Sixteenth Edition

Photovoltaics International

THE TECHNOLOGY RESOURCE FOR PV PROFESSIONALS

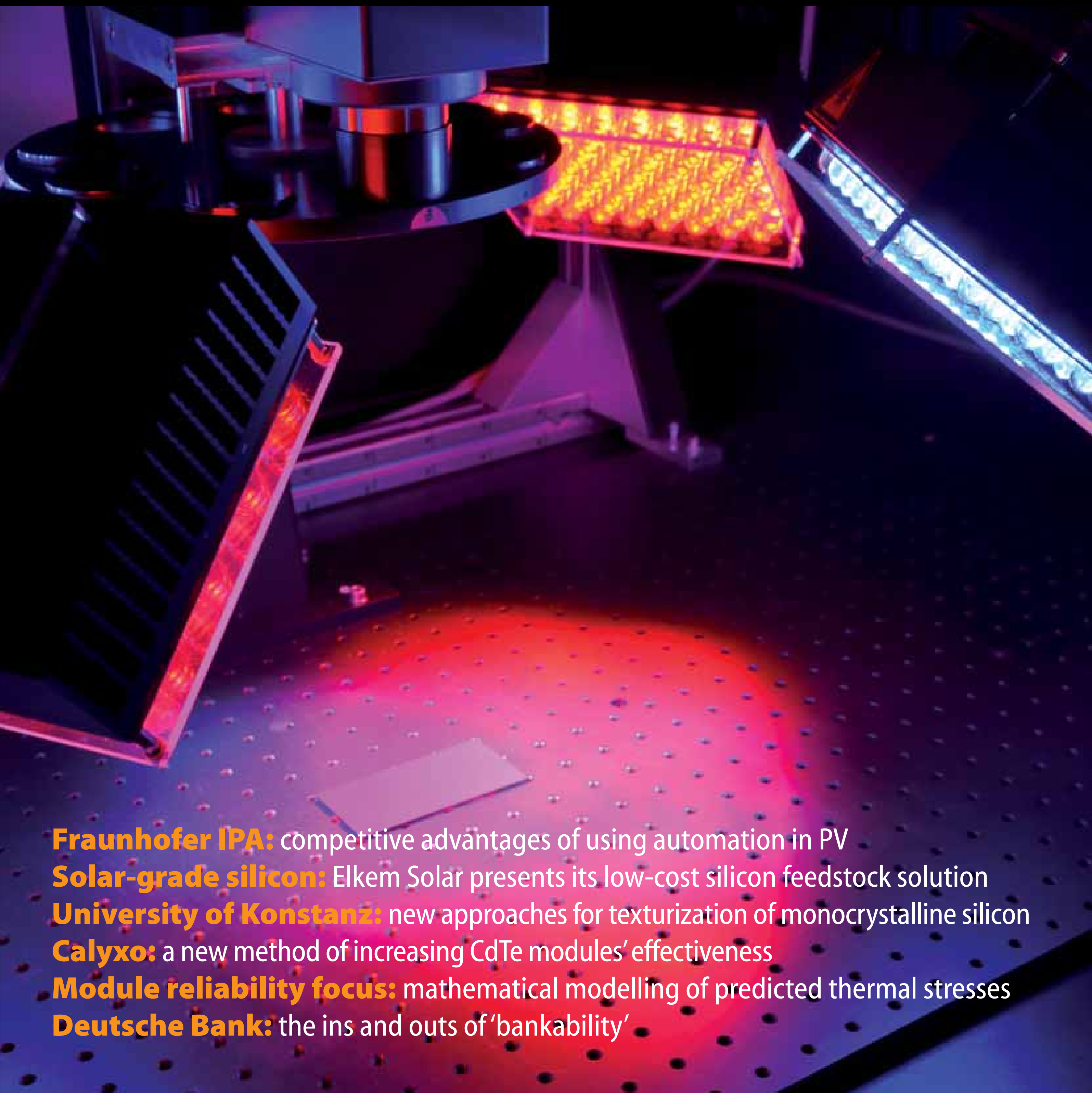

Fraunhofer IPA: competitive advantages of using automation in PV
Solar-grade silicon: Elkem Solar presents its low-cost silicon feedstock solution
University of Konstanz: new approaches for texturization of monocrystalline silicon
Calyxo: a new method of increasing CdTe modules' effectiveness
Module reliability focus: mathematical modelling of predicted thermal stresses
Deutsche Bank: the ins and outs of 'bankability'

Second Quarter, May 2012

www.pv-tech.org

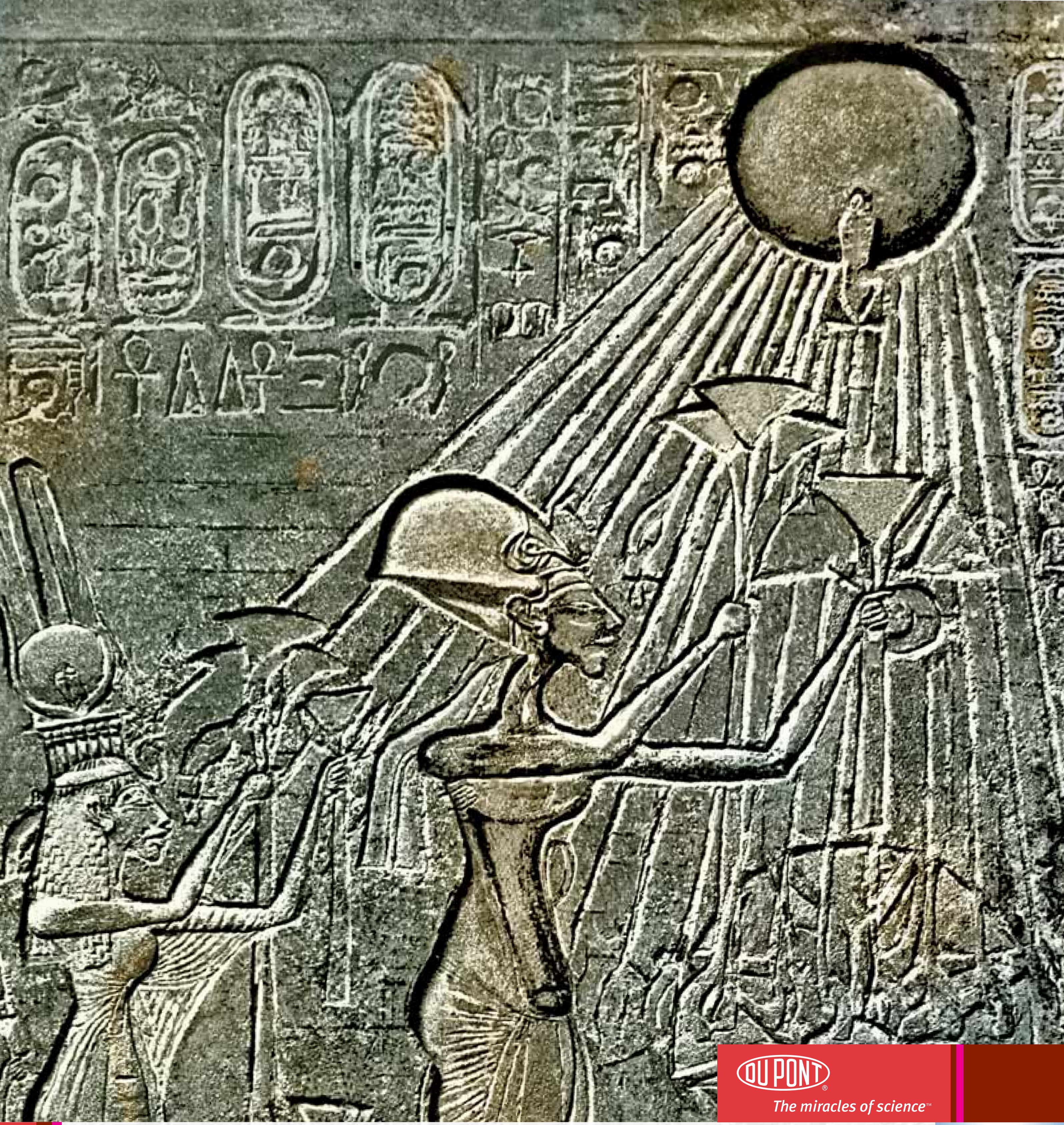

Photovoltaics International

Published by:
Solar Media Ltd.,
Trans-World House, 100 City Road, London
EC1Y 2BP, UK
Tel: +44 (0) 207 871 0123
Fax: +44 (0) 207 871 0101
E-mail: info@pv-tech.org
Web: www.pv-tech.org

Publisher: David Owen

Managing Editor: Síle Mc Mahon

Design & Production: Daniel H Brown
Production: Viki Hämmerle
Senior News Editor: Mark Osborne
Web & Publications Editor: Nilima Choudhury
News Editors: Syanne Olson & Anne Zimmermann
Contributing Editors: Felicity Carus,
Emma Hughes & Pete Bennett

Sub-Editor: Steve D. Brierley
Commissioning Editor: Adam Morrison

Sales Director: David Evans
Account Managers: Adam Morrison, Graham
Davie, Daniel Ryder, Gary Kakoullis,
Nick Richardson, Ben Irving & Peter Gibson
Germany Office Representative: Martin Lehmann
Marketing & Operations Director:
Joy-Fleur Brettschneider

Cover image shows EL & PL measurement setup in the laboratory at the Institute of Mechatronics and Medical Engineering. Image courtesy of University of Applied Sciences Ulm.

Printed by Buxton Press
Photovoltaics International
Sixteenth Edition
Second Quarter 2012
Photovoltaics International is a quarterly journal published in February, May, August and November.

Distributed in the USA by Mail Right International, 1637 Stelton Road B4, Piscataway, NJ 08854.

ISSN: 1757-1197

USPS Information
USPS Periodical Code: 025 313

Periodicals Postage Paid at
New Brunswick, NJ
Postmaster: Send changes to:
Photovoltaics International,
Solar Media Ltd., C/o 1637 Stelton
Road, B-4, Piscataway, NJ 08854, USA

Foreword

With the global events season well and truly underway, the industry is coming alive again. Companies are flocking to events in a bid to showcase their ranges of products and services that offer cost-reduction features and promises of higher yields to address that most ubiquitous of manufacturing goals: higher cell efficiencies.

Supply and demand issues, ASP declines and regional government subsidy decisions continue to plague the majority of manufacturers and equipment suppliers in the PV realm. As 2012 rolls along, it's likely that we will hear more and more reports of once-successful companies falling by the wayside, while the fully integrated business model is fast becoming an attractive route for many manufacturers, an option that is being embraced by Chinese companies in particular.

Nevertheless, in defiance of these difficult times, there's a wealth of evidence that suggests that things are actually going pretty well. Large-scale PV projects are on the up; materials and module supply contracts are still being announced and new markets continue to emerge, markets including Serbia, Chile and that most strategically placed PV region of the Middle East. And new markets are being created as companies add project development to their repertoire in the face of module price declines.

Growth is being supported in these and other emerging markets, with some announcing installations totalling over 100MW despite a lack of government subsidies. Grid parity is far closer than was forecasted only a few years ago, and the dependence on FiTs is waning.

This sixteenth edition of *Photovoltaics International* marks four years of production of the quarterly journal, and we continue in our aim to provide the most technologically relevant, timely and in-depth articles to ensure that you are kept up to speed on technology developments in this ever-changing industry of ours.

Our focus, as always, is on efficiency and quality improvement and cost reduction in manufacturing. We've got two papers in our PV module section that look at stresses in PV modules: **TÜV Rheinland** (p. 112) focuses on dynamic stress tests while **University of California** teams up with **Flextronics** and the **University of Bordeaux** to provide a mathematical model for predicted thermal stresses (p. 119).

We've also got articles on a new approach to solar-grade silicon production from **Elkem Solar** on p. 45; single-side chemical processing from **Fraunhofer ISE** on p. 61; selective emitter technology transfer (**Schmid & Sunrise Global Solar**, p. 75); and luminescence characterization for CIGS cells (**University of Applied Sciences Ulm**, p. 87).

The importance of automation in PV manufacturing is the focus for **Fraunhofer IPA** (p.15); **SEMI PV Group** presents the result of its international technology roadmap survey for 2011 on p. 26, while **EPIA** (p. 154) presents its outlook for the coming year.

Be sure to drop by one of our booths at some of this year's major global events to pick up a copy of *Solar Business Focus* or PV-Tech *PRO*, our new Simplified Chinese publication, or register your details online to get your free digital copy.

I would like, as always, to extend a warm thank you to all our advertisers, authors, advisory board members and contributors. We greatly appreciate your support as we strive to inform and educate the industry of its capabilities in the face of economic adversity.

Let's hope that the market can act smart and persevere!

Síle Mc Mahon
Managing Editor
Photovoltaics International

Photovoltaics
International

Photovoltaics International's primary focus is on assessing existing and new technologies for "real-world" supply chain solutions. The aim is to help engineers, managers and investors to understand the potential of equipment, materials, processes and services that can help the PV industry achieve grid parity. The Photovoltaics International advisory board has been selected to help guide the editorial direction of the technical journal so that it remains relevant to manufacturers and utility-grade installers of photovoltaic technology. The advisory board is made up of leading personnel currently working first-hand in the PV industry.

Editorial Advisory Board

Our editorial advisory board is made up of senior engineers from PV manufacturers worldwide. Meet some of our board members below:

Gary Yu, Senior Vice President, Operations

Mr. Yu served as Trina Solar's Vice President of Manufacturing since May 2007 and in July 2010 was promoted to the position of Senior Vice President of Operations. Mr. Yu has 17 years' manufacturing management experience in semiconductor-related industries. Before joining Trina Solar, he was Managing Director of Wuxi Lite-On Technology, an LED assembly company based in China. Prior to Wuxi Lite-On Technology, he served as a Director of Manufacturing for 1st Silicon Sdn. Bhd. in Malaysia, prior to which he worked at Macronix International, a semiconductor integrated device manufacturer in Taiwan. Mr. Yu has a master's degree in Industrial Engineering and Management from National Chiao Tung University in Taiwan and a bachelor's degree in Chemical Engineering from Tunghai University.

Takashi Tomita, Senior Executive Fellow, Sharp Solar

Takashi Tomita has been working at Sharp for 34 years and is widely recognised as a fore-father of the solar industry in Japan. He was responsible for setting up Sharp's solar cell manufacturing facilities in Nara and silicon production in Toyama. Takashi's passion for solar power has led him to hold numerous posts outside of his roles at Sharp, including: Vice Representative at the Japan Photovoltaic Industry Association; Committee Member of Renewable Energy Portfolio Standard of METI; Adviser Board Member of Advanced Technology of Nara; Visiting Professor of Tohoku University; Adviser of ASUKA DBJ Partners (JAPAN) and Adviser of Global Catalyst Partners (US).

Dr. Peng Heng Chang, CEO, Motech Industries, Inc.

Dr. P.H. Chang was elected CEO of Motech in March 2010. Dr. Chang has over 30 years of experience in management at multinational technology companies and in-depth knowledge in Materials Engineering. Prior to joining Motech, Dr. Chang was VP of Materials Management and Risk Management, VP of Human Resources and Senior Director of Materials Management at Taiwan Semiconductor Manufacturing Co. (TSMC); VP of Administration at Worldwide Semiconductor Manufacturing Co. and Professor of Materials Science and Engineering at National Chiao Tung University in Hsinchu, Taiwan. Dr. Chang also worked for Inland Steel Co. and Texas Instruments in the US prior to 1990. He received his Ph.D. degree in materials engineering from Purdue University in 1981.

Professor Eicke R. Weber, Director of the Fraunhofer Institute for Solar Energy Systems ISE in Freiburg

Professor Eicke R. Weber is the Director of the Fraunhofer Institute for Solar Energy Systems ISE in Freiburg. Weber has earned an international reputation as a materials researcher for defects in silicon and III-V semiconductors such as gallium arsenide and gallium nitride. He spent 23 years in the U.S. in research roles, most recently as Professor at the University of California in Berkeley. Weber is also the Chair of Applied Physics, Solar Energy, at the University of Freiburg, and during his career has been the recipient of several prestigious awards including the Alexander von Humboldt Prize in 1994, and the German Cross of Merit on ribbon in June 2006.

Dr. Zhengrong Shi, Chief Executive Officer, Suntech

Dr. Zhengrong Shi is founder, CEO and Chairman of the board of directors of Suntech. Prior to founding Suntech in 2001, he was a Research Director and Executive Director of Pacific Solar Pty., Ltd., the next-generation thin-film technology company, before which he was a Senior Research Scientist and leader of the Thin Film Solar Cells Research Group in the Centre of Excellence for Photovoltaic Engineering at the University of New South Wales in Australia. Dr. Shi holds 11 patents in PV technologies and is a much-published author in the industry. His work has earned him such accolades as "Hero of the Environment" (TIME magazine 2007) and "Corporate Citizen of the Year" at the China Business Leaders Awards 2007. A member of the NYSE advisory board, Dr. Shi has a Bachelor's degree in optical science, a Master's degree in laser physics and a Ph.D. in electrical engineering.

Dr. Sam Hong, President and COO of Neo Solar Power

Dr. Hong has more than 30 years of experience working in the solar energy industry. He has served as the Research Division Director of Photovoltaic Solar Energy Division at Industry Technology Research Institute (ITRI), a research organization that serves to strengthen the technological competitiveness of Taiwan, and Vice President and Plant Director of Sinonar Amorphous Silicon Solar Cell Co., which is the first amorphous silicon manufacturer in Taiwan. In addition, Dr. Hong was responsible for Power Subsystem of ROCSAT 1 for the Taiwan National Space Program. Dr. Hong has published three books and 38 journal and international conference papers, and is a holder of seven patents. Dr. Hong was the recipient of Outstanding Achievement Award from the Ministry of Economic Affairs, Taiwan, and was recently elected as chairman of the Taiwan Photovoltaic Industry Association.

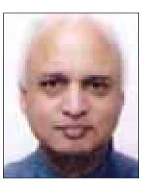

Dr. G. Rajeswaran, President and CTO of Moser Baer Photovoltaic Ltd

Raj served as President and CTO of Moser Baer Photovoltaic Ltd. from July 2007 until October 2008, since which time he has been Group CTO for all the Moser Baer business units and holder of the CEO function for launching new businesses. He spent 22 years with Eastman Kodak Company as the Vice President of Advanced Development & Strategic Initiatives, where he managed Kodak's Japan display operations including technology & business development in Japan, Taiwan, Korea and China. He has also served as Vice President and on the board of SK Display Corporation, and worked in technology development with Brookhaven National Laboratory. Raj has a Ph.D., an M.Tech. and a B.E. in electrical engineering. A much-published author, speaker and patent holder, Raj is a member of the Society for Information Display (SID) and has chaired several international conferences in the field of OLEDs.

Contents

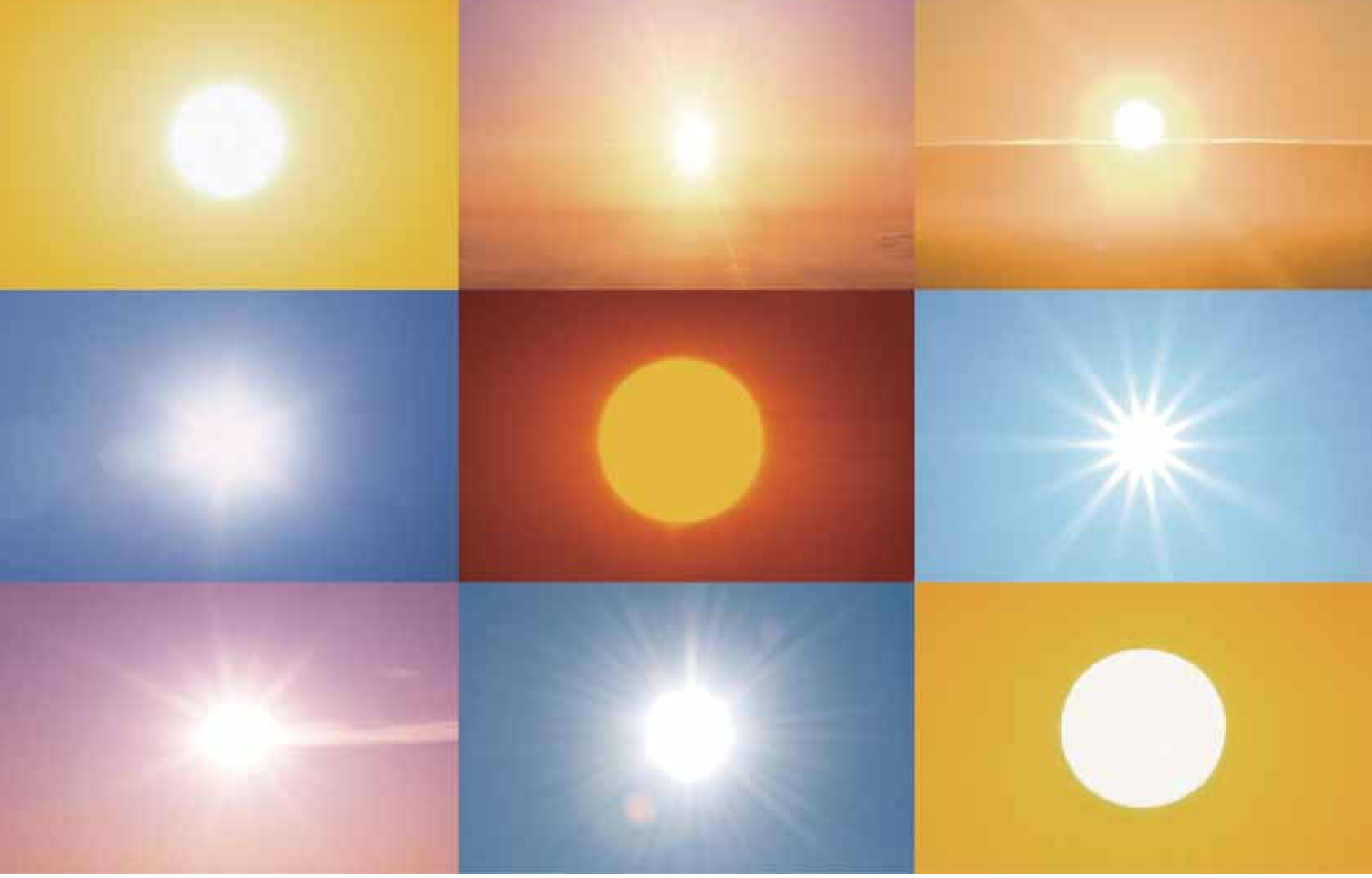

Contents


www.hyundaisolar.com
Imagine
How a single Solar Module
Can save a polar bears home
With a 240Wp solar module
It can replace 3 barrels of oil energy
Solar Energy, that reduces risks of global warming…
Supports a younger, healthier earth
We need Solar!

Fab & Facilities

News

Laid off SolarWorld employees granted aid by US Department of Labour

Considered to be one of the first major rulings for the trade case filed against Chinese trade practices by SolarWorld last year, the US Department of Labour has granted all manufacturing employees that were laid off from SolarWorld Industries' Camarillo, California, plant as being eligible for federal trade-adjustment assistance, including grants for education that will lead to re-educating them for new work.

The decision was handed down at the end of April, stipulating that Chinese imports helped cause the shutdown that resulted in as many as 186 employees from SolarWorld's Camarillo plant being let go.

US law stipulates that the Labour Department can certify works for trade-adjustment assistance only if it finds that an increase in competing imports "contributed importantly" to the decline in sales or production of a firm and to the cause for worker layoffs.

Source: Dallas South News

The US DOL has granted aid to laid-off workers from SolarWorld's Camarillo plant.

Capacity News Focus

Yingli sets up regional headquarters in Tokyo, Japan

Yingli Green Energy has furthered its reach across Asia with its establishment of a regional headquarters in Tokyo, Japan. In conjunction with this new location, the company has also set up a new wholly owned subsidiary in the form of Yingli Japan, or more formally, Yingli Green Energy Japan Corporation, Ltd. The news is a move on the part of the vertically integrated manufacturer to further its business development in Japan.

Source: Yingli

The news is a move on the part of the vertically integrated manufacturer to further its business development in Japan.

"We are pleased to announce the opening of our regional headquarters in Japan," commented Liansheng Miao, Yingli's chairman and CEO. "Japan is an important PV market for us. With the establishment of the Japanese subsidiary, we expect to be closer to our customers and penetrate deeper into this market."

Rio de Janeiro state announced as the site for new US$1 billion solar production facility

Brazil's richest man, Eike Batista, looks set to develop a solar panel manufacturing complex in Rio state, in alliance with Taiwanese electronics provider Foxconn.

Half of the money for the US$1 billion project will be provided by one of Batista's

Source: Bruno Astuto

Forbes ranked Batista as the richest man in South America and one of the top 10 richest men in the world in 2011.

companies, with the other half coming from Foxconn. Exactly which of Batista's companies will provide the proceeds in unclear, though his oil company OGX recently reported loses of US$265,000 for 2011.

The manufacturing plant will produce solar panels, batteries and energy efficient street lamps, though no completion date has been announced.

SunPower to stop using Fab 1 facility

Having already reduced production capacity to control inventory build, SunPower is making further manufacturing cost reductions that had not previously been cited within its 'Manufacturing Step Reduction Program.' The company said it would stop using its Fab 1 facility in the Philippines and consolidate production at Fab 2 in the Philippines and its newer facility, Fab 3 in Malaysia, operated as a JV with AU Optronics.

Source: SunPower

Fab 3 had 10 lines in production at the end of the third quarter of 2011.

SunPower said that it would transfer some equipment from Fab 1 to Fab 2 to reduce manufacturing constraints during the current quarter, reducing nameplate capacity by 125MW.

SunPower also said it would be seeking new tenants at Fab 1, potentially including Deca Technologies. Workers affected by the closure would also have the chance to work at Fab 2 as well as possibly transferring to potential tenants at Fab 1.

Source: REC

SiC Processing has said that it would also close its four production lines at plant Herøya II with an annual capacity of 44,000 tons.

SiC Processing permanently closes wafer slurry operations in Herøya, Norway

As a direct result of REC's announcing the closure of its 650MW multicrystalline wafer plant at Herøya, Norway, by the second quarter of 2012, slurry recycling sub-contractor, SiC Processing has said that it would also close its four production lines at plant Herøya II with an annual capacity of 44,000 tons. The company said that 100 jobs would be lost.

The closure of the Herøya plant signalled the end of all REC's wafer operations in Norway.

Sustainable Energy Technologies to produce Ontario's first factory-built PV systems

Sustainable Energy Technologies has announced it aims to reduce design and on-site labour costs by 90% by producing Ontario's first factory-constructed solar systems. The product will be available through ProFab Solar only, a subsidiary of the partnership between Sustainable Energy and Steeltree Structures. The new systems also claim to offer project developers a reduction in risks during the installation process.

The product will comprise all DC-side components, including prefabricated racking as well as PV modules and the Paralex inverter in the majority of cases. All of the system components will be pre-assembled and certified to meet Ontarian industry safety standards.

Other News

SunPower sells 25MW Californian PV plant to K Road

K Road Power has bought the 25MW McHenry solar project in California

Source: SunPower

K Road has acquired 25MW McHenry solar project in California from SunPower

from SunPower, it has been announced. The project has been designed and is currently being constructed by SunPower in Modesto, California, and is expected to commence commercial production in September 2012. Modesto Irrigation District (MID) will buy the generated energy under a 25-year PPA.

Union Bank, Rabobank and CIT will function as joint lead arrangers for K Road's term project financing and a non-recourse construction financing.

ISO 9001:2008 certification awarded to Nanosolar's German production facility

The German Technical Control Board, TÜV Süd Germany, has awarded Nanosolar's Luckenwalde panel assembly plant the ISO 9001:2008 certificate. The certification will cover all manufacturing steps, as well as testing of the company's thin-film solar panels. The ISO 9001:2008 certificate applies to specific quality management systems and is awarded when all applicable statutory and regulatory requirements are met.

Source: Rath

The ISO 9001 certification applies to specific quality management systems.

Eosol's US$300,000 funds Chile's first solar PV lab at Adolfo Ibáñez University

Eosol New Energy has invested US$300,000 into Chile's first solar PV laboratory at the Adolfo Ibáñez University, inaugurated recently in Santiago, Chile, giving developers an additional reason to keep a close eye on the Chilean market. The laboratory, which will serve as a testing facility for both university students and private companies, features four 12kW grid-connected PV systems. Two of the systems rely on tracking technologies, while the other two are fixed systems. The laboratory also includes temperature, irradiation and solar simulation software technologies.

Source: cmchile.cl

The Adolfo Ibáñez University is playing host to Chile's first solar PV lab.

Wacker officially opens 15,000MT polysilicon plant

As part of plans to increase hyperpure polysilicon production to meet customer demand, Wacker has officially started volume production at its latest plant in Nünchritz, Germany. Wacker said it had invested €900 million in the facilities, creating more than 500 new jobs. The 15,000MT polysilicon plant was scheduled to reach full capacity within a few weeks of its commencement of volume production.

The company reiterated that it was continuing to ramp up its total polysilicon capacity to around 52,000MT by the end of 2012, with total annual production capacity reaching 70,000MT by 2014 when its US plant, currently under construction, comes on stream.

Proinso announces opening of new PV centre in Thailand

PV module and inverter manufacturer, Proinso, has announced that it has established a base in Bangkok, Thailand, to serve Southeast Asia's fastest-growing solar market. From here the company intends

Source: Proinso

Proinso will be looking to increase its influence in the emerging Asian markets.

to extend its reach in Asia even further, with possible development into Vietnam, Laos, The Philippines, Malaysia and Indonesia by the end of next year.

Proinso's global network employs over 2,000 qualified installers and has operations in the US, UK, France, Germany, China, Canada and Italy. The large majority, 88%, of the company's revenue comes from its US and European networks, while emerging markets comprise just 5% of sales.

Proinso has already accumulated a global install total of more than 1.1GW for its products and Asian PV markets look set to top 10,000MW of projects in the next two years.

TÜV Rheinland grants health and safety certification to Canadian Solar

Canadian Solar has passed the required tests for compliance with the OHSAS 18001 international standard for occupational health and safety as set out by TÜV Rheinland. This standard certifies that the Canada-based solar wafer, cell and module manufacturer has an efficient occupational health and safety procedure and management system in place for its employees.

The company also holds ISO 14001, REACH (registration, evaluation, authorization and restriction of chemicals) and QC080000 environmental management system certifications.

Jurasolar's 60MW module facility in Deagu, South Korea to open soon

Situated in Deagu, Gyeongsangbuk-do Province of South Korea, Jurasolar's new 60MW module manufacturing facility is nearing completion and was scheduled for opening in May, according to the company. Equipped with tools including a fully automated PV module manufacturing line from German company JvG Thoma, the factory will produce the company's JvG Desert Modules, named to reflect their ability to perform in extremely high temperatures of over 125°C.

The modules feature a thermally-conductive ultra-thin film that ensures high transparency and light transmission. They are also said to be PID-free and 100% recyclable.

Source: Proinso

Chile's Atacama Desert can receive up to 9.28kWh of sun per square metre per day.

Developers eye Chilean solar market with 2,500MW of proposed projects

Chile's Renewable Energy Center has released a report suggesting that projects amounting to 685MW are awaiting the start of construction after receiving environmental permits and a further 1903MW are awaiting permits.

Chile has been receiving an increasing amount of attention from solar developers in recent months. The Atacama Desert in the north of the country receives some of the highest levels of solar irradiance on earth; coupled with very low rainfall, this makes Chile an ideal place for solar farms. Interested parties include German solar giant juwi, First Solar and Ingenostrum, which plans to build six solar PV projects totalling 688MW generating capacity and costing close to US$2 billion.

Despite having no feed-in tariff or incentive scheme, Chile has set a target of obtaining 10% of its electricity from renewable sources by 2024. However, Chilean president Sebastián Piñera has recently said that the use of renewable energy sources could increase by as much as 20%. Currently just 4% of Chile's electricity is produced from non-conventional renewable sources.

TÜV InterCert Saar India officially opens in Bangalore

TÜV InterCert Saar India officially opened its new office in Bangalore in April. The company originally announced its intent to open an office on November 3, 2011. Rajesh Krishna Iyer will lead staff members to provide management system certification, product certification, inspection, engineering and training for both the automotive and renewable energy markets in the middle Asia region.

Source: emchile.cl

The Adolfo Ibáñez University is playing host to Chile's first solar PV lab.

Product Reviews

Edwards

TMP pump from Edwards offers 32% reduction in energy

Product Outline: Edwards has launched the STP-iXR1606 series of magnetically-levitated turbo-molecular pumps (TMP) with a fully-integrated onboard controller. Edwards' new TMP incorporates a new rotary design that delivers approximately 40% improvement in throughput at high gas flow rates and an increase of nearly 90% in maximum gas flow, compared to existing products

Problem: The reduction of energy consumption and footprint of PV manufacturing equipment and support facilities is a key focus in reducing overall cost of ownership. Providing high-uptime components reduces CoO and improves throughput and productivity.

Solution: Edwards' new pump features a fully-integrated controller that eliminates the connection cable and rack conventionally required with a non-integrated controller. This helps reduce footprint, saving valuable fab real estate, as well as installation time and cost. In addition, the onboard controller incorporates a small power supply, which compared to existing products, delivers approximately 32% reduction in energy consumption at high gas flows. The STP-iXR1606 matches the peak pumping speed of Edwards' highest performing pump in the 8-inch TMP class, but with significant improvements in throughput performance and maximum allowable gas flow.

Applications: Viewed as an all-in-one TMP solution for all applications with reduced footprint, simplified installation and reduced energy costs for PV manufacturing equipment requiring vacuum functions.

Platform: The STP-iXR1606 series delivers high reliability in dirty environments with equivalent IP54 protection against dust and humidity.

Availability: April 2012 onwards.

Eyelit

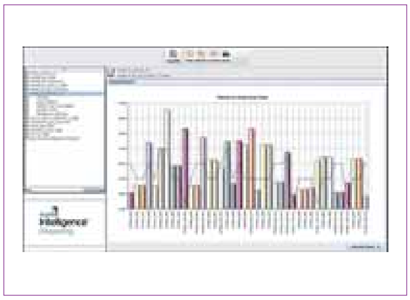

Eyelit's Intelligence Mobile Web Portal remote access to manufacturing data

Product Outline: Eyelit has made available its Intelligence Mobile Web Portal, which provides operational information in real time through tablet devices, smart phones or androids, enabling 'anywhere access' to key manufacturing and quality data from the manufacturing floor.

Problem: Manufacturers have to become more adaptable to multi-site and global operations by striving to use every inch of factory floor space and by promoting a dynamic 'work from anywhere' environment to reduce costs and optimize productivity.

Solution: With portable access to the current state of the factory, personnel can monitor and respond to dynamic conditions remotely and take appropriate action to prevent serious problems. The Mobile Web Portal also supports transactions from a mobile device. This powerful capability is ideal in areas where it is impractical for maintenance personnel to have a traditional computer device.

Applications: Manufacturing Execution and Quality Management (MES and QMS) solutions for visibility, control and coordination of manufacturing operations.

Platform: The Mobile Web Portal works in conjunction with all business intelligence capabilities available throughout Eyelit's product suite; real-time alerts, key performance indicators (KPIs), dashboards, statistical process control (SPC) charts, and production reports with metrics on yields, throughput and cycle times are all available and include drilldown to view detailed equipment and lot information. Users can easily zoom into displays on mobile devices since the portal uses Scalable Vector Graphics (SVG) and Hypertext Markup Language (HTML) technologies.

Availability: April 2010 onwards.

Wastech

Wastech offers new designs for heavy metal removal systems

Product Outline: Wastech Controls & Engineering offers heavy metal removal systems that treat rinse waters from plating lines used to add soldering contacts to PV wafers. Rinse waters are acidic in nature and contain heavy metals such as copper, nickel and tin. Heavy metal removal systems can be a batch or continuous flow system, using a combination of pH adjustment, precipitation, flocculation, clarification and filtration to remove heavy metal oxides.

Problem: Heavy metals are contained in a number of processing steps that need to be treated correctly to meet numerous statutory environmental requirements. However, systems that are scalable and offer lower cost are required for high-volume production.

Solution: Wastech offers the MetFloc chemical line claimed to reduce the process steps, lower chemical consumption and minimize sludge generation. Using MetFloc is claimed to simplify the control strategy, requiring only pH adjustment. The clear water can be routed to an AWN or discharged directly, depending on the discharge limits. The filtrate is disposed of as solid waste.

Applications: The system handles the removal of 21 identified heavy metals in one pass and reduced sludge volumes.

Platform: Design criteria include flow rates from < 1gpm to 100gpm and influent metal concentration range of 10 to 1,000+ ppm with effluent metal concentration range of < 1 to 10ppm. Configuration options include batch or continuous operation. Traditional reagent chemical supplies can be used as can MetFloc chemicals. Reagent day tanks can be supplied direct from drums or totes. Integral post-treatment pH adjustment is made prior to direct final discharge.

Availability: Currently available.

How automation can benefit the PV industry

Roland Wertz, **Fabian Böttinger**, **Christian Fischmann**, **Tim Giesen** & **Marcus Michen**, Fraunhofer Institute for Manufacturing Engineering and Automation (IPA), Stuttgart, Germany

ABSTRACT

Although the different roadmaps for PV vary somewhat from each other, the bottom line always remains the same: exponential growth is predicted over the next 5–10 years. The latest cell technologies meet the demand for grid parity even in central Europe and PV will therefore continue to be the most popular source of renewable energy. In consequence, the whole PV industry has developed from a niche product towards mass production. Every player along the entire value chain is now faced with the need to stay profitable while meeting the ever-increasing demands of the market. Implementing suitable automation can improve competitiveness and thus pave the way to becoming or remaining successful in this turbulent market.

Introduction

The PV industry currently faces a time of consolidation. All players, without exception, are being asked to rethink their own strategies and make the right decisions. This phase of market adjustment has been observed in other areas ever since the beginning of mass production. If a close look is taken at the issues that cell/module manufacturers are currently experiencing, the well-known triple constraint of time, cost and quality can be observed.

The time factor is ever present in production. The overall output of a factory is directly linked to cycle times and equipment downtimes. An optimal process layout can help to decrease both of these and therefore lead to an increase in throughput.

The definition of costs in PV production is made up of two main components. One major cost driver is the quantity of expensive/rare materials that is required. As this is determined by the technology itself, it cannot be affected by the actual production. The second one is the waste of resources – such as consumables, labour and energy – and is therefore the one mostly related to automation and process control.

The quality of production – the third constraint – is mainly described by the ratio between the number of good units coming out of a process and the overall number of units going into it. Referred to as 'yield', this relationship can be optimized by ensuring low breakage rates and implementing accurate, fine-tuned processes.

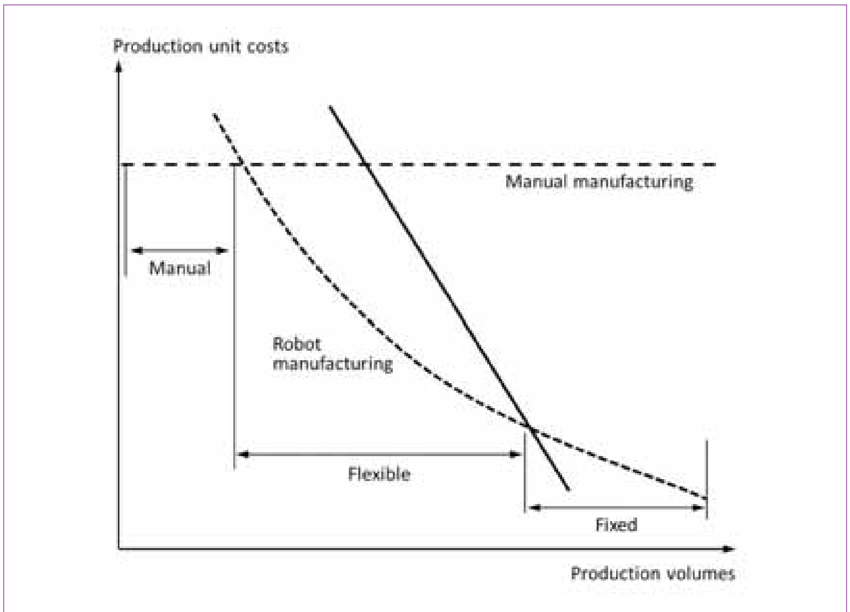

Figure 1. Useful degree of automation as a function of production volumes and production unit costs [1].

Automation in PV

Automation in production has a long history. Edmund Cartwright's weaving loom is mentioned as being the first automated production machine in 1785. The use of steam engines instead of manual labour speeded up the growth of automation, which has continued to the present day.

Because of ongoing improvements to various technologies in the field of sensors and control, automation has become more flexible and capable of more complex tasks. The introduction of computer-controlled equipment gave a further push towards mass production, by reducing the costs while simultaneously increasing quality.

Without significant, ongoing improvements in the field of automation in all branches of industry, manufacturing would be completely different from what it is today. As soon as manufacturing touches one of the DDDs (dangerous, dirty and dull), a suitable automation should be implemented. Although the cost-saving potential is seen to be the major benefit, there are many more advantages of automation. The predictive repeatability of programmed steps, the ability to meet ever-increasing throughput requirements and the capability of handling huge amounts of (sensor) data are also closely related to automation as such.

The basis of a suitable automation concept always lies in understanding the production itself. To optimize the benefits, a knowledge of, and experience in, both the field of automation and PV production are needed. Maximum productivity can only be achieved if the optimum solution for the process step concerned is actually capable of fulfilling requirements.

Factory automation is the versatile interaction of different hardware and software systems – so-called computer-integrated manufacturing (CIM). Determining the optimum degree of automation in manufacturing facilities or process chains is a complex decision for factory planners. To understand the background to this challenge, it may help to take a closer look at history. In the 1970s, the term 'CIM' equated to development efforts to transform shop floors into areas without a human workforce. Because most of the experience possessed by operators could not be implemented into the software of the automation system, the idea of making the shop floor human-free was reconsidered. From then on, CIM began to change. The concept of a fully automated production line turned into the aim of implementing the right amount of automation, i.e. only as much automation as necessary. Calculations to ascertain the optimum degree of automation are based on conflicting targets, relating to labour costs, automation costs, manufacturing quality and production uptimes.

"For PV producers, the most important argument for an automated production process is the need for high-volume manufacturing."

One of the most difficult questions now facing PV producers is how to determine a manufacturing strategy that includes the optimum degree of automation for the future PV market. As in other industries, the initial motivation for companies to consider (further) automation is the problem of increased production costs and the need for more reliable and reproducible manufacturing processes with appropriate capacities. Many other reasons may also be found, such as the desire to increase productivity, speed up time-to-market and realize flexible made-to-order production. However, for PV producers, the most important argument for an automated production process is the need for high-volume manufacturing.

Fig. 1 shows the general automation trade-off based on production volumes. The graph in this figure strictly considers the economic relationship between manual, flexible and fixed production processes. Technical considerations affecting the decision between robot manufacturing and hard automation may play a more important role in certain cases. Owing to the large number of solar products manufactured daily, hard automation is widespread in the production of silicon wafers and crystalline cells. Hard automation is also advantageous because of the low diversity of workpieces in a PV production line. The manufacturing of today's standard 156mm × 156mm wafers with a thickness between 160 and 220μm is an almost stable process. A certain degree of automation therefore enables producers to optimize the overall production system.

While looking at the benefits and advantages of automated systems in the production of PV goods, the challenges and efforts related to implementation should not be forgotten. As well as the monetary investment, the development of a new automation solution also involves systematic planning and design in order to master the technical complexity. In consequence, to ensure a sustained successful solution, the scope of automation needs to take both current and future requirements into consideration. First, the analysis of a fundamental and systematic evaluation concerning the technical challenges in combination with expected future savings is necessary [2]. Based on this, the possible and feasible solutions for automating a dedicated sequence have to be identified and realized.

If the worldwide distribution of industrial robots is taken as a general indicator of hardware automation, 45% of the automation solutions implemented in industries worldwide perform handling tasks, followed by 27% for welding activities and 10% for assembly work [3].

Automation vs. manual work

In principle, it is necessary to differentiate between fully/partially automated and manual work. Automation is useful in the case of large quantities or if, as mentioned before, at least one of the DDD aspects is a factor.

> The pressure to reduce cost and to increase quality rose tremendously within the last few months. Automation is the key to reduce breakage and to minimize contamination on the wafers. Since Asia is facing a significant rise in labour cost every year the return on investment for automation systems becomes more and more attractive. The mass production environment in the PV industry is the ideal setup for the use of automation systems, it combines high production volume with minimal variations in the product range.
> *(Florian Nachbauer, Head of Supplier Management, centrotherm cell & module GmbH)*

The motivation to fully automate a production line is not just the reduction of labour costs: automation can also ensure increased production capacities and significantly improve product quality. In combination with an ongoing process of standardizing interfaces, manufacturing efficiency can be enhanced and ramp-up phases shortened at the same time. Since factories are flexible and capacities are on the increase, the effort involved in adapting automation to the needs of growth can be planned and realized more easily than the effort required to organize larger amounts of manual work. In other words, a suitable automation solution makes life easier.

Credit: centrotherm cell & module GmbH.

Figure 2. Handling prior loading of a carrier.

"An adapted, optimally balanced automation solution can help to minimize problems associated with wafer breakage or quality defects such as micro-cracks, and thus improve yield and quality."

Handling procedures for (un-)loading and transportation can be optimized, and process steps assessed individually. Manual handling is a non-measurable procedure that cannot be repeated exactly and is highly dependent on the person concerned. Regarded as a single task being performed manually, this operation can clearly be categorized as dull and is therefore predestined for automation. Ever-increasing throughput and reliability require a high repetition of simple and complex tasks with constant precision. In theory, simple tasks executed manually should have a low failure rate. But, in practice, doing the same, simple repetitive tasks for eight hours or more is extremely tedious, making it difficult to concentrate throughout the entire period, with the result that failure rates are higher than expected. An adapted, optimally balanced automation solution can help to minimize problems associated with wafer breakage or quality defects such as micro-cracks, and thus improve yield and quality.

When (un-)loading wet-chemistry benches, operators are exposed to the risk of injury from caustic fluids or vapours. The use of automated systems can reduce this risk to a minimum and therefore increase safety at work.

In contrast to the semiconductor industry, PV manufacturing does not require highly sophisticated clean-room conditions. Nevertheless, bilateral studies have shown that the use of mini-environments for dedicated process steps could increase the overall efficiency of the final product, especially in thin-film technologies. Investing in such local clean environments will therefore pay off if

implemented in the right place and in the right dimensions.

"It is much more difficult to assign quality defects or failures to manual handling steps."

Factory automation is more than just a matter of transporting objects – it is also the excellent interaction between software and hardware. Measurement and control systems have to be integrated to ensure the consistent high quality of the product. Quality-related data and sensor signals are used to control process flows, to adapt individual processes and to track and optimize the influence of single process steps on the quality of the end product. Compared to manual work, automation systems have the advantage that the configuration or state at a specified time can be tracked and reproduced in order to investigate the influence of the system or to detect failures. A compatible software system also facilitates wafer and cell traceability to improve quality checks along the whole production line. It is much more difficult to assign quality defects or failures to manual handling steps, and wafer and cell traceability can only be partly achieved. A broad overview of the capabilities of factory IT systems will be given later.

Suitable instruments of automation

In PV manufacturing, automation is highly dependent on the process step, and therefore on the product being manufactured. Throughout the entire process chain, the various products and consumables have to be forecasted, scheduled, transported and supplied with the required quality at the right time. A closer look at the value chain reveals that the object to be transported changes significantly – from polysilicon to the finished solar panel – and thus the automation requirements also change. In particular, transport and handling during wafer and cell processing is a challenging issue in PV industry automation projects. A thin, fragile substrate – 156mm × 156mm in size and between 160 and 220μm in thickness – has to be handled between the various process steps. Special needs result in dedicated solutions, mainly for pre-separation, feeding, positioning, pick-and-place and assembly.

The challenge in these transport operations is not only the delicacy of the object to be handled but also the high throughput of up to 3600 wafers or cells per hour. For a standard handling operation, this means that the automation system has a time frame of only one second for each wafer. There are different ways of managing this situation using automation systems. One solution is a really fast handling system that is capable of functioning at such speeds with the required sensitivity; another solution is a slower method whereby several automation systems act in parallel. Both methods use grippers to handle the substrate. With today's manufacturing lines, the standard gripper is invariably integrated by the supplier. Studies at Fraunhofer IPA have shown that, dependent on the different process steps, a dedicated choice of gripper and gripping principle is beneficial to production quality. Because the surface structure of the substrates changes during processing, handling parameters need to be adapted accordingly.

An inflexible automated production line for photovoltaic cells is only useful in high-volume processing if the required quality of the workpiece can be assured. The term 'quality' in automated PV production, therefore, has different meanings. In consequence, it is not only process output quality due to certain factor combinations in subordinated processes that needs to be taken into consideration: quality inspection and checks to ensure the reliable operation of automated sequences, such as handling by pick-and-place, are also relevant.

For the PV industry, automated handling is one of the most interesting areas of automation. Since the necessary feasibility analysis for a handling automation solution is a challenging task for solar cell producers, the Fraunhofer IPA offers/carries out dedicated handling tests and automation developments for the PV industry. A professional feasibility study of handling tasks for delicate wafers helps to identify the quality and function of the automation solution as well as minimum cycle times and total costs of ownership. Decreasing wafer thicknesses to reduce silicon consumption and new solar cell technologies require the adaptation and testing of appropriate handling equipment and components. By using the design of experiments (DOE) method to make a comprehensive handling evaluation, the achievable position accuracy of a handling component, such as a Bernoulli gripper, can be determined.

One complete pick-and-place cycle is a combination of a number of single steps to be performed, as shown in Fig. 5 [4]. In total, a pick-and-place cycle is made up of a

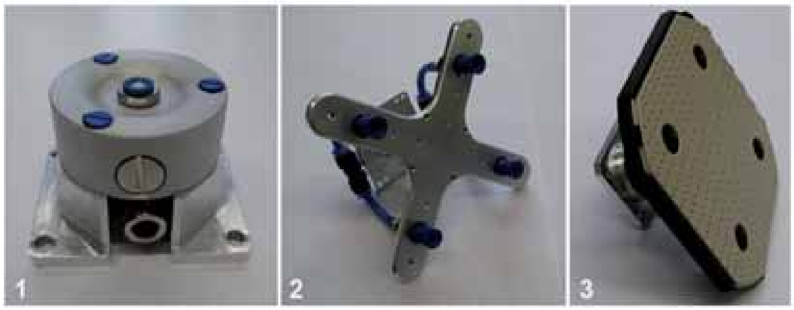

Figure 3. Different grippers for PV handling: 1) Bernoulli gripper, 2) vacuum cups, and 3) area gripper.

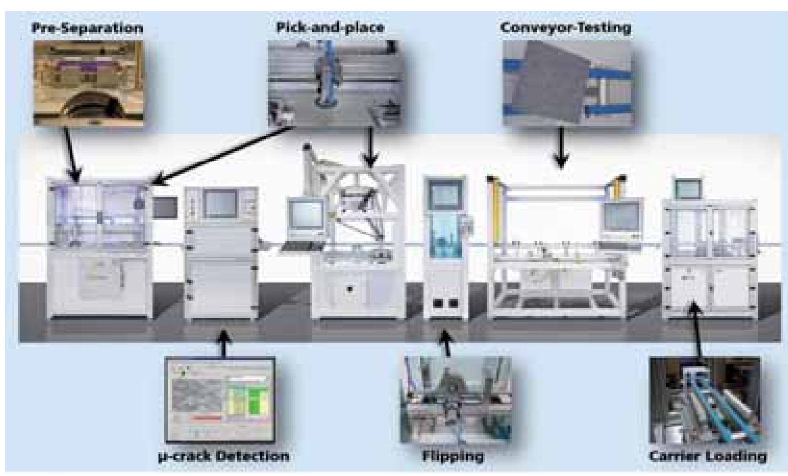

Figure 4. PV test and demonstration centre at Fraunhofer IPA.

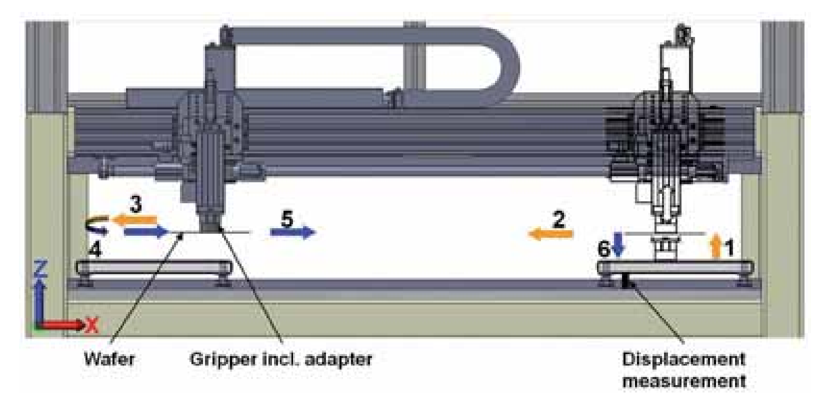

Figure 5. Pick-and-place cycle.

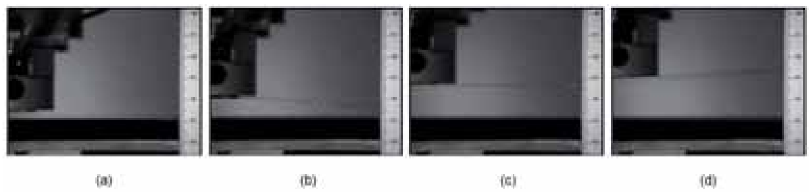

Figure 6. High-speed images (at the points indicated on the graph in Fig. 7) of a wafer being picked up.

sequence of seven movements. To achieve comparable results, test conditions such as lifting height and lateral distance are kept constant for each test batch.

1. The first step is to pick the substrate by utilizing either a positive pressure or a vacuum, depending on the gripping principle.

2. As soon as the substrate is held by the gripper, it is lifted up by a dedicated vertical axis.

3. The lateral movement along one axis simulates the movement from A to B in a production line (i.e. out of the box and along the conveyor belt).

4. To simulate changes in direction and therefore the horizontal forces applied to a substrate due to negative and positive acceleration, a U-turn is performed.

5. The movement performed in step 5 is the same (with the same parameters) as in step 3, but in the opposite direction.

6. The last movement is placement of the substrate in the target position.

7. To complete the cycle, the adhesive forces between the gripper and substrate have to be eliminated, i.e. by turning off the vacuum (depending on the system utilized).

A particular group of data gathered by these experiments relates to the vibrations impacting on the wafer. The high-speed images (Fig. 6) already indicate what the sensor records (Fig. 7) [4].

> "Optimization and cost reduction along the whole value chain are key factors in remaining competitive."

Factory IT

Optimization and cost reduction along the whole value chain are key factors in remaining competitive. While, in the past, companies focused on production processes, new materials and material handling, there is today an increasing awareness of the potential for improving manufacturing systems. Suitable IT systems, having proved their aptitude and gained wide acceptance in many industrial sectors with mass manufacturing systems, are now implemented at all hierarchical levels of a factory organization. On the management (strategic) level, established software – such as Enterprise Resource Planning (ERP), Supply Chain Management (SCM) and Product Lifecycle Management (PLM) – support the long-term planning and supervision of company activities. Below this level, systems can be found that support the operation, monitoring and control of the actual production. They are typically connected

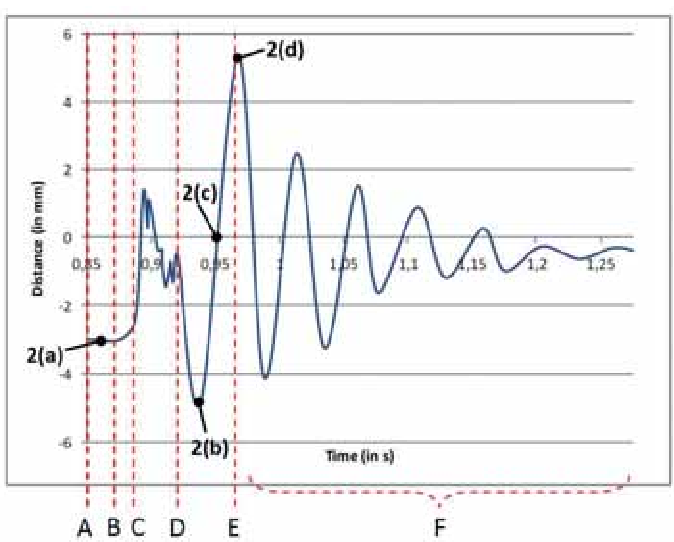

A Gripper at a height of 3mm; no forces applied
B Gripper on; air flow starts
C First contact of wafer with gripper
D Gripper starts moving upwards
E Gripper stops at a height of 20mm
F Wafer is held at a height of 20mm

Figure 7. Graphical illustration of substrate vibration during pick-up.


THE LINDE GROUP
Linde

to the lowest (process) level and serve as an intelligent link between the other hierarchical levels (vertical integration within one single production facility). Although not yet widely used in the PV industry, these tools are considered to offer great potential for optimizing production control and are known as manufacturing execution systems (MES). Depending on the software supplier, not all of the features explained below form part of a single system; in some cases, several applications are used to fulfil these MES tasks. The list is not intended to be complete, but aims to highlight the most valuable features for optimizing the degree of automation.

Data capture and analysis

A key benefit of an integrated MES is the automated capture, correlation and aggregation of data. Production data is linked to equipment data, allowing in-depth analysis of certain scenarios, as well as the calculation of the high-level key performance indicators (KPIs) of interest.

Low-level equipment parameter settings (recipes) can be correlated with process results and quality data. These data sets can be used for statistical process control (SPC) software which feeds analysis results back to the MES to enable active process control. Advanced process control (APC) tools extend this approach by considering data from multiple, interconnected pieces of equipment when adjusting recipes. The focus of these automated systems is to keep processes at a stable level to achieve higher yields and improved cell efficiency. Manual intervention is only required when certain critical conditions occur. Despite these advantages, the underlying – partly very complex – rules for process control need to be defined and maintained manually. Moreover, operators may lose some authority for manually adjusting equipment parameters.

An MES allows end users to define KPIs that can be calculated in real time in order to support operative or tactical management decisions. Automated notifications and alerts can be specified to minimize equipment idling or standby times. Additionally, the data analysis can help planners to predict upcoming maintenance actions on the basis of historical data, equipment utilization, recipe parameters and quality-related data.

Material tracking and identification

For full production system control, the software and planning team need to know the location of materials at any point in time. In combination with actual equipment and material-handling states, this allows equipment utilization and throughput to be optimized. Furthermore, a historical database comprising material identification, process recipes applied and quality-related data can be set up. This may be useful in dealing with warranty issues, quality problem identification and inventory management. Nevertheless, material tracking in crystalline PV production can be quite challenging because of the high takt (cycle) times and the changes being made to the material surface during the process flow. Physical systems, such as laser-based cell marking developed by Q-Cells SE, are available, as well as MES-integrated virtual (software-based) material tracking.

Detailed production planning and execution

On the basis of the production demand from a management-level IT system, the MES is able to calculate and execute detailed production orders regarding material, resources (e.g. equipment) and material flow. A schedule is generated utilizing actual shop-floor data, for example on equipment's and other resources' states. Automated execution will result in the distribution of recipes to equipment, wafer starts and material-handling jobs. Some MESs facilitate the local dispatch of material to equipment and may also allow ambitious targets defined by the management to be achieved.

Major drawbacks of IT-based automation

To tap the benefits of a partly software-controlled manufacturing system, a number of conditions and requirements need to be carefully evaluated and fulfilled. Costly software and hardware have to be purchased and maintained. Rules for handling exceptions (software failures, updates, manual interventions, etc.) need to be well defined, and an option to run the production 'offline' must also be considered. Equipment and material-handling systems from different suppliers have to be integrated into the production IT. Despite the increasing acceptance of SEMI PV2 as a unified equipment communication interface standard and the availability of commercial PV2-compliant connectors, a significant amount of heterogeneous software interfaces can still be found on the market. Sometimes no interface exists at all; in this case, customized graphical user interfaces are required at operator terminals, with manual data acquisition.

No neutral, comprehensive analysis of measurable benefits emerging from the use of production IT in automating PV manufacturing appears to be available on the market. Nevertheless, experience from similar industries with related manufacturing systems indicates positive outcomes from the use of such software. The increasing number of software suppliers offering solutions tailored to the needs of the PV industry confirms this. Ultimately, the selection of an appropriate software solution to fulfil manufacturing requirements, combined with an adjusted integration and operation concept, leads to a more efficient factory operation.

Digital image processing

Digital image processing has become indispensable for PV manufacturers and helps to identify weak points in the production line with regard to required cycle times. Inspecting the contours and shapes of wafers, checking for microscopic cracks in the brittle silicon material, and scanning the printed contacts are just a few of the image-processing methods that can be applied to ensure the automated production of high-quality PV goods. To guarantee the quality of a wafer at a certain point in the production process, the substrate needs to be positioned in the correct orientation for processing, such as for screen printing or edge isolation.

By using direct IR lighting, advanced image processing with an absolute precision of less than 12µm is capable of detecting the exact position of handled wafers. The wafers are placed directly in the field of lens coverage and their positions measured immediately in order to correct travel for the next positioning sequence. Through consideration of two regions of interest in assessing an object's position, the object to be handled can thus be aligned more precisely (e.g. by an accurate alignment tool) to compensate for deviations in position during the handling process. The position aspect has become of more interest ever since cell technology development came up with the idea of back-contacted cells, because that particular process requires higher positioning accuracy.

> "The focus of interest – to drive down the costs per unit – will therefore shift from cell efficiency to yield and throughput."

Outlook

The shake-out has already begun. For a manufacturer to remain competitive, it is essential to make mass production more efficient and thus drive down manufacturing costs. A suitable automation solution that takes handling as well as sensors and related IT structures into consideration is vital in order to meet the demands of future mass production. Each fabrication process has individual boundary conditions and requires a tailored automation solution to meet the conflicting

demands of time, cost and quality.

Time will show whether the main driver for investments in PV cell and module factories will continue to be the improvement of cell efficiency or become instead the improvement of manufacturing efficiency. The focus of interest – to drive down the costs per unit – will thus shift from cell efficiency to yield and throughput. Investments made today in R&D in the field of production and automation will therefore pay off immediately. Lessons learned by other industries can be adapted to the needs of PV and consequently guarantee further success in the future.

References

[1] Cruz Di Palma, R.J. & Scavarda Basaldua, M. 2009, "Production, supply, logistics and distribution", in *Springer Handbook of Automation*, Nof, S.Y., ed. Berlin, Germany: Springer.

[2] Wößner, J. 2012, "Strukturierte Vorgehensweise bei der Planung von Automatisierungslösungen", in: *Entscheidungskompetenz Robotersysteme: Wirtschaftliche Roboterlösungen erfolgreich planen und umsetzen* (Workshop), Verl, A. & Bauernhansl, T., eds. Stuttgart: Fraunhofer-Institut für Produktionstechnik und Automatisierung IPA, pp. 120–153.

[3] Litzenberger, G., ed. 2010, *World Robotics Industrial Robots 2010 – Statistics, Market Analysis, Forecasts and Case Studies*, Frankfurt/Main: International Federation of Robotics / Statistical Department.

[4] Wertz, R. et al. 2011, "Optimized handling of solar substrates in mass manufacturing", *Proc. Intl. Conf. Industr. Eng. Theory, Appl. & Prac.*, Stuttgart, Germany.

About the Authors

Roland Wertz is a group manager at the Fraunhofer Institute of Manufacturing Engineering and Automation (IPA), and responsible for planning and control of productions critical to contamination. He received an M.S. degree in applied cybernetics from the University of Stuttgart. Roland works in the field of factory automation, including equipment automation, material-handling solutions, logistics and data modelling/processing. His field of responsibility includes setting up and leading several industry- and public-funded projects.

Fabian Böttinger holds a diploma in computer engineering and a master's in logistics business engineering. He joined Fraunhofer IPA in 2005 and is currently a project manager for factory planning and optimization in photovoltaics and related industries. Fabian's main expertise is the analysis, modelling and simulation of logistics and automation processes. He also works in the field of factory IT and equipment integration.

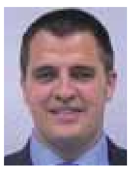

Christian Fischmann joined the Fraunhofer IPA in 2005 after completing his studies in mechanical engineering at the University of Applied Sciences Konstanz. He is a project manager, focusing on the development and evaluation of logistics concepts. Christian also has experience in equipment automation in both the semiconductor and photovoltaic industries.

Tim Giesen graduated in industrial engineering from the University of Applied Sciences Kaiserslautern. After graduation he joined the Fraunhofer IPA, where he works as an international project manager for photovoltaic-related automation. Tim focuses on production engineering, material flow automation and product prototyping in both public-funded and private research projects.

Marcus Michen is a project leader for factory optimization and data analysis, mainly in the photovoltaic and semiconductor industries. After graduating in computer engineering, Marcus joined the Fraunhofer IPA in 2008, where he specializes in validation and verification of production data, as well as modelling and simulation of logistics and automation processes.

Enquiries

Roland Wertz
Fraunhofer Institute for Manufacturing Engineering and Automation (IPA)
Nobelstraße 12
70569 Stuttgart
Germany
Tel: +49 (0) 711 970 1505
Email: wertz@ipa.fraunhofer.de

International technology roadmap for PV: Results 2011

Stephan Raithel, SEMI PV Group, Berlin, Germany

ABSTRACT
What does an industry need for sustainable, long-term success? A market, customers and suppliers, and – most certainly – excellent products that can be sold. When looking at various different mature industries there is one thing they all have in common – they have industry-initiated roadmaps! With SEMI's experience in the semiconductor industry over the last 40 years, the example of the International Technology Roadmap for Semiconductors (ITRS) has proved that pre-competitive industry collaboration among the supply chain and among competitors leads to a reduction in costs, a better time to market and an increased efficiency. Moreover, it helps all players to benefit from jointly solved manufacturing challenges.

Introduction

The photovoltaic (PV) industry is at the stage where it is moving from an 'emerging technology' to a 'mature industry'. Not surprisingly, the call for roadmaps and standardization is getting louder. Working with a group of leading European cell manufacturers, SEMI PV Group facilitated the first edition of the International Technology Roadmap for PV (ITRPV) in 2010, followed by a second edition in 2011 that included wafer and module manufacturers. The acceptance within the community was there from the beginning – certainly with a justified call to go beyond including only European players and to become truly international. The latest edition of ITRPV, published in March 2012 [1], now includes direct input and feedback from PV manufacturers from around the world. The industry is one step closer to having an internationally accepted document that offers technical guidance on production-relevant parameters within the crystalline silicon PV industry. The clear vision is to extend the roadmap along the value chain (including polysilicon and systems) and, of course, to increase the number of international participants within the next few months.

This year's edition gives a status update on the published parameters from the previous year's, but also includes some new, current aspects, such as the market share of quasi-mono-Si vs. mono-Si vs. mc-Si (multicrystalline) products, cost of ownership (CoO) perspectives for different value-chain elements, and wafer-sawing technologies. This paper presents an outline of the newest elements of the current version of the ITRPV. Data preparation is done anonymously by summarizing the input of each participating company. The expected trends up to the year 2020 are shown in graphs, and colour marking is used for some parameters to indicate the maturity of the technology today (see Table 1). All parameters are median values, and answers are given on the basis of data from the latest-generation production line. The topics are split into three areas: materials, processes and products.

Green	An industrial solution exists and is being optimized in production
Yellow	An industrial solution is known but is not yet in mass production
Orange	An interim solution is known but is too expensive or not suitable for production
Red	An industrial solution is not known

Table 1. Colours used in graphs to indicate the maturity of today's technology.

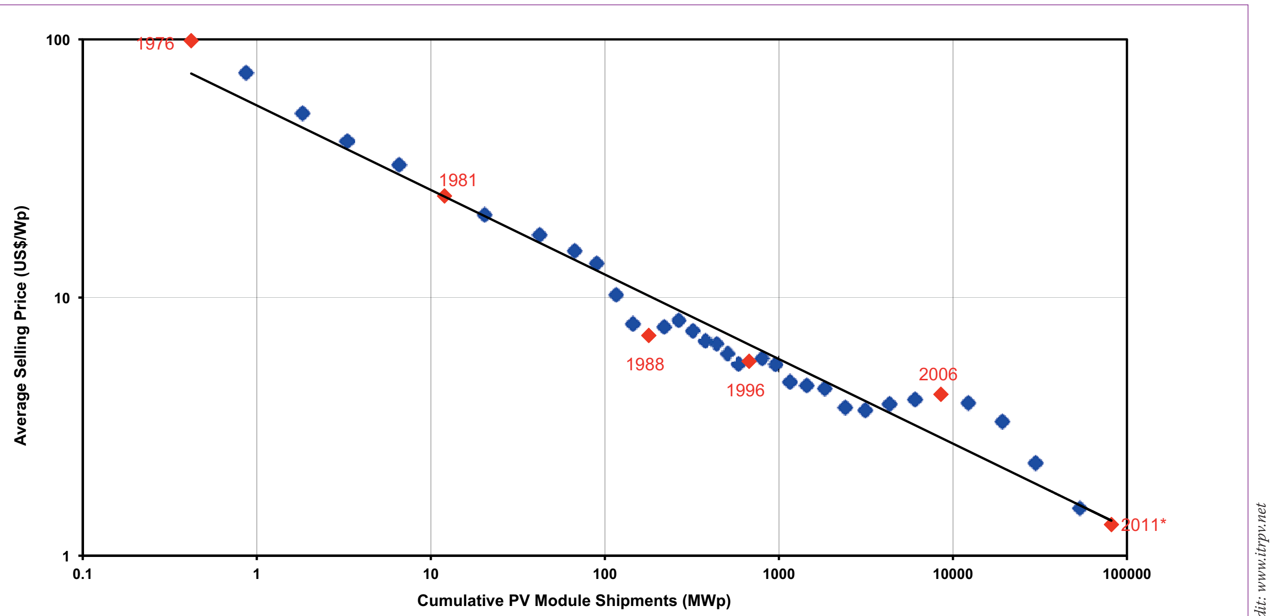

Figure 1. Learning curve showing module prices as a function of cumulative PV module shipments (*estimated value).


Innovative backsheets.
Proven experience.
+25
years
practical
experience

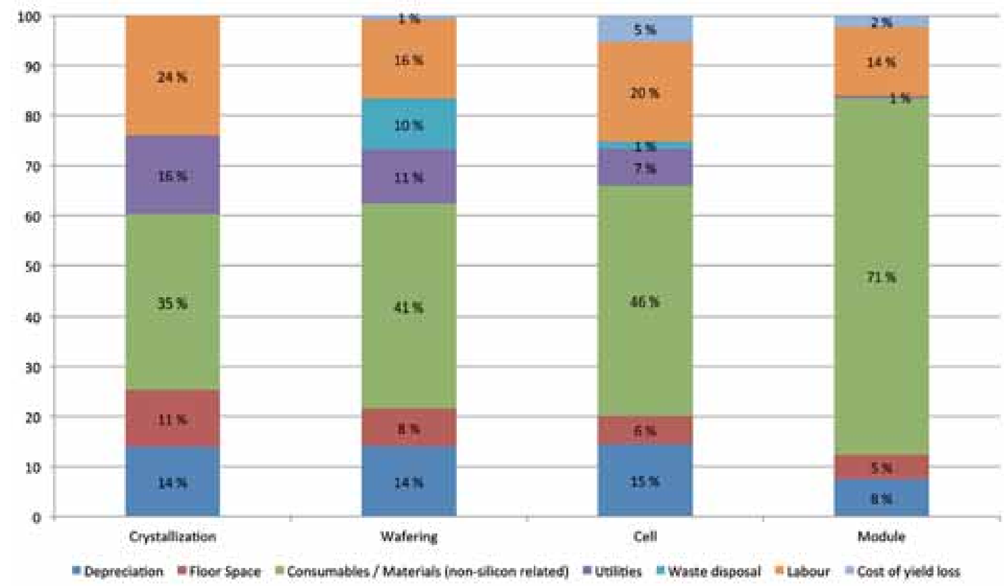

Credit: www.itrpv.net

Figure 2. Relative distribution of cost elements in the different steps of the crystalline silicon PV value chain.

"Only a combination of increased module performance and considerably reduced manufacturing costs will enable the PV industry to reach long-term competitiveness in power generation."

Cost reduction

Cost reduction in the production process has to result in price reductions. The chart in Fig. 1 shows the learning curve for PV modules and displays the average module selling price (in US$/Wp) as a function of modules sold over time (in MWp). When plotted on a log-log scale, the graph becomes approximately linear and reveals that, for every doubling in cumulative PV module shipments, the average selling price decreases by about 20%. Analyses in the last edition of ITRPV in 2011 [1] suggested that improvements in efficiency were important but contributed less significantly to the learning rate than reductions in production costs per piece. Only a combination of increased module performance and considerably reduced manufacturing costs will enable the PV industry to reach long-term competitiveness in power generation.

Cost elements and CoO considerations

In order to reduce costs the main cost factors have to be identified. The companies participating in the ITRPV have been using a standardized CoO calculation model based on the following specifications: SEMI E35 (calculation), E10 (utilization) and E79 (efficiency). The main elements considered are throughput, productivity, depreciation, floor space, materials/consumables, utilities, waste disposal, labour and cost of yield loss. Assuming that throughput and productivity of state-of-the-art machines is very competitive, differentiation for each production step can be identified by an in-depth analysis of the specified main cost elements.

Fig. 2 shows the current situation of the relative distribution of cost elements for crystallization, wafering, and cell and module production according to an analysis of existing production lines among participating companies. Differences are clearly visible between the value-chain elements. In general, critical cost drivers are consumables (wear and spare parts) and materials that are non-silicon related. Expensive wear parts are crucibles (crystallization), and slurry and wire (wafering). Critical materials, for instance, have so far been metallization pastes (cells), and the glass and backsheets (modules). Depreciation (capex) and floor space are cost drivers at all stages of the value chain. Depreciation in cell manufacturing, however, is not considered in our analysis, because of the higher frequency of investments in tool upgrades and line retrofits due to the speed of innovation in cell processing. Utilities (energy plus water) have a high share in crystallization, wafering and cell processing. Yield loss influences the cost in wafering, cell and module manufacturing. Because of recycling in the case of integrated crystallization and wafering lines, the cost of yield loss in wafering is significantly lower than in cell and module manufacturing. The share of labour costs strongly depends on the automation level of the lines considered, but is significant in all steps. This overview highlights that – besides the costs of materials, consumables and

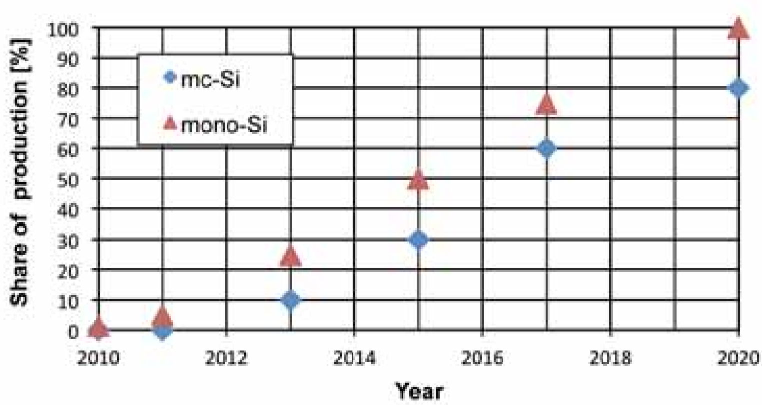

Credit: www.itrpv.net

Figure 3. Share of wafering based on diamond-wire technology vs. wafering based on slurry, for mono- and mc-Si (2010 = 100% slurry-based wafering).

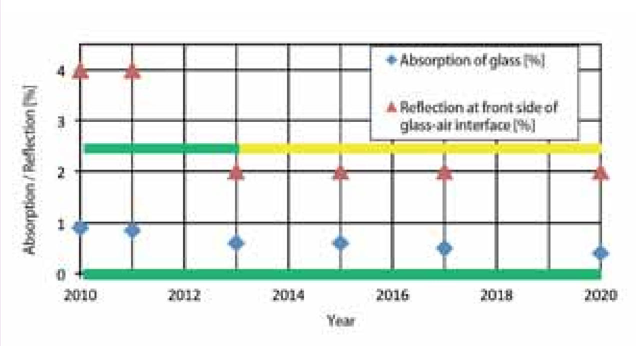

Credit: www.itrpv.net

Figure 4. Requirements for the absorption of glass, as well as for the reflection at the front side of the glass–air interface.

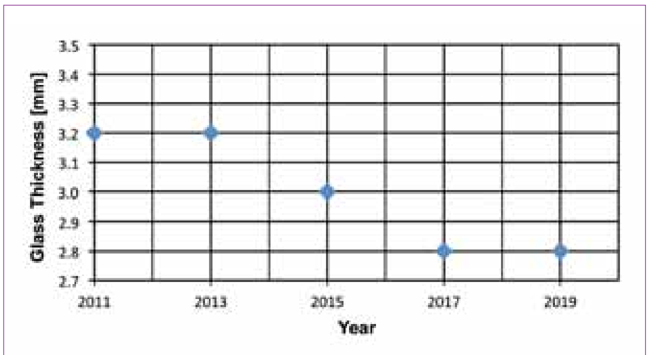

Credit: www.itrpv.net

Figure 5. Trend of the thickness of glass used in module assembly.

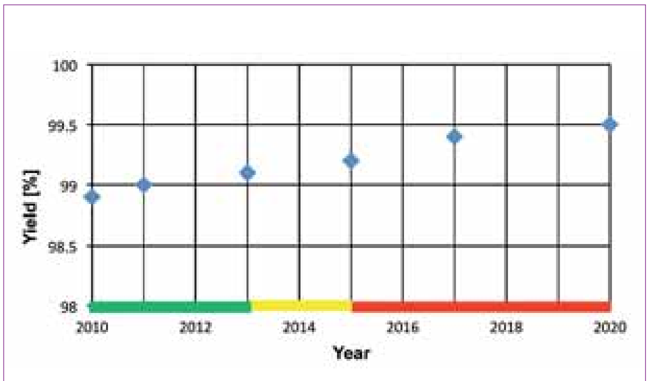

Credit: www.itrpv.net

Figure 6. Trend of expected yield in module manufacturing (the ratio of good cells in good modules out, to good cells in).

utilities – the tool price, layout and user friendliness are important aspects in achieving further cost reductions along the PV value chain.

Crystallization and wafering

Continuous progress in standard poly production and in the development of alternative technologies is needed to enable further cost reduction without sacrificing silicon quality, as described in the SEMI Standards SEMI PV 17-0611 and SEMI PV 22-1011.

> "A significant improvement in cost reduction in the wafering process is expected by the introduction of diamond-wire sawing."

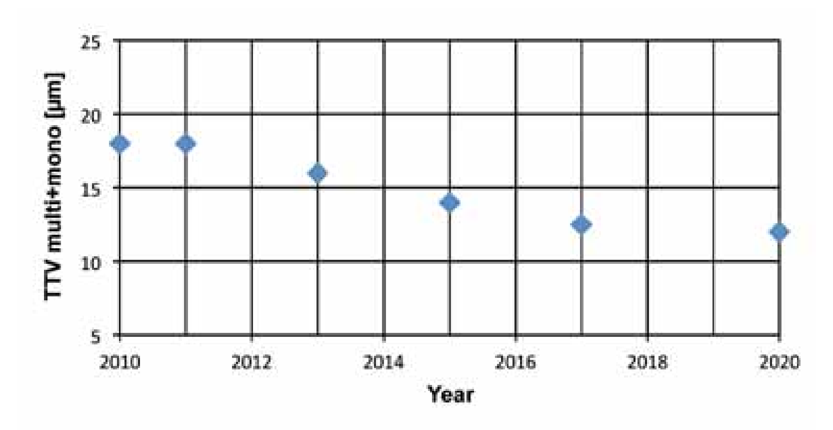

Credit: www.itrpv.net

Figure 7. Expected trend of wafer total thickness variation (TTV).

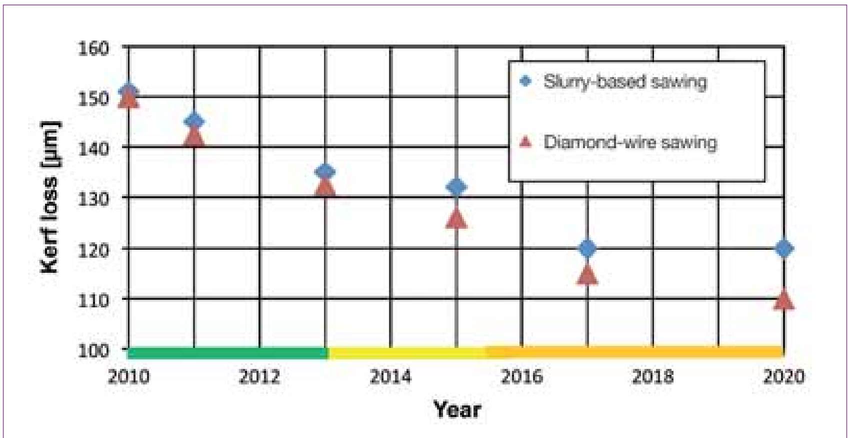

Credit: www.itrpv.net

Figure 8. Kerf-loss reduction trend.

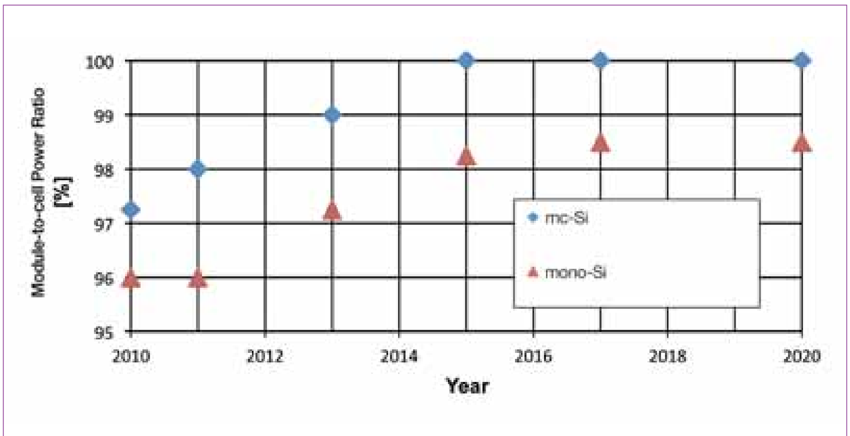

Credit: www.itrpv.net

Figure 9. Expected trend of the module-to-cell power ratio.

Further adjustment opportunities for cost reduction in crystallization and wafering are in the area of consumables, such as crucibles, graphite parts, slurry and sawing wires. It is assumed that prices will approach cost with these goods as well, and a price reduction of about 7% per year is possible. A significant improvement in cost reduction in the wafering process is expected by the introduction of diamond-wire sawing; Fig. 3 shows the projected share of this type of sawing in volume production. The roll-out of this technology requires synchronization with cell process development.

Module materials

By looking at the module cost structure shown in the analysis of the different cost elements, it can be seen that consumables and materials are the main components which need performance improvements and price reductions. The reflectivity at the front side of the glass–air interface will be reduced from typically 4% to 2% by introducing anti-reflection glass into the mainstream from 2013 onwards. The absorption of glass and encapsulant needs to be reduced in order to minimize the cell-to-module power loss. This is especially necessary for blue light, because of the improved spectral response of solar cells in that region of the spectrum.

The reduction of the glass thickness is considered to be a potential cost reduction, as shown in Fig. 5. Thermal hardening of the glass seems to be a possible way of achieving the required temperature stability and stiffness for thicknesses down to 2.8mm. Only non-hardened or chemically hardened glass can be used at thicknesses below 2.8mm. Chemical hardening has to be performed in tanks with liquid molten salt, so thicknesses below 2.8mm are considered to be too difficult and too expensive to produce for larger formats like those used in modules. Even for thicknesses below 3mm, cells have to be very thin (< 80µm) in order to be flexible enough to follow the bending without breakage, otherwise stabilization elements or new back-cover materials that can carry the required mechanical load have to be introduced. Glass thickness reduction will therefore be challenging. Glass and backsheet foils have been identified as being an important cost driver in module building. Besides glass and backsheet foils, the other consumables are frames, encapsulants, interconnections and junction boxes, which have approximately equal contributions in the distribution of costs. All materials should therefore contribute equally to the ongoing reduction in module manufacturing costs.

Copper is expected to remain the chief interconnection material in the coming years. The junction box is the electrical interface of the module, and the material used for mounting it to the back side of the module is still expected to be silicone. Starting in 2015, it is anticipated that the actual internal electrical interconnections will change from being soldered/clamped to being welded. All materials used in the module contribute to the reliability of the PV installation. Reliability considerations will become important in developing new standards and guidelines and may be considered in future ITRPV issues as well.

Process – manufacturing

The trend of expected yield in module manufacturing is shown in Fig. 6. Continuous improvements are implied, despite ongoing reductions in wafer thickness and implementations of new wafer-sawing technologies. In order to process cells of thicknesses less than 150µm with greater than 99.3% yield from 2015 onwards, a dramatically improved interconnection technology is needed, in addition to stress-relieving supporting structures. By 2015 at the latest, lead-free soldering must be implemented into mass production at the same time as the introduction of lead-free cell metallization technologies.

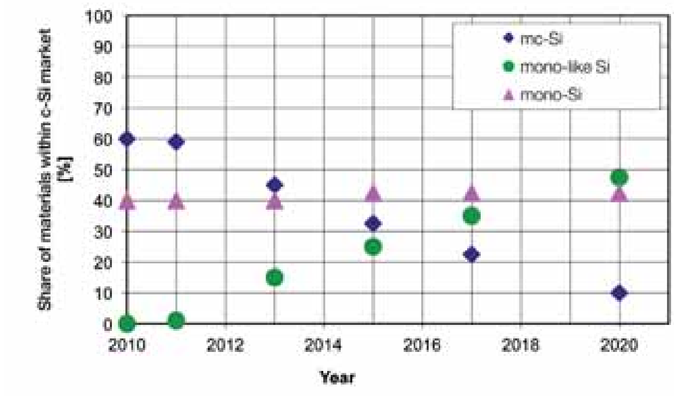

Credit: www.itrpv.net

Figure 10. Expected market share of mc-Si, mono-like Si and mono-Si materials.

Process – technology

Besides production parameters, cell efficiency is also expected to improve; the process parameters that are necessary for achieving this improvement will be discussed next. One essential requirement for thinner solar cells, reflecting the needs from a cell-production point of view, is the reduction of total thickness variation (TTV): the TTV of wafers should not exceed 10% of the wafer thickness without any additional cost (see Fig. 7).

Another challenging parameter is kerf loss. Along with wafer-thickness reduction, kerf loss must also be decreased accordingly, to achieve a significant reduction in silicon consumption.

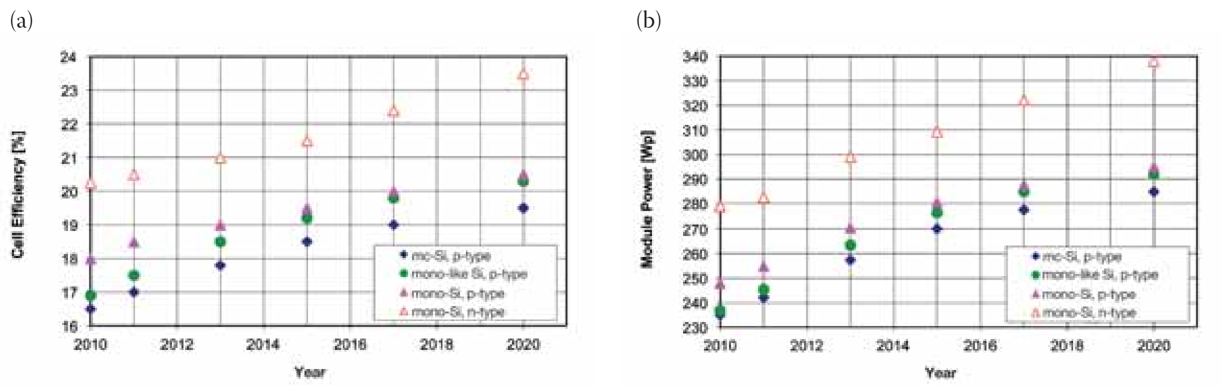

Credit: www.itrpv.net

Figure 11. (a) Stabilized cell-efficiency trend curve. (b) Module-power trend curve.

Additional reductions are expected by the introduction of diamond-wire sawing processes (Fig. 8).

It is crucial to get as much power out of the assembled solar cells as possible. A good parameter expressing this achievement is the module-to-cell power ratio, defined as: module power/(cell power × number of cells). As shown in Fig. 9, for 2011 this ratio was around 98% for multicrystalline silicon cell technology and about 96% for monocrystalline silicon cell technology. In 2013 the power ratio will show an improvement of +1% absolute as a result of the introduction of anti-reflective glass. The launch of new interconnection and encapsulation technologies (for thinner wafers, back-contacted cells, etc.) from 2015 onwards will result in a second improvement step of about +1.0% absolute.

Products

Mono-like silicon material is an emerging new technology that utilizes mc-Si crystallization equipment to grow silicon ingots which have larger volume fractions than mc-Si but with monocrystalline properties. As this material is well suited for high-efficiency cells, an increasing market share for mono-like silicon material is expected within the coming years, as shown in Fig. 10. The market share of n-type mono-Si wafers is expected to increase over the next few years, starting at around 10% in 2012 and increasing to 50% in 2020. The roadmap predicts a much lower market share for n-type mc-Si wafers.

Over the next few years, the efficiency of p-type silicon solar cells will continue to improve. Fig. 11(a) shows the expected trend of average stabilized efficiencies for mc-Si, mono-like Si and mono-Si solar cells with double-sided contacts, manufactured in state-of-the-art mass production lines. Because of the improved material quality of mono-like silicon, the difference between p-type mono-Si and mono-like material is likely to decrease in the coming years. Moreover, n-type mono-Si will show significantly higher efficiencies.

"The market share of n-type mono-Si wafers is expected to increase over the next few years, starting at around 10% in 2012 and increasing to 50% in 2020."

The chart in Fig. 11(b) illustrates the corresponding development of module power, taking into account that, starting in 2013, there will be a transition in mono-Si wafers from a semi-square to a full-square format. Cell-to-module power losses were assumed on the basis of the values mentioned in the full edition of the latest roadmap [1] for the different material types. For mono-like silicon, the same module-to-cell power ratio as for mono-silicon was used.

Conclusion

The data shown here (extracted from the latest ITRPV edition) was collected in 2011 from leading international PV manufacturers along the c-Si value chain. A yearly update of this information is planned, and the next edition of the ITRPV, based on data collected in 2012, will be published in March 2013. Topics such as wafer thickness require cooperation between tool suppliers, cell manufacturers and other players along the value chain. The current issue of this document, as well as information about how to get involved in the roadmap activities, can be downloaded from the ITRPV website [1].

Reference

[1] International Technology Roadmap for PV (ITRPV), March 2012 [details available online at http://www.itrpv.net].

About the Author

Stephan Raithel is currently the director of PV Europe within SEMI PV Group, and the key SEMI spokesperson for the PV community in Europe. One of his main functions is the facilitation of the International Technology Roadmap for PV, ensuring the data collection and data protection, antitrust environment, and recruitment of new participants. Stephan is concurrently the managing director of the Berlin branch office of SEMI.

Enquiries

Stephan Raithel
Director PV Europe, SEMI PV Group
Helmholtzstrasse 2–9
House D / 3rd Floor
D-10587 Berlin
Germany

Email: sraithel@semi.org

Materials

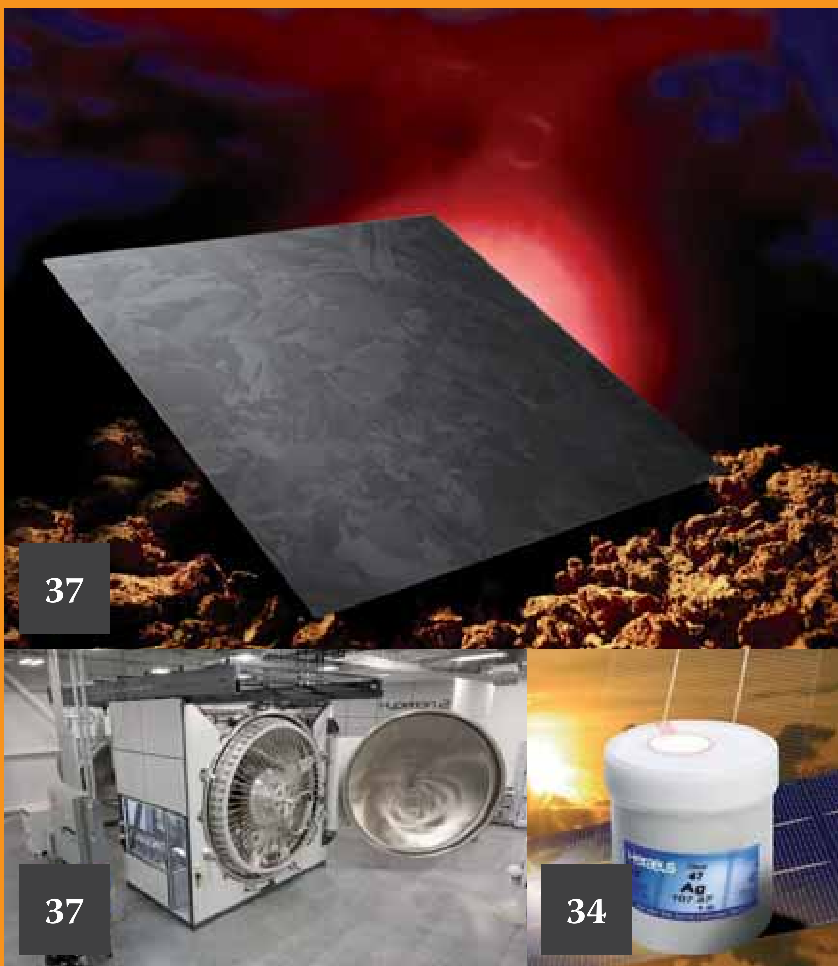

Sales plummet at LDK Solar as losses soar

Delayed fourth quarter and full-year 2011 results at LDK Solar have shown the full extent of the challenges facing the integrated PV manufacturer. Losses from operations for the fourth quarter of fiscal 2011 were US$531.4 million on the back of heavy write-downs across the company, leading to a net loss of US$588.7 million. Revenue reached US$2.15 billion in 2011, compared to US$2.5 billion in 2010.

LDK Solar reported net sales in the fourth quarter of US$420.2 million, compared to US$471.9 million for the third quarter of fiscal 2011 and US$920.9 million for the fourth quarter of fiscal 2010. In previously revised guidance the company had expected sales to be in the range of US$440 to US$450 million.

Having already revised downwards its fourth-quarter figures, the company missed revenue guidance and guided first-quarter revenue to levels not seen since the second quarter of 2009.

LDK Solar's TCS plant. Metallurgical silicon is used as a raw material to produce TCS, which is then used to produce polysilicon.

Business News Focus

Weak demand for specialist PV materials hits Ferro's earnings

Poor demand for silver paste, primarily used in solar cell production, was highlighted by Ferro management as a key reason for lower quarterly earnings at Ferro Corporation. The company reported net sales of US$466 million for the three-month period ended March 31, 2012, compared with net sales of US$573 million in the first quarter of 2011.

Ferro reported gross profit for the quarter of US$88 million, down from US$120 million, during the first quarter of 2011. The company said that sales of electronic materials products were expected to be lower in 2012 compared with 2011, noting that it had limited visibility regarding the strength and timing of a recovery in demand for solar pastes. Ferro also noted that it was unsure of the pace of adoption by customers of its range of new solar paste products launched last year.

Hemlock Semiconductor bemoans polysilicon overcapacity in 2012

Declining prices – be they on the spot market or long-term supply agreements – are making business conditions very tough for polysilicon producers, regardless of their market size or purity of the material they produce. According to the latest financial results from Dow Corning, its JV subsidiary Hemlock Semiconductor expects overcapacity in the sector to continue throughout 2012.

As a result, the company said that Hemlock was aggressively seeking further cost reductions and yield improvements to better manage pricing pressures, which are therefore most likely to continue, despite spot market prices already being below US$30/kg and heading towards US$20/kg. Only the largest producers have manufacturing costs below the US$20/kg mark.

Source: blog.mlive.com

Hemlock Semiconductor expects overcapacity in the sector to continue throughout 2012.

Source: Heraeus

Heraeus will develop next-generation silver metallization pastes for use in Yingli's 'PANDA' cells.

STR Holdings cuts solar material prices to maintain market share

A key supplier of PV module encapsulant materials to the likes of First Solar, STR Holdings said that a 14.3% decline in average selling prices (ASP) q-on-q was due to the need to maintain its market share with key customers. Falling module prices due to overcapacity is continuing to put pressure on the entire PV supply chain to lower prices.

The company reported a net loss from continuing operations in the quarter of US$82.1 million, compared to a net loss of US$68.5 million for the previous quarter. Gross profit for the first quarter was US$2.0 million, or 6.4% of sales, compared to US$4.2 million, or 11.6% of sales, from the previous sequential quarter.

Heraeus teams with Yingli Green on 'PANDA' cell silver metallization pastes

A one-year, US$70 million R&D and supply project is underway between materials supplier Heraeus and Yingli Green. Resources are being allocated from Heraeus's three global technology centres to develop next-generation silver metallization pastes for Yingli's N-type 'PANDA' silicon solar cells.

The new collaboration comes on the back of other deals done with DuPont this year to both improve cell efficiencies and reduce the cost-per-watt. Silver is the second largest cost contributor in cell production, after polysilicon.

Development work will take place at Heraeus's US, German and Singapore-based technology centres.

RENA acquires water treatment specialist to expand outside solar sector

Water treatment specialist Stulz H + E has been acquired by RENA for an undisclosed

Source: Stulz H + E

Water treatment specialist Stulz H + E has been acquired by RENA for an undisclosed sum.

sum. The company said that the German Federal Cartel Office had approved the transaction, which is expected to be completed in the second half of 2012.

RENA noted that the acquisition was intended to provide a "second strategic pillar" to its wet chemical processing technology used in the PV industry. Stulz H + E had revenue of €250 million last year, while RENA reported sales of €400 million.

SINTEF and ECN renew long-standing contract

SINTEF Materials & Chemistry ECN have renewed their agreement to strengthen their long-standing collaboration in the field of crystalline silicon photovoltaics. With this agreement, SINTEF and ECN will combine the operation of pilot infrastructure for silicon feedstock production, crystallization, wafering and solar cell manufacturing. It is hoped that this collaboration will increase the effectiveness of their R&D efforts.

Torstein Haarberg, vice president SINTEF Materials & Chemistry said, "We are very enthusiastic to team up with ECN in the PV field, where ECN is recognized as an internationally leading research institute in the field of solar cells and PV modules."

Dunmore supplying Advanced Solar Photonics with backsheet material

US-based crystalline silicon PV module manufacturer Advanced Solar Photonics (ASP) has selected backsheet material from Dunmore for its 100MW facility. The backsheet material will be used on ASP's high-performance modules which are expected to be used several utility-scale PV power plant projects in the US this year.

Source: Advanced Solar Photonics

The ASP manufacturing plant is a state-of-the-art facility located near Orlando, Florida.

Other News

Arkema, CEA set up two joint research labs for micro- and organic electronics in France

Arkema and CEA have announced their development of a collaboration to go outside of the PV field and into the

Source: Arkema

Arkema and CEA expand partnership into micro- and organic electronic market.

microelectronics and organic electronics sectors with the creation of two joint research laboratories. The CEA-Leti and CEA-Liten labs aim to develop new high-performance materials and manufacturing processes for France's electronics market.

The labs will tap into Arkema's design and production of high performance polymers and polymer nanostructuring, combined with CEA researchers' background with the design and processes for the development of electronic components. The aim of the labs is to reach an ultimate goal of producing new materials that will better the performances of silicon components and reduce their manufacturing costs in next generation integrated circuits.

MEMC issues statement regarding rumours of CEO Chatila's departure

MEMC Electronic Materials, parent company of SunEdison, has issued a formal statement in regards to what is deems misinformation regarding its CEO, Ahmad Chatila, and the company's restructuring. "We have been made aware of rumors relating to the company which may be causing concern," said John Marren, chairman of the MEMC board of directors, "and we wish to make it absolutely clear that Ahmad Chatila remains our CEO."

Meyer Burger raises US$121.3 million in long-term capital

Meyer Burger Technology advised that it has raised US$121.3 (CHF110 million) in long-term capital through a Swiss Franc-dominated straight bond issuance. The bond holds a coupon of 5% payable annually and maturity date of May 24, 2017. Zürcher Kantonalbank, Credit Suisse and UBS Investment Bank collectively offered the bond issue to institutional and private investors.

The company noted that proceeds from the bond will primarily be used to finance its research and development with partial funds used for investments that support its integration of Roth & Rau, the focus on one location from different sites in Thun and for general corporate purposes.

Trident Solar offers new warranty on inkjet print head technology

Trident Solar has introduced a new one-year warranty program on its '256Jet-S' inkjet technology, claiming longevity 25 times greater than alternative inkjet print heads and over 100 times greater than lithographic screen technology. The company claims that the longevity of its technology is due to its inherent design, which was specifically designed for production applications for solar cell volume production applications, having a repairable and inert stainless steel construction. The warranty relates to jetting of acid or alkaline solutions, as well as other chemistries.

ThomasNet

Trident Solar has introduced a new one-year warranty program on its '256Jet-S' inkjet technology.

REC awarded Top Brand PV approval from EuPD Research

EuPD Research recently awarded REC with its Top Brand PV seal of approval for the sales markets in Germany, France and Italy. The award is based on independent surveys of installers and end customers conducted by EuPD. Through the surveys, it was concluded by the research company that REC had the best performance in Germany, where it scored the best ranking as a European, non-German brand.

The seal of approval is granted to a company after a multilevel analysis from statements made by market liaisons and end customers. According to EuPD, the research allows for manufacturers to receive straight-from-the-source assessments of their brand and feedback on how to improve their brand management.

Source: Solar Media Ltd.

REC had the best performance in Germany, where it scored the best ranking as a European, non-German brand.

Product Reviews

Arnold Gruppe

Pilot production system at Arnold Gruppe offers demo and selection of systems

Product Outline: Arnold Gruppe is demonstrating the automated brick glueing process in their technology centre in Weilburg, Germany, with a specially installed pilot production system for customized glueing process development. The company is offering a complete product line of automated silicon brick glueing systems based on an industrial robot system with high accuracy as well as a highly precise adhesive dosing system for reproducible adhesive beads.

Problem: Precise glueing of silicon bricks onto wire-saw beams is of high significance for wafer production. Only a constantly reproducible and durable adhesive bonded joint guarantees a high cutting yield in the later wafer cutting process.

Solution: About 90% of all glueing processes are still done manually in the photovoltaic industry and hence are very dependent on the skills of the individual worker. With an automated process the consumption of glueing material can be typically reduced by approximately 50% compared to the manual process. The Arnold Easy Programming System glueing process is claimed to reduce the breakage rate during wafering in the later wire sawing process by at least 2% and is said to considerably reduce production costs.

Applications: Silicon brick glueing process.

Platform: Depending on the complexity and customer requirements, the basic system is completed with an automated cleaning unit, a brick commissioning storage for optimization of wire saw utilization and a storage unit for resting glued bricks during curing. The system also allows the automation of the joining process of bricks with glass plate and wire saw beam.

Availability: Currently available.

BT Imaging

The iLS-W2 from BT Imaging offers quasi-mono wafer grading

Product Outline: BT Imaging has launched the next-generation iLS-W2 for photoluminescence (PL) inspection of wafer quality; the all-new iS-G1 for inline cast mono grain inspection; a new automation unit, the iQ, that houses the iLS-W2 and/or iS-G1 so that existing production lines can be upgraded; and the QS-W2, a fully integrated inspection tool that can automatically sort wafers. With this suite of tools, wafer makers and fully integrated PV manufacturers can inspect every wafer in production and understand its electrical performance before they make it into a cell.

Problem: The main benefit of the mono-like wafer is that an alkaline texture process can be used which increases the cell efficiency by about 0.5% absolute. Thus, the current industry practice is to manually sort wafers based on the fraction of mono-crystalline area in a wafer.

Solution: Even though the Grade A wafers look optically perfect, there is often a wide efficiency spread due to defects like dislocations that go undetected by standard optical inspection technologies. BT Imaging claims that with its tools, manufacturers can efficiently grade cast mono wafers. The iS-G1 is an optical inspection module, which grades wafers based on mono area fraction. The iLS-W2 is a PL module, which grades mono-like wafers based on dislocation count. The iLS-W2 offers on-the-fly inspection at 3,600 wafers per hour – a 2× increase over the iLS-W1.

Applications: The iLS-W2 inspects and grades the electrical quality of silicon PV wafers at full wafer line speeds using PL imaging and integrated image processing algorithms.

Platform: Existing production lines can easily integrate the iLS-W2 with any wafer inspection system.

Availability: Shipping from July 2012.

GCL-Poly

GCL-Poly offers high efficiency multicrystalline wafer

Product Outline: GCL-Poly has successfully developed a high efficiency multicrystalline wafer, 'GCL Multi-Wafer S1+,' which is said to have achieved customer feedback after trial runs of average conversion efficiencies of 17.6%, with an increase of 0.5–0.7% when compared with its current benchmark wafers.

Problem: Improvements in quality and purity of bare silicon wafers has a direct impact on cell/module efficiencies. Although monocrystalline wafers offer such improvements over multicrystalline wafers, extra cost of production limits adoption. Higher quality multicrystalline wafers at close to current production costs are required to boost conversion efficiencies and lower the cost per watt.

Solution: The new wafer is made from electronic grade polysilicon materials produced by GCL-Poly under the most stringent quality control in the industry and was based on innovative developments from the theory of silicon material and a new design of thermal field coupled with precise process development. The GCL Multi-Wafer S1+ has improved microstructure and precisely controlled crystal defects such as dislocations, stacking faults and grain boundaries. As a result, the wafer has the characteristics of a low concentration of carbon, oxygen and metal impurity and also high minority carrier lifetime as well as uniform doping profile.

Applications: High efficiency multicrystalline wafer (156 × 156mm)

Platform: GCL-Poly expects that the output of the GCL Multi-Wafer modules (60 units, 156 × 156mm) and GCL Quasi-Mono Wafer modules (60 units, 156 × 156mm) will reach 270W and 285W respectively.

Availability: March 2012 onwards.

Product Reviews

SCHMID

SCHMID's Metrology Sorter with Analyzer Software for wafer inspection

Product Outline: Designed for diamond wire cut and slurry cut monocrystalline, quasimono and multicrystalline wafers, SCHMID's Metrology Sorter with Analyzer Software option provides critical wafer process inspection. SCHMID's analyzer software compiles the measurement data of the finished wafers in a three-dimensional brick, which establishes the basic information for the specific intervention in the upstream production steps.

Problem: A key factor in the long process of crystallization and cutting of solar wafers is the prompt recognition of the effects on the wafer quality, especially to identify the origin of different defects.

Solution: The Metrology Sorter System is a user-friendly final inspection system with a three-dimensional brick display of the surface roughness distribution on a wafer. The distribution on all the wafers in the entire brick allows important conclusions to be drawn about the cutting parameters. The optical preparation of a multitude of measurement data is therefore always clearly arranged and the software operation proves to be intuitive. From the measurement results, the four parameters – thickness, TTV, roughness and waviness – are calculated and visually displayed. No mechanical back-fitting is necessary when switching between wafer types.

Applications: Designed for diamond wire cut and slurry cut wafers as well as for monocrystalline, quasimono and multicrystalline wafers.

Platform: The Metrology Sorter is the on-the-fly inspection in the SCHMID Wafer Backend, which also includes upstream machines like Precleaning + Degluing, Singulation and Horizontal Wafer Cleaning and the necessary handling machines and covers all processes after the cutting with SCHMID's own equipment.

Availability: Currently available.

Twin Creeks Technologies

Twin Creeks Technologies offers Hyperion 3 for ultra-thin wafer production

Product Outline: Twin Creeks Technologies has launched its first commercial tool Hyperion 3, which is a commercial wafer production system that is claimed to dramatically reduce the cost of solar modules and semiconductor devices by reducing the amount of silicon and other substrate materials used by up to 90%.

Problem: The thickness of wafers is based on wafer slicing capabilities and the handling requirements for device processing. In reality, only the very top layer of a substrate plays an active role in generating energy or transmitting signals. Replacing conventional wafering technologies has the potential to lower costs and provide ultra-thin substrates that can be employed in more flexible packages and applications, while reducing wafer breakage.

Solution: Hyperion 3 uses a process called Proton Induced Exfoliation (PIE) generating monocrystalline wafers claimed to be less than 1/10th the thickness of conventional wafers. Hyperion embeds a uniform layer of high-energy protons into monocrystalline wafers to a depth of up to 20 microns. When heated, this new layer expands, cleaving the top surface from the donor wafer to form an ultra-thin wafer that is otherwise identical to the original. Twin Creeks estimates that Hyperion will permit manufacturers to produce solar cells for under US$0.40/W in commercial-scale volume production.

Applications: Hyperion is compatible with a wide variety of monocrystalline wafers.

Platform: A single Hyperion 3 system is claimed to process over 1.5 million thin wafers per year, enough for more than 6MW worth of solar cells.

Availability: March 2012 onwards.

Market dynamics of materials supply for PV in China

Mark Thirsk, Linx Consulting LLC, Mendon, Massachusetts, USA

ABSTRACT

China has become the largest manufacturing base for crystalline silicon modules in the world, and is becoming increasingly reliant on a domestic supply base. This article discusses the emergence of local supply chains and the strategic responses of global suppliers to this domestic competition. It proceeds to review a set of conclusions from four case studies of formulated material supply within China that can apply to supply-chain participants in the PV industry, concluding with some strategic considerations for suppliers on the cusp of entering the Chinese market.

Introduction

In the last three years, China has quickly established itself as the major manufacturing site in the world for PV cells and modules. In 2011, supply from China accounted for more than 65% of the global PV demand, and total capacity installed in China came close to equalling global demand. While established manufacturing capacity in China historically relied on imported materials for support, the expansion of the manufacturing base led to purchase suppliers seeking domestic supply of high volumes of chemicals and materials that were used in cell and module manufacturing.

A domestic supply base existed in China for many chemicals and commodity materials, and these companies rapidly took advantage of the growing demand for the products in the PV industry. Materials such as inorganic acids, solvents, alkalis, silicon carbide grit and other non-formulated materials were quickly sourced from domestic supply in China. By 2007, most single-component, pure materials were sourced from domestic chemical suppliers.

Complementary to these pure chemicals – and critical to the long life of a finished module and the high efficiency of the cells – are formulated materials that must be produced with tight quality controls and product-specific compositions. Materials such as metallization pastes, encapsulant polymers and backsheets are all highly predictive of module performance and lifetime, and are specified to the appropriate level of functionality required by the module design, without incurring extra cost. The suppliers of these products have typically been Japanese, European or North American, and have enjoyed high market share because of the know-how required to produce these materials.

Over the last two to three years, domestic Chinese suppliers have developed the competencies and supply chains required to best service the domestic module supply base with formulated materials. These challenge imported materials in functionality, and can offer price advantages to the end-users. This shift has meant significant changes in strategy for global suppliers operating in the Chinese market.

In general, the manufacturing technology for crystalline silicon PV modules is little changed from that used several decades ago for the first modules. As the global PV industry has ramped up in the last decade, standardization of manufacturing equipment and module testing has led to a market largely supplied with modules with minimal differences in process and functional design. New technologies and materials competing to displace incumbent processes face a stringent selection process, and, prior to their being widely adopted, the lifetime testing process. Thus, manufacturing change occurs relatively slowly. Relentless pressure to reduce prices means that new materials and processes have to bring significant savings in manufacturing cost in order for them to be adopted.

In the last 18 months, the PV industry has continued its dramatic growth in terms of installed generating capacity coupled with similarly dramatic reductions in module cost and market price. Cost reductions have been underpinned by the slide in price of the main raw material, polysilicon, which was responsible for up to a third of a module's total cost at the end of 2010. In 2012, we are seeing that the average polysilicon price is below the cash cost of many small-volume manufacturers, and is challenging large manufacturers such as OCI, Hemlock, Wacker and GCL to further reduce their manufacturing costs while maintaining product quality.

As polysilicon prices come ever closer to manufacturing costs, price reduction pressure moves to other key materials in the module manufacturing chain. Some of this pressure is also taken on by manufacturing efficiencies and support supply-chain optimization in the tier 1 manufacturing environment.

Figure 1. Hemlock Semiconductor is among the large polysilicon manufacturers that have had to reduce manufacturing costs in order to remain competitive.

Many of the products in the bill of materials for cell and module manufacturers are commodities on global markets. A characteristic of a commodity is that the price is to some extent dependent on market supply and demand conditions, and price elasticity with increased demand is relatively weak. As the PV industry makes up a small part of the total global demand of these commodity materials, it is quite difficult to envisage the added demand for PV production yielding further cost reductions in these materials. Examples of commodity materials whose price is very independent of PV demand include silver bullion, glass, oil derivatives and energy.

We will now provide a review of the conclusions from four case studies of formulated material supply within China that can apply to supply-chain participants in the PV industry.

Chemical and material market segmentation

At a high level, materials required for crystalline silicon cell and module manufacture can be separated into pure


Moscone Center,
North Hall, Booth 5713
inter solar
connecting solar business
NORTH AMERICA

Pure chemicals	Formulated chemicals and materials, and specialty materials
Poly	Polysilicon
SiC	Specialty texturization mixes
Wet chemicals (HF, KOH, ethylene glycol, Nitric acid, etc.)	Specialty cleaning mixes
$POCL_3$	Metal pastes (Ag and Al based)
Process gases (silane, nitrogen, ammonia, etc.)	Silicon inks and dopant pastes
Encapsulants	Backsheets

Table 1. Pure chemicals and formulated chemicals, materials and specialty materials required for crystalline silicon cell and module manufacture.

chemicals, and formulated chemicals and materials; most of the key PV-relevant materials can fall into these two segments, as illustrated in Table 1.

Case studies

Polysilicon

Polysilicon is a key raw material for crystalline silicon modules. Generally sold either as chunks produced from a modified Siemens CVD process or as granules from a fluidized bed reactor, the supply of polysilicon is concentrated in the hands of a few of large producers. However, on a global scale, there are upwards of 50 smaller producers capable of manufacturing between tens and thousands of tons of polysilicon per year. In 2011, polycrystalline prices crashed, driven partly by significant overcapacity in the industry and partly because of strong competition among leading suppliers to supply the available market. Reductions in the selling price of polysilicon translated into significant price reductions of finished modules, which have maintained end-market demand even as government subsidies have declined or are withdrawn completely.

In China, approximately 40 suppliers have been established in the polysilicon space. A select few, such as LDK and Yingli, are captive, but most offer polysilicon on the merchant market. The largest, GCL Polysilicon, has focused on only selling wafers that for the most part are manufactured with internally produced polysilicon.

"In China, approximately 40 suppliers have been established in the polysilicon space."

In the latest five-year plan for renewable energy, published in 2012, the National Development and Reform Commission (NDRC) has made it clear that, while it expects an increase in domestic capacity to approximately 50,000 metric tons this year, it will also concentrate its support on the top 20 suppliers, leaving others to fend for themselves. The imbalance between domestic supply and demand has led to volatility in polysilicon imports, and suppliers from Korea and the USA have been able to meet the added demand from their expanded capacities as this domestic supply is ramping up.

The high value and relative ease of transport of polysilicon means that local supply does not always carry an advantage. Additionally, a stable high-quality production plant may take many quarters to ramp up production, and require a highly trained staff to run the capital-intensive equipment. Such suppliers seek long-term supply contracts with their customers that include an element of price indexing to ensure plant loading and consequent high-quality production. Once a wafer maker has selected a polysilicon supplier, change will only be made on the basis of price and supply capability for equivalent quality.

Sawing wire

Wafer production is dominated by the use of multiple wire slurry sawing (MWSS), which uses brass-plated steel wire and silicon carbide abrasive. Wafer sawing requires between 50,000 and 150,000km of wire per megawatt of wafers produced, depending on saw loading and desired wafer quality. The wire used for wafer sawing must be of exceptional quality, with no defects that could cause breakage during a cut. Suppliers of sawing wire have historically been based in Europe, Japan and the USA; however, in the last few years, competitive Chinese suppliers of sawing wire have emerged.

Cost-reduction efforts also favour migration to diamond wire cutting, which eliminates the need for slurry and slurry recycling. In addition to new steel wire suppliers, multiple diamond wire suppliers are beginning to compete for business in this emerging application.

In the case of MWSS and diamond wire, the basis of competition is primarily that of technical performance, with yield and sawing performance driving supplier selection. Chinese suppliers have been able to develop high-quality sources of steel and wire-drawing processes capable of matching those of leading global suppliers. As a result, these Chinese suppliers are gaining market share in competition with foreign suppliers.

Metallization pastes

Metallization pastes are considered to be among the most complex materials used in the manufacture of solar cells. The silver pastes used in forming front grids and busbars are the most difficult to produce, with the rear-side silver pastes somewhat easier. Back-surface field aluminium pastes are usually considered the least technically challenging to manufacture within this group.

The supply of front-side silver pastes continues to be quite a niche market and is concentrated among a small number of suppliers who have significant experience and know-how in formulating pastes for low contact resistance, high conductivity, reliability and consistent supply. In contrast, aluminium pastes are somewhat easier to formulate and have fewer performance requirements.

In the early days of PV production, Chinese paste suppliers attempted to

Figure 2. DuPont's Solamet thick-film metallization paste is among the materials imported by Chinese PV manufacturers.

formulate full lines of metallization pastes. However, early silver formulations were variable, and customers saw yield problems, leading to their favouring the import of silver pastes from foreign suppliers such as DuPont, Ferro and Heraeus.

Domestic aluminium paste manufacture, however, has continued to go from strength to strength in China. In fact, foreign suppliers such as Ferro have built and are operating aluminium paste manufacturing facilities in China to compete with domestic suppliers such as GRTC.

As GRTC has grown, it has devoted resources to R&D, and has recently introduced silver pastes for front- and back-side metallization. Moreover, although not strictly a mainland Chinese company, Gigasolar of Taiwan has also joined the fray to compete with a silver paste range of its own. The entry of these two domestic competitors is a significant change in the last preserve of technically differentiated materials.

Challenges	Pure chemicals	Formulated chemicals
Unique segment challenges	Cost leadership Localization	Technical differentiation
Common challenges	Price leadership and scale	
Long-term challenge	Adequate returns to meet reinvestment requirements	

Table 2. Summary of strategic challenges for the different materials segment suppliers.

Module encapsulant

A key component in module encapsulation is the adhesive that is layered on both sides of the strings of a cell. This material, usually ethyl vinyl acetate (EVA), is cured on module lamination to produce a hard, continuous encapsulation around the cells. Typically two sheets are used per module, extending across the full size of the module. A large proportion of modules are still finished in China, and the domestic consumption of EVA is significant. We estimate Chinese consumption of EVA to be well in excess of 100,000,000m^2.

EVA is a globally supplied commodity that is manufactured by large chemical suppliers and supplied as resin granules. These granules are converted into film and supplied to module makers for lamination. Major EVA film suppliers include DuPont, SKC, Mitsui and Bridgestone. All of these companies, with the exception of DuPont, are vertically integrated suppliers of film to the PV industry.

In China, EVA film was also historically supplied through import from foreign suppliers. Although domestic supply of film was established as early as 2003, in the last three to four years the domestic supply has ramped up dramatically; we estimate that greater than 60% of demand for EVA film is satisfied by domestic production. The largest supplier of solar-grade EVA film in China is now Hangzhou First PV Material Co.

Drivers for supplier selection of EVA film include price, quality, ease of doing business and end-product yield.

- Price: locally produced products are usually competitive on price, quoted in RMB and import duty exempt.

- Quality: although domestic film suppliers often source polymer from global producers, film quality can be dependent on the local manufacturing capability. While domestic producers are often not perceived to be of the highest quality, acceptable final product quality can indeed be achieved.

- Ease of doing business: all suppliers are expected to have a domestic presence, although local product support is not always perceived as absolutely necessary.

- Product yield: EVA film quality has a significant input in final product yield, and higher quality films can support the price premium. This can offset cost penalties incurred by foreign suppliers.

Since manufacturing scale is critical for tier 1 suppliers, it is difficult for market entrants to start small, which in effect favours large incumbent suppliers that are recognized by the module producers. Some large global suppliers do not have significant brand recognition among tier 1 and tier 2 module makers, which can present quite a challenge in terms of gaining market acceptance.

Lessons to be learned when supplying in China

There are several important lessons for chemical and material suppliers that derive from the case studies outlined in the previous section. Apart from having to be identified by the NDRC as a key strategic supplier, critical dimensions for competitive differentiation include cost leadership, technical differentiation, localization, customer intimacy and scale (see Table 2).

In today's cost-driven environment, cost leadership – be it derived from load factor costs, cheap capital or superior technology – is critical to being chosen as a key supplier to leading PV companies. In the area of pure chemicals, Chinese companies can compete almost entirely on price and have largely succeeded in closing out foreign competition. As domestic suppliers gain technical and manufacturing experience, they have also been able to challenge importers on technical capabilities for most formulated materials.

In the case of a few formulated materials – silver pastes and diamond wire in particular – foreign competitors in China have been able to protect premium pricing with technically superior products. However, as the market expands, domestic suppliers are finding that they are able to invest returns into R&D and develop competitive technologies to compete against imported materials.

There is no reason why foreign companies cannot develop a localized presence that takes advantage of low factor costs in China and allows them to compete on an equal footing. This has occurred in several industries, and will continue in the PV industry as manufacturing scale increases. Closely linked to this local presence is the customer intimacy that a supplier must develop with its customer base. Domestic companies arguably have an advantage in this respect, although new entrants with recognizable brand names and well-trained local employees can certainly challenge domestic suppliers in this regard.

A daunting aspect of the solar industry is the speed at which manufacturing scale has grown. Suppliers that cannot offer manufacturing scale to match demand are at a severe disadvantage when competing for business with tier 1 module manufacturers. Any strategic plan to grow in this market must address scale of manufacture, as well as quality and consistency of supply.

In addition to these strategic elements there is a structural concern that suppliers must address. The pricing of most of the pure chemicals and many of the formulated chemicals used in module manufacture are approaching their cash costs. As a result, the end-market price of these materials will start to resemble commodities, and external factors will impact suppliers' capability to maintain a particular price level. This has already been seen in the case of silver paste because of the volatility of silver bullion pricing in the recession, but recent history has shown us that materials such as HF (hydrogen fluoride) and oil-derived polymers can experience significant high price spikes due to market volatility. In the supply chain, operating on narrow margins, some of these price spikes will be passed on to the end customer, which will run contrary to the expectation of continued price reductions for economically viable PV power.

A final consideration of competing at low prices with narrow margins is the need for reinvestment and capacity addition (particularly in polysilicon). As returns reduce, the attractiveness of upgrading or adding capital to a business with low IRR plummets, leading to possible demand tightness and price increases in the long term.

Strategic alternatives for material suppliers

For many current suppliers of chemicals and materials, participating in China is a must. While technical advantage can be sustained and domestic product exported to China with local representation may be a viable business model, in the long term, suppliers must expect the Chinese competition not only to start offering competitive products but also to have structural cost advantages. Setting up domestic manufacturing is not an uncomplicated business by any means, but it has been successfully achieved by many companies in this and other industries. This may well be the best approach to share gains in the Chinese market.

In order to maintain a differentiated technical advantage, a supplier can also pursue material reduction strategies. Major paste suppliers already offer silver pastes with reduced precious metal content or formulations tuned for double printing, and ultra-fast-cure EVA has the ability to reduce lamination time for enhanced productivity.

"Addressing scale requirements as part of a strategic plan is vital to gaining share with tier 1 suppliers."

Addressing scale requirements as part of a strategic plan is vital to gaining share with tier 1 suppliers. On the flip side, however, using manufacturing scale as both a competitive and a cost advantage has proved to be an effective defence against smaller competitors; this makes Hangzhou First PV a difficult competitor to contend with in the encapsulant market.

The final strategic consideration from suppliers giving consideration to entering the Chinese market is that as demand for PV modules grows in other regions of the world, localized manufacture will be the most economic approach. An example of this is Suntech assembling its modules in the USA. Chemical and material suppliers can bid for business as and when such manufacturing is established. While such a "wait and see" strategy may be attractive to some, it is worth considering that domestic Chinese suppliers may well be considering expansion in foreign markets at that point, as GRTC is already doing.

About the Author

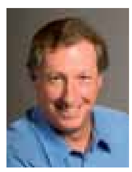

Mark Thirsk is a managing partner and co-founder of Linx Consulting, which provides market-defining analysis and strategic insights across major markets in electronic materials. He has over 25 years' experience in economic and business forecasting, strategic planning, technical marketing, product management and M&A, spanning many segments and processes in electronic materials. Mark has served on the SEMI Chemicals and Gases Manufacturers Group (CGMG) since 1999, acting as chairman between 2001 and 2003. He holds a B.Sc. (Hons.) in metallurgy and materials science from Birmingham University and an MBA from The Open Business School, and has authored multiple publications in both academic and trade publications, as well as contributing to several patents.

Enquiries

Mark Thirsk
Managing Partner
Linx Consulting LLC
PO Box 384
Mendon, MA 01756-0384
USA

Tel: +1 617 273 8837
Email: mthirsk@linx-consulting.com
Website: www.linx-consulting.com

Solar-grade silicon – is 'Siemens' the only answer?

Jan Ove Odden, **Anne Karin Søiland**, **Erik Enebakk**, **Steinar Braathen**, **Bjørn Sandberg** & **Kenneth Friestad**, Elkem Solar, Kristiansand, Norway

ABSTRACT
Solar-grade silicon (SoG-Si) based on metallurgical refining processes, often called upgraded metallurgical-grade silicon (UMG-Si), is expected to play an important role in achieving the solar industry's necessary cost targets per Wp in order to compete with other energy sources. The broad term 'UMG-Si' currently embraces types of silicon feedstock that differ quite substantially in product quality and performance. This paper presents a summary of the work carried out by Elkem on low-cost production of silicon feedstock via a flexible, recycling metallurgical processing route with the lowest carbon footprint on the market. Results are given that qualify Elkem Solar Silicon® (ESS™) as a SoG-Si, with comparable efficiencies to polysilicon (poly-Si) from the traditional Siemens process. The latest results on the performance of modules based on ESS are reported. An indication of the stability of older modules based on SoG-Si feedstock from Elkem is also considered. On the basis of the results, there is no reason to expect modules based on ESS to differ from other commercial modules based on poly-Si. ESS is therefore shown to be a viable alternative to conventional poly-Si, but with the additional benefit of lowering specific energy use and cost per Wp.

Introduction

Elkem has been working with metallurgical routes for solar-grade silicon (SoG-Si) since the late 1970s, and several approaches have been tested and evaluated. The results indicate that the outcome of a metallurgical route will depend on the different process steps included. In the early stages, Elkem focused on employing high-purity raw materials, and then, during the 1990s, introduced several additional purification steps, before arriving at the concept that was industrialized in 2009. This concept includes silicon-reduction furnace operation, slag treatment, leaching, one-directional solidification and post-treatment (see Fig. 1). The first step is simply a form of production of metallurgical silicon, but designed to fulfil the criteria for the subsequent refining of the silicon to a solar-grade quality. This is followed by three purification steps in the process chain, which are:

1. Slag refining – removal of dopant
2. Leaching – removal of dopant and metallic elements
3. Solidification – further reduction in dopants and metallic elements.

> "The emissions of CO_2 equivalents (CO_2-eq) per kg SoG-Si from Elkem are between 10 and 30% of those from the Siemens process route."

Subsequent to the three purification steps is the post-treatment, which includes cleaning and packing of the finished product. As indicated in Fig. 1, the Elkem metallurgical route is flexible regarding the use of recycled material. In addition to the internal recycling, the Elkem process can also potentially recycle ingot cuts – often known as carbide cuts – from the solar industry, which normally do not end up as solar cell material. This practice also contributes to the Elkem metallurgical process route being the most environmentally friendly SoG-Si process route in the world, for which the energy payback time of a finished solar module is less than one year because of the low energy intensity of the Elkem process compared to any of the different versions of the Siemens process. The emissions of CO_2 equivalents (CO_2-eq) per kg SoG-Si from Elkem are between 10 and 30% of those from polysilicon production by a traditional Siemens process route (11g vs. 40–150g CO_2-eq/kg SoG-Si), depending on the specific

Figure 1. The five steps in the metallurgical route industrialized by Elkem: reduction furnace, slag treatment, leaching, one-directional solidification and post-treatment. The robustness and flexibility of the process in terms of handling recycled ingot cuts is highlighted.

Elements		Specification SEMI PV17-0611	Elkem Solar Silicon typical values
Boron	Target tolerance	≤ 0.38 ppmw ± 0.06 ppmw	0.22 ppmw ± 0.05 ppmw
Phosphorus	Target tolerance	≤ 0.79 ppmw ± 0.17 ppmw	≤ 0.62 ppmw ± 0.15 ppmw
Carbon		≤ 43 ppmw	25 ppmw
Aluminium		-	< 0.01 ppmw
Transition and post-transition metals Ti, Cr, Fe, Ni, Cu, Zn, Mo		≤ 200 ppba	< 50 ppba
Alkali and earth alkali metals Na, K, Ca		≤ 4000 ppba	< 200 ppba

Table 1. The specifications of the SEMI PV17-0611 standard compared to typical values obtained from chemical analyses of the ESS SoG-Si feedstock.

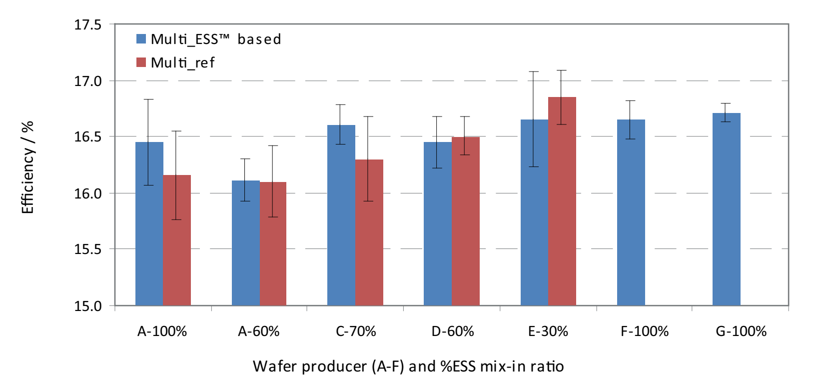

Figure 2. Cell efficiencies obtained by different producers (A–G) using ESS in different blending ratios. Polysilicon reference data are provided where available, and the standard deviations for all batches are indicated. The results are based on cells processed by ISC Konstanz or industrial cell manufacturers using their standard cell production lines in a similar way to that for polysilicon material.

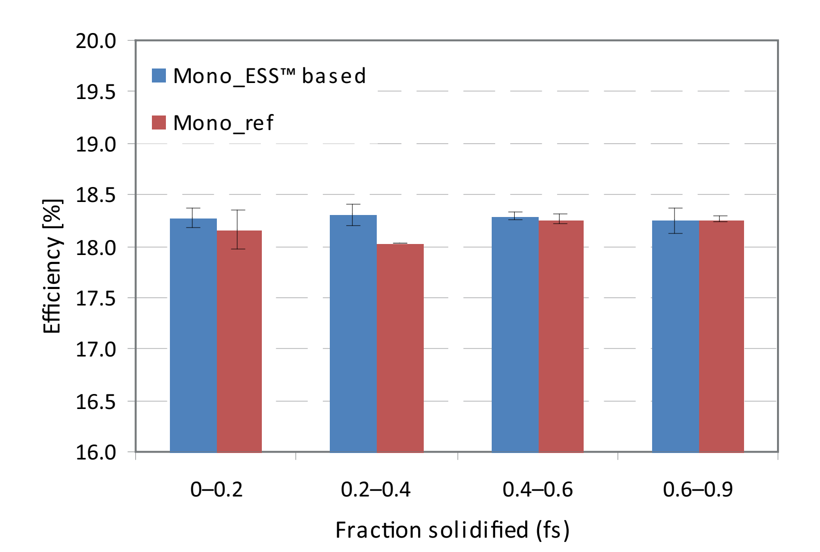

Figure 3. Cell efficiencies as a function of fraction solidified for crystals from a mix of 50% ESS and 50% virgin polysilicon (Mono_ESS), and for crystals from 100% virgin polysilicon (Mono_ref). The results for Mono_ESS are the average obtained from wafers from four crystals grown by four different crystal growers; the results for Mono_ref are from two different monocrystals grown by two different crystal growers. The standard deviations are indicated. All wafers were processed by the standard industrial cell production line at ISC Konstanz.

process details and location of the polysilicon plant [1].

An industrial prototype plant was constructed in Kristiansand, Norway, with an initial production capacity of 5000MT/year, which later increased to 6000MT/year in 2011. A further increase in capacity to ~7500MT/year during 2012 will strengthen Elkem's position even more in terms of cost per kg SoG-Si. In parallel to this increase in production capacity, the content of boron (B) and phosphorus (P) in Elkem Solar Silicon® (ESS™) has decreased: typical values are now 0.22 ppmw B and 0.62 ppmw P.

In the last 30–40 years several companies have explored metallurgical routes for the production of solar-grade silicon (SoG-Si). The above-mentioned efforts have made the Elkem process the leading route within this category in terms of both quality and cost. Silicon produced from these different metallurgical refining routes is often called upgraded metallurgical-grade silicon (UMG-Si). This term, however, can be very misleading. The silicon quality – or the quality of the UMG-Si – is obviously dependent on the route chosen, so it is therefore possible to find significant variations in the chemical purity, homogeneity and physical appearance of the so-called UMG-Si on the market. In order to clarify the quality requirements of SoG-Si, SEMI has published a standard, namely SEMI PV17-0611. Elkem has developed an SoG-Si that currently falls in group IV of this standard – this feedstock is branded under the name ESS. A typical analysis of the feedstock is given in Table 1.

Cell results for wafers based on ESS

During the last decade Elkem Solar has regularly presented the test results obtained for cells with ESS-based mono- and multicrystalline wafers [2–4]. A large test consisting of 150,000 multicrystalline cells was presented by Q-Cells in 2008 [5]. Since then, several producers of multicrystalline ingots have used ESS mixed with polysilicon in various blending ratios. Elkem Solar has supervised the quality of its wafers by continuous testing at ISC Konstanz in Germany. Fig. 2 shows the results from ISC Konstanz for cells made from wafers produced by different industrial competitors in their normal wafer production lines. The results obtained for ESS-based cells correspond to reference cells, and the efficiencies mostly fall in the range 16.5–17%. An important point has been to demonstrate that ESS is not limited to a standard cell process, but has the potential for future use in high-efficiency cells [6].

"An important point has been to demonstrate that ESS is not limited to a standard cell process, but has the potential for future use in high-efficiency cells"

Elkem Solar has been testing the use of ESS in monocrystalline wafer production for the past few years. In the initial trials the wafers were limited by the boron content, but during the last two years the boron level in ESS has been significantly reduced. Monocrystalline cells based on a mix of 50% ESS and 50% virgin polysilicon show comparable efficiencies to reference cells based on 100% virgin polysilicon, with very small variations along the crystal (see Fig. 3). Light-induced degradation (LID) has been measured on cells from the different crystals and is comparable to that of the reference cells, with a typical degradation loss of 1–3% relative. Several recent papers have pointed out that LID in compensated silicon seems to be dependent on the net dopant quantity ($N_A - N_D$) rather than on N_A itself, where N_A is the concentration of acceptor atoms and N_D is the concentration of donor atoms. However, consensus has not yet been reached on this issue [3,7]. Nevertheless, ESS has demonstrated its suitability for monocrystalline ingot production, and it has been shown that it is possible to reach very uniform resistivities over the crystal length [8]. Elkem Solar is currently in the process of also testing a higher percentage mix of ESS for monocrystalline wafer production, with up to 100% ESS in the crystals.

Stability of cells based on ESS

The ESS production process today consists of five separate steps, including a silicon furnace, slag treatment, leaching, one-directional solidification and post-treatment, where the three middle steps are designed to remove different types of impurity. There has been a particularly large focus on the boron (B) and phosphorus (P) content, since these elements are directly related to the resistivity of the ingot in the final customer solar cell. Over the years, Elkem has lowered the content of B and P for ESS from less than 4 ppmw in the early 1980s, to today's typical values of 0.22 ppmw B and 0.62 ppmw P.

It has been challenging for customers to distinguish between the different UMG-Si qualities on the market; the large variation between different UMG-Si qualities also raises the question of how reliable solar cells based on UMG-Si will be. This problem was not pinpointed in the early stages of UMG-Si development, and for old modules there are no published data that relate to long-term degradation. Elkem, however, has recently measured one module from the early stages of the development, as well as even smaller demo modules, in order to get an indication of the degradation. The results (< 7% degradation after 15 years and ~20% after 27 years) indicate that the module based on UMG-Si (< 2 ppmw B and P) should not be worse than commercial modules from the late 1980s or early 1990s. Modules from that time period have been reported as showing a linear degradation of approximately 0.7% per year [9,10], which is comparable to the oldest demo module containing ESS (see Fig. 4). The results have encouraged Elkem to start a programme to systematically measure degradation of solar modules that are based 100% on industrial-produced ESS. Results for degradation of both older demo modules and more recent modules based on industrially produced ESS are shown in Fig. 4.

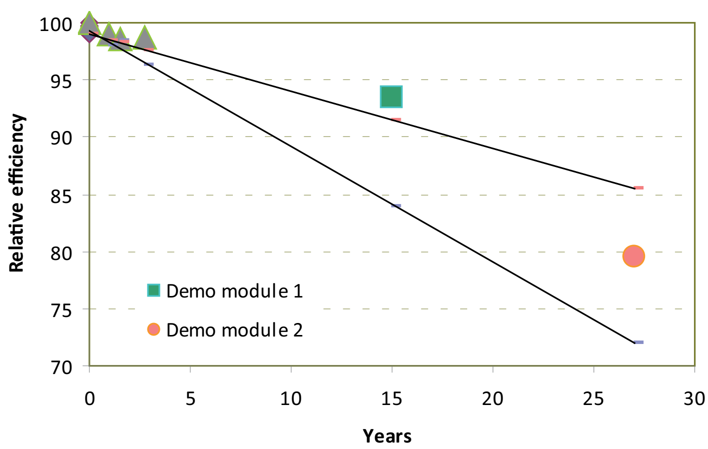

Figure 4. Change in relative efficiency over time, measured for different 100% ESS-based solar modules. The more recently produced modules (green symbols in the top left corner) are highlighted and explained later in Fig. 5. The degradation for a test module based on Elkem SOG-Si from 15 years ago is represented by demo module 1, whereas the average for smaller demo modules made from Elkem solar-grade silicon from 27 years ago is indicated by demo module 2. The upper and lower solid lines correspond to linear long-term degradations of 0.5% and 1% per year, respectively.

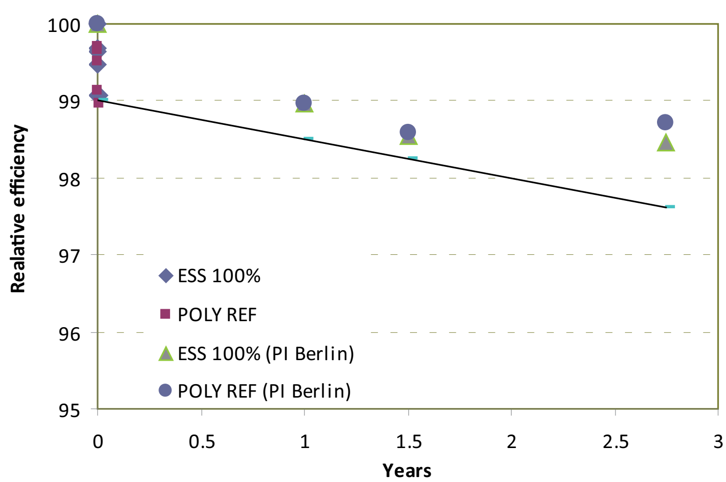

Figure 5. The initial change in the relative efficiency for different ESS-based and corresponding polysilicon reference solar modules. The modules labelled 'PI Berlin' were tested at the certified solar module test facility Photovoltaic Institute Berlin. The solid line corresponds to a linear long-term degradation of 0.5% per year.

"All the results so far regarding the degradation of solar modules based on 100% ESS show comparable results to polysilicon after the first few years of operation."

The results obtained from more recently produced ESS and polysilicon reference modules are highlighted in Fig. 5 for their first years of operation. The points that are scattered on the *y* axis indicate LID, which is commonly seen within the very first hours of operation of any silicon-based solar module. The results indicate equal amounts of LID – below 1% on the module level – for both the ESS and polysilicon modules. Note that the last two data points in the figure show lower degradation than the previous measurements. The differences, however, are small and within the analysis accuracy for the measurements at the certified institute PI Berlin.

All the results so far regarding the degradation of solar modules based on 100% ESS show comparable results to polysilicon after the first few years of operation. According to Osterwald et al. [11], the anticipated degradation for today's solar modules is of the order of 0.5% per year, and, as can be seen from Fig. 5, all the modules show lower degradation than this trend. In any case, the primary causes of performance loss in solar modules are claimed to be related to mechanisms that are external to the solar cell material itself [12]. Some of the solar module research projects initiated by Elkem now focus on the performance of ESS modules relative to polysilicon references during high-temperature and low-light conditions, for example < $300W/m^2$. This is because there are indications that ESS performs better than polysilicon under such conditions – results will be published when this research is complete.

Summary

ESS will always be a cost-competitive alternative to polysilicon from a Siemens process route. Technical cooperation with the customer, including guidance on dopant addition strategies based on in-house resistivity-profile modelling, helps in achieving the optimal use of ESS. The flexibility of the Elkem metallurgical process route to SoG-Si is also used in cooperation with the customer, by potentially recycling customer carbide cuts back to SoG-Si. The results presented above show that efficiencies obtained for ESS-based multicrystalline cells, using standard industrial cell processing conditions, are comparable to those for polysilicon reference material. This is valid throughout the whole range of blending ratios, and the efficiencies range from 16.5 to 17%. Even for monocrystalline cells, comparable results to those for polysilicon have been obtained, specifically efficiencies of between 18 and 18.5%.

The results so far show no indications of a higher degradation rate for solar modules containing 100% ESS than for polysilicon reference modules. Measurements performed on older demo modules containing SoG-Si from Elkem show a degradation which is to be expected for a module produced at that time. The ESS is the 'greenest' SoG-Si on the market mainly because of the low energy intensity of the process, which leads to an energy payback time of less than one year for ESS-based solar modules. This also leads to a carbon footprint of 11g CO_2-eq/kg SoG-Si as compared to polysilicon, which varies between 40 and 150g CO_2-eq/kg SoG-Si, depending on the process route and plant location.

> "As a relatively new silicon feedstock in the market, ESS has now shown that it is a compatible alternative to conventional Siemens polysilicon."

As a relatively new silicon feedstock in the market, ESS has now shown that it is a compatible alternative to conventional Siemens polysilicon. Further verification and documentation of the performance and compatibility of ESS will entail identifying potential advantages such as high-temperature and low-light performance. To this end, Elkem Solar is working actively with different research institutes to carry out various cell and module long-term tests, with the aim of exploiting its product's potential even further than has been indicated in this paper. In conclusion, as a solar-grade feedstock, ESS will bring down the cost of a finished solar module and will offer a clear environmental benefit.

References

[1] Braathen, S. et al. 2012, "High performance solar cells based on low cost solar silicon with low carbon footprint", *Proc. SOLARCON China 2012*, Shanghai, China.

[2] Rein, S. et al. 2010, "Cz-Silicon wafers and solar cells from compensated solar grade silicon feedstock: Potential and challenges", *Proc. 25th EU PVSEC*, Valencia, Spain.

[3] Peter, K. et al. 2008, "Future potential for SoG-Si feedstock from the metallurgical process route", *Proc. 23rd EU PVSEC*, Valencia, Spain.

[4] Friestad, K. et al. 2004, "Solar grade silicon from metallurgical route", *Proc. 19th EU PVSEC*, Paris, France.

[5] Hoffmann, V. et al. 2008, "First results on industrialization of Elkem Solar Silicon at Pillar JSC and Q-Cells", *Proc. 23rd EU PVSEC*, Valencia, Spain.

[6] Kaes, M. et al. 2006, "Over 18% efficient mc-Si solar cells from a 100% solar grade silicon feedstock from a metallurgical process route", *Proc. IEEE 4th World Conf. PV Energy Conver.*, Waikoloa, Hawaii, USA.

[7] MacDonald, D. et al. 2009, "Light induced boron-oxygen defect generation in compensated p-type Czochralski silicon", *J. Appl. Phys.*, Vol. 105, p. 093704.

[8] Søiland, A. et al. 2011, "Investigation of Cz-monocrystals, p- and n-type, produced from a 50/50 mix of Elkem Solar Silicon® and polysilicon", *Proc. 5th Int. Worksh. Cryst. Si. Sol. Cells*, Boston, Massachusetts, USA.

[9] Osterwald, C.R. et al. 2002, "Degradation analysis of weathered crystalline-silicon PV modules", *Proc. 29th IEEE PVSC*, New Orleans, Louisiana, USA, pp. 1392–1395.

[10] Skoczek, A., Sample T. & Dunlop, E.D., 2009, "The results of performance measurements of field-aged crystalline silicon photovoltaic modules", *Prog. Photovolt: Res. Appl.*, Vol. 17, pp. 227–240.

[11] Osterwald, C.R. et al. 2006. "Comparison of degradation rates of individual modules held at maximum power", *Proc. IEEE 4th World Conf. PV Energy Conver.*, Waikoloa, Hawaii, USA, pp. 2085–2087.

[12] Quintana, M.A. et al. 2002, "Commonly observed degradation in field-aged photovoltaic modules", *Proc. 29th IEEE PVSC*, New Orleans, Louisiana, USA, pp. 1436–1439.

About the Authors

Anne-Karin Søiland graduated in 2005 from the Norwegian University of Science and Technology (NTNU) with a Ph.D. degree in materials technology. Her thesis topic was the formation of SiC- and Si_3N_4-inclusions during crystallization of multicrystalline silicon ingots. Anne-Karin joined Elkem Solar in 2004; her main activities have included working on customer processes, mono- and multicrystalline ingot production, and the use of Elkem Solar Silicon in these processes.

Jan Ove Odden graduated from the University of Oslo in 2004 and received his Dr. Scient degree in inorganic chemistry. For his thesis he researched the decomposition of monosilane under high-pressure conditions in free-space reactors. In 2007 Jan began working as an R&D engineer at Elkem Solar, where he focuses on technical customer support and leads research projects evaluating the performance of ESS in solar modules in the field.

Enquiries

Jan Ove Odden
Elkem Solar AS
P.O. Box 8040, Vaagsbygd
NO-4675 Kristiansand
Norway
Tel: +47 38 01 76 52
+47 94 50 10 64

3D multi-physics modelling of unidirectional solidification of mc-Si in an ingot furnace

Anne J. Faber & **Adriaan M. Lankhorst**, CelSian Glass & Solar B.V., Eindhoven, The Netherlands, & **Bo Zhao** & **Cheng Wang**, Jinggong Science & Technology Co., Ltd, Zhejiang, China

ABSTRACT

Unidirectional solidification of large Si ingots from the melt phase is currently one of the most important technologies for producing mc-Si for PV cells. Si ingot furnaces began from casting equipment, and have been improved by DSS (directional solidification system) or DSS-like methods. To improve PV cell efficiency and reduce costs, intensive development has focused on increasing a single ingot's volume, reducing impurities and controlling the growth speed and temperature gradient. One of the latest developments of Si ingot furnaces is mono-like crystalline silicon growth using a seed preservation method and more accurate control. The Si ingot furnaces are optimized with precise control of temperature gradients and growth speed for the formation of a large unit of quasi-monocrystalline Si. This optimization can further improve a PV cell's efficiency by at least 1%. In order to obtain fundamental knowledge about the key process steps that determine the growth and electrical quality of mc-Si via directional solidification in an ingot furnace, a combined modelling-measuring approach is essential. Moreover, a mathematical model of the Si ingot casting process can be used for model-based process control.

Figure 1. Cross section of Jinggong's mono-like crystalline ingot (height 100mm).

Figure 2. Jinggong assembly line for the JJL500N Si ingot furnace.

Introduction

In the first part of this paper, the underlying physical phenomena and physical laws of the Si ingot process are explained on the basis of characteristic dimensionless numbers. The equations for the physical laws are solved numerically in X-stream – CelSian's dedicated 3D computational fluid dynamics (CFD) package. X-stream is a multi-physics CFD package with sub-models representing, for example, flow, melting, radiation heat transfer, turbulence, combustion, kinetic reactions and thin-layer deposition [1,2]. The solver in X-stream is based on the finite volume method as described in Ferziger & Peric [3], the grids are 3D multi-block structured and body fitted, and the code is fully parallelized. Typical results of 3D CFD modelling calculations are presented in the second part of this paper.

Physical characteristics of the Si solidification process

Fig. 3 shows a simplified configuration of a Si ingot furnace: a rectangular quartz crucible, containing the Si load, is placed in a rectangular housing of insulating refractory material. Usually, the bottom of this housing is formed by a water-cooled copper plate. The area around the crucible is flushed with argon gas. The batch process begins with the filling of the crucible with Si chunks and heating them well above the melting temperature of Si to form a Si melt. The unidirectional crystallization process is started by increasing the heat loss via the crucible bottom, with the help of the water-cooled bottom plate, and lowering the power of the heaters, causing a vertical temperature gradient in the Si melt. In this way, solidification starts at the bottom and proceeds upwards until no melt is left.

The physical phenomena that play a role in these industrial Si ingot furnaces include:

- Heat transfer by conduction, convection and radiation from the heaters to the Si load, within the Si load and from the Si load to the cooled crucible bottom.
- Flows and transport of chemical species in the Si melt as well as in the argon gas above the melt.

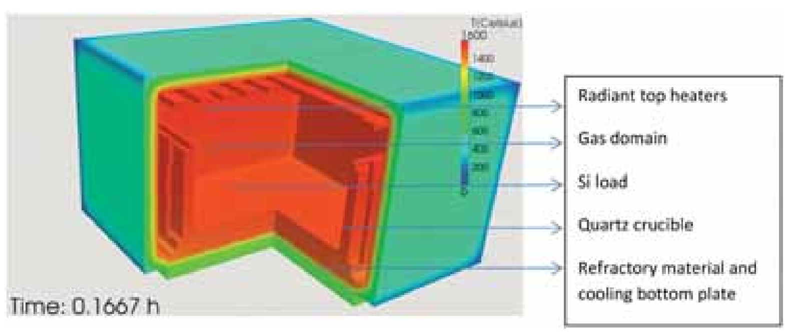

Figure 3. Simplified schematic of a Si ingot furnace, showing different physical domains.

- Release of latent heat by the Si during crystallization.

"Natural convection and turbulent flow must be taken into account for the flow patterns in the very low viscosity Si melt to be correctly described."

The most important physical features of the Si ingot process can be identified by considering some key dimensionless numbers that characterize the heat transfer, the mass flow, and the liquid–solid phase change in the system. Table 1 summarizes the most relevant physical characteristics of Si for this process, as well as the characteristics of water for comparison. By estimating the values of the physical numbers, as given in this table, the following general conclusions for the directional Si crystallization process can be derived:

- Since the Stefan number (the ratio between sensible heat and latent heat) is small, the Si solidification process is dominated by the latent heat release given by

$$k_{Si_m} \frac{dT}{dy}\Big|_m - k_{Si_c} \frac{dT}{dy}\Big|_c = \rho H R_{Si} \quad (1)$$

where H is latent heat, ρ is silicon density, and k_{Si_m} and k_{Si_c} are the melt and crystal thermal conductivities respectively. The Si solidification process is characterized by the crystallization rate $R_{Si} = \frac{dy}{dT}$.

- From the formula in Equation 1, the order of magnitude of the Si solidification rate in the stationary situation can be estimated to be $R_{Si} \approx 1.0$cm/hr.
- At the onset of crystallization (at the bottom of the ingot), the temperature in the top layers of the Si melt is assumed to be about 1460°C.
- Natural convection and turbulent flow must be taken into account for the flow patterns in the very low viscosity Si melt to be correctly described.
- Although typical Si flow velocities are small (of the order of mm/s – see Table 1), the heat transfer in the liquid Si is dominated by convective heat transfer, as the thermal Péclet number is much larger than unity.

Besides these guidelines for the Si domain, the following physical phenomena in the gas domain should be accounted for: laminar or turbulent flow in the gas, and heat transport from the heaters to the Si load by (mainly) radiation. Taking these into consideration, in order to simulate numerically the complete Si solidification process in an ingot furnace by

Properties @ T_m	Symbol	Unit	Silicon	Water	Remarks
Melting temperature	T_m	°C	1414.00	0	
Melting temperature	T_m	K	1687.15	273.15	
Heat capacity	C_p	J/kgK	910.0	4221.0	Water has by far the highest heat capacity
Thermal conductivity	k	W/mK	56.5	0.55	Silicon is much more conductive than water
Density	ρ	kg/m^3	2583	1000	
Dynamic viscosity	η	kg/ms	5.57E-04	1.79E-03	Liquid silicon is less viscous than water
Kinematic viscosity	ν	m^2/s	2.16E-07	1.79E-06	
Thermal expansion coefficient	β	1/K	7.17E-05	7.00E-05	Of the same order for silicon and water
Latent heat	H	J/kg	1.79E+06	2.50E+06	High latent heat for both silicon and water
Gravity	g	m/s^2	9.81	9.81	
Characteristic temperature difference	ΔT	K	10	10	
Characteristic dimension	L	m	0.25	0.25	
Stefan number	Ste	-	5.08E-03	1.69E-02	The smaller the Stefan number, the more that latent heat effects dominate; Si solidification largely dominated by H
Prandtl number	Pr	-	8.97E-03	1.37E+01	Molten Si: hydrodynamic boundary layer much smaller than thermal boundary layer
Grashof number	Gr	-	2.36E+09	3.34E+07	The higher the Grashof number, the stronger the natural convection
Rayleigh number	Ra	-	2.12E+07	4.58E+08	Turbulent flow for Ra > 10^6–10^9
Péclet number	Pe	-	109	5370	Ratio of heat transfer by convection versus conduction
Buoyant velocity scale	V_b	m/s	4.19E-02	4.14E-02	
Maximum velocity in boundary layer	V_{max}	m/s	1.05E-02	2.80E-03	Pr < 1: $V_{max} \approx 0.25 * V_b$ Pr > 1: $V_{max} \approx 0.25 * Pr^{-0.5} * V_b$
Dimensionless distance from velocity maximum to wall	x/L	-	2.21E-03	1.03E-03	
Distance from velocity maximum to wall	x	m	5.53E-04	2.56E-04	Very thin (of the order 0.5mm) boundary layers in both cases

Table 1. Physical properties and characteristic numbers of Si compared to water.

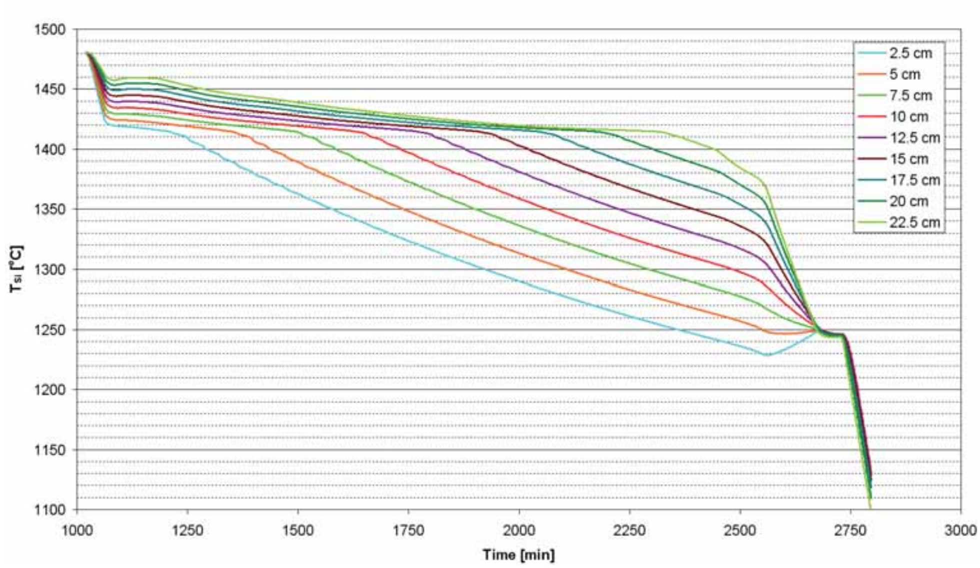

Figure 4. Calculated Si melting temperatures at various vertical positions (distance from the crucible bottom).

a CFD model, the simulation model should involve:

- solving the equations governing the energy conservation laws in all domains (gas, Si and refractory materials);
- solving the laminar or turbulent flow equations in the gas domain surrounding the ingot;
- determining the natural convection and turbulent flows in the Si melt domain;
- solving for detailed radiative heat transfer (discrete ordinates model) in the gas domain surrounding the ingot.

Typical 3D-modelling results for an industrial Si ingot furnace are presented next.

3D simulations of an mc-Si ingot furnace

Full-scale calculations were conducted for one quarter of an industrial 410kg-ingot mc-Si ingot furnace. The grid for this geometry consists of 0.5 million hexahedral grid cells, of which roughly 20% are located in the silicon melt (typical melt cell size 10mm × 6mm × 10mm). The geometry is subdivided into several domains, each domain having a different set of sub-models applied for different physics. Here, the domains are silicon, quartz and support crucibles, refractory housing and the argon-filled space between the box and the housing; each heater is also a separate domain. The energy equation is solved in all domains: the enthalpy formulation is used on the silicon domain, and the usual temperature formulation on the other domains. The solutions are coupled over domain boundaries to ensure continuity of temperature and heat fluxes. Radiative heat transfer in the gas domain is solved by a discrete ordinates model. Laminar flow equations are solved in the argon-gas space.

During crystallization, the heater power and the water cooling are controlled in such a way that the temperature signals from three thermocouples follow a target curve in time. During a specific test run, to locate the crystallization front as a function of time, dip-rod measurements were taken at two positions in the melt: one in the centre, and the other in the corner of the crucible.

Transient heater power and bottom water cooling-rate data were used as input for the model. The model was validated by comparing the transient results with the temperatures of the three thermocouples as well as of the front positions at the two dip-rod locations.

> "As a result of the huge amount of latent heat release, temperatures close to the actual crystallization front remain close to the Si melting temperature (1414°C)."

Simulations were carried out with and without Si melt flow enabled. Fig. 4 shows the calculated temperatures for the case of no Si melt flow, at nine vertically distributed centre points in the Si melt. As a result of the huge amount of latent heat release, temperatures close to the actual crystallization front remain close to the Si melting temperature (1414°C). For points located in the solid crystal, the temperature rapidly decreases because of the heat removal by the bottom cooling plate. Compared to temperature gradients in the crystal, gradients in the melt are small owing to the higher thermal conductivity of liquid Si (k_{Si_m} = 56.5W/mK) compared to the solid Si thermal conductivity, which is given by:

$$k_{Si_c}(T)=1.21\cdot10^{5}\cdot T^{-1.1921} \qquad (2)$$

where T is the temperature in K. At the melting temperature, k_{Si_c} = 17.2W/mK [4].

In Fig. 5 the front positions calculated without melt flow enabled are compared to the dip-rod measurements. As regards the front positions, the agreement on the centre line of the ingot is excellent, whereas the predictions in the corner are somewhat less accurate. The calculations predict a planar (slightly concave) front (as seen from the crystal), but the dip-rod measurements indicate that in reality the surface is convex. Comparison of the front shapes between melt-flow and no-melt-flow calculations after five hours' process time suggests that the convexity is reproduced better when melt flow is switched on in the model.

The small temperature gradients involved make this process very sensitive to process parameters, but, bearing that in mind, the qualitative agreement between measurements and calculations is quite good. Once crystallization starts and latent heat is released at the front, the removal of this latent heat is much more important for the energy flows in the silicon than the removal of the sensible heat, as shown earlier in Table 1 by the low value of the silicon Stefan number.

Fig. 6 shows a snapshot of the (transient) flow pattern on the boundary of the Si melt for the first five hours of the process in the case when a laminar flow model is used. The flow field is the superposition of a large loop and smaller convection cells that vary in size and position during crystallization. The flow is driven by the

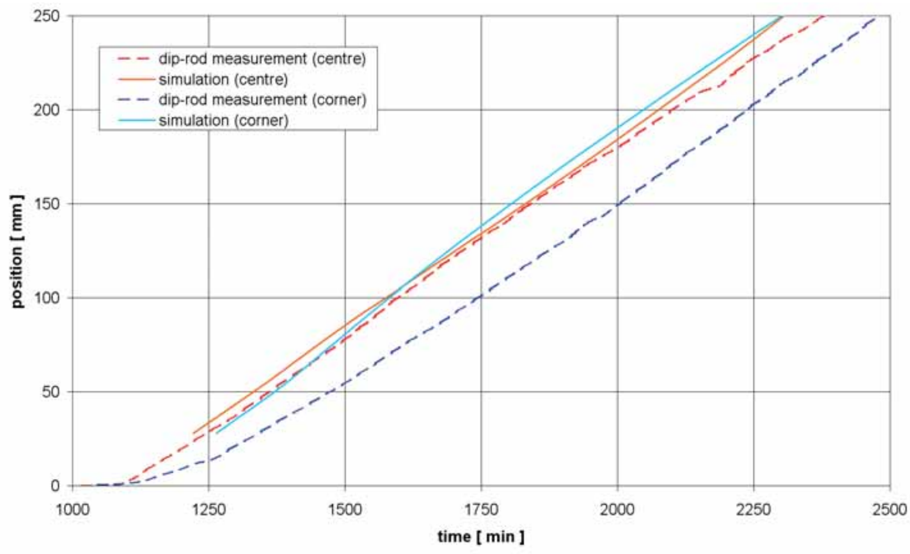

Figure 5. Measured and calculated positions of the Si crystallization front at two locations (centre and corner).

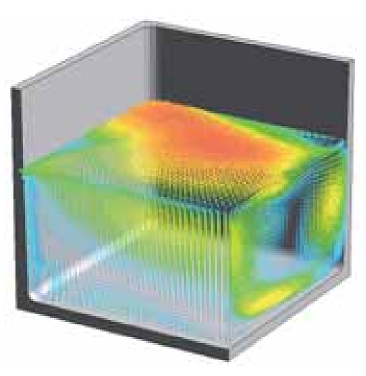

Figure 6. Snapshot of velocity vectors on the boundary of the silicon domain.

deviations from the stratified temperature/density profile, due to the release of latent heat at the front, the developing front curvature and the non-adiabatic side walls.

"The model is ready to support ingot furnace design and can ultimately be used in model-based crystallization process control."

Conclusions

Several basic physical processes interact in a subtle manner in industrial ingot furnaces for the crystallization of mc-Si via the vertical temperature-gradient method. The required components are: flow of melt and gas; energy transport through conduction, convection and radiation; and release of latent heat and solidification. These aspects have been implemented in X-stream – CelSian's dedicated 3D multi-physics multi-domain CFD simulation package.

The results for a complete, industrial 3D mc-Si furnace have been presented. For this furnace, where actual transient heater-power curves provided the main input for the model, the calculated thermocouple temperatures at locations just outside the silicon showed maximal differences of 10–20°C from the measurements. From this it may be concluded that the general energy flows in the complete furnace were well captured by the model. This means that the model can be used to gain insight into the process to investigate the effects of various interacting physical phenomena – radiation, convection, latent heat release, flow, etc. Furthermore, the model is ready to support ingot furnace design and can ultimately be used in model-based crystallization process control.

References

[1] Thielen, L. et al. 2007. "Simulation of multiphysical phenomena in glass melting furnaces", *Proc. NAFEMS World Congr.*, Vancouver, Canada.

[2] Lankhorst, A.M. et al. 2007. "Transient ALD simulations for a multi-wafer reactor with trenched wafers", *Surf. Coat. Techn.*, Vol. 201, pp. 8842–8848.

[3] Ferziger, P. & Peric, M. 2002. *Computational Methods for Fluid Dynamics*, 3rd ed. Berlin Heidelberg: Springer.

[4] Yamasue, E. et al. 2002. "Thermal conductivities of silicon and germanium in solid and liquid states measured by non-stationary hot wire method with silica coated probe", *J. Cryst. Growth*, Vol. 234, pp. 121–131.

About the Authors

Anne Jans Faber completed his studies in experimental physics at Utrecht State University, The Netherlands, in 1985, and is a senior scientist at CelSian Glass & Solar (formerly TNO Glass Group) in Eindhoven. He works as a contract researcher for international companies in the fields of glass science and technology, high-temperature sensors and solar silicon processes. Anne has authored/co-authored numerous scientific publications, and is the holder of several patents.

Adriaan Lankhorst received his doctoral degree in applied physics from Delft University of Technology, The Netherlands, in 1991, and is an R&D manager at CelSian Glass & Solar. He started working at TNO in 1990 as a process physicist, managing and executing projects involving complex physics and chemistry and the development and application of CFD models. Adriaan specializes in high-temperature processes such as glass melting, as well as combustion, turbulence, radiation, and mc-Si processes.

Bo Zhao is the CTO of Jinggong Science & Technology Co. Ltd. and the GM of Jinggong Mechatronic Research Institute. Bo has specialized in automatic control and crystal growth of silicon ingot furnaces for more than 10 years, and has led a number of key innovations in hot-zone design and crystal growth processes.

Cheng Wang is an R&D manager at Jinggong Mechatronic Research Institute. A CAE engineer specializing in numerical simulation for silicon ingot furnace design, Cheng is currently focusing on theoretical research into silicon crystal growth.

Enquiries

Anne Jans Faber
Tel: + 31 6 22973991
Email: anne-jans.faber@celsian.nl

Cell Processing

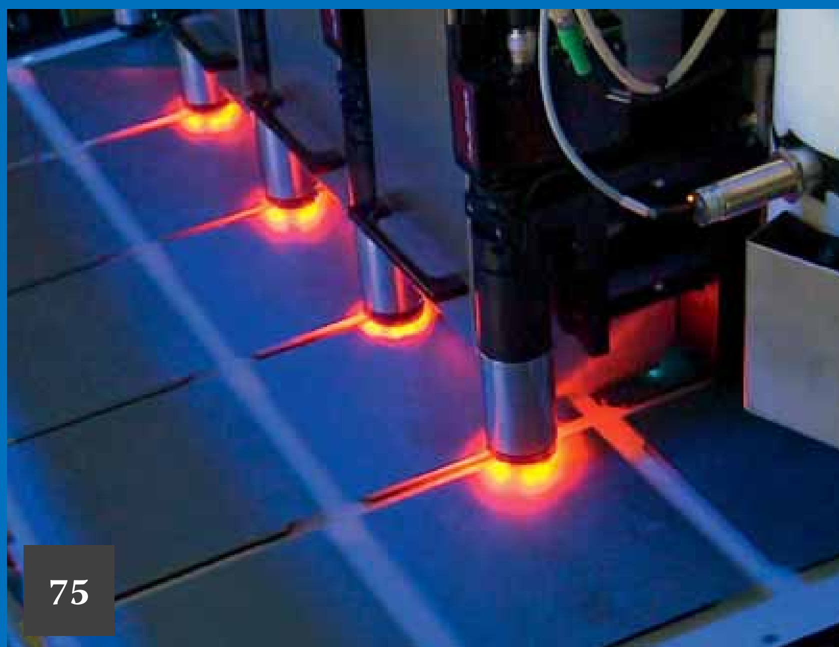

Hyundai Heavy Industries achieves record 19.7% efficiency with selective-emitter cell

Hyundai Heavy Industries (HHI) has announced the achievement of 19.7% conversion efficiency for its copper-contact solar cells. The record, for a selective-emitter cell, was obtained using standard 156mm commercially available p-type silicon wafers and has been verified by Fraunhofer ISE.

HHI researchers have been working on improving the LDSE technology with the addition of copper contacts on the front of the cell, eliminating the need for silver in the process. The use of copper, rather than silver, has led to cost reductions of up to 30% when compared to same-size cells produced by other companies. A key innovation by HHI's newly restructured research and development team was to prevent plating step problems by fitting the deposition method of the front silicon nitride dielectric.

The selective-emitter cell, which has a full-area aluminium-alloyed back electrode, beat the previous record of 19.6% efficiency, held by a Chinese company for 125mm wafers.

HHI researchers have been working on improving the LDSE technology with the addition of copper contacts on the front of the cell.

Cell Production News Focus

bSolar debuts its new bifacial PV solar cells

bSolar has advised that its high-efficiency, bifacial PV crystalline silicon solar cells are ready to be showcased during Intersolar Europe in Munich from June 14–16. The company's bifacial cells use the cells' back side to collect reflected and diffused sunlight in order to produce added electricity. They are manufactured using p-type wafers, standard equipment and production processes.

According to bSolar, the new cells hold a 10–30% higher kWh rate per kWp installed in standard application and up to 50% in vertical installations. The company noted that this is equivalent to a cell efficiency of 21–24% in standard applications. The cells can be used for flat rooftop and ground installations as well as certain BIPV applications such as solar sound barriers, carports, and green houses.

The cells are manufactured in bSolar's industrial plant in Heilbronn, Germany. The company advised that its cell shave been used in bifacial modules by various producers worldwide with bSolar's current

Source: bSolar

bSolar's bifacial cells use the cells' back side to collect reflected and diffused sunlight in order to produce added electricity.

production capacity set at 30MW per year. Expansion is planned in order to meet customer demands.

Suniva ARTisun Select solar cells said to now average 19% efficiency

Suniva revealed that its ARTisun Select series of solar cells are averaging 19% efficiency in plant-wide production. The new cell efficiencies are available to cell customers and have been incorporated into the company's Optimus modules. Suniva additionally noted that it has refined the aesthetic specifications for the cells, including a narrower colour band, which is said to have created a more cosmetically uniform module.

Bruce McPherson, vice president of research and development for Suniva, commented: "With our pioneering proprietary work to produce the ARTisun Select cells, we have overcome the production and cost challenges traditionally associated with high-efficiency manufacturing. We feel confident our select cells will continue to achieve increased production average efficiencies beyond 19.2% during 2012."

SunPower starts commercial production of 24%-efficient Maxeon Gen 3 cell

SunPower's third-generation Maxeon solar cell, which claims world-record efficiencies of up to 24%, has entered commercial production. The all-back contact cell is 160mm^2 in size and features low reverse-bias breakdown voltage and better temperature coefficient, claiming an increase in energy yield in high-temperature environments and in shady, dusty conditions.

Up to 128 of the Maxeon cells will be integrated into SunPower's solar panels to deliver efficiencies of over 20%. The modules will be limited in their availability throughout 2012.

"We're pleased to move our world-record breaking efficiency solar cell from the lab into commercial production," said Tom Werner, SunPower president and CEO. "With the new Maxeon solar cells, offering efficiencies of up to 24%, SunPower continues to lead the industry in technology innovation, delivering to its customers the highest efficiency, most reliable solar panels for guaranteed performance."

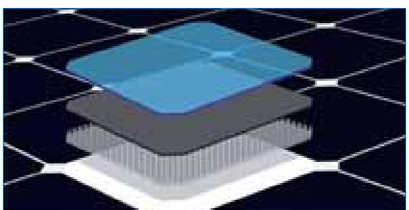

Source: SunPower

SunPower's Maxeon solar cell claims world-record efficiencies of up to 24%.

Business News Focus

Trina Solar picks Applied Materials for second consecutive year as best supplier

Outstanding efforts on new technology development and cost efficiency initiatives has ensured Applied Materials won Trina Solar's 'Outstanding Contribution of the Year 2011 - World Purchasing Award' for the second year in a row. Applied noted that it was the only equipment supplier to be recognised by the integrated PV module manufacturer in its annual awards. One of the key Applied Materials technologies employed by Trina Solar is its Baccini screen-printing technology.

However, NPD Solarbuzz recently reported that Applied Materials could well lose its equipment supplier top spot in 2012. Having relinquished its number one spot in the semiconductor industry last year – the first time in several decades – Applied Materials could also lose its leadership position in the PV industry which has been a 14-quarter reign since 2008.

According to the market research firm, Applied Materials is expected to be overtaken in the revenue stakes in the first half of 2012 by Meyer Burger.

HYET Solar acquires all Helianthos assets from Nuon

HYET Solar, a relatively new company founded by Rombout Swanborn, recently bought all assets of Helianthos from Nuon. The company plans to further develop Helianthos's technology with a team of 15 to 20 employees. HYET advised that its long term goal is to eventually bring the Helianthos flexible solar cell foil to market on a large scale.

Nuon noted that the auctioning of the individual parts of the Helianthos business had already been completed when a final agreement was reached with HYET Solar. Nuon had reserved the right of allotment after auctioning the business's assets in order to keep the possibility of re-launching Helianthos.

BTU International sales up 9.4% but solar equipment orders weak

Thermal processing equipment specialist BTU International expect further weakness for solar equipment orders as the industry continues to be impacted by overcapacity and very low capital expenditure. The company posted a first-quarter 2012 loss of US$2 million, compared to a net loss of US$2.3 million in the preceding quarter on the back of sales that were up 9.4% to US$16.3 million, yet

Source: Trina Solar

One of the key Applied Materials technologies employed by Trina Solar is its Baccini screen-printing technology.

Source: BTU

BTU International's Tritan firing furnace.

down 35.8% compared to US$25.4 million for the same quarter a year ago.

Management noted that equipment sales in the electronics sector was growing but would only partially offset the fall in orders from the PV industry in the second quarter. The company guided second quarter revenue to be in the range of US$14 to US$15 million.

A STAR Institute of Microelectronics and Picosun Oy to partner on new ALD technique development

Research organization A*STAR Institute of Microelectronics (IME) will join forces with Finnish ALD equipment manufacturer Picosun Oy to create new innovative ALD and plasma-enhanced ALD techniques. It is hoped that these new techniques will facilitate continual growth in the solar and next-generation memory sectors.

The primary objective of the partnership will be to enable the integration of industrial devices with the target processes. Other areas targeted for potential development by the joint venture include processes for multilayer metal-insulator-metal (MIM) capacitors, advanced complementary-metal-oxide-semiconductors (CMOS), novel dielectrics and metals for applications in resistive switching non-volatile memories (NVM) as well as processes for solar cells.

Establishing the IME-Picosun partnership ties closely also to the recent opening of Picosun's first Asian subsidiary, Picosun Asia Ltd. in Singapore.

Picosun, an international ALD manufacturer with headquarters in Europe, North America and Asia, has over 35 years' experience in the development and sales of ALD systems. Its ALD equipment is used by various high-profile industries and research institutes around the globe.

Source: Picosun

Picosun's ALD process tools.

European Union awards €10m to solar cell research consortium

The University of Luxembourg's Laboratory of Photovoltaics has received a sizable grant to develop technologies for more efficient and cheaper solar cells. The University is part of a consortium of 14 partners, known as the Scalenano project, which has been awarded €10 million by the European Union. The project has just begun and will run until 2015.

Led by Dr. Phillip Dale, Head of the Electrodeposition Group at Luxembourg's Laboratory of Photovoltaics, the Scalenano project will use cutting-edge research tools to specifically examine how to improve the process of solar cell development in order to reduce production costs.

"Our main objective is to develop low cost and efficient solar cell technology. Increasing the competitiveness of this technology will bring the cost down for everyone, which will eventually allow solar technology to reach the masses," explained Dr. Dale.

The Scalenano project consortium includes the Catalonia Institute for Energy Research, EMPA- Swiss Federal Laboratories Materials Science and Technology, Istituto Italiano di Tecnologia, Commissariat àl'Energie Atomique et aux Energies Alternatives, Helmholtz Zentrum Berlin, the University of Nottingham, University of Luxembourg, Scuola Universitaria Professionale della Svizzera Italiana, Free University Berlin, Merck KGaA, Nexcis Photovoltaic Technology, Innovative Materials Processing Technologies Ltd. and Semilab.

Source: Flickr

The consortium of 14 partners, known as the Scalenano project, has been awarded €10 million by the European Union.

Product Reviews

centrotherm

centrotherm offers upgrade package for 20% cell conversion efficiencies

Product Outline: centrotherm photovoltaics is offering an upgrade package for its centaurus technology, combining a selective emitter with a dielectric passivated backside, already blended with fine line printing, reducing paste consumption of the front side silver paste by more than 20%.

Problem: The performance of present standard industrial solar cells with extensive screen printed Al-BSF backside is limited by both rear surface recombination velocity and low internal reflection of the Al-backside. Outweighing these limitations by backside passivation concepts is generally associated with a high degree of risk and effort caused by new process and material developments.

Solution: centrotherm has developed a solar cell rear side technology with local Al-BSF in combination with a dielectric reflector. The reduced surface recombination velocity increases the V_{oc} by more than 10mV. The improvement of the internal light reflection for long wavelengths leads to a gain in J_{sc} of about 1.5mA/cm^2. Both effects are claimed to lead to an overall efficiency improvement of about 1% (absolute), allowing average production efficiencies of more than 19.5%.

Applications: Upgrade package for centrotherm photovoltaics centaurus technology, which combines a selective emitter with a dielectric passivated backside.

Platform: In addition to the laser tool for selective emitter, three additional tools are required: for the formation of the rear dielectric layer, centrotherm's PEVCD system; a laser tool to ablate the local BSF fraction of the dielectric layer and an additional wet chemical tool is needed to smooth the rear side for optimal reflection and passivation.

Availability: April 2012 onwards.

Engineered Conductive Materials

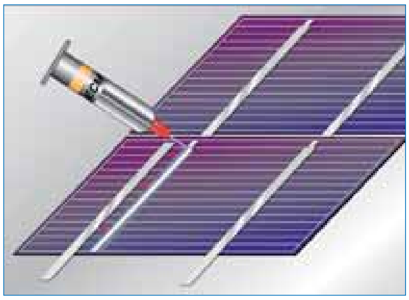

ECM's spot curing conductive adhesive DB-1590 designed for thin wafers

Product Outline: Engineered Conductive Materials (ECM) has introduced a fast curing conductive adhesive, DB-1590, for use as a solder replacement in next-generation crystalline silicon solar modules using thinned silicon and/or plated bus bars. This material formulation has been optimized to provide improved conductivity and stability on various substrates when cured at 200°C.

Problem: Thinner wafers are more susceptible to high-temperature processes that could possibly cause excess bending, warping or cracking. Faster curing times and low temperatures could also improve process throughput and lower production costs and support the migration to thinner, sub-180 micron wafers.

Solution: DB-1590 is designed to gel in five seconds or less at 200°C, developing sufficient strength to withstand the applied stresses induced by the manufacturing process until the adhesive cure is completed during the encapsulant lamination process. DB-1590 has optimized rheology for dispensing, improved damp heat resistance and conductivity stability on tin, tin-silver and silver-plated ribbons. DB-1590 is also stable on OSP treated copper and nickel bus bars.

Applications: The DB-1590 features a rubber-like flexibility that is designed for flexible photovoltaic applications.

Platform: DB-1590 is the latest addition to Engineered Conductive Materials' full line of conductive stringer attach adhesives, conductive adhesives for back contact crystalline silicon, thin-film and via fill applications, as well as conductive grid inks for photovoltaic applications.

Availability: April 2012 onwards.

Konica Minolta

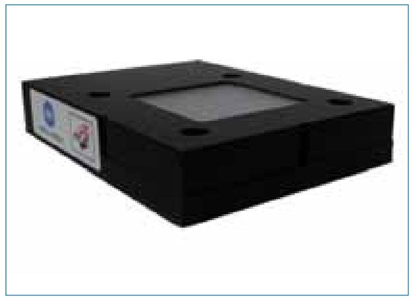

Konica Minolta's triple-junction solar reference cells for spectral mismatch suppression

Product Outline: Developed in conjunction with the National Institute of Advanced Industrial Science and Technology in Japan, Konica Minolta Sensing Americas has launched the first triple-junction solar reference cells: AK-120/130/140. Spectral mismatch, which had been a major problem with conventional cells, can be suppressed to 1% or less even when evaluating solar cell performance using JIS C-8942 Class C solar simulators, according to the company.

Problem: In general, reference standard cells using optical filters have low durability against exposure to light, resulting in changes in characteristics. AK Series reference cells have a high durability against exposure to light, greatly reducing solarization, ensuring stability even when used over a long period of time.

Solution: The AK-120/130/140 is a completely integrated cell with connectors for I−V and temperature measurement. The built-in temperature sensor can be connected to a commercially available temperature controlled stage to easily achieve and maintain the standard test condition of 25°C. Also included are short-circuit current (I_{sc}) values used for solar simulator adjustment. Errors in I_{sc}, due to multiple reflections, are greatly reduced. Improvements in the optical structure suppress multiple reflections and reduce the 1.3% error of conventional products to 0.0%.

Applications: Triple-junction solar reference cells.

Platform: The AK-140 can be used with the AK-120 and AK-130 for triple-junction cells or as a standalone reference. All AK Series reference PV cells come ready to use with a PT-100 temperature sensor and a test report of I_{sc}. They can also be delivered with calibration traceable to AIST.

Availability: April 2012 onwards.

Product Reviews

Manz AG

New chemical edge isolation tool from Manz offers higher process stability

Product Outline: Manz AG's IPSG CEI 4800 is designed for chemical edge isolation (CEI) and phosphor silicate glass (PSG) post process removal. The tool is capable of handling 4800 wafers per hour.

Problem: Wet chemistry isolation is accomplished by the rear side and edges of the wafer being coated in a HF-based chemistry, due to the surface of the emitter layer on the front side not being exposed to the etchant. Wafers are coated with a thin layer of silicon nitride which improves device reliability and serves as an anti-reflection layer. Combining wet chemical processes in short sequential phases provides greater process control and improved throughput for lower production costs.

Solution: The IPSG CEI 4800 is specifically designed to remove the highly doped layer from the backside and the edges of a wafer, thereby producing a chemical edge isolation. In a second process step, the remaining phosphor silicate glass layer on the front side of the wafer that was created during the previous diffusion process step is removed. The newly developed soft sponge roller process concept enables faster inline transportation speeds and ensures at the same time higher process stability combined with gentle wafer handling.

Applications: Crystalline silicon wafer PSG removal process.

Platform: The machine will be sold as a bundle with the Manz SpeedPicker for loading and unloading.

Availability: May 2012 onwards.

SoLayTec

SoLayTec Lab to Fab solution offers superior passivation and high flexibility

Product Outline: SoLayTec has introduced its Process Development Tool for ultrafast ALD for depositing Al_2O_3. The tool is said to be capable of a highly effective surface passivation of the cell (front and rear) with a throughput of 100wph.

Problem: Leading research institutes have recently reported superior solar cell passivation properties of thin aluminium oxide layers grown by ALD. However, no cost-effective production tool has been available for high-volume ALD deposition for solar manufacturing applications.

Solution: SoLayTec's ALD PDT can process about 100wph of 10nm thickness due to a deposition rate of 0.5nm/second. Process parameters, like layer thickness, temperature, concentration TMAl and H_2O and amount of flows can be changed very easily. In parallel, SoLayTec is developing its lab to fab solution with a claimed lowest cost of ownership for aluminium oxide deposition, which is called the High Volume Tool (3,600wph). This tool is expected to be ready by the end of 2012.

Applications: The passivation can be used for front and rear side passivation for p- and n-type cells. The passivation of low resistivity p-type silicon by the negative charge dielectric aluminium oxide is confirmed at the device level by an independently confirmed energy conversion efficiency of 20.6%.

Platform: The PDT is a cassette-to-cassette system, with wafers floating on air from left to right and pass the injector head. At this the point, the layer is created by spatial ALD under atmospheric pressure.

Availability: March 2012; a high-volume tool is expected by the end of 2012.

Sun Chemical

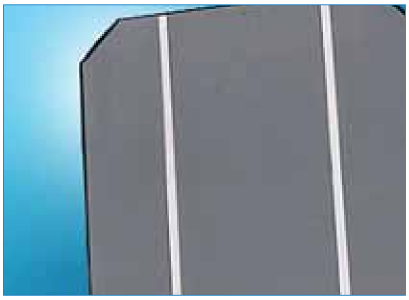

Sun Chemical offers one-stop shop for solar cell metallization solutions

Product Outline: Sun Chemical is showcasing a broad range of metallization solutions for both additive and subtractive processes as well as module materials for use in the crystalline silicon (c-Si), thin-film, printed electronics and other emerging markets at global events this year.

Problem: Solar cell manufacturers are continually searching for new ways to reduce the cost of solar cells in both additive and subtractive processes for metallization pastes, insulators and resists.

Solution: One of the key products being featured includes SunTronic Cellmet Aluminum metal pastes, formulated for screen-printing processes. Cellmet 437 was developed for use as the back electrode on mono-or multicrystalline silicon solar cells 180-220mm thick. These low bow, green environmental and health hazard friendly aluminium pastes are specially designed to form p+ doped layers when fired on a p-doped silicon PV device. This paste has been optimized to eliminate Al bead formation during the firing process and has been optimized to be co-fireable with Sun Chemical's front side and back side silver metallization pastes.

Applications: Back-surface electrode on mono-or multicrystalline silicon solar cells.

Platform: Cellmet 437 is fritted using an environmentally friendly lead- and cadmium-free glass composition and can be fired over a broad range of conditions including co-fire process techniques with front contact silver inks.

Availability: Currently available.

Challenges for single-side chemical processing

Jochen Rentsch, **Rupprecht Ackermann**, **Gero Kästner**, **Christoph Schwab**, **Martin Zimmer** & **Ralf Preu**, Fraunhofer ISE, Freiburg, Germany

ABSTRACT
Wet chemical process equipment is widely used in industrial solar cell production, and inline etching systems in particular have attracted more and more attention since their introduction 10 years ago. The horizontal wafer transport within these systems has made it possible to think about single-side wafer treatments even for wet chemical process applications. Since its market introduction in 2004, the chemical edge isolation process based on the single-side removal of the parasitic emitter at the rear side of the solar cells has gained an increasing share of the market in comparison to competing technologies that use laser techniques. However, stabilization and control of such a process under mass production conditions remains challenging. The introduction of new high-efficiency cell concepts involving passivated rear sides will increase the importance of single-side wafer treatments, as the final solar cell performance is significantly affected not only by the complete removal of the parasitic emitter but also by an ideally polished surface on the rear side of the wafer.

Introduction

Single-side wet chemical processing techniques are gaining importance in industrial solar cell manufacturing as they increasingly replace the once widely used laser technologies, especially for edge isolation [1,2]. Performed directly after emitter diffusion, the wet chemical process completely or partly removes the parasitic emitter from the wafer's rear side and edges. For standard screen-printed solar cells, this means that the aluminium-alloyed rear no longer has to overcome the phosphorus diffusion on the rear of the solar cell in order to create an alloyed aluminium/silicon back-surface field (BSF) layer, which is the requirement for plasma or laser-edge junction isolation. A higher quality BSF can therefore be obtained, leading to higher efficiencies. By removing the emitter from the rear of the cell, chemical edge isolation is compatible with the development of future cell technologies that do not utilize screen-printed contacts and require single-sided diffusions. Inline etching systems with acidic etch chemistry based on HF/HNO_3 are typically used, resulting in a surface that is still rough [3]. An industrially applicable etching process for single-side emitter removal must therefore fulfil several requirements:

- Etch back of the emitter layer at the cell's rear side is homogeneous
- The process is completely single sided
- Process conditions are stable in order to create a robust process

Because of the use of thinner wafers and the goal of achieving higher conversion efficiencies, future industrial solar cell concepts are mainly based on the use of rear passivation concepts and local rear contacts (PERC concept) [4–6]. Besides the different passivation and metallization techniques used, single-side removal of the parasitic emitter layer, as well as surface cleaning issues at the cell's rear, turns out to be a key technology step for an industrial realization. Depending on the actual process scheme, dry or wet chemical etching and conditioning approaches might be preferable. In high-efficiency laboratory processes, the solar cell's rear is usually polished to reach optimum passivation quality; the polishing itself, however, is often achieved by additional masking of the non-etched wafer side. Transferring such a polishing process into mass production is a very challenging proposition, as will be discussed in the following sections.

This paper reviews different possibilities for the technical realization of single-side wet chemical etching processes, as well as summarizing the challenges for implementation and quality assurance of wet chemical edge isolation and chemical polishing processes.

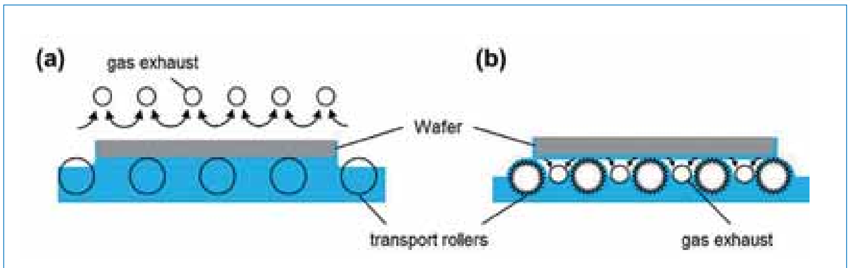

Figure 1. Two different basic principles for the single-side wet chemical etching process: (a) the wafer is 'floating' on the surface of the etching solution; (b) the transport rollers themselves are supplying the wafer surface with fresh etching solution from the bath.

Technical realization of single-side processes

On the equipment market today, it is mainly horizontal processing solutions within industrially suitable inline etching systems that are available for single-side wet chemical etching applications. As etching solutions, diluted acidic chemicals with the main components hydrogen fluoride (HF) and nitric acid are commonly used. To suppress the strong etching reaction, as well controlling the viscosity of the solution, additives such as sulphuric or acetic acid might be added. As the etching in those acidic mixtures is strongly exothermic, constant cooling of the overall etching bath has to be ensured in order to control the process and to minimize the resulting reaction gases. To implement the etching sequence within these inline systems and to maintain the single-sidedness, two basic etching principles can be distinguished (see Fig. 1):

(a) The silicon wafer is transported on the surface of an etching bath. The liquid surface of the etching bath is regulated in such a way that a small gap of a few millimetres is formed between the wafer and the liquid surface. With the correct distance attained, the wafer itself enables the adhesion of the liquid to the wafer. The resulting meniscus of the solution towards the wafer surface should not collapse during the etching process; on the other hand, dipping of the wafer into the solution has to be avoided. In order to avoid a wrap-around of reaction gases (HF, nitrous oxides), gas exhaust lines are typically installed above the wafer surface.

(b) The wafer is transported via 'wetted' transport rollers. In this case a homogeneous liquid film on the rollers has to be ensured in order to enable sufficient fresh media supply to the wafer's surface. The amount of etching solution that can be brought to the wafer surface by this method typically depends on, for example, the transport velocity, the viscosity of the etching solution and the overall liquid surface level in which the rollers are immersed. The resulting reaction gases can be drawn off between the rollers, directly at the wafer surface.

Most existing etching systems on the market rely on one of the above-mentioned etching principles, and often the available systems can only be distinguished by the types of roller material, different transport mechanisms or gas exhaust set-ups.

"A major challenge of the chemical edge isolation process is ensuring that the front emitter remains dry throughout the process while the rear is etched."

Chemical edge isolation

A major challenge of the chemical edge isolation process is ensuring that the front emitter remains dry throughout the process while the rear is etched. This requirement is even more challenging due to the fact that, typically, the chemical etch is done directly after emitter diffusion, with the phosphorus silicate glass layer still present on all wafer surfaces. That results in an overall hydrophilic surface, which, on the one hand, alleviates the homogeneous distribution of the etching solution on the rear side, but, on the other hand, also promotes a wrap-around of the etching solution towards the front-emitter side of the wafer. The latter effect is even more critical because the emitter has to be properly removed not only on the rear side but also on the wafer edges; this is illustrated in Fig. 2. In the case when the emitter is not sufficiently removed from the wafer edge, potential edge disturbances, already caused during wafering, are not separated from the front-side emitter. Minority charge carriers which are generated near the wafer edge are therefore more likely to recombine at these recombination centres than to be collected from the front emitter. Total removal of the emitter layer from the wafer edge, together with an effective SiN_x anti-reflection and passivation layer, suppresses such an effect.

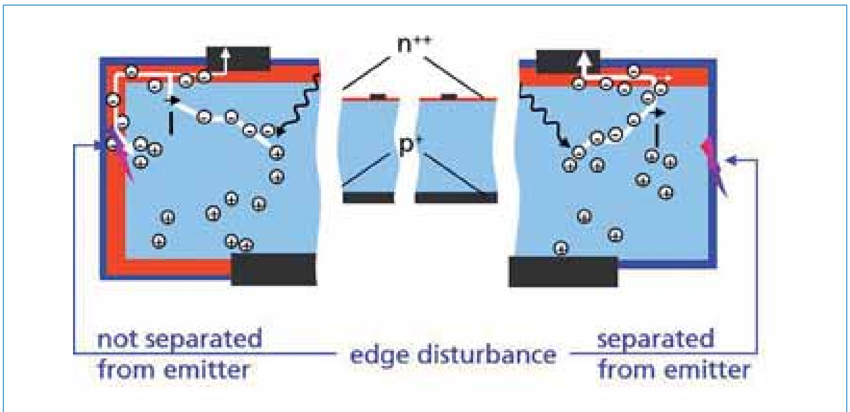

Figure 2. Sketch of the wafer-edge region: with the emitter layer (left), and without it (right).

For the implementation of the chemical edge isolation process, a number of parameters have to be optimized in order to obtain a robust production process. Many process settings are closely related to each other: for example, in general an etch depth of around 0.6µm should be sufficient for the removal of a standard industrial emitter layer. However, that would assume a totally homogeneous etch rate throughout the whole wafer surface. As this is not typically achieved, the etch depth has to be slightly increased to a value of around 1µm. Increasing the etch depth can usually be realized by extending the etching time. The easiest method of controlling the etch depth, however, is changing the transport speed, but this does not work for single-side etching processes. Owing to the etching mechanisms discussed earlier, the transport speed might already influence the formation of the liquid meniscus towards the wafer surface in the case of principle (a), or affect the amount of etching solution transported via the rollers in the case of principle (b). Moreover, the overall transport speed typically represents a fixed parameter in an industrial production line; the variation of the etch depth, therefore, has to be adjusted either by the temperature or by the composition of the etching solution itself.

Besides the challenges of establishing and controlling the etching process itself, quality assessment as process control also tends to be critical. To decide whether the process has been carried out successfully, the corresponding sheet-resistance distributions at the wafer's front emitter side as well as at the rear side have to be controlled. As mentioned earlier, for chemical edge isolation, it is important to characterize in particular the wafer-edge regions. However, to characterize the sheet resistance in the near-edge region (e.g. using the well-known 4-point probe measurement technique), the edge itself has a highly detrimental effect on the results. Fig. 3 shows 4-point probe track measurements of the front side of a wafer after chemical edge isolation. The measurements were carried out on all four sides of the wafer by measuring a track of 30mm towards the wafer edge. In all cases,

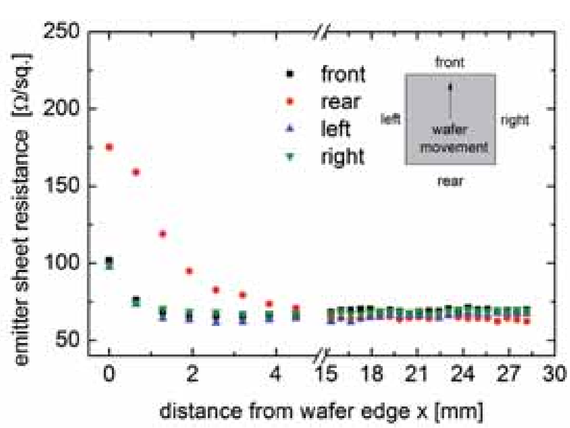

Figure 3. 4-point probe line scan measurements, taken on the four different sides of the wafer, of the front emitter after chemical edge isolation.

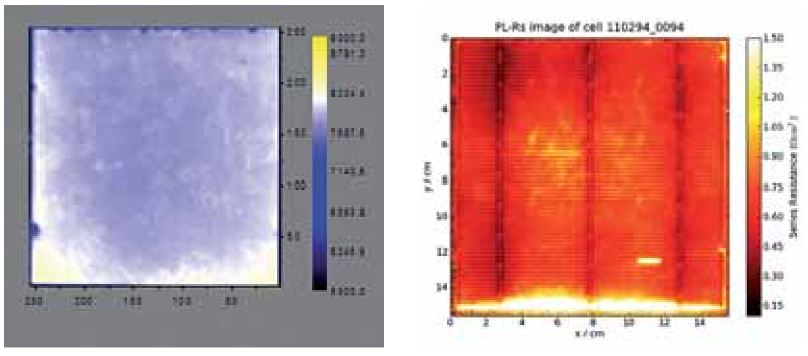

Figure 4. Left: sheet resistance imaging (SRI) of a front emitter layer after chemical edge isolation. Right: series resistance image of a finished solar cell using the C-DCR technique [9].

an increase in emitter sheet resistance was observed when approaching the edge.

In order to understand such an increase in sheet resistance, the basic principles of a 4-point probe measurement technique have to be kept in mind. This technique is typically used for homogeneous layers, as the assumed geometrical current distribution underneath the contacts only holds true in that particular case. However, as one approaches a non-conducting wafer-edge region, this assumption is no longer valid. The current distribution is confined by the edge itself, and the measured voltage (and therefore the resulting resistance) is significantly increased because of the smaller available area. In the case of a conducting wafer edge (i.e. where an emitter layer still exists on the wafer edge), current might also flow around the edge, resulting in an actual lower voltage and therefore in a lower sheet resistance. It is possible to show that, up to a distance of about 3mm from the wafer edge, sheet resistance values can be determined with sufficient measurement accuracy.

For the measurement example in Fig. 3, the observed increase of the emitter sheet resistance on all four wafer sides therefore demonstrates the removal of the emitter from the wafer edge (i.e. the case of a non-conducting wafer edge). On the other hand, there are differences in the increases in sheet resistance between the wafer sides. Whereas the front, as well as the left and right sides of the wafer's front emitter (in the direction of the wafer movement through the etching bath), seems to be undisturbed in terms of resistance, there is a significant increase in sheet resistance observable at the rear side of the wafer. Such an increase is often observed and can be attributed either to an actual etching media wrap-around (in the case of a textured front side, often capillary forces alleviate such a wrap-around) or to reaction gases that are concentrated especially at the wafer's rear side. In both cases, the phosphorus silicate glass layer still present on the front surface is no longer able to sufficiently protect the emitter layer. In order to analyze these effects further, spatially resolved measurement techniques are necessary to localize the affected wafer areas.

Fig. 4 presents two different possible inline-capable measurement techniques.

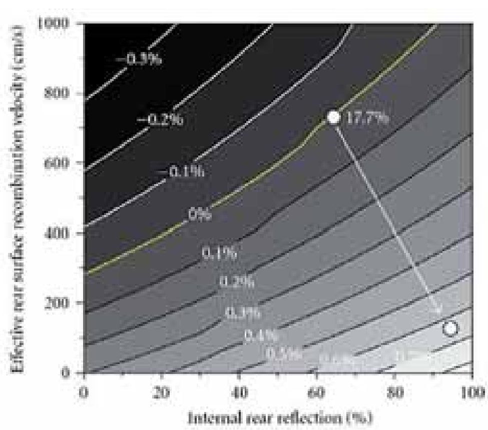

Credit: Glunz [11].

Figure 5. Changes in efficiency due to variation of the surface recombination at the rear surface S_{rear} and the internal reflection R_{back}. The point marked on the 0% isoline (yellow) represents a 220µm-thick industrial solar cell with 60Ω/sq emitter and Al-BSF on 1Ωcm monocrystalline silicon. The second point relates to a rear-passivated and locally contacted (PERC) solar cell with the same front side.

The first method (Fig. 4, left) is the so-called sheet resistance imaging (SRI) [7], which can be carried out directly after the etching process. This method gives an initial overview of the homogeneity of the resulting emitter sheet resistance; unfortunately, no calibration is as yet available between the measurement signal and the real sheet resistance, so only quantitative information can be extracted. The measurement clearly indicates areas of higher emitter sheet-resistance (darker blue regions) and can therefore help to localize areas of stronger etch attack during chemical edge isolation.

For a final cell analysis, luminescence images of silicon solar cells are useful, since they contain information about local recombination properties and local series resistance. The increase in series resistance due to the detrimental effect of the etch attack on the front-side emitter can be visualized and qualitatively evaluated (Fig. 4, right) using a fast method based on photoluminescence imaging for a spatially resolved coupled determination of the dark saturation current and series resistance (C-DCR) [8].

In principle, all the measurement techniques presented could also be realized as inline measurements; however, only sheet resistance measurements are widely accepted as a quality assurance tool in standard industrial production lines. Imaging methods such as SRI or luminescence methods may provide a much more detailed data set of the process outcome, but further research in this area is needed to extract more quantitative information.

> "Not only is the removal of the parasitic emitter layer at the rear side necessary, but also the rear surface of the wafer must be polished."

Rear-side polishing

For high-efficiency, all-side-passivated solar cell concepts, not only is the removal of the parasitic emitter layer at the rear side necessary, but also the rear surface of the wafer must be polished in order to optimize the electrical quality of the rear passivation layer and to facilitate effective light trapping within the solar cell bulk [10]. Such an approach is becoming even more important as wafer thicknesses decrease, since the passivation quality needs to be improved because of the increased surface-to-volume ratio. Additionally, the path length of the light inside the wafer is shortened for thinner

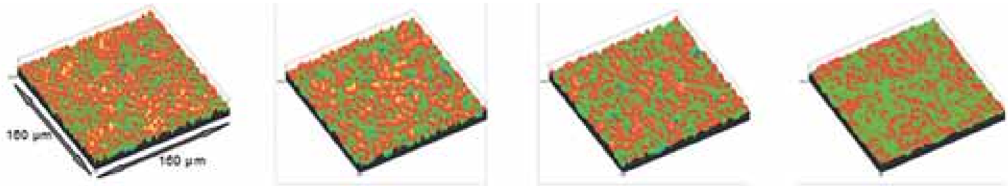

As textured $f_S = 1.64$ | Low removal $f_S = 1.24$ | Medium removal $f_S = 1.14$ | High removal $f_S = 1.03$

Figure 6. Resulting surface topography and surface enlargement factor f_S measured by confocal microscopy after different polishing processes with increasing amount of etch (from left to right), starting from a surface that was originally alkaline textured [13].

wafers, so out-coupling of light at the rear interface needs to be minimized. The influence of the corresponding physical parameters of the solar cell – the surface recombination velocity S_{rear} (electrical quality of the passivated surface) and the internal reflection R_{back} (optical quality of the rear interface) to the conversion efficiency – is shown in Fig. 5 [11].

The implementation of a polishing process for the wafer's rear side would ideally be combined with the single-side chemical edge isolation step to remove the parasitic emitter on the rear surface. Etching mixtures for polishing purposes, although also mostly acidic, usually have a much higher concentration of HF and HNO_3 than typical mixtures used for chemical edge isolation. The challenges concerning etch media and reaction gas wrap-around effects that were mentioned earlier are therefore even more distinctive for the polishing process. For that reason, at the moment the polishing can only be implemented in a solar cell process sequence before emitter diffusion, directly after texturing [12]. But, as the parasitic emitter removal at the rear side would still be necessary for the production of a rear-passivated and locally contacted (PERC) solar cell, two single-side process steps are currently still required.

The polishing, however, entails different requirements for the etching process when the original texture (either alkaline or acidic for a typical two-sided texturing process) needs to be flattened. In order to obtain a truly polished surface from an originally alkaline-textured surface, it is necessary to etch off almost 20µm of silicon (see Fig. 6). The decrease in the surface enlargement factor f_S with increasing etch depth is clearly demonstrated in Fig. 6 for surfaces that have been pre-textured differently. Due to the variation in morphology of acidic- and alkaline-textured surfaces, the required amount of silicon to be removed differs: 3–5µm silicon removal should be sufficient to polish the rear of an acidic-textured surface; in the case of alkaline-textured surfaces, 10µm or more will be necessary in order to achieve a target of around 10% surface area enlargement (medium removal in Fig. 6).

A major drawback of implementing such a process step, especially with monocrystalline silicon wafers, is the fact that such an etch depth results in a significant thinning of the overall wafer. Nevertheless, *I-V* data of PERC type solar cells, when a rear polish process is applied with different silicon removal rates, demonstrate the efficiency improvement potential of such a process (see Table 1). An overall efficiency gain of more than 2% absolute could be realized by implementing the rear polishing process. The large increases in V_{oc} and J_{sc} demonstrate the improved electrical (low S_{rear}) and optical (high R_{back}) performance of the solar cell's rear side, independent of the choice of passivation layer (the same results were obtained with either thermal oxidation or PECVD AlO_x passivation).

These results provide initial evidence that a polished rear surface yields a high passivation quality for PERC-type solar cells. Further progress in process optimization (particularly by technologically solving the detrimental wrap-around effects) might also allow a future combination of rear polishing and chemical edge isolation within one process step.

"These results provide initial evidence that a polished rear surface yields a high passivation quality for PERC-type solar cells."

Si removal (no. of cells)	Passivation	f_S	V_{oc} [mV]	J_{sc} [mA/cm^2]	*FF* [%]	η [%]
As textured (6)	SiO_2	1.64	618	36.9	75.4	17.2*
Low removal (5)	SiO_2	1.24	646	38.5	74.9	18.6*
Medium removal (5)	SiO_2	1.14	646	38.7	76.2	19.0*
Medium removal (7)	AlO_x	1.14	644	38.7	76.0	19.0*
High removal (6)	SiO_2	1.03	649	39.0	76.7	**19.4***
Best cell, stabilized	SiO_2	1.03	646	38.6	77.2	**19.3****

*Measured on an industrial cell tester after processing.
**Confirmed by Fraunhofer CalLab.

Table 1. Surface enlargement factor f_S extracted from confocal microscopy measurements, and the median values of the *I-V* parameters of the best firing group as a function of the Si removal. Total cell area is ~239cm^2. The best cell after degradation for 24 hours under illumination of approximately 0.6 suns is indicated. (The highest efficiencies achieved are highlighted in bold.)

Conclusion

Single-side wet chemical etching processes are increasingly being utilized in industrial manufacturing of crystalline silicon solar cells, mainly for chemical edge isolation. Independent of the individual technological realization, keeping the single-sidedness of the process remains the major challenge of this approach. Liquid media and/or reaction gas wrap-around effects have a strong influence on the performance of the front-side emitter layer and have to be strictly avoided. Common measurement techniques need to be adapted in order to correctly interpret the measurement results. The challenge becomes even greater when the single-side etching process must not only remove the parasitic emitter layer at the rear surface, but also provide an effective polishing of the surface. These processes, mandatory for many rear-passivated and locally contacted high-efficiency cell concepts, represent a key factor in improving the electrical and optical qualities of the rear side of a solar cell.

References

[1] Delahaye, F. et al. 2004, "Edge isolation: Innovative inline wet processing – ready for industrial production", *Proc. 19th EU PVSEC*, Paris, France.

[2] Löhmann, M. & Delahaye, F. 2007, "Report on industrial use of inline wet edge isolation for solar cell production", *Proc. 22nd EU PVSEC*, Milan, Italy.

[3] Melnyk, I. et al. 2005, "High throughput in-line acidic texturisation and edge isolation: An industrial reality", *Proc. 20th EU PVSEC*, Barcelona, Spain.

[4] Swanson, R.M. & Sinton, R.A. 1986, "Point contact silicon solar cells", *Proc. 7th EU PVSEC*, Seville, Spain.

[5] Schultz, O., Glunz, S.W. & Willeke, G.P. 2004, "Multicrystalline silicon solar cells exceeding 20% efficiency", *Prog. Photovolt: Res. Appl.*, Vol. 12, No. 7, pp. 553–558.

[6] Gautero, L. et al. 2010, "Comparison of different rear contacting approaches for industrial PERC solar cells on MC-SI wafer", *Proc. 25th EU PVSEC*, Valencia, Spain.

[7] Isenberg, J., Biro, D. & Warta, W. 2004, "Fast, contactless and spatially resolved measurement of sheet resistance by an infrared method", *Prog. Photovolt: Res. Appl.*, Vol. 12, No. 7, pp. 539–552.

[8] Glatthaar, M. et al. 2009, Spatially resolved determination of the dark saturation current of silicon solar cells from electroluminescence images", *J. Appl. Phys.*, Vol. 105, p. 113110.

[9] Glatthaar, M. et al. 2010, "Spatially resolved determination of dark saturation current and series resistance of silicon solar cells", *physica status solidi (RRL)*, Vol. 4, No. 1, pp. 13–15.

[10] Angermann, H., Henrion, W. & Röseler, A. 2001, "Wet-chemical conditioning of silicon: Electronic properties correlated with the surface morphology", in *Silicon-Based Materials and Devices*, Nalwa, H.S., Ed. San Diego, CA: Academic Press, pp. 267–298.

[11] Glunz, S.W. 2007, "High-efficiency crystalline silicon solar cells", *Adv. in OptoElec.*, Vol. 2007, pp. 1–15.

[12] Queisser, S. et al. 2009, "Inline single side polishing and junction isolation for rear side passivated solar cells", *Proc. 24th EU PVSEC*, Hamburg, Germany.

[13] Schwab, C. et al. 2012, "Passivation of inline wet chemically polished surfaces for industrial PERC devices", submitted to *Energy Procedia*.

About the Authors

Jochen Rentsch is the head of the Wet Chemical and Plasma Technologies / Process Transfer department at Fraunhofer ISE. He received a diploma degree in physics in 2002 from the Technical University of Braunschweig, Germany, and a Ph.D. degree in physics in 2005 from Albert-Ludwigs University of Freiburg, Germany. Jochen's current research activities at Fraunhofer ISE focus on innovative wet chemical and plasma technologies and their application to industrial solar cell processing.

Rupprecht Ackermann received his diploma in chemistry in 1998 from the University of Freiburg, Germany. He completed his Ph.D. in 2001 in the field of inorganic solid-state chemistry at the same university, and joined Fraunhofer ISE in 2009. Working in the department of Wet Chemical and Plasma Technologies at ISE, Rupprecht currently focuses on chemical edge isolation and emitter etch back.

Gero Kästner was awarded a diploma in process and environmental engineering by the University of Applied Science, Offenburg, in 2006. He joined Fraunhofer ISE in 2008 and currently works in the department of Wet Chemical and Plasma Technologies, where he specializes in process development, systems engineering and facility management. Gero has been a student in the master's programme in photovoltaics at the University of Freiburg since 2010.

Martin Zimmer is head of the "wet chemical processes and analytics" group. In 2005, he received his diploma in chemistry from the Ruprecht-Karl's-University, Heidelberg, specializing in spectroscopic methods for microbiological applications. He joined Fraunhofer ISE in 2006 and finished his Ph.D. 2011 in the field of wet chemical analysis and process development within the department for Wet Chemical and Plasma Technologies of ISE.

Ralf Preu is the director of the Division for PV Production Technology and Quality Assurance at Fraunhofer ISE. Ralf received a diploma degree in physics in 1996 from the University of Freiburg, Germany, followed by a Ph.D. in electrical engineering in 2000 and a diploma degree in economics in 2003 from the University of Hagen.

Enquiries

Dr. Jochen Rentsch
Fraunhofer ISE
Heidenhofstrasse 2
D-79110 Freiburg
Germany
Tel: +49 761 4588 5199
Email: jochen.rentsch@ise.fraunhofer.de

Solutions used in the texturization of monocrystalline silicon

Jose N. Ximello-Quiebras, **Johannes Junge**, **Sven Seren & Giso Hahn**, Department of Physics, University of Konstanz, Konstanz, & **Ernst Epple**, Lotus Systems GmbH, Geisingen, Germany

ABSTRACT

Texturization of (100) monocrystalline silicon (mono-Si) for solar cells is still an issue in the industrial production of standard screen-printed mono-Si solar cells. This fact is due to the properties of isopropyl alcohol (IPA), which is used together with potassium hydroxide (KOH) in the standard etching solution KOH-IPA (or used with sodium hydroxide NaOH in NaOH-IPA). The low boiling point of IPA (82.4°C) limits the etching temperature and thus the processing speed. Furthermore, KOH-IPA etching solution is very sensitive to the wafer pre-treatment characteristics of as-cut mono-Si wafers. Two ways to overcome these disadvantages are presented in this paper. The first approach involves the use of a high boiling alcohol (HBA) instead of IPA in the standard KOH-IPA etching solution. This allows higher etching temperatures to be used, without evaporation losses of the alcohol, but with reduced etching times. The second approach consists of using a closed etching bath in which vacuum (low-pressure) steps (i.e. pressure oscillations between atmospheric and below-atmospheric pressure) are achievable; in addition, a cooling system located on top of the etching bath allows the liquefaction of the evaporated IPA. The second texturing approach considerably decreases the etching time of mono-Si wafers. Examples of mono-Si wafers were textured using the new KOH-HBA etching solution and then processed into solar cells; the current-voltage results of the processed solar cells are presented.

Introduction

The industrial production of standard screen-printed (p-type) monocrystalline silicon (mono-Si) solar cells consists of a relatively small number of process steps. It begins with the texturization of the as-cut mono-Si wafers. In this first step, by using an aqueous solution of potassium hydroxide (KOH) and isopropyl alcohol (IPA), the saw damage is removed and a random pyramidal texture is produced on both wafer surfaces – the pyramidal texture decreases the total light reflection of mono-Si wafers. After that, a phosphorus ($POCl_3$) diffusion on textured mono-Si wafers is carried out in order to form the emitter (n-type region). Then, by using (for example) the plasma etching method, the edges of the silicon wafers are removed in order to electrically isolate the front side (n-type) from the bulk of the wafer (p-type). Subsequently, a thin film of hydrogenated silicon nitride (SiN_x:H) is deposited on the front side of the wafer using the plasma-enhanced chemical vapour deposition (PECVD) process in order to further decrease the total light reflection and to passivate the front surface. Front silver and back aluminium contacts are printed by using screen printing. Finally, a firing step is used to sinter the metal contacts and establish good front and back contacts. After completion, the solar cells are characterized by current-voltage measurements under AM1.5 illumination conditions [1].

Besides the chemical etching method used [2,3] to texture mono-Si wafers, texturing can be carried out through mechanical grooving [4], laser grooving [5] or plasma etching [6]. Out of these methods, chemical etching is the only one that allows a random pyramid structure because of the anisotropy of the chemical etching process. Here anisotropy means that the etch rate depends on crystal orientation of the mono-Si wafer [7]. The wet chemical texturization process of mono-Si wafers is mainly carried out using an aqueous solution of deionized water, IPA and potassium hydroxide (KOH). The etching solution is heated to a temperature of 80°C and the silicon wafers are placed in it. After approximately 30 min of etching time, the silicon surface (on both sides) is covered with small pyramids (size ≈ 10µm), referred to as a pyramidal texture, and about 10µm of silicon is removed from each side of the silicon wafers. This etching process is well known in the photovoltaic industry as the standard KOH-IPA texturization process for mono-Si wafers. Although this chemical etching method is well established in industrial production of screen-printed mono-Si solar cells, new developments in the wafering processes hinder the effectiveness of the standard KOH-IPA etching solution, as will be explained below.

Because the photovoltaic community is always trying to decrease the cost of solar cells, and therefore the price of solar electricity, new approaches have been tried in order to achieve this goal. For example, the thickness of Si wafers has been reduced (from 240µm to currently around 180µm), and new improved wire-sawing technologies for cutting silicon ingots have been introduced. Thus, less silicon is wasted during the cutting of silicon ingots. But, unfortunately, both the sawing method used for the cutting process and the washing/cleaning procedure employed vary between the different silicon wafer producers, which means that as-cut silicon wafers show different surface characteristics [8]. As a consequence, the same standard KOH-IPA solution cannot be used for all types of as-cut silicon wafers, because the KOH-IPA solution is very sensitive to the surface characteristics of the wafers [9]. Because of the constant evaporation of IPA during the etching process, another disadvantage of the KOH-IPA solution is the cost of replenishing the IPA.

In order to overcome these disadvantages, the search for a substitute for IPA in the aqueous solution of KOH-IPA is a topic of current investigation in the photovoltaic community. To this end, some efforts have been made in the last few years and some of them have been successfully carried over to the mass production of solar cells. For example, Birmann et al. [10] used 1,4-cyclohexanediol instead of IPA. Because of the high boiling point of the alcohol, an etching temperature of 90°C was used, and therefore the etching time was reduced to 10 min; additionally, the pyramid size was decreased. Wijekoom et al. [11] used a polymer (with a boiling point above 100°C) as a substitute for IPA. By using the new additive in the etching solution, a pyramidal texture with pyramid heights of approximately 1µm was obtained. The same authors also produced standard screen-printed mono-Si solar cells that achieved a solar cell efficiency of up to 17.8%. It follows from the work of these authors that good results can be achieved by using IPA substitutes with a higher boiling point in the KOH etching

solution; on the one hand, this allows texturing processes to be carried out at higher temperatures and therefore for shorter etching times, and, on the other, evaporation losses of the alcohol are reduced and thus texturing costs are lower.

"With KOH-HBA, higher etching temperatures of around 100°C can be used, without evaporation losses of the alcohol, but with reduced etching times."

In this paper, two approaches for solving the IPA problems are proposed. The first approach involves the use of another alcohol, referred to as high boiling alcohol (HBA) because it has a boiling point above 200°C; the new etching solution will therefore be referred to as KOH-HBA solution. Thus, with KOH-HBA, higher etching temperatures of around 100°C can be used, without evaporation losses of the alcohol, but with reduced etching times [12]. A further reduction of the etching time (15 min) is possible if, in an initial etching step, the saw damage of the as-cut silicon wafers is removed [13].

The second approach proposed involves recovering the evaporated IPA. For this a new etching bath setup has been developed by the wet-etching company Lotus Systems. IPA is cooled down (liquefied) in a cooling chamber located on top of the new etching bath, and is then conducted to a reservoir. Apart from the cooling system of the new etching bath setup, a vacuum system has been adapted, allowing the application of vacuum to the etching chamber; the etching process is therefore accelerated and a considerable reduction in etching time is achieved. This texturization process with vacuum pulses was introduced for the first time in Ximello et al. [14]; no previous studies have been found that mention the use of this technique for texturing mono-Si wafers.

This paper shows that the pyramidal texture obtained using the KOH-HBA solution can be successfully achieved in the production of solar cells via the standard industrial screen-printing method, a selective emitter process [15] and an advanced photolithography-based process [16]. Czochralski (Cz) and float zone (FZ) silicon wafers were textured and processed into solar cells.

Experimental

Texturization

Two etching solutions were used to texture (100) p-type Si wafers. The first consisted of deionized (DI) water, KOH and HBA. A temperature of 100°C and an etching time of 30 min were used with this etching solution to texture Cz-Si (200µm thick) and FZ-Si (230µm thick) wafers with resistivities of 1–3Ωcm and 1Ωcm, respectively. The etching process took place in a glass beaker heated by a hotplate.

The second etching solution consisted of DI water, KOH and IPA. A temperature of 80°C, and etching times of 30 min and 16 min were used to texture 12.5cm × 12.5cm Cz-Si wafers. To do this, the new etching equipment was used, which allowed the application of vacuum in the etching chamber. Compared to the standard KOH-IPA texturization process, which takes place at atmospheric pressure, vacuum (or more precisely lower pressure than the atmospheric pressure) is applied in the closed etching chamber (around 65% of atmospheric pressure is applied for one second). The frequency of the vacuum pulses can be varied from a few seconds to several minutes during the etching process, and it was possible to reduce the etching time to 16 min. Without vacuum pulses during the etching process, an etching time of 30 min was required. In addition, with the new etching equipment, it was possible to recover IPA from the etching chamber. To characterize the pyramidal texture, reflection measurements and scanning electron microscope (SEM) pictures were taken.

Solar cell processes

Only wafers textured with the KOH-HBA solution were processed into solar cells. Textured Cz-Si wafers were processed into solar cells using the standard industrial screen-printing method and the advanced industrial selective-emitter method. Textured FZ-Si wafers were processed into solar cells via an advanced photolithography-based process.

The screen-printing-based process starts with a $POCl_3$ diffusion to form a p-n junction on textured silicon wafers; the emitter has a sheet resistivity of 50Ω/sq. After that, the phosphorus glass is removed. A silicon nitride (SiN_x:H) layer with a thickness of approximately 75nm is then deposited as an anti-reflective coating, and front silver and rear aluminium contacts are applied by the screen-printing method. After co-firing, the edges of the cells are removed by sawing to achieve electrical isolation.

The processing scheme of the selective-

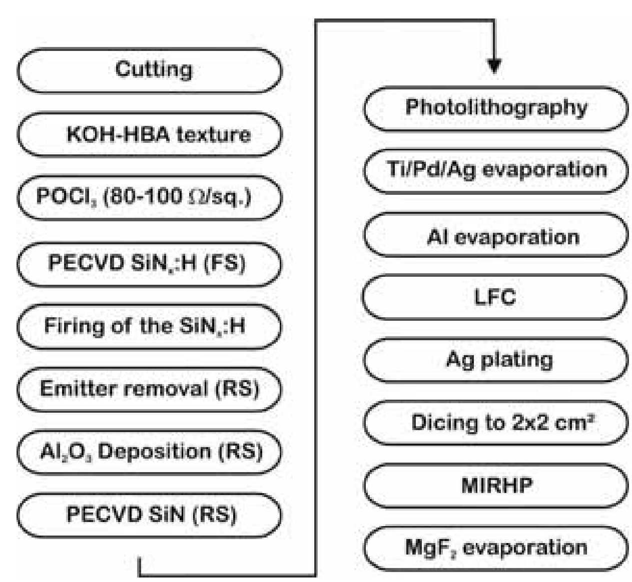

Figure 1. Process flow chart showing the photolithography-based process, featuring a Al_2O_3 rear side (with an optional SiN_x:H rear-side capping layer).

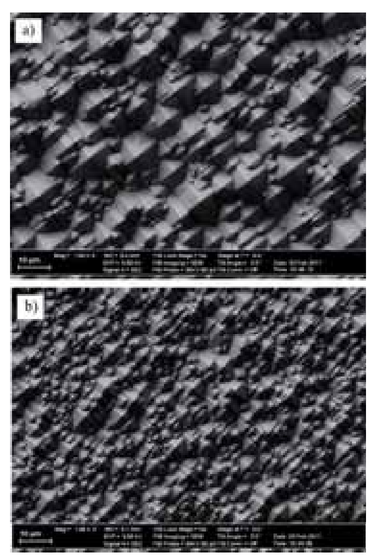

Figure 2. SEM images of Si wafers textured in a KOH-IPA solution: (a) textured at atmospheric pressure; (b) textured using the vacuum process.

Figure 3. Texturing of a mono-Si wafer in a KOH-IPA etching solution by using a closed etching bath in which vacuum steps are applied: (a) a mono-Si wafer covered by hydrogen bubbles (vacuum off), thus slowing down the etching process on this wafer; (b) the same wafer, with hydrogen bubbles detaching from the surface when a short vacuum-process step (vacuum on) is applied; (c) a picture taken immediately after the vacuum step in (b), showing the wafer to be almost free of hydrogen bubbles (vacuum off), and therefore allowing the etching process to accelerate again. The vacuum steps are applied periodically during the etching process – by doing this, the etching time is considerably reduced.

emitter process is very similar to the one just described for screen printing, with only two differences. The first is that the selective-emitter process starts with a stronger emitter diffusion, which leads to an emitter with a sheet resistivity of 30Ω/sq. The second difference is in the formation of a selective emitter, which is carried out as follows: after $POCl_3$ diffusion, an acid-resistive mask is selectively screen printed on the emitter to protect it from further acid etching. By using an acid solution (DI water, HF, HNO_3) the emitter is then lightly etched through the formation of porous Si until it reaches a sheet resistivity of 50Ω/sq. After this, the printed mask, the porous Si and the P-glass are removed. Front contact fingers are printed on regions with high phosphorus doping, i.e. the regions that were not etched away.

The photolithography-based process (see Fig. 1) starts with the cutting of the FZ-Si wafers to a size of 5cm × 5cm, to satisfy the requirements of the photolithography equipment at the University of Konstanz. After this has been done, the wafers are textured as explained earlier. The $POCl_3$ diffusion process is carried out to form an emitter with a sheet resistivity of 80–100Ω/sq. Subsequently, the wafers receive a PECVD SiN_x:H layer as an anti-reflective coating. This is followed by a firing step carried out in a conventional belt furnace to ensure good hydrogenation from the SiN_x:H layer. The front side is then masked with a hot melt ink, and the emitter at the rear side is removed in a polishing etch consisting of HF, HNO_3 and CH_3COOH. The next step is the application, by atomic layer deposition, of a dielectric rear-side passivation layer of aluminium oxide (Al_2O_3); an optional SiN_x:H layer is deposited to protect the very thin

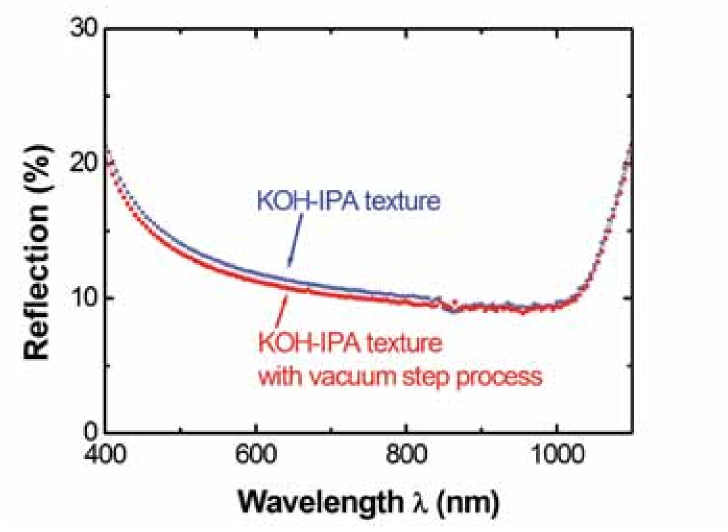

Figure 4. Reflection measurements of Cz-Si wafers textured with a KOH-IPA solution. Vacuum pulses during the texturization process were used to accelerate the etching process.

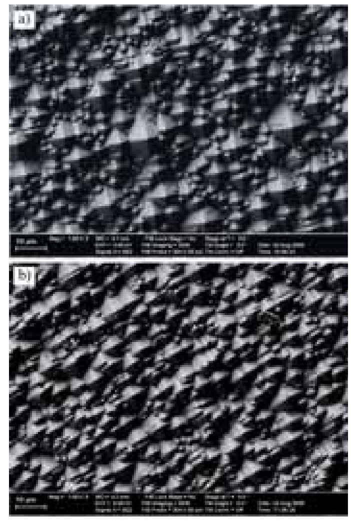

Figure 5. SEM images of surfaces textured with a KOH-HBA etching solution: (a) Cz-Si wafer; (b) FZ-Si wafer.

passivation layer. Afterwards, the front contacts are defined by photolithography and evaporation of Ti, Pd and Ag; aluminium is evaporated on the rear side. The rear contact is then established using a laser-fired contact (LFC) process, and the front contacts are thickened by silver plating. Finally, four solar cells (2cm × 2cm) are cut with a dicing saw. After preliminary characterization, a microwave-induced remote hydrogen plasma (MIRHP) step is implemented to enhance hydrogen passivation, improve the rear surface passivation and sinter the front contacts. When *I-V* characterization of all solar cells is complete, the best cells additionally receive a second, dielectric, anti-reflective coating (DARC) by means of thermally evaporated magnesium fluoride (MgF_2).

Results and discussion

Texturization results: vacuum

SEM images of a KOH-IPA textured surface are shown in Fig. 2. Comparing Figs. 2(a) and (b), a decrease in pyramid size can be observed in (b) and is due to the vacuum process used during the texturization. The application of vacuum steps in the etching chamber allows a quick detachment of hydrogen bubbles (which form during the chemical etching process) from the silicon surface. An extra force is applied to the hydrogen bubbles by the change in pressure during the vacuum cycling (see Fig. 3); a better recirculation of the etching solution is also provided. These two facts mean that the etching process is speeded up. The resulting small pyramid size is comparable to that observed with KOH-HBA textured Si wafers (see next section).

Fig. 4 shows reflection measurements of the textured silicon wafers in Fig. 2. It is observed that Cz-Si wafers textured with KOH-IPA solution and with the vacuum process show slightly lower reflection values for wavelengths below 850nm. An etching time of 16 min was used for the vacuum-assisted etching process; compared to the etching time used in the standard KOH-IPA etching process, which lasts between 30 and 40 min, a decrease in etching time of around 50% was achieved.

Texturization results: HBA

SEM images of KOH-HBA textured surfaces for the two types of wafer are shown in Fig. 5; an etching time of 30 min was used for both materials. The best homogeneity is observed on the textured FZ-Si wafer: this high homogeneity may be attributed to the correspondingly higher quality of the FZ-Si wafer material.

Fig. 6 shows reflection measurements

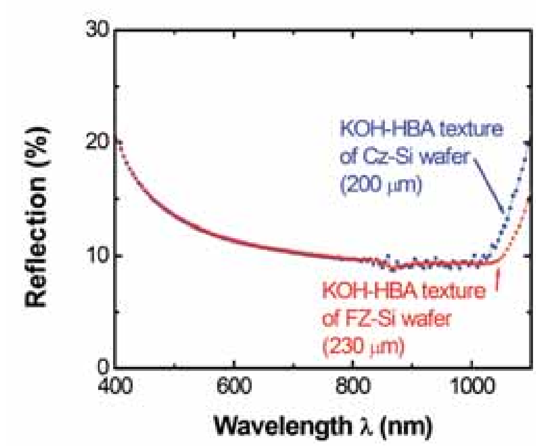

Figure 6. Reflection measurements of Cz-Si and FZ-Si wafers textured in a KOH-HBA etching solution.

Material/Cell process	J_{sc} [mA/cm^2]	V_{oc} [mV]	*FF* [%]	η [%]
Cz / Screen printing	35.5	628	79.0	17.6
Cz / Selective emitter	36.5	637	78.3	18.2
FZ / Photolithography	39.3	660	77.6	20.0

Table 1. *I-V* results of the processed solar cells. Cz-Si wafers (12.5cm × 12.5cm), textured using the KOH-HBA solution, were processed into solar cells by the standard screen-printing method (average over eight cells) and by the selective-emitter method (average over ten cells). Textured FZ-Si wafers (5cm × 5cm) were processed into 2cm × 2cm solar cells by an advanced photolithography-based cell process (best cell).

of the textured Si wafers in Fig. 5: it can be seen that the two kinds of textured Si wafer (Cz-Si and FZ-Si) have almost the same reflection values. A small variation is observed at wavelengths above 1050nm, which is due to the difference in thicknesses of the wafers.

Solar cell results

The current-voltage (I-V) data of the processed solar cells are shown in Table 1. It is important to note here that only wafers textured using the KOH-HBA etching solution were processed into solar cells.

A comparison of the results of both industrial processes reveals a gain in solar cell efficiency of 0.6% absolute for solar cells processed via the selective-emitter process. This increase is mainly due to the higher short-circuit current J_{sc} and open-circuit voltage V_{oc} of these cells. The increase in J_{sc} and V_{oc} is attributed to the better blue response on the etched back regions (thinner dead layer and thus less Auger recombination) and the resulting better surface passivation.

Although reflection values are almost the same for both types of silicon wafer textured with the KOH-HBA solution, the solar cell created from the FZ-Si wafer via the advanced process achieves the highest J_{sc} (39.3mA/cm^2), which is near the theoretical value of J_{sc} (42.5mA/cm^2), estimated for the technologically achievable AM1.5G efficiency limit of Si solar cells [17]. This result demonstrates that the texture exhibits appropriate characteristics for developing solar cells with efficiencies close to the technological limit, at least with FZ-Si wafers.

> "The etching process with the vacuum steps reduces the etching time of mono-Si wafers by about 50% – to 16 min compared to the etching time of 30–40 min used in the standard KOH-IPA etching process."

The photolithography cell process allows the definition of very narrow front metal contact fingers, which, in combination with a lightly doped emitter, explains the high short-circuit current J_{sc} achieved for this solar cell. It also shows the importance of the high-quality passivation layer of Al_2O_3 on the rear side, which results in a high open-circuit voltage V_{oc}. Moreover, this cell process shows very encouraging results due to its low thermal budget.

Conclusions

A new alcohol – HBA – has been used as a substitute for IPA in the standard KOH-IPA texturing solution. Because of the high boiling point of HBA, lower evaporation losses are realized than with IPA. The new KOH-HBA solution has been used successfully to texture both Cz and FZ mono-Si wafers. A very homogeneous texture with small pyramid size was observed, as was the fact that the KOH-HBA etching solution was less sensitive to the pre-treatment of as-cut mono-Si wafers.

The KOH-HBA textured Si wafers were processed into solar cells by the standard industrial screen-printing method, a selective-emitter method and an advanced cell process. Cz-Si wafers etched with the KOH-HBA solution and processed via the standard industrial screen-printing method and the selective-emitter method demonstrated solar cell conversion efficiencies of 17.6% and 18.2%, respectively. FZ-Si wafers textured with the KOH-HBA solution and processed into solar cells via an advanced photolithography-based cell process achieved an efficiency of up to 20.0%.

A new etching bath setup, developed by the wet-etching company Lotus Systems, was used with the standard KOH-IPA solution to texture silicon wafers, making it possible to recover IPA and accelerate the etching process. Evaporated IPA is cooled down in a cooling system and is then conducted to a reservoir, and the etching process is accelerated by an innovative vacuum procedure during texturization. Vacuum steps are employed and thus an extra force is applied to the hydrogen bubbles situated on the silicon surface. These hydrogen bubbles are removed very effectively from the wafer surface, and the growth of large hydrogen bubbles is avoided, resulting in an accelerated etching process and a homogeneous pyramidal texture with small-sized pyramids. The etching process with the vacuum steps reduces the etching time of mono-Si wafers by about 50% – to 16 min compared to the etching time of 30–40 min used in the standard KOH-IPA etching process.

Acknowledgements

The financial support for the processing equipment from the BMU project FKZ 0325079 in particular is gratefully acknowledged. We also thank L. Mahlstaedt for the diffusion processes, and F. Mutter and A. Dastgheib-Shirazi for their collaboration on the processing of solar cells.

References

[1] Neuhaus, D.-H. & Münzer, A. 2007, "Industrial silicon wafer solar cells", *Adv. in OptoElec.*, Vol. 2007, Article ID 24521.

[2] Singh, P.K. et al. 2001, "Effectiveness of anisotropic etching of silicon in aqueous alkaline solutions", *Sol. Energy Mater. & Sol. Cells*, Vol. 70, pp. 103–113.

[3] Seidel, H. et al. 1990, "Anisotropic etching of crystalline silicon in alkaline solutions", *J. Electrochem. Soc.*, Vol. 137, pp. 3612–3626.

[4] Gerhards, C. 2002, "Mechanisch texturierte, großflächige, multikrystalline Siliziumsolarzellen", Dissertation, *Universität Konstanz*.

[5] Abbot, M. & Cotter, J. 2006, "Optical and electrical properties of laser texturing for high-efficiency solar cell", *Prog. Photovolt: Res. Appl.*, Vol. 14, pp. 225–235.

[6] Dekkers, H.F.W. et al. 2000, "Silicon surface texturing by reactive ion etching", *Optoelec. Rev.*, Vol. 8, No. 4, pp. 311–316.

[7] Seidel, H. 1986, "Der Mechanismus des Siliziumätzens in alkalischen Lösungen", Dissertation, *Freie Universität Berlin*.

[8] Holt, A. et al. 2010, "Etch rates in alkaline solutions of mono-crystalline silicon wafers produced by diamond wire sawing", *Proc. 25th EU PVSEC*, Valencia, Spain, pp. 1617–1620.

[9] Aoyama, T. et al. 2010, "Fabrication of single-crystalline silicon solar cells using wafers sliced by a diamond wire saw", *Proc. 25th EU PVSEC*, Valencia, Spain, pp. 2429–2432.

[10] Birmann, K., Zimmer, M. & Rentsch, J. 2008, "Fast alkaline etching of monocrystalline wafers in KOH/CHX", *Proc. 23rd EU PVSEC*, Valencia, Spain, pp. 1608–1611.

[11] Wijekoon, K. et al. 2010, "Production ready novel texture etching process for fabrication of single crystalline silicon solar cells", *Proc. 35th IEEE PVSC*, Honolulu, Hawaii, USA, pp. 3635–3641.

[12] Ximello, N., Haverkamp, H. & Hahn, G. 2009, "A new KOH-etch solution to produce a random pyramid texture on monocrystalline silicon at elevated process temperatures and shortened process time", *Proc. 24th EU PVSEC*, Hamburg, Germany, pp. 1958–1960.

[13] Ximello, N. et al. 2010, "Influence of pyramid size of chemically textured monocrystalline silicon wafers on the characteristics of industrial solar cells", *Proc. 25th EU PVSEC*, Valencia, Spain, pp. 1761–1764.

[14] Ximello, N. et al. 2011, "Up to 20% efficient solar cells on monocrystalline silicon wafers by using KOH-High Boiling Alcohol (HBA) texturing solution", *Proc. 26th EU PVSEC*, Hamburg, Germany, pp. 849–852.

[15] Dastgheib-Shirazi, A. et al. 2008, "Selective emitter for industrial solar cell production: A wet chemical approach using a single side diffusion process", *Proc. 23rd EU PVSEC*, Valencia, Spain, pp. 1197–1199.

[16] Junge, J. et al. 2010, "Evaluating the efficiency limits of low cost mc Si materials using advanced solar cell processes", *Proc. 25th EU PVSEC*, Valencia, Spain, pp. 1722–1726.

[17] Aberle, A.G. et al. 1995, "Limiting loss mechanism in 23% efficient silicon solar cells", *J. Appl. Phys.*, Vol. 77, No. 7, pp. 3491–3504.

About the Authors

Jose Ximello-Quiebras studied physics at the National Polytechnic Institute (IPN), Mexico, and received an M.Sc. in 2005 for research on the properties of cadmium sulphide (CdS) thin films deposited by chemical bath and sputtering methods for CdS/cadmium telluride (CdTe) solar cells. From 2006 to mid-2008 he worked as a researcher on the photoluminescence of porous silicon at the University of Stuttgart, Germany. Since mid-2008, Jose has been working towards his Ph.D. at the University of Konstanz and is investigating texturing solutions for monocrystalline and multicrystalline silicon wafers for solar cells.

Johannes Junge studied physics at the University of Karlsruhe, Germany, and received his Ph.D. in physics from the University of Konstanz in 2012. Johannes is currently working in the New Materials group within the photovoltaics division of the University of Konstanz, where his research interests include defect engineering and the determination of solar cell efficiency potential for all kinds of Si wafer material.

Sven Seren studied at the University of Konstanz, where he earned his Ph.D. in 2007 for research on low-cost solar cells fabricated from fast-grown silicon ribbon materials. Since then Sven has headed the New Materials group at the University of Konstanz, with a research emphasis on the characterization and processing of multicrystalline silicon ribbon materials.

Giso Hahn studied physics at the University of Stuttgart, Germany, and received a Ph.D. degree in the same subject from the University of Konstanz in 1999. Since 2009 he has been a professor in the physics department at the University of Konstanz, and is currently the head of the photovoltaics division, which focuses on crystalline silicon materials and solar cell process development. Giso's research interests include the characterization of promising low-cost materials for photovoltaic applications and the development of adapted solar cell processes for these and other materials.

Ernst Epple studied at the University of Hohenheim in Stuttgart and graduated in engineering. After having worked for around 20 years for several wet-process technology companies, Ernst took on the position of chief technology officer at Lotus Systems GmbH. His work there focuses on process and system engineering with the aim of lowering production costs in the manufacture of solar cells.

Enquiries

J.N. Ximello-Quiebras
University of Konstanz
Department of Physics
Jacob-Burckhardt-Str. 29
78464 Konstanz
Germany
Tel: (+49) 7531 883731
Fax: (+49) 7531 883895
Email: jose.ximello-quiebras@uni-konstanz.de

E. Epple
Lotus Systems GmbH
Sautierstraße 23
78187 Geisingen
Germany
Tel: (+49) 7704 9233-155
Fax: (+49) 7704 9233-60
Email: Ernst.Epple@lotussystems.de

Selective emitter (SE) technology – the transfer from laboratory to optimization in full-scale production

Helge Haverkamp, Schmid Group, Freudenstadt, Germany, & **Budi Tjahjono**, Sunrise Global Solar Energy Co. Ltd., Wujie Township, Taiwan, R.O.C.

ABSTRACT

The selective emitter (SE) concept features two different doping levels at the front surface of the cell. Both doping profiles are tailored individually to best suit their specific purposes, thus achieving both low contact resistance of the emitter electrode and low recombination in the emitter and at the Si/SiN_x:H interface. This paper details the experience gained since the first tools for generating an SE structure were installed two years ago. The approach taken is discussed and a presentation given of the physical concept and properties of SE technology, along with the different aspects that have to be considered when integrating SE into an otherwise unchanged production facility.

Introduction

In standard cell architecture using p-type wafers, uniform phosphorus doping of the front surface is applied to create the n-type emitter. The depth profile of the dopant concentration is chosen so that it allows a low contact resistance of the emitter electrode to the doped silicon, while at the same time attempting to minimize carrier recombination in the highly doped layer and at the interface between the silicon and the passivation layer. When screen printing the conventional silver paste for metallization, low contact resistance to the emitter is achieved best through applying a high dopant concentration to the emitter [1]. On the other hand, in order to reduce recombination at the front surface, it is essential that doping levels be kept low [2]. This conflict between doping requirements is the main source of electrical loss occurring in homogenous emitter designs.

A selective emitter (SE) separates the doping requirements by providing a highly doped area intended for metallization and a lightly doped area for reduced emitter and surface recombination. Thus, it becomes possible to minimize resistive and recombination losses.

While many SE approaches are discussed in the literature only a few are actually suitable for mass production. Considerations of process stability, tool cost, process cost

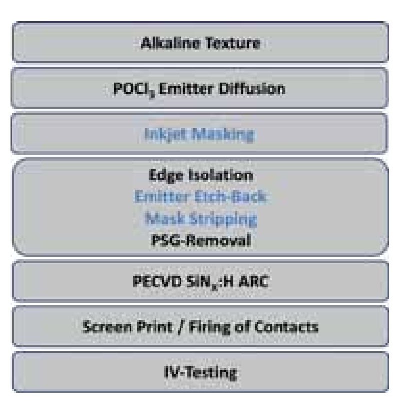

Figure 1. Process flow for cells with the etch-back SE structure. Three additional process steps are added to the standard production process, two of which are integrated into the wet bench that is used for edge isolation and PSG removal.

of ownership and ease of integration have led to only a handful of concepts being deemed practical [3]. This paper reports the experience gathered in almost two years of SE production at Sunrise Global Solar Energy Co. Ltd., a solar cell manufacturer in Taiwan. The production method used is based on the etch-back approach originally developed at the University of Constance, Germany [4].

> "A selective emitter separates the doping requirements by providing a highly doped area intended for metallization and a lightly doped area for reduced emitter and surface recombination."

Process description

The cell fabrication process begins with alkaline etching to produce a random-pyramid texture; after this, the wafers are subjected to a batch-type phosphorus diffusion using $POCl_3$ as the precursor to create an n-type layer at the front surface. The areas intended for metallization are then masked with an inkjet system. Edge isolation, emitter etch-back, stripping of the inkjet mask and PSG removal are carried out using a single wet bench. The wafers then follow the standard production process consisting of PECVD SiN_x:H anti-reflection coating (ARC), followed by screen printing and firing of the electrodes. A schematic of the process flow is shown in Fig. 1.

Choice of masking technology

Initial development work in the laboratory employed screen-printing technology for partial masking of the emitter. Several technological challenges – such as thermal treatment of the mask, ease of removal and alignment precision – prompted the adoption of a different technique for carrying out the masking step. Replacing screen printing with inkjet printing of hot-melt wax offered several advantages:

- No thermal treatment of the mask required; the hot-melt wax used freezes upon contact with the wafer.
- Superior alignment precision (±7µm); no gradual distortion of the mask from screen warping.
- Tight control over deposited amount of masking material; exact reproducibility, eliminating process deviations found in screen printing.
- Touchless technology, minimizing mechanical stress on the wafer.
- High throughput of up to 2400 wafers/hour in a single tool; in-line integration with subsequent wet bench.

The inkjet system had originally been designed for printed-circuit board applications. Apart from a few niche applications, it had not previously been used in the production of solar cells, but a few technical changes to the alignment technique and transport system made it suitable for crystalline wafers. Today, the inkjet system prints 25 wafers in a single cycle, making use of different alignment algorithms according to customer requirements.

Emitter etch-back technique

Etching back the emitter removes the very highly doped layer at the surface, also called the 'dead layer.' Removal of the dead layer leads to an increase in emitter transparency and facilitates surface passivation. Both effects increase short-circuit current (I_{sc})

Figure 2. Inkjet system (left) including loading/unloading section. Alignment system (right) recognizes wafer position for accurate placement of the printed mask.

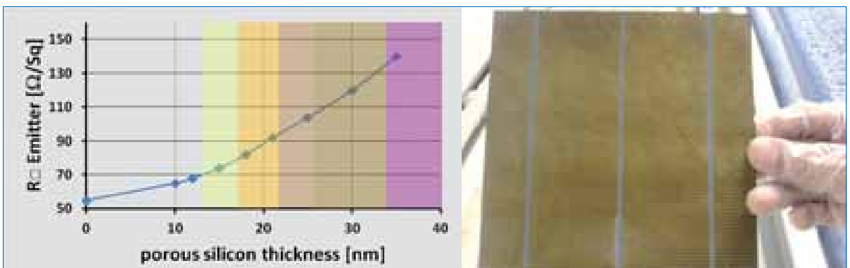

Figure 3. Left: Emitter sheet resistance vs. porous silicon thickness created in the etch-back process for an initial sheet resistance of 50Ω/sq. Right: Porous silicon layer after inkjet masking and emitter etch-back.

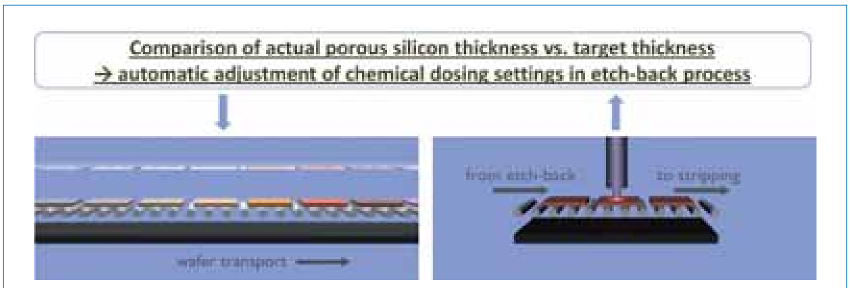

Figure 4. Schematic of the etch-back technique and process control. The thickness of the porous silicon layer is measured online immediately after the etch-back process. The measurement data is fed into a control system that adjusts the chemical concentration in the etch-back process if necessary. After the measurement, the porous silicon layer is stripped, along with the inkjet mask (not shown).

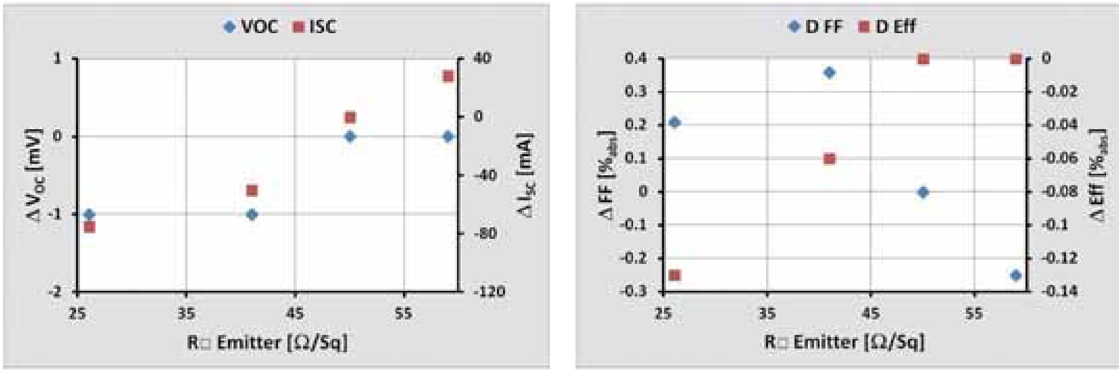

Figure 5. Dependence of V_{oc} and I_{sc} on initial emitter sheet resistance (left). All groups have been etched back to a sheet resistance of 80Ω/sq. In general, a higher initial emitter sheet resistance tends to produce a higher cell efficiency (right).

and open-circuit voltage (V_{oc}). To benefit from an etched-back emitter it is essential to have excellent control over the etch depth: etching too deeply will lead to an excessive increase in emitter sheet resistance, causing a decrease in fill factor (*FF*) and efficiency, while shallow etching will not fully remove the dead layer. In order to determine the etch depth exactly, a special technique is employed. During the process, the etch-back solution creates a thin layer of porous silicon whose thickness correlates with the etch removal. The more silicon is etched, the thicker the porous silicon layer created. The layer is removed later in the stripping process along with the inkjet mask using a caustic etch solution.

As a result of the growth of the porous silicon layer, the wafer will change its colour, enabling the operator to detect with the naked eye any process deviations and local inhomogeneous etching. The porous silicon layer thickness is measured online using an optical spectrometer in the wet bench, thus allowing the operator to exert precise control over the etch-back depth.

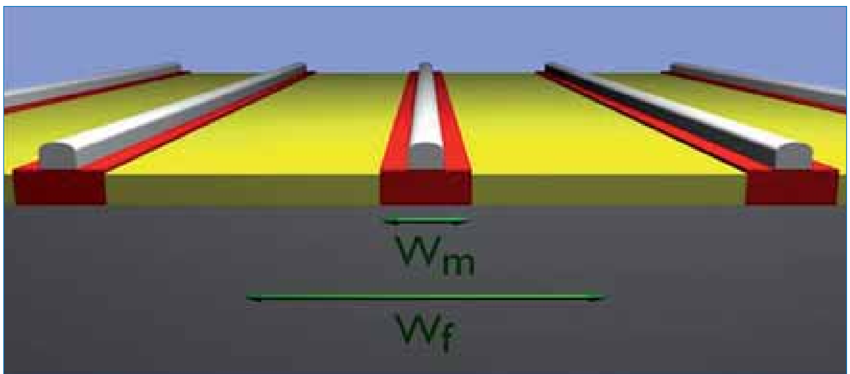

Figure 6. After masking and etch-back of the emitter there are two areas with high (red) and low (yellow) surface dopant concentration. Depending on the ratio of masking width (W_m) to finger pitch (W_f), the initial phosphorus diffusion process must be tuned to optimize cell performance.

In addition, a closed-loop feedback cycle is integrated in the control software and this automatically adjusts the concentration of the chemicals to achieve the desired etch-back depth. A schematic of the control method is shown in Fig. 4.

Optimizing SE technology in production

Aside from the etch-back process parameters themselves, several parameters in the preceding and subsequent processes can be adapted in order to maximize the benefit of implementing SE technology. These parameters include emitter diffusion, mask design, etch-back depth, emitter passivation and design of the emitter electrode. Each technology will be discussed separately. Although many process parameters are interdependent, it is still helpful to consider the basic characteristics independently.

Adapting phosphorus emitter diffusion

The first process that had to be adapted in the production sequence was the dopant-depth profile of the n-type phosphorus emitter. The standard production process typically features an emitter sheet resistance of 60–70Ω/sq, diffused in a batch furnace system. While sheet

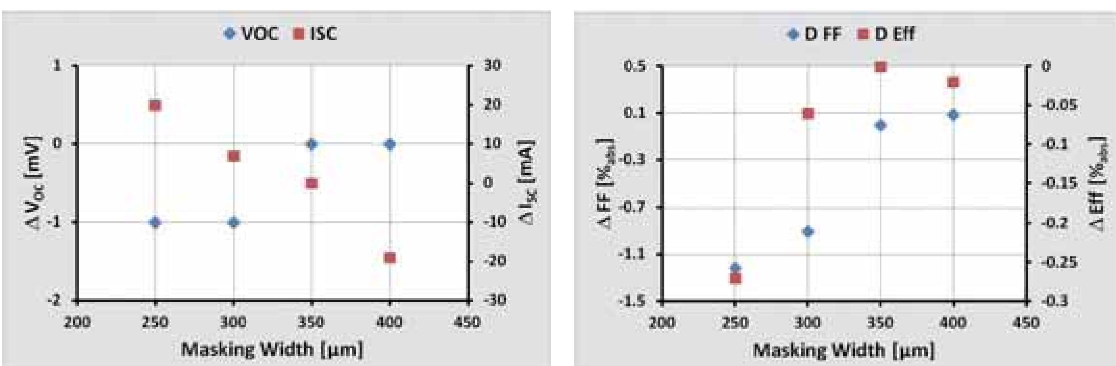

Figure 7. Influence of masking width on V_{oc} and I_{sc} (left) and on *FF* and cell efficiency (right).

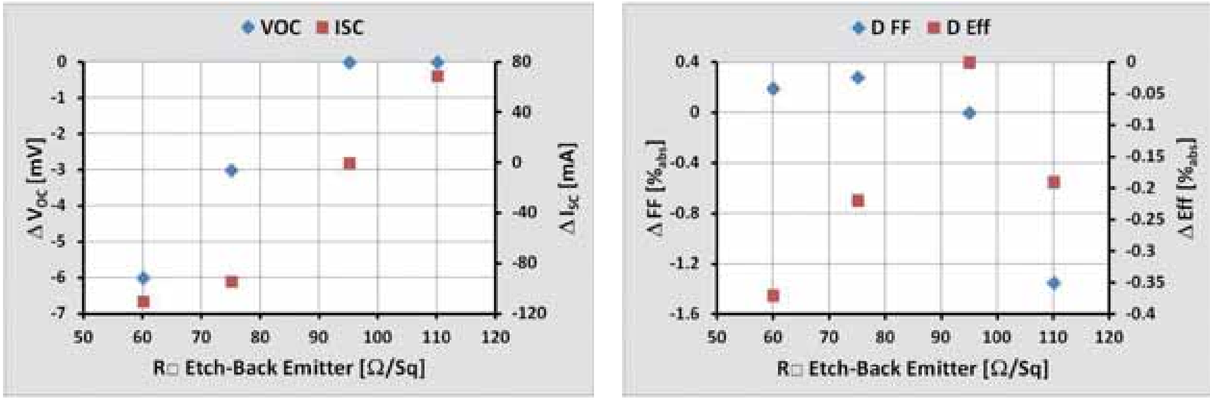

Figure 8. Influence of etch-back emitter sheet resistance on V_{oc} and I_{sc} (left) and on *FF* and cell efficiency (right). Initial emitter sheet resistance was 40Ω/sq.

	Eff [%]	I_{sc} [A]	V_{oc} [mV]	*FF* [%]	R_s [mΩ]	R_{shunt} [Ω]	I_{rev} [A]
Avg.	18.968	8.953	640	79.09	2.92	1358.59	0.126
Std dev.	0.0874	0.0335	1.5	0.2960	0.2	413.11	0.1487

Table 1. Daily average values of electrical parameters in Sunrise's production line.

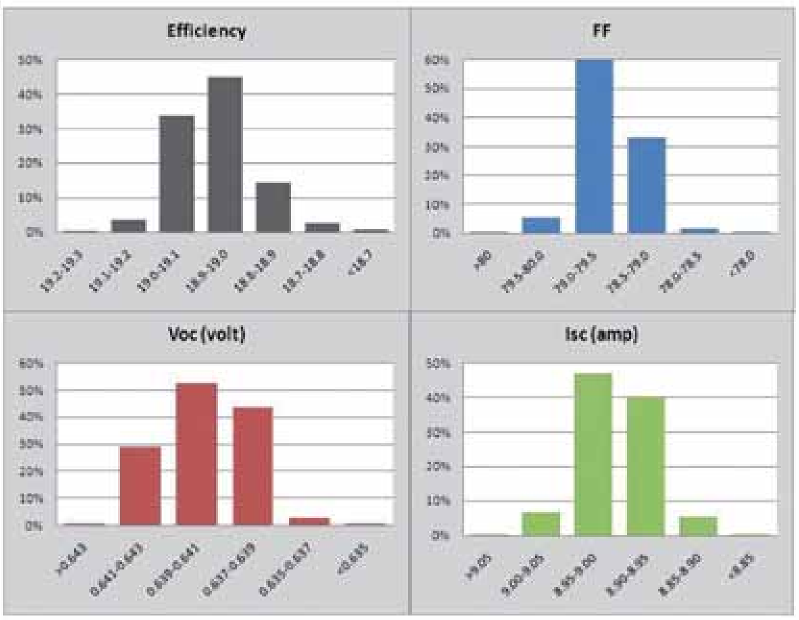

Figure 9. Distribution graphs for efficiency, *FF*, V_{oc} and I_{sc} of the etch-back SE cells produced at Sunrise.

resistance uniformity plays a critical role in homogeneous emitter designs, it becomes less important in SE technology. The first tests in production were carried out by varying emitter sheet resistances between 25–60Ω/sq. Although contact resistance of the emitter electrode to the emitter decreases with lower emitter sheet resistance, recombination in the emitter and at the SiN_x:H/n-Si interface increases with higher dopant concentration.

Typical findings show that, even though the emitter of all groups has been etched back to 80Ω/sq, a better cell efficiency is achieved when starting from a higher emitter sheet resistance before etching. The reason for this behaviour is well understood. To maintain high dopant concentration, part of the emitter surface is masked during emitter etch-back, and this area suffers from increased carrier recombination.

Depending on the ratio of masking width (W_m) to finger pitch (W_f), recombination in the masked area can offset some of the gain that an etched-back emitter will produce. Thus, the initial sheet resistance of the emitter should not be chosen too low, otherwise excessive carrier loss will occur in the area protected from the etch-back process. The slightly higher initial emitter resistance should not pose any problem in the region where the electrode contacts the silicon, because recent developments in Ag paste allow the metal to form a low-resistance contact with a more lightly doped emitter.

> "Typical findings show that a better cell efficiency is achieved when starting from a higher emitter sheet resistance before etching."

Masking width

In order to benefit from low contact resistance of the emitter electrode, it is essential that high dopant concentration at the Si/Ag interface is maintained. Thus, for screen printing, the emitter electrode should be correctly aligned with the areas masked before the etch-back process. Since the areas that are required for alignment tolerances are a source of electrical loss, it is important that these are kept as small as possible. Ideally, masking of the highly doped emitter before etch-back would be limited to just the area covered by the emitter electrode. This can be done in a laboratory environment, where overlay of masking and metallization can be very precise. In large-scale production, however, the positioning accuracy of the inkjet tool used both for masking and for metallization (screen printer) has to be taken into account when choosing the masking width.

Typically, during ramp-up of the process, a masking width W_m of 450µm was chosen. As operators and engineers gained more experience in overall process tuning, the masking width was able to be reduced. It was found that alignment accuracy becomes limited by gradual distortion of the screen during printing.

Normally, reducing W_m to 300µm and below does not lead to an increase in average efficiency on a mass-production scale. This is because there is higher likelihood of misalignment of the heavily doped area and the emitter electrode. This misalignment will cause two distinct effects:

1. Contact resistance of the emitter electrode to the emitter increases locally; cell series resistance increases, thus lowering *FF*.

2. Emitter electrode (Ag finger) contacts the lightly doped emitter, which causes increased recombination and leads to a decrease in V_{oc}.

Passivation of the contacts will be reduced because of lower emitter doping at the n-Si/Ag interface, causing increased recombination that leads to an increase in the emitter saturation current density j_{0e} [2] and a decrease in V_{oc}.

Choosing a masking width that is too narrow to allow accurate alignment of the emitter electrode generally leads to a larger spread in cell efficiency and a lower average cell efficiency. Apart from inkjet- and screen-printer alignment accuracies, distortion of the screen-printing mask over time has to be considered. In contrast to other SE technologies, the etch-back approach features a deep p-n junction. This is helpful as it avoids shunting of the cell in the case of minor misalignment, thereby retaining production yield. In 2011 more advanced equipment became available that allowed online monitoring of alignment precision, further facilitating process control [5]. An example of such equipment is the high-precision alignment camera in screen-printing tools.

> "To achieve the desired etch depth, measurement of the layer thickness is used to fine-tune the etch-back process in-line."

Etch-back process control

It is essential to exert very tight control over the etch-back process. This is realized through the generation of a porous silicon layer during the etch-back process, as mentioned earlier. To achieve the desired etch depth, measurement of the layer thickness is used to fine-tune the etch-back process in-line. The etch-back process is self-adjusted through the implementation of a closed-loop feedback controller. By using this cycle of direct feedback for process control, it is possible to achieve very high process stability in the etch-back process, resulting in high line yield. From knowledge of a simple correlation between etch-back depth and emitter sheet resistance (Fig. 3, left), the target sheet resistance of the emitter can be adjusted very precisely. Electrical cell data from a test in which the etch depth was varied are shown in Fig. 8.

If the etch-back is too shallow, the final emitter sheet resistance is low, resulting in only a small increase in I_{sc}. If the emitter is etched too deeply, the increase in I_{sc} will be offset by a low *FF* due to the higher emitter lateral resistance of the cell. The etch-back thickness optimization is strongly related to the final electrode pattern design as well. Moreover, in the case of multi-wafers, longer etching will cause excessively deep etching, commonly observed in the acid etching of multi-wafer material.

Recent result in mass production

Recent results of the implementation of etch-back SE technology in mass production at Sunrise are shown in Table 1 and Fig. 9. An average efficiency close to 19% is regularly achieved in large-scale production. Typically, over 90% of efficiency distribution falls within a 0.3% range, whereas 99% of the distribution falls within a 0.5% range. The distribution spreads and standard deviations of all the electrical parameters are quite small, showing that very tight process control is possible in a mass-production setting. Secondary electrical parameters, such as shunt resistance and reverse current, that are critical in module assembly are generally good.

Cell-to-module (CTM) loss in module assembly

SE cells inherently have higher short wavelength responses. It is therefore a common assumption that the benefit of higher efficiency SE cells will be lost at the module level because of EVA cut-off of the short wavelength light, resulting in a high CTM loss. However, such a problem is not specific to SE cells. Most higher efficiency p-type cells with homogeneous emitters typically rely on a lightly doped surface emitter, which is made possible by the front Ag pastes that are capable of making good contact to such a surface, resulting in a higher short wavelength response.

> "Applying a selective emitter to pursue high efficiency concepts has become imperative."

An SE cell typically has the additional benefits of a higher V_{oc} and *FF* owing to the low recombination in the emitter and at the Si/SiN_x:H interface, and low contact resistance of the emitter electrode, respectively. These cell features are generally preferable in modules. An improved spectral response at long wavelengths, resulting from better passivation at the surface, also partly contributes to the higher I_{sc}; such a benefit is completely retained at the module level.

The optimization effort during module assembly and superior module material (such as the use of narrower but thicker ribbons, more UV-transparent encapsulant such as silicone, and AR-coated front glass) can lead to considerably lower power losses. A CTM loss as low as 1.5% for monocrystalline SE cells, with efficiencies above 18.6%, has been achieved, resulting in 265W+ power output from a 60-cell module.

Outlook

In 2011 many cells were produced based on SE technology and different cell architectures, resulting in record efficiencies being achieved [6–8]. Applying a selective emitter to pursue high efficiency concepts has become imperative, since carrier surface recombination is now the dominant source of electrical loss in most monocrystalline cells. Recently, dielectric passivation of the rear surface has been shown to significantly increase electrical and optical performance of the cell, making reduction of front-surface recombination even more critical. For rear-side passivation, several concepts are currently under investigation or transitioning to pilot production, with an Al_2O_3 coating showing the highest promise. As soon as such cell architectures can be introduced into mass production, it will then be possible to exploit the full potential of SE technology to achieve the highest cell and module efficiency.

References

[1] Hilali, M.M. et al. 2004, "A review and understanding of screen-printed contacts and selective-emitter formation", *Proc. 14th Worksh. Cryst. Si. Sol. Cells & Mod.*, Winter Park, Colorado, USA.

[2] Cuevas, A. et al. 1996, "Surface recombination velocity of highly doped n-type silicon", *J. Appl. Phys.*, Vol. 80, pp. 3370.

[3] Hahn, G. 2010, "Status of selective emitter technology", *Proc. 25th EU PVSEC*, Valencia, Spain.

[4] Haverkamp, H. et al. 2008, "Minimizing the electrical losses on the front side: Development of a selective emitter process from a single diffusion", *Proc. 33rd IEEE PVSC*, San Diego, California, USA.

[5] Voltan, A. et al. 2011, "Advanced alignment methods for precise printing over selective emitter in c-Si solar cells", *Proc. 26th EU PVSEC*, Hamburg, Germany.

[6] Sunrise Global Solar Energy Ltd., Press Release, April 2011.

[7] Schott Solar GmbH, Press Release, August 2011.

[8] Schott Solar GmbH, Press Release, November 2011.

About the Authors

Helge Haverkamp is the head of solar cell process technology development at Gebr. Schmid GmbH. He received his doctorate from the University of Constance, Germany. Before joining Schmid, Helge worked for various solar cell and equipment manufacturers as a technology consultant.

Budi Tjahjono is the CTO of Sunrise Global Solar Energy Co. Ltd. He received his doctorate from the Centre of Excellence for Photovoltaics and Advanced Photonics at the University of New South Wales (UNSW). Before Sunrise, Budi worked at UNSW as a research fellow and was the technology transfer consultant for various PV manufacturers worldwide.

Enquiries

Dr. Helge Haverkamp
SCHMID Group | Gebr. SCHMID GmbH
Robert-Bosch-Str. 32–36
72250 Freudenstadt
Germany

Tel: +49 7441 538 368
Email: haverkamp.he@schmid-group.com

Thin Film

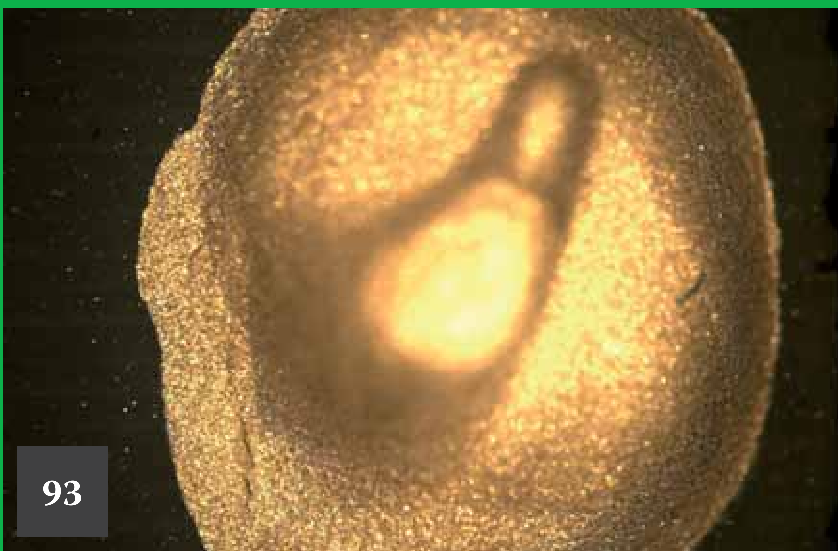

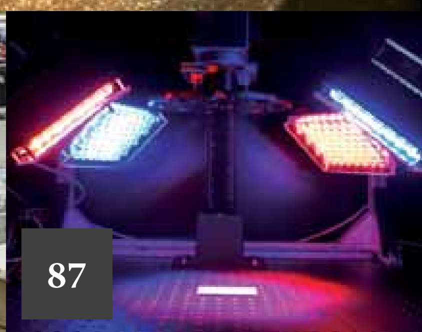

Calyxo's CdTe technology claims 16.2% cell efficiency

Calyxo has revealed that its CdTe cell technology has reached 16.2% efficiency, a figure that has been verified by Germany's SGS testing body. The company uses its proprietary low-cost "hot and fast" atmospheric deposition process in the manufacture of its CdTe cells. Calyxo's CTO Michael Bauer also expressed confidence in the technology's potential to reach 17–18% cell efficiency and 14–15% top module efficiency by the end of the year.

Calyxo's 25MWp production line in Bitterfeld/Wolfen-Thalheim employs over 150 staff. A second production line, with a capacity of 60MWp, is scheduled to start commercial production later this year. Calyxo split from Q-Cells in February 2011 and is now owned by the original technology provider Solar Fields, LLC, based in Toledo, Ohio.

Source: Calyxo

A second production line, with a capacity of 60MWp, is scheduled to start commercial production later this year.

R & D News Focus

ISO 9001:2008 certification awarded to Nanosolar's German production facility

The German Technical Control Board, TÜV Süd Germany, has awarded Nanosolar's Luckenwalde panel assembly plant the ISO 9001:2008 certificate. The certification will cover all manufacturing steps, as well as testing of the company's thin-film solar panels. The ISO 9001:2008 certificate applies to specific quality management systems and is awarded when all applicable statutory and regulatory requirements are met.

Heliatek's organic tandem solar cell verified at 10.7% record conversion efficiency

Dresden, Germany-based OPV thin-film developer Heliatek has achieved a new organic tandem solar cell world record with 10.7% cell efficiency on a 1.1cm^2 substrate. SGS undertook the testing and validated the figures, and also confirmed the OPV cell's merits in low light and high temperature operation.

Standard testing conditions (STC) were undertaken by SGS, which also established that under low light conditions and an irradiation of 100W/m^2, the efficiency is 15% higher compared to the standard efficiency measured at 1,000W/m^2. High temperature operation also demonstrated constant efficiency, claimed to be a unique characteristic for OPV technology in contrast to traditional solar technology where efficiency drops from 15% to 20% at elevated temperatures.

Heliatek is also claiming that real-world outdoor conditions testing has shown its OPV technology has a 15% to 25% greater power output harvest, compared to that of crystalline and thin-film solar technologies.

Source: PR Newswire

Heliatek has achieved a new organic tandem solar cell world record with 10.7 % cell efficiency on 1.1 cm^2 substrate.

Konarka's organic solar modules pass TÜV IEC tests

Konarka has announced that its OPV modules were the first OPV technology to pass individual critical tests for IEC 61646, an accelerated lifetime testing protocol, by TÜV Rheinland. The company has now stated that its organic solar modules have passed IEC stress tests under IEC 61646. The testing was conducted by TÜV Rheinland at its Solar Energy Assessment Centre (SEAC) in Cologne, Germany.

Source: Mrsec

Konarka's organic solar modules have passed TÜV's IEC tests.

Fraunhofer presents new PolAR process at the International Vacuum Conference

Fraunhofer has developed a new method of providing high-area polymer films with an anti-reflective film layer through the utilisation of plasma-etching. The development was unveiled at the recent International Vacuum Conference and will be used to help provide solar cells with optimal light conditions.

The anti-reflective layer programme, named PolAR, was developed by an alliance including Rodenstock, Southwall Europe, Leica Microsystems and Fraunhofer's IOF and FEP programmes. The project was funded by the Federal Ministry of Economics and Technology and focussed on developing a roll-to-roll process to manufacture anti-reflective polymer films.

The manufacture process creates minute indentations while also enhancing the base roughness of the film. The indentations are smaller in size than the wavelengths of visible light, this prevents light scattering and keeps the film clear. Whilst this process is ongoing, the depressions change the refraction index between the film and external medium continuously, which can dramatically reduce the optical reflection.

Source: IDW Online

Fraunhofer researchers with a roll of their anti-reflective polymer film.

Optical reflection on PET films, for example, may be reduced from 12% to 0.2%.

Business News Focus

Soltecture opens insolvency proceedings

Executive management of Soltecture have applied to open insolvency proceedings. Having extensively explored new financing options, including rebranding and restructuring initiatives towards the end of last year, the company has stated it saw no other viable option for averting the company's impending insolvency at the present time.

The company blames a high surplus capacity on the market leading to a drop in solar module prices, which – despite the company's greatest efforts to further reduce costs – could not be compensated.

Hartwig Albers, from Brinkmann & Partner, has been appointed by the insolvency court in Berlin Charlottenburg as preliminary insolvency administrator. Soltecture is confident that operations can be continued at its headquarters in Adlershof with an industrial investor, claiming it is already at an advanced stage of discussion with prospective partners. Details have not been disclosed.

Energy Conversion Devices' auction bid fails

An auction planned for May 8, 2012 to flush out a buyer for Energy Conversion Devices (ECD), which is currently in Chapter 11 administration, was withdrawn only a matter of days before the planned auction. The company immediately moved to lay off approximately 300 employees worldwide. Hilco Industrial has been retained to begin preparations for an asset sale, suggesting flexible thin-film producer ECD could be finally wound down.

Management inferred in a statement that bids had been received in advance of the previously planned auction yet none had been "an acceptable qualified bid by the bid deadline."

However, investment bank Quarton Partners was said to be continuing to work with ECD management and prospective buyers on alternative ways to sell the company as a growing concern. ECD said it would retain a smaller workforce to support the bankruptcy process and asset sales procedures

First Solar sales fall in first quarter

First Solar reported first-quarter sales that showed quarter-on-quarter sales declines. Net sales of US$497 represented a decrease of US$163 million from the fourth quarter of 2011.

The company also announced that James Hughes had been appointed chief executive officer. Hughes succeeds Mike Ahearn (pictured), First Solar's founder and chairman, who has been serving as interim CEO since October 2011. Hughes joined First Solar in March as chief commercial officer. Ahearn will continue in his role as chairman of the board.

Mike Ahearn, First Solar's founder and chairman, who has been serving as interim CEO since October 2011, has been replaced in the CEO role by James A. Hughes.

The company also made further management announcements including chief technology officer, Dave Eaglesham retiring and his replacement would be Raffi Garabedian, First Solar's vice president of Advanced Technologies.

Adler to manage First Solar European warranties

Following reports on First Solar shutting down production in Germany, it has contracted German PV services provider Adler Solar to take over responsibility for European warranties. First Solar stated that it will continue to play an active role in handling customer complaints, but Adler will be the main point of contact and will provide the bulk of warranty services.

Toronto Stock Exchange reviewing delisting Day4 Energy

The Toronto Stock Exchange notified Day4 Energy that it is reviewing the

Source: Share Quotes

Day4 Energy under delisting review by Toronto Stock Exchange.

company's eligibility for continued listing of its securities on the Exchange under its Remedial Review Process. Day4 Energy has 120 days to comply with all TSX requirements for continued listing.

If Day4 fails to demonstrate meeting all TSX requirements by August 13, the securities will be delisted 30 days from such date. The review comes on the heels of the company's expressed financial fragility, for which the company states, it is looking for financing and strategic alternative to help.

Global Solar Energy to sell portable solar business

Global Solar Energy has announced that it is to sell its portable solar business, including the Sunlinq and P3 product lines. The company assures that it does not anticipate any disruption in production or service to its portable solar business customers during the sale process. Global Solar insists the purchase will allow it to better position its focus on and grow other key business units serving the BIPV market. FTI Capital Advisors, the wholly owned investment banking subsidiary of FTI Consulting, will conduct an asset sale of its portable products business.

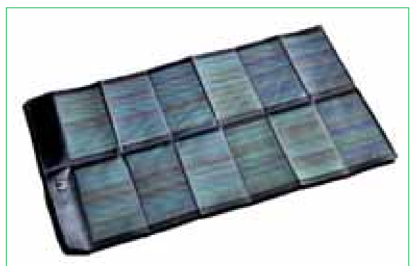

Source: Global Solar Energy

Global Solar Energy's Sunlinq charger.

Other News

GTM Research report notes tough times for thin-film PV; projects upswing around 2015

It is no surprise that thin film has had some trouble for the past few months and GTM Research's latest report, Thin Film 2012–2016: Technologies, Markets and Strategies for Survival, points out that the

Source: Miasolé

MiaSolé is expected to be the front runner for thin-film CIGS over the next four years.

technology's global market share dropped to 11% in 2011, after peaking at almost 20% in 2009. These days, the report states, thin film is surrounded by a highly competitive PV supply market with oversupply bringing c-Si technology to global markets at less than US$1 per watt.

GTM predicts that by 2016, CIGS technology will see the biggest growth, with the report anticipating 4GW in four years. Companies like Solar Frontier, MiaSolé and TSMC are expected to be the lead thin-film suppliers over the next few years with the cost of manufacturing inching towards US$0.50 per watt.

The report advised that the technology's production and total market value is expected to fall below US$3 billion in 2012; however, hope is on the horizon, as GTM predicts an upswing for thin film in 2015 to 2016 with a market recovery of US$7.6 billion. According to the report, the industry's comeback will depend on the success of First Solar and the completion of efficiency, yield and scale road maps from other thin-film manufacturers.

Ball Aerospace & Technologies taps Emcore to supply solar panels for new spacecraft

Emcore has entered a new partnership with Ball Aerospace & Technologies (BATC), which will see the company design, manufacture, test and deliver solar panels for a new spacecraft. The solar panels will utilize Emcore's ZTJ multi-junction solar cells, which, along with the panels, will be produced at the company's New Mexico facility.

The contract is valued at almost US$6 million for a period of nearly two years.

Nanosolar completes all major tasks for US$42 million TPP grant from US DOE

Six years after the US Department of Energy (DOE) awarded Nanosolar a US$42 million Solar American Initiative (SAI) Technology Pathway Partnership (TPP) grant, the company has advised that all 10 major tasks have been achieved or surpassed. The grant was originally awarded in 2006 for the development of large-scale PV systems for commercial buildings that would offer the best price per watt performance in the industry.

The DOE signed off on the company's achievements earlier this month, which included reaching more than 13% cell power conversion efficiency on the production floor that now holds an annual capacity of 115MW, deploying 3.4MW of panels for pilot installations, a 550kW deployment for Camp Perry and a 2.88MW deployment in Oregon.

Additionally, the company is expected to reach grid parity economics by 2015 and continues to gather performance and reliability data from third-party testing laboratories, which is to be analysed by independent engineering firms and institutions. Finally, Nanosolar has produced, sold and deployed at 14 sites around the world.

Source: Nanosolar

Nanosolar has advised that all 10 major tasks have been achieved or surpassed.

Product Reviews

DuPont MCM

DuPont's Solamet PV416 silver metallization paste for lower processing temperatures

Product Outline: DuPont Microcircuit Materials (MCM) has introduced Solamet PV416 photovoltaic metallization paste used to raise the efficiency of thin-film photovoltaic cells. The front-side silver paste material has the capability of being processed at temperatures below 140°C, designed to provide improved contact resistance, conductivity, adhesion and fine line resolution when printed on Transparent Conductive Oxides (TCOs).

Problem: Improving thin-film cell efficiencies requires the ability to print fine lines with a high aspect ratio for greater conductivity, while maintaining a low-cost process.

Solution: Solamet PV416 PV metallization paste can be processed at lower temperatures than similar pastes used in crystalline silicon cells and its special chemistry provides performance characteristics such as high conductivity, adhesion and line resolution. With improved printed conductivity (10mΩ/sq@25micron), low contact resistance (3mΩ.cm^2), and improved line resolution (<100 micron), it is ideal for solar cells built on thin-film PV substrates. It offers excellent fine line printability with minimal flow-out on TCOs as well as excellent electrical properties. It is particularly suited for use on CIGS and other thin-film PV technologies.

Applications: Designed for screen printing front-side conductor in CIGS, a-Si and other thin-film solar cells.

Platform: Solamet PV416 PV metallization paste has a silver-based polymer composition and is designed to be screen printed in high volume applications. It can be dried at temperatures between 130°C and 180°C. Drying times can vary depending on the efficiency of the drier. Longer drying times and higher drying temperatures will improve the adhesion, resistivity and abrasion resistance.

Availability: April 2012 onwards.

Konica Minolta

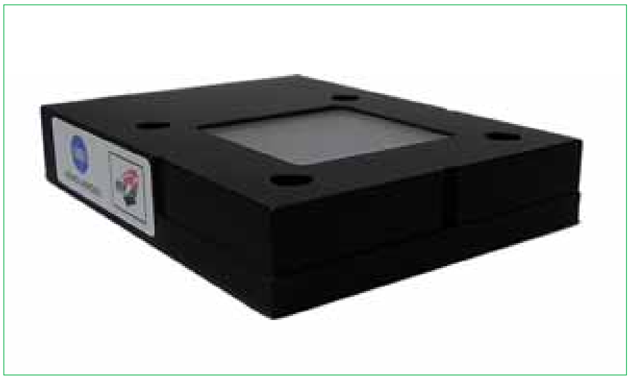

Dye sensitized solar reference cell from Konica Minolta offers temperature stability

Product Outline: Konica Minolta Sensing Americas has introduced the AK-300 PV Reference Cell, which is claimed to be the world's first for dye-sensitized solar cells. The AK-300 was developed in conjunction with the National Institute of Advanced Industrial Science and Technology and utilized Konica Minolta's advanced optical filter technology. The reference cell has been designed using an optical filter mounted on a stable crystalline silicon solar cell rather than using traditional dye materials.

Problem: Spectral mismatch, which had been a major problem with conventional cells, can be suppressed to 1% or less even when evaluating solar cell performance using JIS C-8942 Class C solar simulators.

Solution: The AK-300 is a completely integrated cell with connectors for I-V measurement as well as temperature measurement. The built-in temperature sensor can be connected to a commercially available temperature controlled stage to achieve and maintain 25°C. Also included is the short-circuit current (I_{sc}) values used for solar simulator adjustment. AK Series reference cells have a high durability against exposure to light, greatly reducing solarization and ensuring stability even when used over a long period of time. Improvements in the optical structure suppress multiple reflections and reduce the 1.3% error of conventional products to 0.0%.

Applications: The AK-300 can be used as a standalone reference for DSC/DSSC type cells.

Platform: All AK Series reference PV cells come ready to use with a PT-100 temperature sensor and a test report of short circuit current (I_{sc}). They can also be delivered with calibration traceable to AIST.

Availability: April 2012 onwards.

Luminescence characterizations and parameter drifts of CIGS solar cells

Thomas Ott & **Thomas Walter**, University of Applied Sciences Ulm, **Oliver Kiowski** & **Dimitrios Hariskos**, Centre for Solar Energy and Hydrogen Research (ZSW), Stuttgart, & **Raymund Schäffler**, Manz CIGS Technology GmbH, Schwäbisch Hall, Germany

ABSTRACT

Lifetime guarantees of more than 20 years are a target for the long-term stability of solar modules. An important point for the future of CIGS solar cells is to understand the impact of metastable behaviour on long-term stability. Accelerated ageing under open-circuit conditions leads to a drop in open-circuit voltage (V_{oc}). A decrease in the net doping density is responsible for the drop in V_{oc} and consequently the drop in the photoluminescence (PL). In the initial state the electroluminescence (EL) ideality factor exhibits a value close to unity, as expected from theory. After the dark anneal an increase in the EL ideality factor is observed, and an EL measurement at constant voltage shows a decrease in EL: both these behaviours are due to a pile-up of negative charges at the heterointerface. The application of a positive bias or an illumination during the endurance test leads to an optimization of stability. This paper shows that PL and EL can distinguish between bulk and interface properties and are well suited for the detection of degradation mechanisms.

Introduction

The importance of CIGS in terrestrial photovoltaics is steadily increasing [1–3]. A significant aspect of all PV technologies is long-term stability, which can be assessed by accelerated ageing. This paper presents the use of luminescence techniques, in particular electroluminescence (EL) and photoluminescence (PL), in a study of the accelerated ageing of CIGS-based solar cells. The electrical characteristics (*I-V*, *C-V*) and luminescence properties were therefore detected before and after dark anneals at elevated temperatures. Furthermore, the EL properties were characterized by measuring the EL intensity as a function of the applied bias. From these curves of intensity versus voltage, diode parameters – such as an EL ideality factor – were extracted. The parameter drifts obtained were compared to simulation results utilizing SCAPS (a solar cell capacitance simulator developed at the University of Ghent, Belgium).

Reliability testing

Endurance tests under different conditions were undertaken in order to investigate the behaviour of luminescence in the context of accelerated ageing. The tests were done at elevated temperatures of up to 165°C; in some cases a low positive (max. 0.4V) or negative (max. 0.2V) bias was applied to the cells during the endurance test. The devices were annealed for up to 200h. The following parameter drifts were measured before and after the endurance test:

- Open-circuit voltage (V_{oc})
- Fill factor (*FF*)
- EL
- PL
- *C-V* values

PL was detected using a pco.1300 digital 12-bit CCD camera with an exposure time of 10 seconds. For EL, an InGaAs photo detector was used. *I-V* curves were mapped with an Agilent 4155C Semiconductor Analyzer and measured under a halogen spot. The *C-V* measurements were detected with an HP 4192 Semiconductor Analyzer at a frequency of 100kHz. All measurements were taken at a temperature of 300K. The analyzed high-efficiency CIGS solar cells were produced by Manz CIGS Technology GmbH and typically exhibit a V_{oc} of 700mV, an $FF > 72\%$ and efficiencies exceeding 14%.

V_{oc} parameter drifts

Fig. 1 shows the parameter drift of V_{oc} for an applied bias at 165°C. For the long-term test at elevated temperatures, biases of 0.4, 0.2, 0.1 and –0.1V were applied to the cells for 200h during the accelerated ageing. As a reference, a device was dark annealed under open-circuit conditions, and this device shows a decrease in V_{oc} [4]. *C-V* measurements indicate that a decrease in the net doping density is responsible for this degradation.

Fig. 1 shows that a bias during the endurance test influences the V_{oc} parameter drift: a positive bias leads to a stabilization or enhances V_{oc}; a negative bias leads to a decrease in V_{oc}. An endurance test under 0.2 suns also results in stabilization, which leads to the assumption that this is due to an internal bias across the heterointerface [5].

Simulations of PL

All simulations were carried out using SCAPS. From theory it is known that luminescence intensity depends on the splitting of the quasi Fermi levels [6]. In the previous section a decrease in V_{oc} was obtained after the endurance test because of a decrease in the net doping density. In the next section a decrease in *FF* due to a pile-up of negative charges at the interface will be presented. These two mechanisms – V_{oc} and *FF* – affect the electrical characteristics of the device. As a consequence, the splitting of the

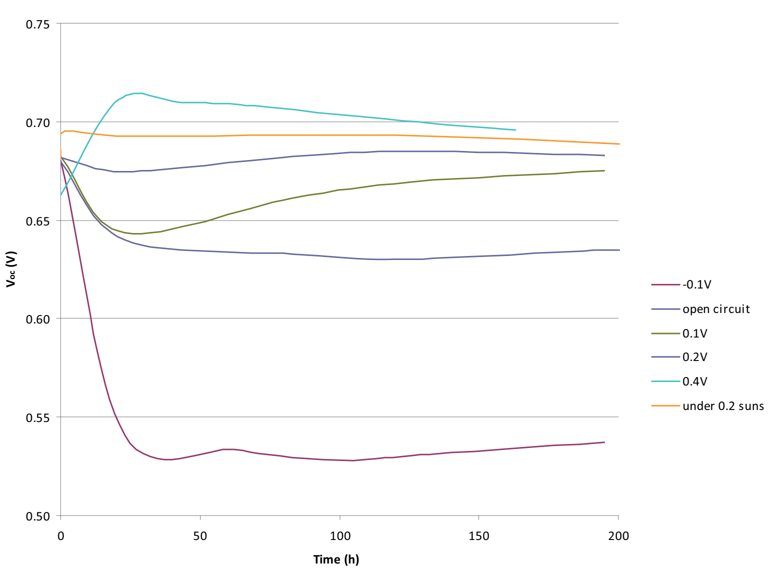

Figure 1. V_{oc} parameter drifts after the endurance tests.

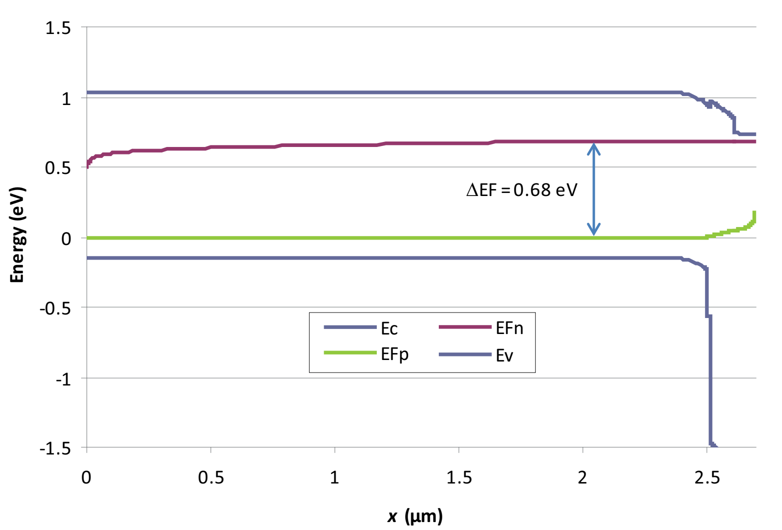

Figure 2. Simulated reference band diagram for PL.

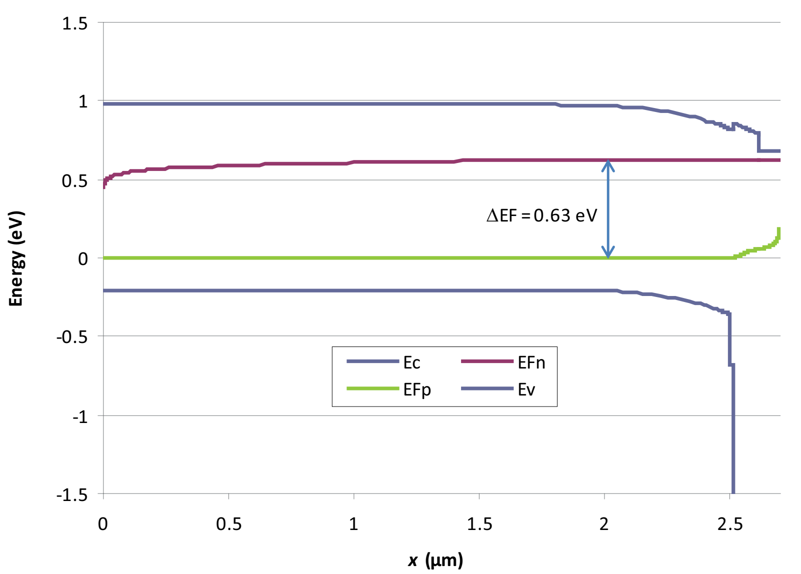

Figure 3. Simulated band diagram for PL with reduced N_A.

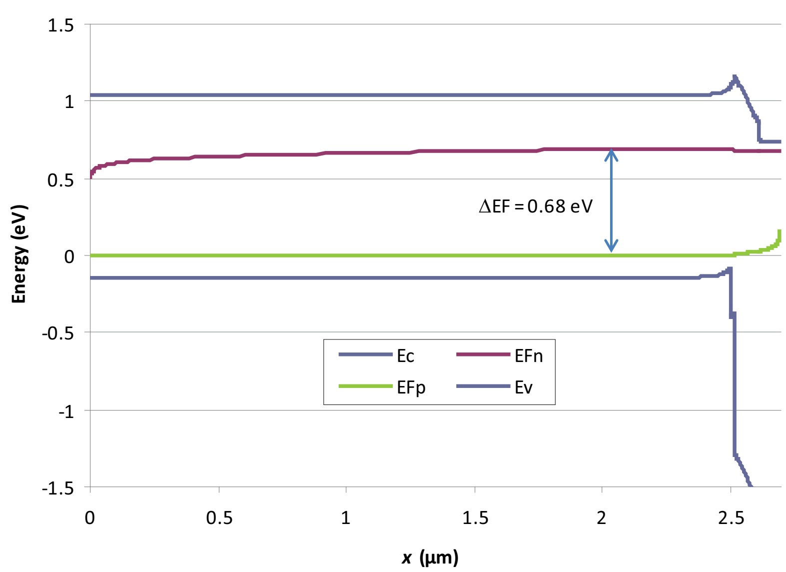

Figure 4. Simulated band diagram for PL with a pile-up of negative interface charges.

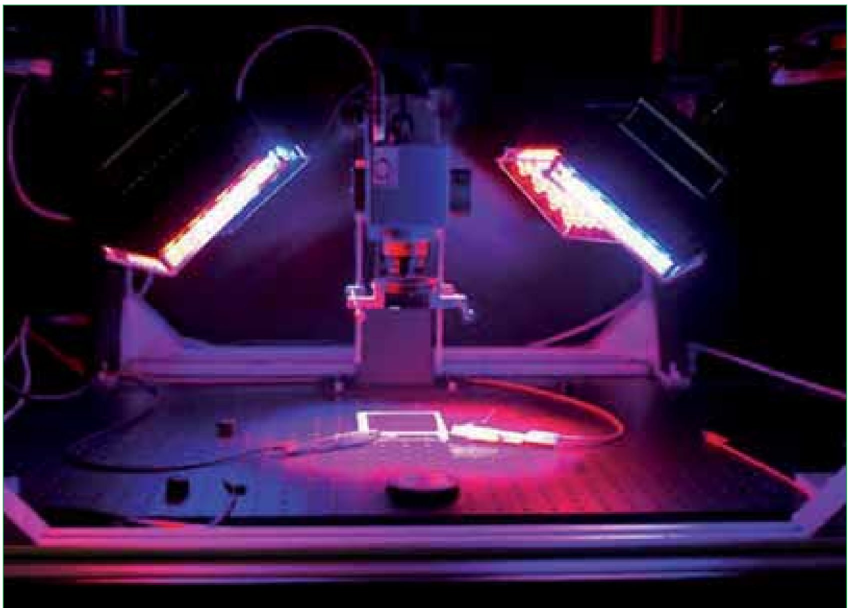

Figure 5. Setup for PL measurements.

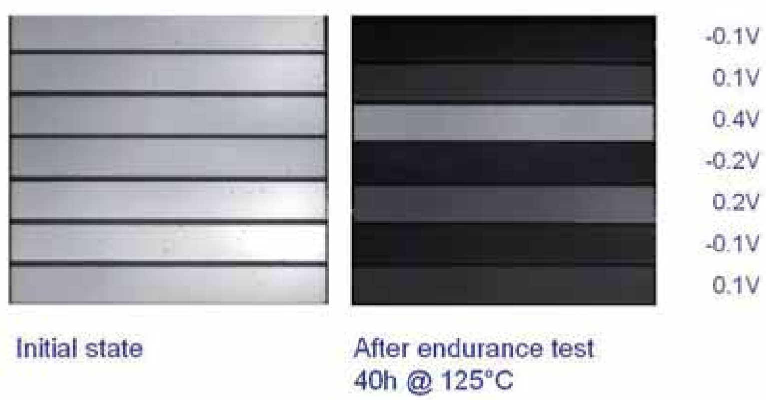

Figure 6. PL images before and after the endurance test.

quasi Fermi levels, and therefore the luminescence intensity, is affected by certain operating conditions.

Fig. 2 shows the band diagram of the heterointerface under illumination and open-circuit conditions which correspond to the measurement configuration of PL. The splitting of the quasi Fermi levels in this reference state at a certain position is roughly 680meV ($\Delta E_F(x=x_0)$ = 680meV). If the net doping density (N_A) is reduced, ΔE_F decreases to 630meV (Fig. 3), resulting in a reduced PL intensity (Φ_{PL}) compared to the reference. A simulation of interface charges (Fig. 4) exhibits no significant change in ΔE_F (680meV) and therefore Φ_{PL} is constant.

Photoluminescence

The theory of PL is well known [7]. In this study the influence of accelerated ageing on PL intensity is investigated. Fig. 5 shows the measurement setup for the PL procedure: a CCD camera was used, and the test device was illuminated by four LED arrays operating at a wavelength of 630nm. In order to separate the luminescence and the excitation wavelength, a GaAs filter with a cut-off wavelength of about 870nm was employed.

"A positive bias tends to maintain the PL intensity of the initial state, whereas a negative bias or an open-circuit condition reduces the luminescence significantly."

Fig. 6 shows PL images of a device with eight interconnected cells before and after endurance testing for 40h at 125°C. During the endurance test, different low-voltage biases between +0.4V and –0.2V were applied to the cells. In the initial state the PL intensity is homogenous over the whole device. As can be deduced from the figure, the PL intensity is affected by the induced metastabilities. A positive bias tends to maintain the PL intensity of the initial state, whereas a negative bias or an open-circuit condition reduces the luminescence significantly. These results agree with those of the SCAPS simulations, which leads to the conclusion that the underlying ageing mechanism for the PL is the N_A parameter drift, and the PL intensity is therefore governed by the net doping density. *C-V* measurements taken during the investigation confirm this result.

FF parameter drift

The parameter drift of the *FF* was also investigated. Fig. 7 shows the *FF* measured (i) in the initial state, (ii) after a dark anneal at 165°C for 24h, and (iii) after a light soak for 3h following the dark anneal. The devices were measured under illumination through spectral edge filters, which only transmit light exceeding a certain cut-off wavelength. Only illumination with

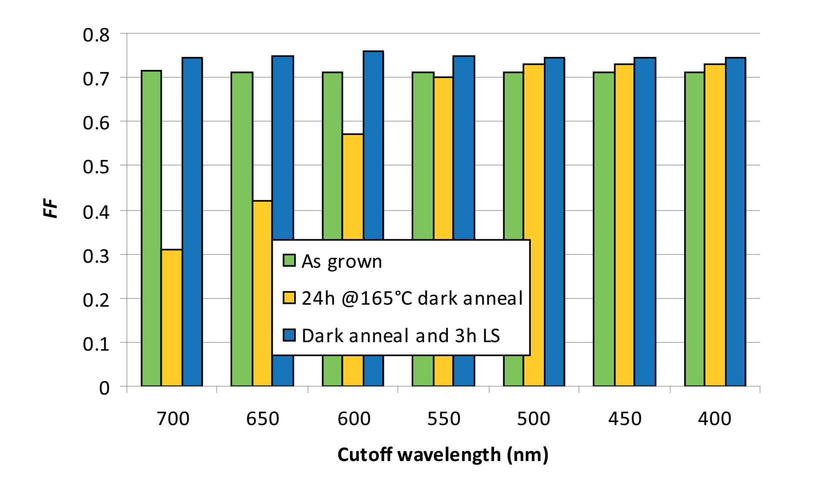

Figure 7. *FF* measured with spectral edge filters after the endurance tests.

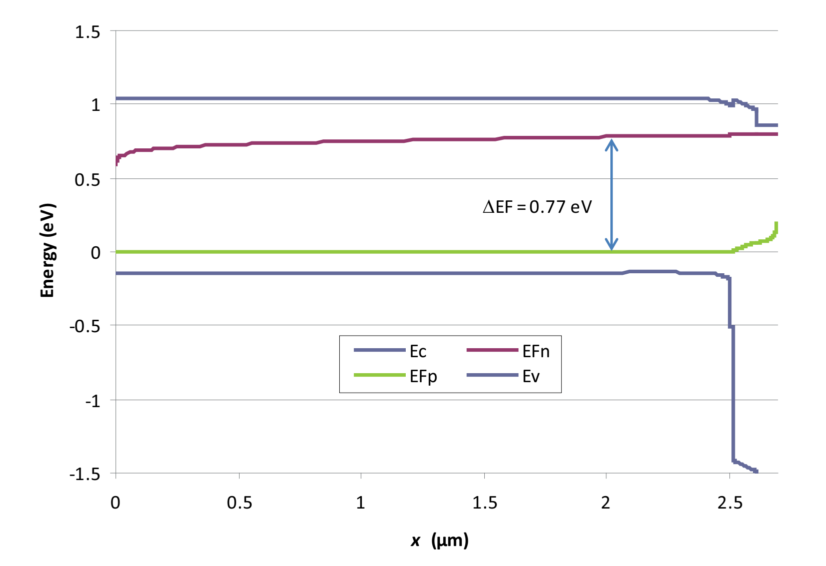

Figure 8. Simulated reference band diagram for EL.

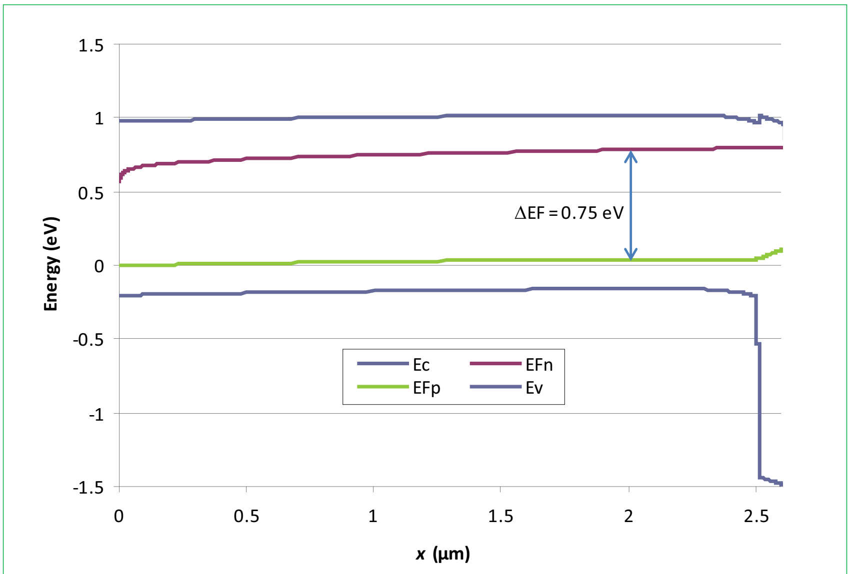

Figure 9. Simulated band diagram for EL with reduced N_A.

wavelengths greater than 550nm shows a decrease in *FF*. This effect is known as the 'blue metastability'. The reason for this behaviour is a pile-up of negative charges at the heterointerface as a consequence of the endurance test, and this restricts the collection of current. An illumination of the CdS buffer (UV) is necessary to avoid this metastable influence, but a light soak can also reverse this effect as shown in Fig. 7.

Simulations of EL

Figs. 8–10 show simulated band diagrams (reference, reduced N_A, negative interface charge pile-up) in the dark, which correspond to the EL situation when a constant bias of 800mV is applied to the device during the measurement. For a reduced N_A, a minor decrease of 750meV in ΔE_F is exhibited, compared to the reference ($\Delta E_F(x=x_0)$ = 770meV), and this results in a relatively unchanged EL intensity (Φ_{EL}). A simulation of interface charges indicates a reduction in ΔE_F (660meV), leading to a decrease in Φ_{EL}.

EL with lock-in amplifier

The fact that the EL is related to the V_{oc} is shown in Kirchartz & Rau [8], but for our study it is desired to correlate the behaviour of EL to the endurance tests. Fig. 11 shows the setup for the EL lock-in measurement: a function generator applies the bias to the sample, and the emitted luminescence is detected by an InGaAs photodiode and amplified by a lock-in amplifier. With this measurement setup it is possible to measure the EL intensity as a function of the applied voltage; the resulting characteristics exhibit similar properties to *I-V* characteristics.

Fig. 12 shows the EL intensity (photodiode current) and applied voltage characteristics. The sample was measured (i) in the initial state, (ii) after a dark anneal at 125°C for 160h, and (iii) after a 4h light soak (including a 2h soak at room temperature, followed by a 2h hot, light soak at 80°C) after the dark anneal. At the end of the endurance test, a reduced EL intensity for the same applied voltage was observed – this decrease in intensity (under constant *V* conditions) indicates transport restrictions at the interface. The results correspond to the SCAPS simulations, leading to the conclusion that the underlying ageing mechanism for EL intensity is due to negative charges at the heterointerface. However, light soaking reverses this degradation mechanism, and the same EL intensity as in the initial state is observed.

As in the case of electrical *I-V* characteristics, an EL ideality factor (derived from the intensity versus the applied bias characteristics) can be defined. In the initial state the EL ideality factor exhibits a value close to unity as expected from theory [9]. After the endurance test an increase in the EL ideality factor is observed, as can be deduced from the slope of the blue curve in Fig. 12, but the light soaking tends to reverse the observed parameter drift of the EL ideality factor. An EL ideality factor greater than one requires

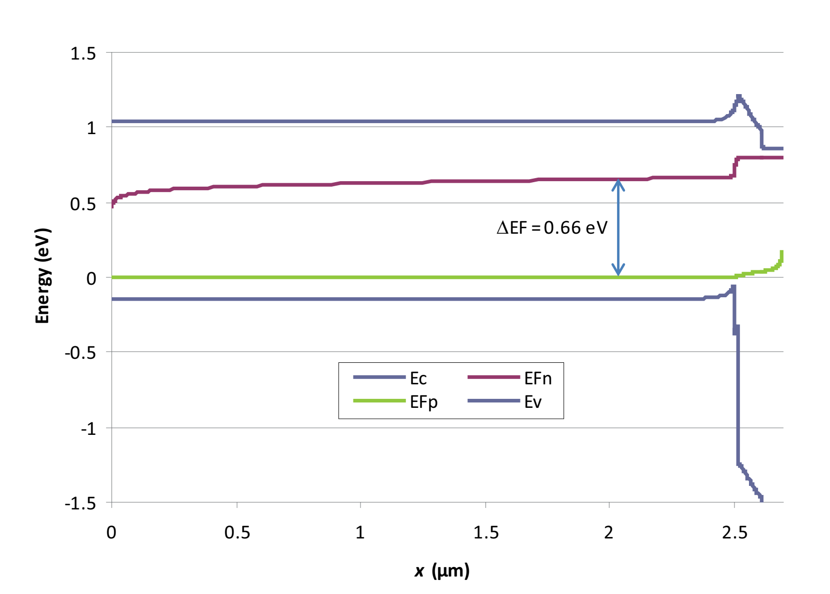

Figure 10. Simulated band diagram for EL with a pile-up of negative interface charges.

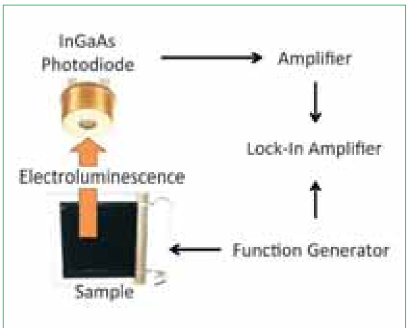

Figure 11. Setup for EL lock-in measurements with an InGaAs photodiode.

that the increase in the externally applied bias does not correspond to the internal increase of the splitting of the quasi Fermi levels, which can be related to interface charges or reduced carrier mobility at the heterointerface. The step in the electron quasi Fermi level (Fig. 10) results from the reduced interface mobility and can be considered as a kind of internal series resistance. As a consequence, depending on the current density, an internal bias drop across this internal series resistance occurs, leading to the rather sharp drop of the quasi Fermi level at the interface. It therefore appears to be possible to separate parameter drifts of bulk properties (N_A) from interface properties (interface charges) by the appropriate operating conditions during the luminescence measurement, i.e. PL or EL under a constant applied bias.

Discussion

The investigations revealed that PL and EL exhibit a metastable behaviour after endurance tests. These findings were correlated with the V_{oc} and *FF* parameter drifts. To obtain the principal degradation mechanisms of the luminescence, the band diagram was simulated for several cases and compared with the measurements. Simulations and measurements of the PL reveal that the net doping density is responsible for this metastable behaviour. For EL (constant voltage) the externally applied bias does not correspond to the internal splitting of the quasi Fermi levels, and therefore interface charges or reduced carrier mobility at the heterointerface is the main degradation mechanism for EL. In the initial state an EL ideality factor close to unity was obtained, but measurements show that this factor is also affected by the metastabilities. Illumination or a bias during the endurance test can enhance or stabilize the cells.

> "EL and PL are well suited for the detection of degradation mechanisms and can distinguish between bulk and interface properties."

Conclusions

Observed parameter drifts of CIGS solar cells after endurance tests included those for EL, PL, *FF* and V_{oc}. The PL intensity was governed by the net doping density, whereas the EL intensity was governed by interface charges. In the initial state the EL ideality factor exhibited a value close to unity, but this factor increased because of negative charges at the interface. The application of a positive bias or an illumination during the accelerated ageing resulted in optimization of the stability. This study has demonstrated that EL and PL are well suited for the detection of degradation mechanisms and can distinguish between bulk and interface properties.

Acknowledgement

This work was supported by the German

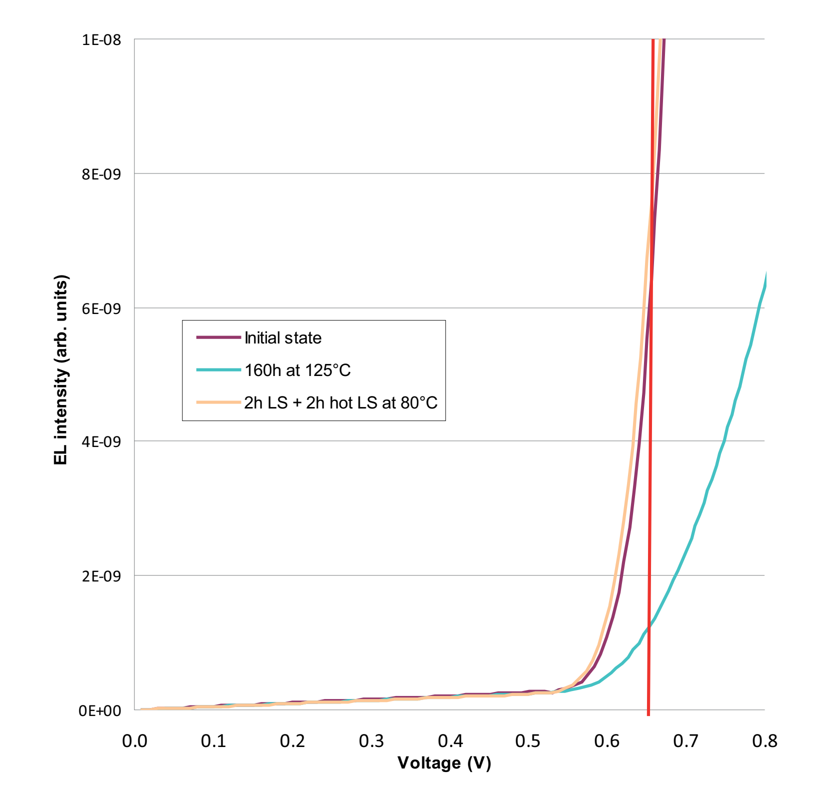

Figure 12. EL intensity versus applied voltage.

Federal Ministry for the Environment, Nature Conservation and Nuclear Safety.

References

[1] Powalla, M. et al. 2011, "CIGS solar cells with efficiencies > 20%: Current status and new developments", *Proc. 26th EU PVSEC*, Hamburg, Germany, pp. 2416–2420.

[2] Ramanathan, K. et al. 2005, "High performance CIGS thin film solar cells: A laboratory perspective", Conf. Paper NREL/CP-520-38987, DOE Solar Energy Technol. Meet., Denver, Colorado, USA.

[3] Hariskos, D. et al. 2007, "The ZnS/ZnMgO buffer combination in CIGS-based solar cells", *Proc. 22nd EU PVSEC*, Milan, Italy, pp. 1907–1910.

[4] Mack, P. et al. 2009, "Endurance testing and accelerated ageing of CIGS thin film solar cells", *Proc. 24th EU PVSEC*, Hamburg, Germany, pp. 2439–2442.

[5] Mack, P. et al. 2010, "Optimization of reliability and metastability of CIGS solar cell parameters", *Proc. 25th EU PVSEC*, Valencia, Spain, pp. 3337–3340.

[6] Würfel, P. 2009, *Physics of Solar Cells*. Berlin, Germany: Wiley-VCH, p. 74.

[7] Unold, T. & Gütay, L. 2011, "Photoluminescence analysis of thin-film solar cells", in *Advanced Characterization Techniques for Thin Film Solar Cells*, Abou-Ras, D., Kirchartz, T. & Rau, U., Eds. Weinheim, Germany: Wiley-VCH, p. 151.

[8] Kirchartz, T. & Rau, U. 2007, "Electroluminescence analysis of high efficiency Cu(In,Ga)Se_2 solar cells", *J. Appl. Phys.*, Vol. 102, p. 104510.

[9] Rau, U. 2007, "Reciprocity relation between photovoltaic quantum efficiency and electroluminescent emission of solar cells", *Phys. Rev. B*, Vol. 76, p. 085303.

About the Authors

Thomas Ott received his diploma degree in mechatronics engineering from the University of Applied Sciences Ulm, Germany. Since 2009 he has been working as a research assistant on the RECIS project at the university, where his work focuses on the long-term stability of CIGS thin-film solar cells.

Thomas Walter received his diploma degree in electrical engineering and his Ph.D. on the electrical defect characterization of CIGS thin-film solar cells from Stuttgart University, Germany. He then joined Bosch, working on microsystem technology and SiGe-based millimetre-wave electronics. Since 2005 he has been teaching microelectronics, microsystem technology and photovoltaics at the university, where he is also currently conducting several research projects on the long-term stability and luminescence characterization of CIGS thin-film solar cells.

Oliver Kiowski studied chemistry at the Karlsruhe Institute of Technology, Germany, and at UMass, Amherst, USA, where he received his Ph.D. for work on carbon nanotubes. He is currently employed by the Centre for Solar Energy and Hydrogen Research in Stuttgart, Germany, where he is carrying out research into thin-film photovoltaics using optical and electrical metrology.

Dimitrios Hariskos studied chemistry at RWTH Aachen University. He received his Ph.D. from the University of Stuttgart and the Technical University of Darmstadt. In 1998 he joined the Centre for Solar Energy and Hydrogen Research, where he is currently working on the up-scaling of CIGS technology from a small-area cell to a full-size commercial module on a 30MW production line.

Raymund Schäffler received his diploma degree in electrical engineering from Stuttgart University, Germany, after which he worked at the university in the field of analytics, TCO and CIGS. This was followed by employment at ZSW Stuttgart (focusing on module technology and encapsulation) and then at Würth Solar. In 2012 he began working for Manz CIGS Technology GmbH as a scientific associate.

Enquiries

Thomas Ott
Mechatronics and Medical Engineering Department
University of Applied Sciences Ulm
Albert-Einstein-Allee 55
89081 Ulm
Germany

Tel: +49 (0) 731 50 28575
Email: th.ott@hs-ulm.de
Website: www.hs-ulm.de

Flexible CIGS modules – selected aspects for achieving long-term reliable products

Markus Münch, **Annegret Reithe**, **Melina Wachsmuth**, **Michael Meißner** & **Eva-Maria Stahr**, Solarion AG, Leipzig, & **Mike Röllig**, Fraunhofer Institute for Non-destructive Testing (IZFP-D), Dresden, Germany

ABSTRACT

Flexible copper-indium-gallium-(di)selenide (CIGS) absorbers offer a wide range of possible applications in rigid as well as flexible and lightweight solar module designs. The main advantage of CIGS in comparison to the well-known flexible module technology based on amorphous silicon is its currently higher efficiency and the promising optimization potential of its efficiency in the future. Because of low cell thicknesses of less than 40µm and the general sensitivity of CIGS to moisture, it is a challenge to develop suitable interconnection and encapsulation technologies that promote long-term reliability of solar modules. Selected aspects of our work in this area will be discussed in this paper.

Introduction

Solarion manufactures flexible copper-indium-gallium-(di)selenide (CIGS) solar cells on highly flexible polymer substrates in a proprietary low-temperature ion-beam-assisted deposition (IBAD) process. The core technology was developed in 1996 at the Leibniz Institute for Surface Modification in Leipzig, and Solarion was founded in 2000 as a spin-off company. Focus was placed thereafter on the development of the process and equipment for roll-to-roll (R2R) manufacturing. Today Solarion operates an R2R solar cell pilot line and a solar module pilot line, as well as a module test facility. A mass production line with a nominal annual capacity of 20MW is currently under construction.

Figure 1. A highly flexible CIGS solar cell from Solarion.

The solar cells are manufactured on an ultra-thin polymer substrate employing the IBAD manufacturing process, which deposits a thin layer of CIGS on the lightest substrate available at a reduced deposition temperature of about 400°C. The cell materials are deposited in a continuous R2R process, and a thin, silver-based contact grid is printed on top of the cell. This is converted to a batch of single cells, each having an area of 56cm^2, which are then sorted into several power classes in a similar way to that used for crystalline solar cells (Fig. 1). A sophisticated marking and tracking system ensures the traceability of all materials and process parameters from the raw materials of the cells to the completed module.

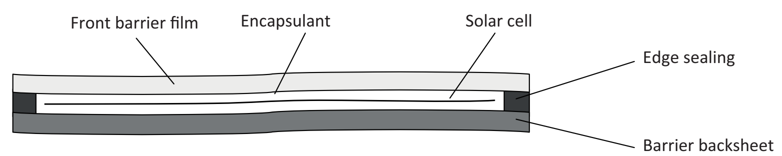

Figure 2. Typical cross section of a flexible CIGS solar module.

"Because of low cell thicknesses of less than 40µm and the general sensitivity of CIGS to moisture, it is a challenge to develop suitable interconnection and encapsulation technologies that promote long-term reliability of solar modules."

A cross section of a glass-free CIGS solar module is illustrated in Fig. 2. Because of the moisture sensitivity of CIGS, in order for an environmentally stable, hermetically-sealed module to perform reliably for more than 20 years in the field, it is necessary to apply the following materials: transparent barrier film, cell encapsulant, edge sealing and barrier-containing backsheet material.

The interconnection between the flexible solar cells inside the module is realized using polymer-based conductive adhesives. These materials are well established in flexible electronics and were included in the investigations.

Owing to their light weight and flexibility, Solarion's CIGS cells lend themselves well to a wide range of possible designs and applications, such as building-integrated photovoltaic (BIPV) and automotive projects, among others.

Module R&D activities

Besides its solar cell R&D, Solarion has undertaken intensive solar module research, focusing on product and technology development as well as reliability and safety testing, with the latter being a widely underestimated concept in PV technology [1]. The majority of the common standard module tests and module materials tests are performed in-house at the module reliability laboratory. Advanced reliability and safety tests are conducted by partners.

A flexible encapsulation technology was developed for Solarion's cell technology after a wide variety of polymeric materials were investigated. The optimal materials and their system compatibility, particularly with the solar cell, were identified by intensive research and testing over the past four years of 25 conductive adhesives, about 20 barrier films, 20 different encapsulants, 6 types of edge sealing and several backsheets.

Methods of investigation

Several methods were employed for determining usable materials and their combinations in order to achieve the development target. IEC 61646 is the baseline standard for the definition of accelerated ageing tests of solar modules. While damp-heat testing at 85°C and 85% relative humidity accelerates hydrolysis and material decomposition as well as interactions in or between polymers, it also allows the investigation of moisture ingression into a solar module package. Temperature cycling between –40°C and +85°C induces thermomechanical stress, mainly due to different coefficients of thermal expansion (CTE) of the module materials.

UV exposure is merely defined as a precondition test in IEC 61646. Given the glass-free, polymer-based composition of flexible modules, UV exposure must be given a greater level of importance by a longer test duration. Combined humidity and UV tests in accordance with ISO EN 4892-3 were therefore undertaken, using increased UV intensity to study the synergistic effect of moisture and UV radiation exposure. The samples were additionally exposed to humidity–freeze cycles at temperature extremes of –40°C and +85°C. All the tests were terminated when a power below 90% of the original rating was observed, or when the samples would fail a visual inspection. Postmortem studies were performed, as required by the IEC norm, in order to identify the degradation mechanism. Typical failure mechanisms of, but not limited to, crystalline solar modules in accelerated ageing are described by Wohlgemuth [2].

Accelerated mechanical ageing of the flexible modules was performed using a cyclic bending test over a roll diameter of 300mm in order to simulate the typical stress imparted by coiling up for shipment and uncoiling for installation. In addition, vibration tests using an electromagnetic

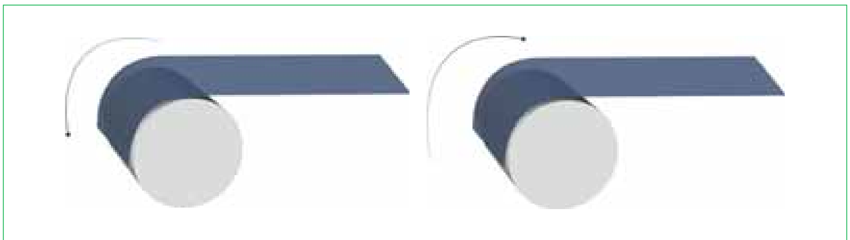

Figure 3. Bending (left) and straightening (right) of a flexible solar module.

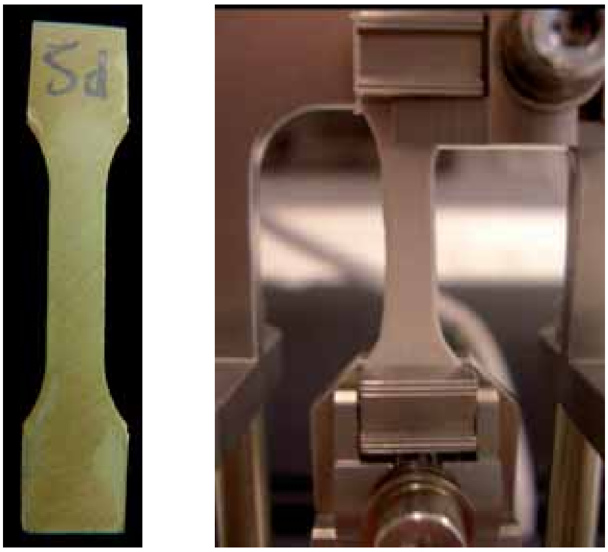

Figure 4. Test specimen made from conductive adhesive (left), and in the testing position (right) for linear DMA.

Figure 5. Effects of moisture ingress due to adhesion loss: delamination (left), and degradation as indicated by an electroluminescence image of a mini-module (right).

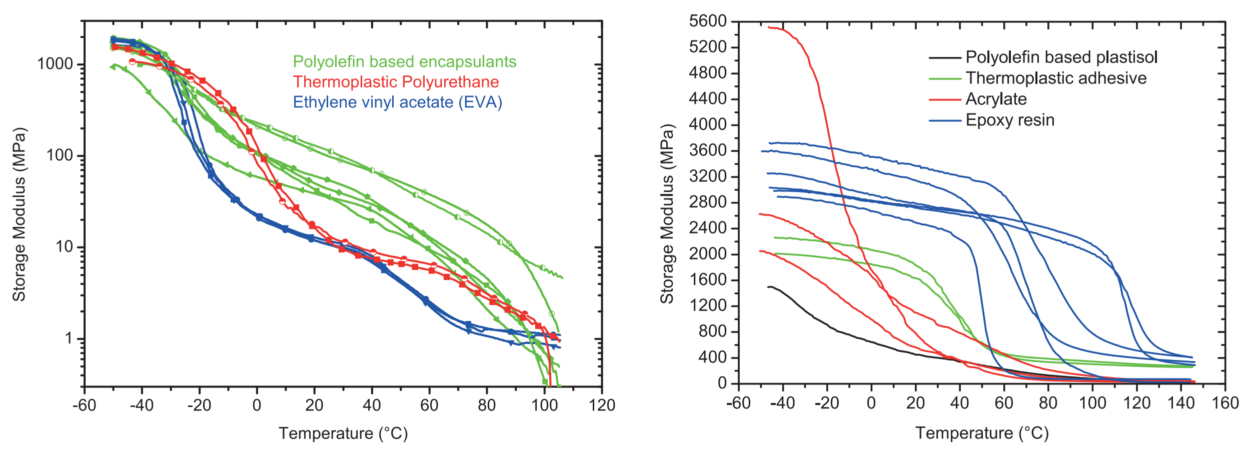

Figure 6. Storage modulus vs. temperature for different encapsulants (left) and polymer conductive adhesives (right).

shaker were carried out to investigate the susceptibility of flexible modules to forced oscillations of up to 200Hz. Frequency and amplitude were measured by a laser vibrometer.

A pulsed AAA sun simulator was used to determine the electrical parameters of the samples, while electroluminescence testing, infrared imaging, laser-beam induced current testing (LBIC), lock-in thermography (LIT) and optical microscopy were used for failure analysis.

A number of material characterization techniques were employed in order to understand the materials' properties and their respective interactions at the module level. The method of choice was dynamic mechanical analysis (DMA) for investigating the thermomechanical behaviour of polymers for encapsulants, barrier films, edge sealings, and polymer-based interconnection materials. The aim was to investigate the elasticity of materials over the typical operating temperature range of solar modules from –40°C to +85°C. As opposed to the procedure used in Kempe [3], linear DMA was conducted for system-adapted test specimens in order to ascertain their respective storage moduli over a range of temperatures (Fig. 4). Adhesion testing between laminated films, encapsulants and edge sealings was performed according to ISO1139:2010 (Adhesives – T-peel Test for Flexible-to-Flexible Bonded Assemblies). Additional mechanical tests, for example a fracture test before and after weathering, were performed to investigate microstructural processes in the polymers. As a further analysis, the dimensional stability of encapsulants with residual stresses was tested under high temperature in accordance with the following procedure – samples of encapsulant were cut to a dimension of 50mm × 50mm, powdered with talcum and placed onto a heating plate at 105°C for 10 minutes.

Key factors for reliable flexible CIGS module encapsulation

The following key factors can be identified by experimentation.

Adhesion and chemical compatibility

Adhesion and chemical compatibility of neighbouring materials are the most important requirements in achieving long-term stable products. The goal is to have neighbouring materials form a sufficiently strong adhesive bond so that cohesive fracture is exhibited during a peel test, not just after lamination but also after accelerated ageing. Inadequate adhesive bonding typically leads to delamination and loss of moisture-barrier protection in module packaging.

During and after the ageing procedures, interactions between materials could be observed: for example loss of adhesion at the interface, outgassing, material decomposition, loss of structural strength and discoloration. Most of these effects could be observed after damp-heat testing or combined UV and damp-heat testing. Consequently, the impact on the module of elevated temperature, moisture and UV radiation may lead to failure mechanisms and subsequent module failure in the field. It is easy to see that stringent testing of materials and their compatibility is vital to the subsequent approval of their use in flexible solar modules.

Thermomechanical behaviour

The thermomechanical behaviour of polymeric materials used as encapsulants and conductive adhesives was characterized by DMA. In this procedure, viscoelastic properties can be gleaned from glass transition and time-dependent deformation behaviour of materials over a significant temperature range from –40°C to above 100°C. A wide variety of storage moduli were observed (Fig. 6). Some of the conductive adhesive materials lose their flexibility at low temperatures and fail under stress. Furthermore, encapsulants are susceptible to creep at high temperatures due to softening.

Encapsulations based on polyolefin (PO), polyurethane (TPU) and ethylene vinyl acetate (EVA) were simultaneously characterized. Distinctive glass transitions at around –20°C were observed for

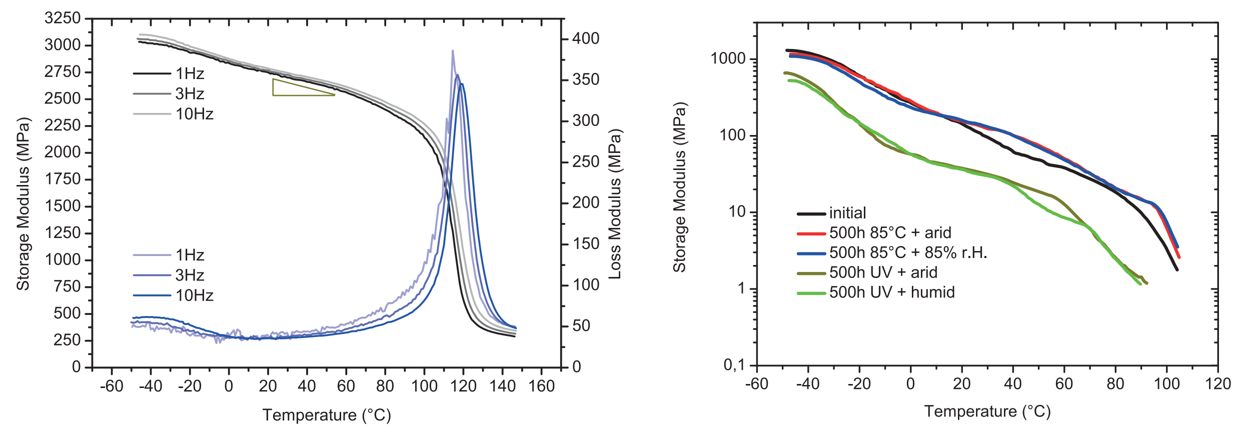

Figure 7. Left: storage and loss modulus vs. temperature of an epoxy-based conductive adhesive with characteristic glass transitions and phase changes. Right: storage modulus vs. temperature of a thermoplastic encapsulant for different environmental influences.

Figure 8. Dimensional changes of different encapsulants before (far left specimen) and after shrinkage tests. Two EVAs and four thermoplastic materials were investigated.

Figure 9. Electroluminescence image of a mini-module showing degradation caused by moisture ingress through the front barrier film.

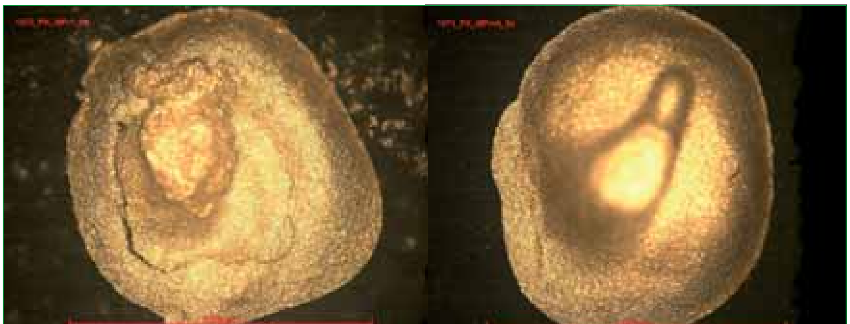

Figure 10. Results of the vibration test. Left: with high-modulus conductive adhesive, mechanical stress has caused the interconnection dot to fracture. Right: with modified conductive adhesive, the interconnection dot is stable.

EVA materials: this represents the thermodynamic phase transition from a crystalline to an amorphous microstructure. The extreme change in material stiffness at very low temperatures leads to high stresses inside an assembled module, and this greatly increases the risk of overloading the encapsulation–neighbour interface. At high temperatures, some EVAs exhibit irreversible material transport that leads to a significant reduction in stiffness. For a long, stable module lifetime, material transport within the module at elevated temperatures and overstressing at low temperatures must naturally be avoided.

Environmental influences

A study was made of the effects on module performance of environmental conditions such as

- Moisture (85% relative humidity at 85°C)
- UV light under dry conditions
- UV light under wet conditions
- Temperature storage (85°C)

The material characterization was then repeated (Fig. 7).

The time-dependent material

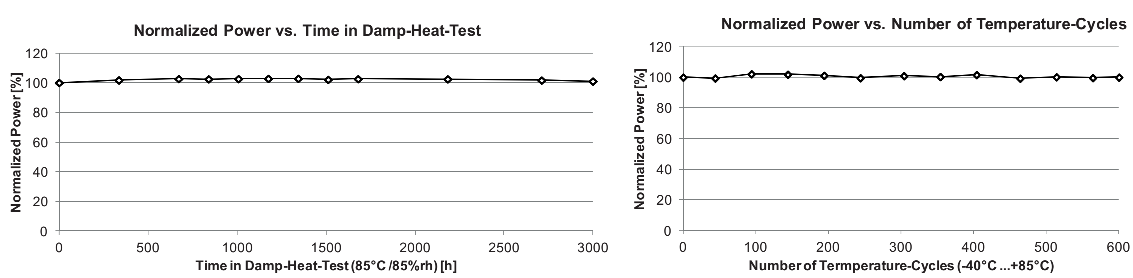

Figure 11. Stability of flexible CIGS modules in temperature-cycle and damp-heat testing.

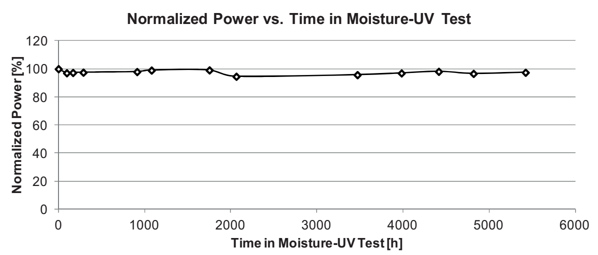

Figure 12. Stability of flexible CIGS modules in combined moisture and UV testing.

deformation and glass transition within the operating temperature range are also critical to the use of polymeric materials in flexible modules. The choice was made to use materials that exhibited linear elastic behaviour over the specified operating temperature and showed no significant modulus changes around the glass transition point. Locally high stresses due to material deformation must be prevented.

Dimensional changes

Besides the specified physical properties of materials, the parameters of the manufacturing process can significantly influence the processability and service life of the module package. For example, volumetric dimensional changes due to residual stresses (Fig. 8) can lead to displacement of the solar cells and ribbons, and can bring about additional mechanical stresses inside the layer composition. In extreme cases, the destruction of the solar cells and/or interconnection structures could be observed.

> “The test modules in the combined moisture and UV testing have been verified to exhibit long-term stability with practically no power degradation.”

Water vapour transmission

Low water-vapour transmission of the materials investigated and very strong resistance to moisture in field applications are additional key factors in flexible CIGS module reliability. These properties are ensured by the transparent front barrier film, the backsheet material and the edge sealing that prevents water vapour ingress via the module edges [4]. CIGS solar cells are known to be sensitive to moisture, and so it was necessary to evaluate a variety of barrier materials with water vapour transmission rates less than $10^{-3}g/m^2$. Otherwise, there could be a large variation of moisture sensitivity, depending on the individual production processes of the different CIGS manufacturers and the materials that they use [5]. Moisture ingress into the module and the resulting cell corrosion can be deduced through the use of electroluminescence imaging (Fig. 9).

Mechanical stress

External mechanical stress can also influence the long-term stability of solar modules. Whereas typical crystalline and thin-film glass modules are rigid and thus susceptible to brittle fracture, flexible solar module materials and their respective interfaces must be able to withstand bending and oscillation forces imparted during production, shipment, installation and operation. Beyond the load tests of IEC 61646, additional cyclic bending tests were applied to flexible modules to ensure their high quality and durability over the guaranteed lifetime. The modules were stressed over a 300mm-diameter drum in convex and concave geometries, and in lengthwise and transverse cell directions. When the preferred interconnection and encapsulation technologies were used, no

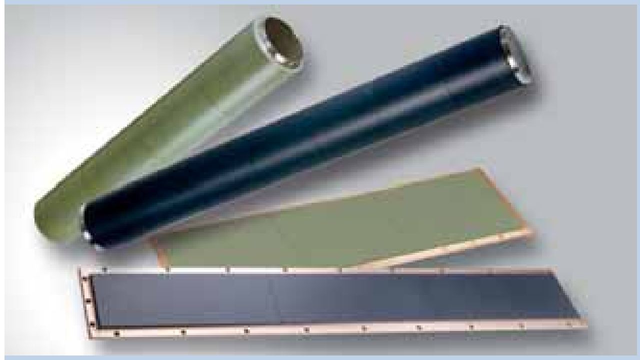

Thin Film

change in power of the modules was evident after 2000 bending cycles.

Further investigations were conducted with vibration tests that showed significant differences in the fatigue behaviour of the cell's interconnection materials. Brittle fracture was observed on high-modulus materials, whereas flexible conductive adhesives exhibited superior stability. The use of modified and matched materials for interconnection and encapsulation leads to excellent vibration stability of the complete system.

"For a long, stable module lifetime, material transport within the module at elevated temperatures and overstressing at low temperatures must naturally be avoided."

Conclusion

Understanding relevant properties of materials and their concomitant interactions is vitally important for developing a general understanding of flexible module packaging. This knowledge allows the development of robust solar modules that could potentially perform far beyond the requirements of IEC 61646, which typically reveals only early failures. The investigations presented in this paper thus define pre-qualification procedures in order to select suitable materials and their combinations in the short term, without the wasted effort of building complete modules in the early phase of product development. Only materials exhibiting positive test results can be brought to process and product qualification. This reduces the risk of premature test failures and avoids significant iterations with, and extensive parallel testing of, multiple material candidates on the module level.

The module technology that has been developed consists of flexible interconnections and a hermetically-sealed cell package that exhibits excellent long-term reliability. In accordance with IEC 61646, damp-heat tests were performed for three times the required length of time, and the temperature-cycle test for three times the required number of cycles: no test sample showed any significant electrical degradation. Likewise, the test modules in the combined moisture and UV testing have been verified to exhibit long-term stability with practically no power degradation.

Acknowledgement

This paper is based on an article by Münch et al. [6]. Parts of this work were supported by financial resources from the European Fund for Regional Development of the European Union and from the German State of Saxony.

References

[1] Sample, T. et al. 2009. "Accelerated ageing of seven different thin-film module types by sequential exposure to damp heat or damp heat with either additional applied voltage or ultraviolet light", *Proc. 24th EU PVSEC*, Hamburg, Germany.

[2] Wohlgemuth, J. 2011. "Failure mechanisms and the use of accelerated tests in the development of reliable PV modules", IEEE Int. Reliab. Phys. Symp., Monterey, California, USA.

[3] Kempe, M.D. 2005. "Rheological and mechanical considerations for photovoltaic encapsulants", DOE Solar Energy Technol. Prog. Rev. Meet., Denver, Colorado, USA.

[4] Kempe, M.D., Dameron, A. & Reese, M. 2011. "Calcium-based test method for evaluation of photovoltaic edge-seal materials", NREL PV Mod. Reliab. Worksh., Golden, Colorado, USA.

[5] Coyle, D.J. et al. 2011. "Life prediction for CIGS solar modules", NREL PV Mod. Reliab. Worksh., Golden, Colorado, USA.

[6] Münch, M. et al. 2012. "Flexible CIGS modules – selected aspects for achieving long-term stable products", NREL PV Mod. Reliab. Worksh., Golden, Colorado, USA.

About the Authors

Markus Münch holds a degree in electrical engineering from Leipzig University of Applied Sciences. He has worked in the PV business since 1997, with responsibilities that have included product development and management. Markus joined Solarion in 2008 and is currently the Solar Module Division Director, leading a team responsible for product and technology development as well as module reliability.

Mike Röllig received a diploma in electrical engineering (M.S. in engineering) from Dresden University of Technology, and completed his Ph.D. in material science and engineering in 2008. His work in the field of microsystems technology, packaging and material characterization focuses on the measurement of the material properties of lead-free solders for industrial applications. Mike is currently employed at Fraunhofer IZFP-D as the head of the department of test and diagnosis methods.

Enquiries

Markus Münch
Solarion AG
Ostende 5
04288 Leipzig
Germany
Email: markus.muench@solarion.de

Mike Röllig
Fraunhofer Institute for Non-destructive Testing
Maria-Reiche-Straße 2
01109 Dresden
Germany
Email: mike.roellig@izfp-d.fraunhofer.de

Calyxo's advanced CdTe module designed for hot climates

Michael Bauer, **Frank Becker**, **Hubert-Joachim Frenck**, **Jochen Fritsche** & **Kenneth Kormanyos**, Calyxo, Bitterfeld-Wolfen, Germany

ABSTRACT

This paper presents Calyxo's recent advances in product design that have resulted in independently confirmed peak aperture-area efficiencies of 13.4% for modules and 16.2% for cells. Some insight is given into a suitable product design for achieving the highest reliability possible, even in hot climates such as Australia, with no signs of degradation during the first three years of deployment in the field. These technical advances and the midterm production-cost target of US$0.50/Wp allow a forecast levelized cost of electricity (LCOE) of under US$0.10/KWh, especially in sunny regions of the world.

Introduction

As the market leader in thin-film photovoltaics, First Solar has demonstrated impressive efficiency and production-cost benchmarks during the last few years, with average aperture efficiencies in production of around 12% and a decrease in manufacturing cost [1]. Calyxo GmbH began successfully following this trajectory, with a manufacturing cost falling below US$0.80/Wp this year and expected to drop below US$0.50/Wp in the future; Calyxo's production yields on average up to 11.9% aperture-area efficiencies and maximum aperture-area efficiencies as high as 13.4% for its modules. Last year Calyxo presented an overview of the decisive cost advantage of its process on the basis of its patented Atmospheric Pressure Physical Vapour Deposition (APPVD) process [2].

"Calyxo's continued increases in efficiency will be a major contributor to further reductions in manufacturing cost."

The targets are clearly defined for increasing CdTe efficiency levels further in the near future, to values that are at least comparable to today's crystalline silicon module efficiencies. Calyxo's continued increases in efficiency will be a major contributor to further reductions in manufacturing cost. The ways in which Calyxo has significantly improved efficiencies during 2011 are discussed in some detail in this paper. Moreover, evidence is presented of the superior semiconductor film quality that is achieved by the hot and fast APPVD process. Product reliability in the field is just as important as initial performance in terms of a prerequisite of success in the photovoltaic industry. This paper presents data supporting the particularly satisfactory long-term performance of Calyxo modules in the field; an example is also given that illustrates why accelerated testing is a useful tool for choosing between different concepts during product development.

Calyxo efficiency development and roadmap

After having achieved product and process stability during early ramp-up of the production line, Calyxo has begun a more intensive improvement programme. Three basic routes for improving efficiency are being followed:

1. Improvement and optimization of the electrical quality of the device stack on the basis of benchmark values.

2. Further improvement of the APPVD semiconductor film quality.

3. Further process improvement to reduce the variation in electrical performance over the entire module area of 0.72m^2.

To fully leverage the device potential, the electrical properties of the Calyxo device were first benchmarked against a former world-record holder – the device made by Wu et al. [3]. Fig. 1 shows a qualitative and quantitative assessment using two powerful tools: an *I-V* analysis and external quantum efficiency (EQE) measurements. From this assessment the following levers were identified and consequently worked on:

- Device-current improvements (labelled 1.1 in Fig. 1) as well as short-wavelength improvements (2.1), which require CdS thickness and substrate optimization (glass thickness and composition, TCO, anti-reflective coating).

- Device-voltage improvements (1.2) as well as long-wavelength improvements (2.2), which require back-contact and semiconductor optimization as well as low-iron glass.

On the basis of these investigations, it was possible to achieve an externally confirmed 16.2% small-cell efficiency (Fig. 2).

Optimization of the semiconductor deposition and of the post-treatment processes of the APPVD process remain important levers in increasing efficiency.

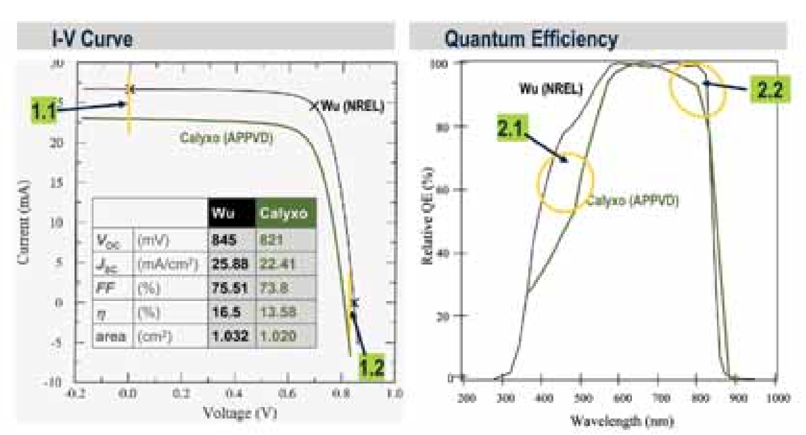

Figure 1. Benchmarking of Calyxo *I-V* curve and external quantum efficiency (EQE) before optimization vs. former world record of performance at the cell level [3].

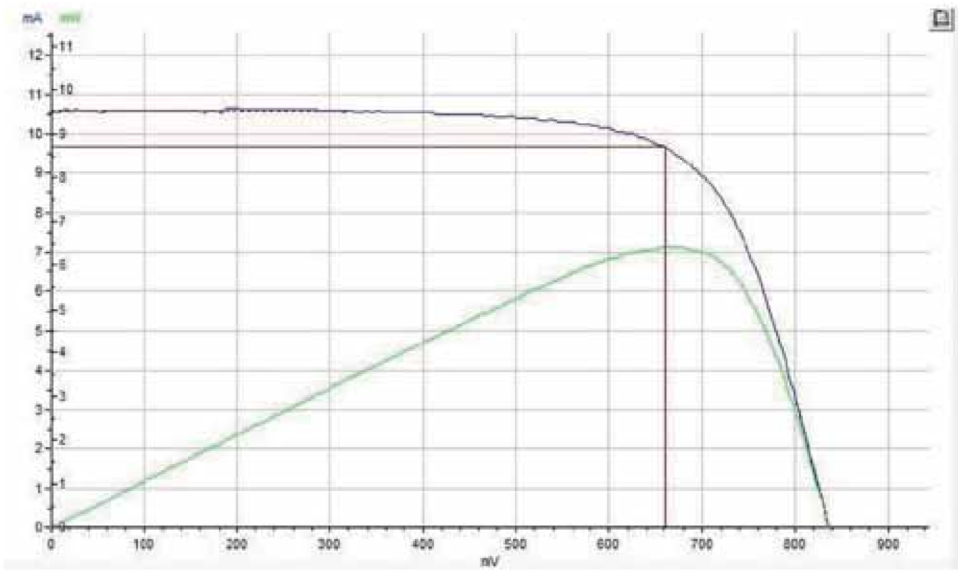

Figure 2. *I-V* curve of the Calyxo 16.2% externally confirmed record cell.

The advantages of the hot and fast APPVD process over vacuum deposition technologies becomes apparent from extensive SEM preparative studies. One finds less non-ideality in the APPVD crystal structure than when vacuum technologies are used; moreover, the growth of the CdTe grains is columnar, which is preferable as it results in less recombination and high V_{oc} values. This work is currently ongoing, but it is planned to publish details of the studies soon.

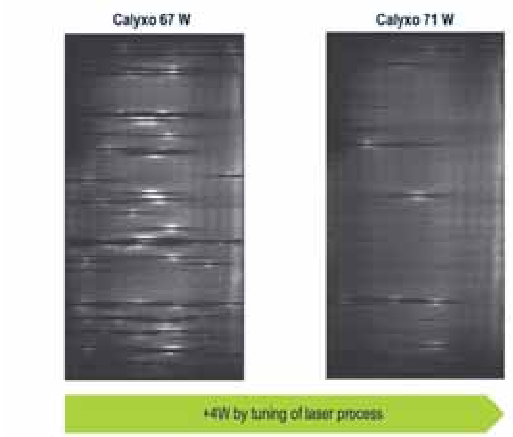

Figure 3. EL (electroluminescence) images for assessing electrical module homogeneity.

> "Optimization of the semiconductor deposition and of the post-treatment processes of the APPVD process remain important levers in increasing efficiency."

A major concern is non-uniformities, which can limit the achievement of high power values for a complete module as well as good overall yields in mass manufacturing. There is no single root cause of poor homogeneity values. Basically every process step and raw material can have an impact on homogeneity, as noted by Becker & Frenck [2] in the recently published systematic approach for line optimization during ramp-up. Qualitative analytical methods such as electroluminescence have been found to be very useful in identifying improvement potential in Calyxo's production line. Fig. 3 gives an actual example showing the impact of identifying and resolving so-called 'point shunts' to enhance device performance.

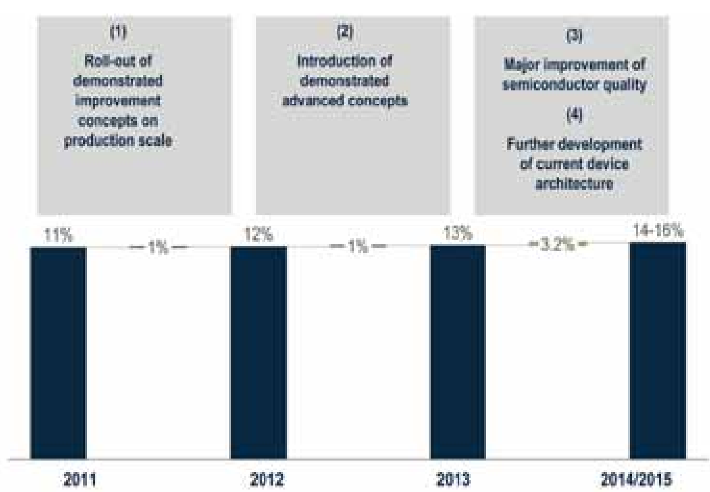

Figure 4. Calyxo's efficiency roadmap.

Outlook for further efficiency development trends

It is certainly fair to say that the leading CdTe module manufacturers have already demonstrated their ability to make modules rated at 13% aperture efficiency as the standard product offering in the near future – for example, First Solar 14.4% full size, Calyxo 13.4% aperture, Primestar 12.8% aperture and Abound 12.2% aperture. No fundamental new scientific advances are required to achieve this goal. Fig. 4 illustrates the basic concept of Calyxo's research and development roadmap for achieving 14–16% average efficiency in mass production. A brief overview of leveraging Calyxo's film potential to efficiencies much higher than 20% was given recently [4].

Field performance of CdTe modules

CdTe modules exhibit several features that are beneficial to the energy yield of a CdTe-powered photovoltaic system. Several independent studies have looked at the real-life energy yield of CdTe photovoltaic systems. The paper by Huld et al. [5] confirmed two major advantages of CdTe modules: 1) the good light-harvesting properties of the modules tested under moderate illumination, well below standard test conditions (STC); 2) the positive impact of the low CdTe temperature coefficient. The temperature coefficient for CdTe modules is around –0.25%/K at Pmpp, and is slightly dependent on the module manufacturer. The CdTe temperature coefficient is significantly lower in magnitude than in the case of crystalline silicon or CIGS modules, which have a temperature coefficient of roughly –0.4%/K at Pmpp. Our own simulations on the energy yield in regions with higher global horizontal solar irradiation (such as in India) have demonstrated up to 10% more electricity per KWp installed compared to crystalline silicon modules. This is a significant result since it basically says that CdTe systems, which are comparably priced to crystalline silicon systems, will generate 10% more delivered energy because of the better performance at realistic module temperatures. A levelized cost of electricity (LCOE) of under US$0.1/KWh in sunny regions is a reasonable short-term goal for CdTe PV systems.

The importance of module stability in different climates

There have been numerous studies about the future of PV technology and its use in various parts of the world (see, for example, Breyer and Gerlach [6] and references cited therein). Most of those studies arrive at the conclusion that PV technology will likely be installed in areas with high irradiation. These include:

- Densely populated regions, which may sometimes have been so since ancient times (India, Mediterranean)
- Territories with a high percentage of people who do not have access to the grid at all (Africa or India)

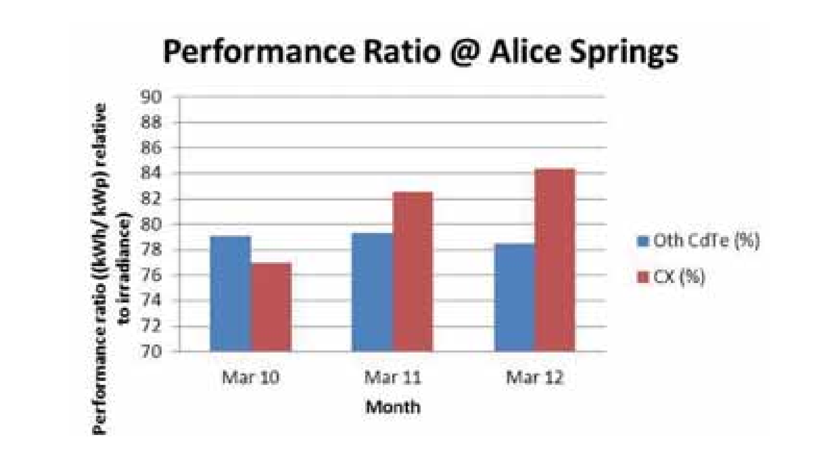

Figure 5. Performance of Calyxo modules in the Australian desert.

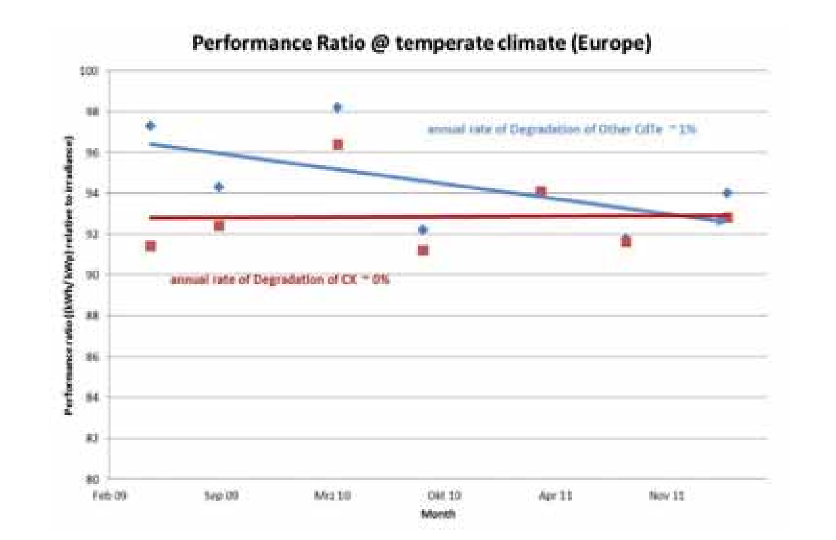

Figure 6. Performance of Calyxo modules in a temperate climate (Germany).

- Areas where the standard of living is exceptionally high (Sun Belt and Hawaii in the USA)

In all cases, the need for alternatives to conventional power stations is as obvious as it is critical, since the necessary cooling medium (in most cases water) is either in short supply or very expensive. Thus the cost of electricity in these areas is higher than in other regions, and often a premium has to be paid for electricity consumption at noon, while at the same time the LCOE from PV is potentially low because of high irradiation [7].

> "Hot climates are said to impose stringent demands on the quality of the module."

On the other hand, these climates place specific demands on the PV systems to be installed. The typical widely used means of evaluating PV module long-term stability may no longer be applicable [8], and there may be additional challenges to overcome. It has been pointed out that for some climate zones there are indications that degradation rates may be higher than in other climate zones [9]. In particular, hot climates are said to impose stringent demands on the quality of the module.

Acknowledging this fact, Calyxo has been thoroughly investigating, since the early days of production, the performance of modules in those climates. Fig. 5 shows that Calyxo modules perform well at a site in the Australian desert: the performance ratio is satisfactory and even increases over the two-year period of investigation. From the data presented in Fig. 5 it can be concluded that the Calyxo modules have a rate of degradation below the 0.5%/yr limit usually assumed to be safe in guaranteeing a minimum 80% power output after 25 years of operation [9]. This particular result is attributed in large part to the careful design of the Calyxo layer stack, which will be discussed in a later section.

The performance of a PV module depends on the climate in which it is installed [10]. Since around 74% of the global PV capacity has been installed in Europe [11], predominantly in Germany, the performance of modules in temperate climates needs to be evaluated. The results for a test array in Germany are shown in Fig. 6. The performance ratio of Calyxo modules is stable over the test period of more than two years; at the same time, different CdTe modules do not exhibit the same behaviour. Together with the data presented in Fig. 5, it is concluded that Calyxo's layer stack and its module perform well in the current market, and will do the same in future ones.

In order to further improve the performance, it is necessary to rely on scientific data and laboratory tests. When introducing new elements to the layer stack or a new module construction, the test procedures as laid out by TÜV, IEC and UL offer good guidelines for testing, and can form the basis of any in-house qualification run. Further information may be gathered by temperature/time matrices of specific stress-test procedures (e.g. V_{oc}). An illustrative example is presented in Fig. 7, taken from a feasibility study relating to two different module features investigated during product development; two different module solutions were evaluated. While both module features yield good initial results, differences in performance are seen at higher temperatures and longer exposure times, thus allowing the better module construction to be identified.

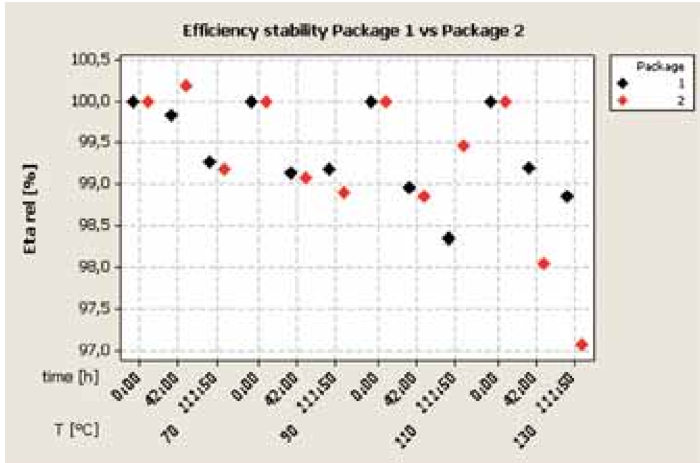

Figure 7. Performance of two different module solutions.

Product development trends

Besides efficiency developments, other product properties are definitely up for discussion, from both customer-value-generating and cost-saving points of view. Module parameters such as product size and weight undergo continuous evaluation and are good candidates for optimization. However, the 1.20m × 0.60m module has become a pseudo 'standard size' for CdTe modules and is part of many of the designs of the balance of system in a PV installation, which makes it difficult to change the standard product size of CdTe modules. Ongoing cost-saving efforts across the entire value chain, from raw-material production to system operations, will certainly have an impact on the module itself.

It has already been pointed out that module construction is often not yet regarded as part of the technology roadmap in PV technology [2], a noteworthy exception being the introduction of Calyxo's new CX3 module. To give but one example, the choice of the encapsulation material will be discussed in some detail. As the encapsulant is just one of many materials to form a module, it is obvious that the choices for combining the various materials are as numerous as the pitfalls that await if no consideration is given to all the interactions and specific demands, from qualification procedures to stability issues.

Historically, PV modules have been encapsulated mostly in ethylene vinyl acetate (EVA), since a highly transparent yet comparatively unreactive thermoplastic material was needed to protect crystalline-Si wafers from moisture and the environment in general [12]. Most of the PV industry has stayed with EVA, because module construction has not been on the agenda. EVA therefore remains the predominant encapsulant and is also used with CdTe superstrate technology, although it has been pointed out that, in this particular case, there is no need for the encapsulant to be transparent [2]. Thus, attention may be focused on different material properties. One specific issue with CdTe material is that cells exposed to high humidity at elevated temperatures are prone to premature degradation [13]. On the other hand, it is known that, in terms of moisture vapour transmission rate (MVTR), there are far better thermoplastics than EVA [14]. EVA loses its initially good properties very quickly; moreover, it has been noted before that EVA may not be the best possible encapsulant to ensure protection, because of corrosion issues and high water diffusivity. Polyolefines and ionomers are suitable, though by no means the only choices [12,15].

Table 1 gives an overview of the range of MVTR data that can be achieved with various thermoplastics. Since thermoplastics can be manufactured in a variety of blends, with every manufacturer having its own special recipe because of intellectual property issues, this in turn results in materials having different specific properties. The set of data in Table 1 is intended to serve as a guideline only. It is up to the PV manufacturer to pick a suitable material on the basis of the demands presented by the place of installation or other boundary conditions. Given the right volume of material to be used, a PV manufacturer can even tailor thermoplastics to optimize certain parameters. Picking the right encapsulant is not determined by simply choosing the thermoplastic with the lowest moisture ingress rate. The encapsulant's viscosity and manufacturability, as well as creep upon thermal exposure, have to be taken into account [17].

Calyxo's new module construction has successfully undergone the standard certification cycle in accordance with the relevant standards in various markets. Even after non-standard testing, such as extended damp-heat tests (multiple IEC cycles), the CX3 module showed no visible features and would have passed

Class or material description	MVTR [g·mm/m²/day]
Ionomer	0.5–1.5
EVA (ethylene vinyl acetate)	15–25
PVB (polyvinyl butyl)	35–65
TPO (thermoplastic polyolefine)	1.5–2.5
TSI (thermoplastic silicone)	50–90
TPU (thermoplastic urethane)	55–100+

Table 1. Comparison of moisture vapour transmission rates (MVTRs) of several potential sealing materials for photovoltaic modules. (Data taken from Kempe et al. [15], Swonke & Auer [16] and data sheets from various suppliers.)

Element	Linear coefficient of thermal expansion (CTE) α [10^{-6} 1/K]
Aluminium	23
Chromium	4.9
Molybdenum	4.8–5.0
Nickel	13
Copper	16.5
CdS	5.9
CdTe	4.0–6.5

Table 2. CTE of some semiconductor and back-contact materials used in CdTe thin-film photovoltaics.

the standard test criteria. Moreover, excellent performance of the CX3 product was demonstrated in non-standard bias damp-heat testing: no critical features were observed, even by extensive electroluminescence analysis.

Another example in which design features affect the durability and the reliability of the module can be given, relating to the design of the metallic back contact of the device. The individual layers need to be matched with regard to the different thermal and mechanical properties of the individual layers. In that respect it is advantageous to have monolithic layers instead of complicated stacks for which, in most instances, only a single parameter is optimized while other parameters that could be of equal importance are disregarded. Calyxo's approach is based on simplicity and straightforward processing to make sure that all layers are monolithic and the interfaces are suitably matched.

Table 2 gives a summary of some of the data that has to be taken into account when designing an optimized layer stack, comparing CTE of the semiconductor compound and some metals that are widely used in PV technology and exhibit sufficiently low electrical resistivity. It is noted that, while a number of metals have CTE values that are close to those of CdS and CdTe, there are also less appropriate choices which, if used as a back-contact material, would eventually lead to high strains during thermal cycling.

Environmental, health and safety aspects

Today's society pays increasing attention to a responsible and sustainable approach in using resources. Among all photovoltaic technologies, one of the most investigated is CdTe module technology, and its positive impact in terms of economic and environmental characteristics has repeatedly been demonstrated. To give just one example, a photovoltaic system built using CdTe thin-film modules is one of the best in terms of energy payback time – this can be well under a year, depending on the installation location [18].

> "Developments regarding product improvement suggest that a reduction in manufacturing cost to US$0.50/Wp is a realistic assumption."

Summary

This paper has presented the recent advances made by Calyxo in improving its product, thereby demonstrating cell efficiencies as high as 16.2% as a result of device optimization and homogeneity improvement in production. These developments regarding product improvement suggest that a reduction in manufacturing cost to US$0.50/Wp is a realistic assumption. In conjunction with the excellent light-harvesting behaviour of CdTe modules, the LCOE will shortly fall below US$0.10/KWh. These economic facts and the good environmental profile of CdTe will support a significant market share of CdTe thin-film photovoltaic technology, especially in areas with high solar irradiation. It has been shown that careful design of the module for reliability leads to outstanding product performance in both hot and moderate climates.

References

[1] First Solar [http://www.firstsolar.com].

[2] Becker, F. & Frenck H.-J. 2011, "CdTe thin film modules: Basic developments, optimizing performance and considerations in module design", *Photovoltaics International*, 12th Edn, pp. 134–139.

[3] Wu, X. et al. 2001, "16,5%- efficient CdS/CdTe polycrystalline thin-film solar cell", *Proc. 17th EU PVSEC*, Munich, Germany, pp. 995–1000.

[4] Bauer, M. 2012, "Technology and developments in CdTe thin film photovoltaics", *Future in Photovoltaics*, Issue 7 [available online at http://www.futurepv.com].

[5] Huld, T.H. et al. 2010, "Mapping the performance of PV modules, effect of module type and data averaging", *Solar Energy*, Vol. 84, pp. 324–338.

[6] Breyer, C. & Gerlach, A. 2010, "Global overview on grid-parity event dynamics", *Proc. 25th EU PVSEC*, Valencia, Spain.

[7] Woodhouse, M. 2011, "An economic analysis of photovoltaics versus traditional energy sources", *Proc. 37th IEEE PVSC*, Seattle, Washington, USA.

[8] Kurtz, S. 2011, "Evaluation of high temperature exposure of photovoltaic modules", *Prog. Photovolt: Res. Appl.*, Vol. 19, p. 954.

[9] Jordan, D.C. & Kurtz, S.R. 2011, "Thin film reliability trends toward improved stability", *Proc. 37th IEEE PVSC*, Seattle, Washington, USA.

[10] Jordan, D.C. & Gotwalt, C. 2011, "JMP applications in photovoltaic reliability", presentation at JMP Discovery Summit, Denver, Colorado, USA, NREL Report PR-5200-51126.

[11] Ardani, K. & Margolis, R. 2011, "2010 solar technologies market report", US Department of Energy (DOE)/GO-102011-3318.

[12] Kempe, M. 2010, "Evaluation of encapsulant materials for PV encapsulation", *Photovoltaics International*, 9th Edn, p. 170.

[13] Visoly-Fisher, L. et al. 2003, "Factors influencing the stability of CdTe/CdS solar cells deduced from stress tests at elevated temperatures", *Adv. Funct. Mater.*, Vol. 13, No. 4, p. 289.

[14] Kempe, M. 2005, "Module encapsulant diagnostic and modeling", NREL Report CP-520-37027.

[15] Kempe, M. et al. 2010, "Evaluation and modeling of edge seal materials for photovoltaic applications", *Proc. 35th IEEE PVSC*, Honolulu, Hawaii, USA.

[16] Swonke, T. & Auer, R. 2009, "Impact of moisture on PV module encapsulants", *Proc. SPIE*, Vol. 7412, p. 74120.

[17] Miller, D.C. et al. 2010, "Creep in photovoltaic modules: Examining the stability of polymeric materials and components", *Proc. 35th IEEE PVSC*, Honolulu, Hawaii, USA.

[18] PVthin [http://www.pvthin.org].Woodhouse, M. 2011, "An economic analysis of photovoltaics versus traditional energy sources", *Proc. 37th IEEE PVSC*, Seattle, Washington, USA.

About the Authors

Michael Bauer studied process and mechanical engineering at Martin Luther University of Halle and at the Technical University Braunschweig. He received his Ph.D. from the University of Halle in engineering, with a focus on the theoretics of scale-up of heat transfer mechanisms in tubular fixed-bed reactors. Michael is the CTO of Calyxo and has been leading operations since 2009.

Frank Becker studied electrical Engineering at the University of Saarland, where he specialized in semiconductor and sensor technology. Since finishing his academic studies in 1993 he has worked for various companies in areas including project engineering, fibre optics, high-speed transponders and metallization. Frank has been part of the technical management team at Calyxo since 2008 and is currently the head of development.

Hubert-Joachim Frenck studied physics at the University of Münster. He changed to the chair of Prof. Kassing at Kassel to conclude his Ph.D. in 1988 on 'Molecular engineering in PE-MOCVD thin-film deposition'. Since then, he has been working in areas related to thin-film technology. Hubert was appointed head of production at Calyxo in 2009.

Jochen Fritsche is responsible for research, IP management and product development at Calyxo GmbH. Jochen received his Ph.D. in material science from Darmstadt University of Technology on electronic properties of semiconductor interfaces of CdTe thin-film solar cells and worked as a research assistant and project leader in CdTe research for six years.

Kenneth R. Kormanyos is the president of Calyxo USA, Inc., the US-based R&D group for Calyxo GmbH. As engineering director for Solar Fields, LLC (2003–07) he developed the APPVD process used by Calyxo GmbH. Earlier affiliations include First Solar (1998–2003), Glasstech (1989–1998) and Owens-Illinois (1971–1989). He has 20 US patents and has contributed to several publications. Kenneth received his qualification in engineering physics at the University of Toledo in Ohio in 1971.

Enquiries

Calyxo
Sonnenallee 1a
D-06766 Bitterfeld-Wolfen
Germany
Email:

PV Modules

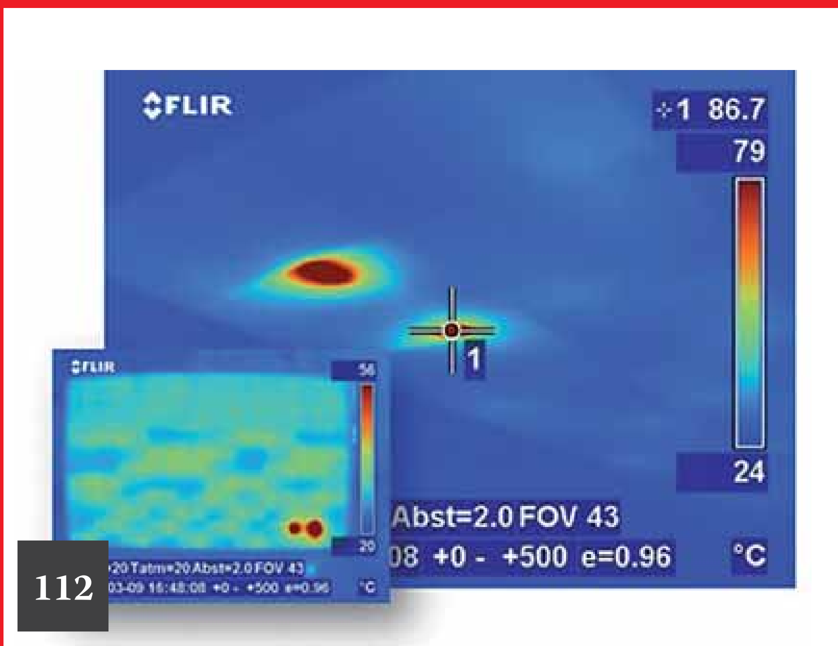

Canadian Solar's shipments drop by 21% in first quarter

As has been the theme throughout 4Q'11 and 1Q'12 quarterly results, it would appear that not even the 'major' manufacturers and suppliers in the PV industry are exempt from revenue and shipment woes. Canadian Solar has reported a drop of over 21% in module shipments, logging 343MW in 1Q'12 compared to 436MW in 4Q'11. Second-quarter shipment guidance is in the range of between 430MW and 450MW.

However, the company's diluted loss per share was US$0.49 – significantly down from US$1.39 in the fourth quarter 2011. Canadian Solar also reported cash, cash equivalents and restricted cash balances of US$625.2 million – up more than US$100 million from the US$522.3 million reported at the end of the last quarter. Canadian Solar attributed the shipment and revenue drops to continued ASP declines, increases in expenses and general market and financial constraints.


Source: Canadian Solar

Canadian Solar has reported a drop of over 21% in module shipments, logging 343MW in 1Q'12 compared to 436MW in 4Q'11.

Business News Focus

Tata BP Solar chief executive resigns

K. Subramanya has resigned as CEO of India's third largest panel manufacturer, Tata BP Solar, effective May 1. No explanation was given for the resignation and Subramanya has stated he has no plans for the immediate future.

Module maker Tata BP Solar, initially a joint venture between British Petroleum and Tata Power Co., has come under increasing competitive pressure from low-cost Chinese manufacturers. Tata Power bought out BP last December, as BP closed all of its worldwide solar operations, but like US and European panel producers, has struggled to compete with Chinese manufacturers.

Indian manufacturers are constructing more than 700MW of renewable energy capacity but the country has received very few orders, forcing the closure of numerous factories throughout India.

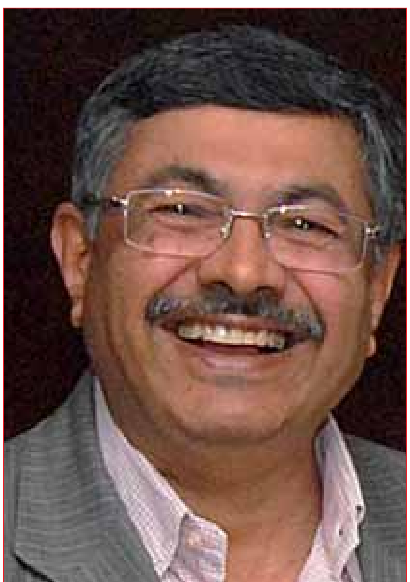
Source: The Hindu

Subramanya gave no reason for his departure and has said he has no plans for his immediate future.

US Department of Commerce aligns final determinations for CVD and AD investigations

The US Department of Commerce (DoC) has announced that final determination of the countervailing duty (CVD) investigation and the final determination of the antidumping duty (AD) investigation of Chinese PV cell imports will be issued at the same time.

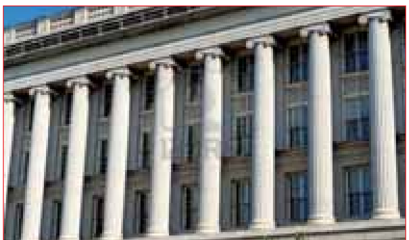
Source: 123rf.com

The DoC decided that since both investigations were initiated together, the deadline should be the same.

Both determinations will be issued no later than July 30 2012. The reason for this is that, due to their simultaneous initiation, both determinations should have the same deadline, the DoC said. The AD's preliminary ruling is scheduled for May 16, while the preliminary ruling for the CVD was already issued back in March. The DoC claims that Chinese manufacturers of PV modules have inappropriately received government subsidies.

Navigant releases 7th annual edition of PV analysis report

Navigant's Solar Services Program advised that its Photovoltaic Manufacturer Shipments, Capacity & Competitive Analysis 2011/2012 is now available. The report gives an analysis of PV industry shipments, capacity and average prices and

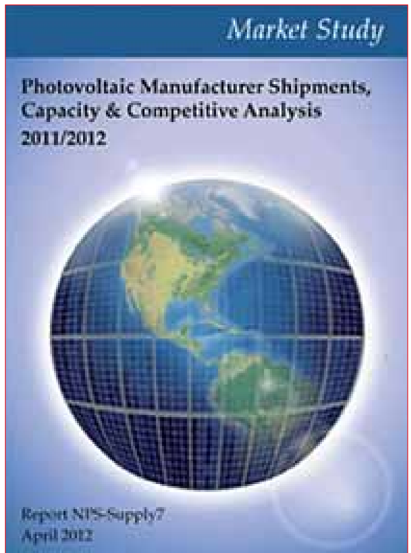

Source: Navigant Consulting

Navigant Consulting's Photovoltaic Manufacturer Shipments, Capacity & Competitive Analysis 2011/2012 is now available.

revenues as well as a five-year forecast of technology shipments.

The seventh annual edition of the report includes, among other features, ASP's for PV technologies with a complete trend line from 1986 to 2011 and forecasts to 2012, annual shipments of PV technologies broken out by region, manufacturer and technology, a discussion of 2011's top PV manufacturers and forecast and discussion for the CSP, HCPV and LCPV industries.

Hanwha acquires three-year US$180 million development loan

Hanwha SolarOne has acquired a three-year US$180 million syndicated term loan facility led by The Korea Development Bank, Standard Chartered Bank (Hong Kong), KEB Hong Kong Branch, KDB Asia and KEB Asia Finance. The loans will be denominated

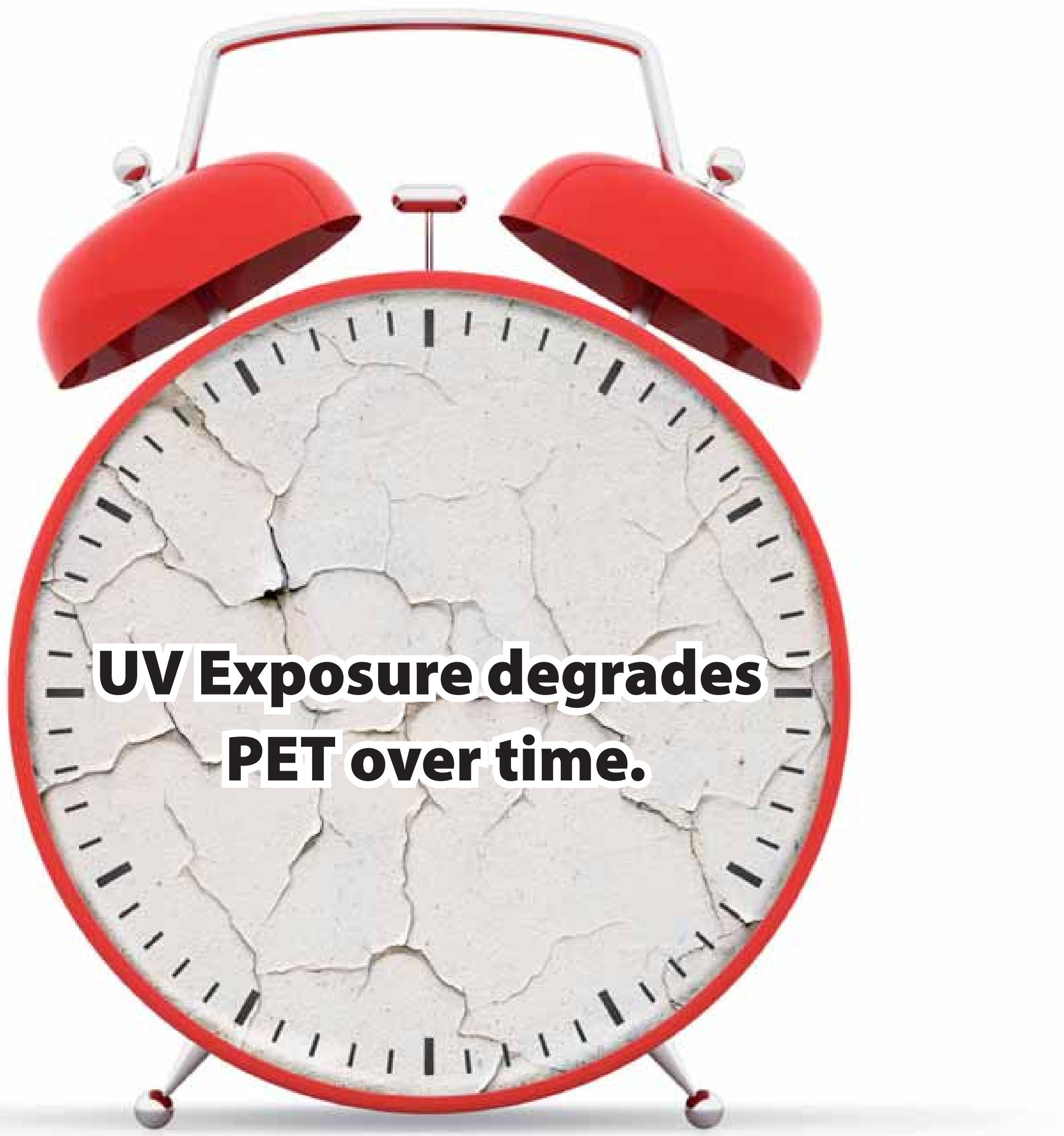
UV Exposure degrades
PET over time.


Source: SAG Next

Hanwha SolarOne has acquired a three-year US$180 million syndicated term loan facility.

in US dollars and will be guaranteed by Hanwha Chemical Corporation.

Testing and Certification News Focus

PV Evolution Labs announces launch of new PID certification program

Canadian Solar has become the first solar company to pass the stringent new PID certification program unveiled by US solar module testing laboratory, PV Evolution Labs (PVEL). The certification program was designed to inform module manufacturers and project developers on intricacies of module degradation from system voltages, a leading cause of module failure.

The PID certification program was designed to recreate the voltage-derived stresses an installed module will experience, conducted by subjecting modules to 600 hours of maximum system voltage levels with damp heat conditioning. Stipulations of the PID certificate require periodic retesting.

Suntech unveils high-performance 305W module

Suntech Power Holdings has unveiled STP 305-24/Vd module with SuperPoly technology. With 305Wp nominal power and up to 15.7% efficiency, the company states that this high-performance module is ideally suited for large-scale commercial projects seeking low levelized cost of energy (LCOE).

The module achieves high efficiency by utilizing an advanced ingot casting process, which combines the benefits of monocrystalline silicon wafers and polycrystalline silicon wafers into one product.

The 72-cell/6-inch module is claimed to have one of the highest fill factors in the industry with a large scale format of 1956 x 992mm, which reduces installation costs


Source: Suntech Power Holdings

The STP 305-24/Vd module was launched at Solarexpo 2012 in Verona, Italy in early May, 2012.

and delivers a lower LCOE. The product line offers Suntech's 25-year power output warranty and a workmanship warranty of 10 years. In addition, the panels feature 0/+5% positive power tolerance and have been built to withstand all weather conditions, well above IEC standard requirements.

Siliken receives EQA Carbon Footprint Certificate

Siliken has taken another step towards environmental sustainability after being awarded the Carbon Footprint Certificate for its SLK60P6L modules. The presentation of the award is based on a calculation of indirect and direct greenhouse gas emissions throughout the manufacture and distribution process, until delivery to the client. Siliken's SLK60P6L modules emit 213.83kg of CO_2


Source: Siliken

Siliken is one of the limited number of PV companies to have achieved the satisfactory standard for the certificate.

per manufactured panel, meeting the satisfactory PAS 2050:2011 standard.

The company's modules have already received a number of industry certificates for a variety of environmental standards. These include the ISO 9001:2008 and 14001:2004 certificates, the TÜV certificate to the IEC 61701:1995 standard and product certificates in accordance with the EN (IEC) 61215:2005 and EN (IEC) 61730:2007 standards.

Other News

Upsolar to expand its technology division

Upsolar has announced an expansion to its technology division, to offer a suite of testing, auditing and consultation services to local organizations in an effort to strengthen technical support for emerging PV companies.

The company intends to provide its clients with component and module testing in compliance with International Electrotechnical Commission (IEC) standards. Current offerings include evaluations on electrical safety, bypass diodes, wet leakage currents and insulation. The technology division is also equipped for durability testing, where products are exposed to extreme environments including high temperatures, UV acceleration, excessive humidity and mechanical stresses.

Outside the lab, Upsolar engineers are available for consultation services ranging from on-site PV plant inspection to comprehensive operational assessments to assist clients with improving their internal manufacturing processes, including productivity improvement and waste management.

ArrayPower and ShinHa partnership will bring sequenced inverters to Korea

ArrayPower's sequenced inverters are being put through their paces yet again. Field tests conducted by juwi recently, appear to have caused a stir in Korea. Sales representative ShinHa has entered into an agreement with ArrayPower for these inverters that are claimed to have demonstrated higher energy harvest compared to conventional string inverters. ShinHa will provide sales and technical support.

ArrayPower's sequenced inverter will be sold to module producers, to integrate the inverter during the module manufacturing process, facilitating cost reductions across the solar value chain and enhancing ease of installation by enabling a plug-and-play AC module. The sequenced inverter is backed by a 25-year warranty.

8minutenergy Renewables Spire sells 250th 4600SLP sun simulator

Spire Corporation has reached a new milestone with the shipment of its 250th 'Spi-Sun' simulator 4600SLP. Spire noted that it had supplied over 600 simulators in total, since having started selling the equipment. Spire reached the 100 shipment milestone in April 2010.

China Sunergy supplies Renewable Energy with 31MW of PV modules

China Sunergy has announced that it has entered into a supply agreement with Renewable Energy, a subsidiary of SUNfarming Group. Sunergy will exclusively supply Renewable Energy with 31MW of its PV modules. The modules will be used for a variety of ground-mounted systems and rooftop installations in Germany. Last year, Sunergy supplied SUNfarming with 23MW of its modules.

Ethiopia to get first PV module assembly plant courtesy of Spire

Spire Corporation has been selected to provide a 20MW turnkey module assembly line to a partnership between renewable energy project developer, SKY Energy International and Metals and Engineering Corporation and an Ethiopian state enterprise, Metals and Engineering Corporation (METEC) that will be the first module plant in Ethiopia. The assembly line will be established in Addis Ababa.

SolarWorld provides 10.6MW to Gujarat solar park

German module manufacturer SolarWorld has provided 10.6MW in PV modules to Asia's biggest solar park in Gujarat, India. The Gujarat solar park, located near Charanka in the Patan district, has a total capacity of 600MW, installed by a variety of developers.

SolarWorld provides 10.6MW to Gujarat solar park

German module manufacturer SolarWorld has provided 10.6MW in PV modules to Asia's biggest solar park in Gujarat, India. The Gujarat solar park, located near Charanka in the Patan district, has a total capacity of 600MW, installed by a variety of developers.

REC signs agreements to supply 20MW for Bulgarian solar projects

REC has announced that it will supply 20MW PV modules for several installations across Bulgaria. Alma-D and REC signed a deal for over 10MW of modules for six Bulgarian projects in which Alma-D is the stakeholder. Among the projects are a 6MW plant in Kamenar and a 4MW plant in Kameno; REC also signed three contacts with Elektro-Solar Systems for a 2MW project called Kosharevo, a 3MW Voinikovo project and a 5MW project dubbed Pop Gruevo.

Phono Solar and SYBAC sign €300 million deal

Phono Solar and SYBAC have solar signed a five-year purchase agreement for €300 million, which equates to a module output of 500MW. Phono Solar's monocrystalline and polycrystalline silicon solar modules range recently passed TÜV Rheinland's ammonia corrosion test.

Moose Power chooses Heliene modules for Ontario project

Toronto-based solar developer Moose Power Inc (MPI) has announced that it has chosen to use Heliene modules for its upcoming 1MW solar project in Ontario. Heliene's manufacturing operation in Sault Ste. Marie produces high-density PV modules that meet the Ontario Power Authority's domestic content requirements. The modules will be installed on four buildings across the city under Ontario Power Authrotity's feed-in tariff scheme, marking the first in a portfolio of over 2MW that has been awarded to FTS Energy Solutions, a joint venture between Wynn Family Properties and MPI.

Hanwha panels selected for Disney's green exhibition

INNOVENTIONS at Epcot has announced it has selected solar panels from Hanwha for its educational facility at the Walt Disney World Resort, Florida. The experiential exhibit has been erected to provide visitors with a practical look at green building technologies. The VISION House is a large home with realistic living space and interior decor.

ET Solar supplies 4MW of modules for rooftop PV projects in France

ET Solar has announced the completion of four rooftop projects, totalling 4MW generating capacity, in partnership with French developer Langa Solar. The projects are expected to begin power production by mid-2012. The two companies jointly designed, installed and financed the four projects with ET Solar supplying the PV modules for the plants.

IKEA Italy installs 7MW of Q-Cells' modules

IKEA has announced that it will equip the roof of its main warehouse in Piacenza, Northern Italy, with 7MW of Q-Cells' CIGS thin-film modules. The rooftop installation was developed in collaboration with GreenTechPower and F. Ili Zaffaroni.

Product Reviews

KÖMMERLING

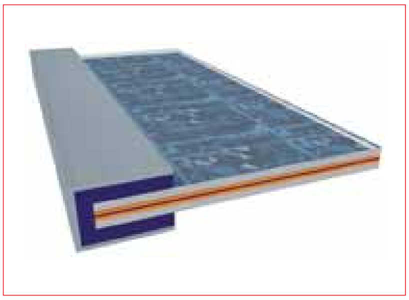

KÖMMERLING's PVS 120 offers improved water and moisture vapour tightness

Product Outline: KÖMMERLING has launched its new butyl based framing sealant 'HelioSeal' PVS 120. In contrast to existing framing sealants on the market, HelioSeal PVS 120 is claimed to provide immediate green strength and superior water and moisture vapour tightness. The sealant is applied hot and can be used by hand or in fully-automated high speed lines.

Problem: Water tightness alone is not enough for the protection of PV modules. It is also necessary to ensure moisture vapour tightness of the whole system especially in the framing area a parameter for long-life durability. The PV industry is looking for sealing systems which can be easily used in the production process.

Solution: HelioSeal PVS 120 is a butyl rubber-based hot melt framing sealant which is delivered ready-to-use. It claims that easy handling allows for simple processing by using pail or drum melting equipment and is said to generate minimal waste. Along with a high level of green strength, superior water and moisture vapour tightness (less than 0.2 g/m^2d) is another main feature. The sealant has primer-less adhesion to glass, aluminium, galvanized and stainless steel.

Applications: Long life sealant for ultra secure framing of thin film and crystalline PV modules.

Platform: Automated application equipment for 20 litre pails and 200 litre drums for easy integration in production lines is available. The sealant can be used for sealing both the inner and outer components of modules with ease and the confidence of long-term durability.

Availability: Currently available.

LayTec

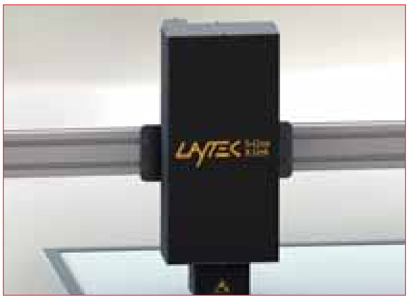

LayTec's in-line metrology system evaluates EVA cross-linking non-destructively

Product Outline: LayTec has introduced a new in-line metrology system X Link that is designed to provide fast and accurate evaluation of the level of EVA cross-linking directly after the module lamination process. It can be integrated in to any c-Si or thin-film-based solar module production line, claimed to offer 100% coverage for process and quality control.

Problem: Gel fraction and creep test are the two main methods used for the detection of the correct cross-linking EVA. However, both are time consuming and destructive, preventing its use in high volume production.

Solution: LayTec developed the X Link metrology system in close cooperation with Fraunhofer USA. This method utilizes a rheological approach. It analyses the response of the laminated EVA back sheet combination. The measured stiffness is directly correlated with the level of cross-linking. The data can also be given as percentage gel content equivalent. Placed directly after the laminator, the tool gives direct feedback to the lamination process for the adjustment of heating zones and exposure times. LayTec X Link is said to improve lamination yield by real-time control and provide a detailed proof of the long-term stability of PV modules thereby increasing bankability. This system replaces the common and coarse gel content test.

Applications: It can be integrated into any c-Si or thin-film based solar module production line.

Platform: The in-line version can be directly connected to production systems and SPC databases by a large variety of protocols.

Availability: May 2012 onwards.

teamtechnik

Teamtechnik's STRINGER TT1200 HS solders at 1400 cycles/hour

Product Outline: teamtechnik's STRINGER TT1200 HS is claimed to solder crystalline solar cell strings in a 2.5 second cycle on just one track. Compared to its previous model, throughput has been boosted by 200 cycles and is claimed to currently be the fastest single-track stringer system on the market.

Problem: The continued drive to reduce module assembly costs can be met by improving throughput and overall productivity of the stinger system. However, developments including dual track systems can increase equipment complexity and manpower resources, negating the full potential for cost reduction.

Solution: teamtechnik uses a unique design of hold-down devices in its systems to separate the actual soldering process from the cell-handling process. Simultaneously, the hold-down devices position and secure the ribbons on the cells. This allows teamtechnik to claim 1400 cycles/hour, with a cycle time of 2.5 seconds with just one track. This hold-down device also ensures a safe process and correct string geometry. At the same time, it is claimed to guarantee extremely low breakage rates – from 0.1–0.3%, depending on the type of solar cell being used, due to the continuous optimization of the pre- and post-heating temperature, which reduces stress on the cells. Tool availability is said to be over 95%.

Applications: For all standard cells' thickness less than 160µm, including 2 and 3 bus bars

Platform: teamtechnik specializes in both non-contact and controlled soldering processes. Both technologies can be integrated as an option into the systems.

Availability: April 2012 onwards.

Fab & Facilities

Materials

Cell Processing

Thin Film

PV Modules

Power Generation

Market Watch

Dynamic stress tests on PV modules – derivation of extended stress scenarios

Florian Reil, TÜV Rheinland, Cologne, Germany

ABSTRACT

With current state-of-the-art PV module tests stipulating only a static mechanical load test in accordance with IEC 61215 and IEC 61646 standards, hardly any fatigue stressing is carried out on cells, cell connectors or rigid component parts such as the glass or framing. This paper presents research on dynamic load testing of PV modules and discusses reliability aspects of these essential requirements that must be considered in future standardization work.

Introduction

On the basis of the current situation of standards, PV modules demonstrate a relatively good mechanical behaviour under the applied loads that are well defined within the IEC type approval tests from IEC 61215/61646 and the safety tests from IEC 61730-2 [1]. A 2011 internal extension of these tests carried out at TÜV Rheinland indicated a failure rate in the mechanical load (ML) test of 12.6% from a set of more than 12,000 c-Si modules (between 2005 and 2010) that had failed the certification processes.

In the type-approval testing, the ML test (IEC 61215 10.16 [2]) is applied to a single PV module out of a set of 10 modules under realistic mounting conditions such as those recommended by the manufacturer. "The purpose of this test is to determine the ability of the module to withstand wind, snow, static or ice loads" [2] – this means external environmental mechanical stresses equivalent to a total load of 2400Pa (or 5400Pa if desired by the manufacturer) impacting vertically on the surface of the module. The ML test is the only stress test which determines the resistivity of the modules with regard to tensile or compressive forces induced only by mechanical forces to simulate wind or snow.

Prior to the ML test, IEC 61215/61646 stipulates that a damp-heat test at 85°C and 85% relative humidity (RH) be conducted on the same module. The module is evaluated by means of its electrical power and isolation characteristics before and after the test, as well as by the presence of any major visual defects that may occur due to the load application. According to this definition, the ML test has to be declared a static load test, since each type of load lasts for three hours, with force directions being varied for one hour between loads. A total load application of six hours is prescribed.

IEC 61215/61646 states that the pressure loads correspond to a real wind velocity of approximately 130km/h [2]. Eurocode EN1991-1-4 (for the calculations of wind actions on structures), for instance, implies aerodynamic load factors that have to be introduced into basic load assumptions. Examples of dynamic wind influences are blast vibrations due to oscillation elements (caused by changing blasts), or curl-stimulated crosswise vibrations such as galloping, judder and rain/wind-induced vibrations. The multiplication of the dynamic factors leads to a 'quasi-static' procedure, so that resonance swinging, caused by gusts, is also covered by this [3]. Unfortunately, neither the Eurocodes nor the national amendments (DIN 1055-4 in Germany, for instance) imply any conclusions on the frequency of occurrence of wind gusts. This would help to estimate how many times theoretically wind-forced pressure accumulations in front of or behind a PV module could be expected for a 25-year exposure. On the basis of these findings, a calculation of the relevant load amplitudes can be applied; however, the derivation of appropriate load sequences and times for a realistic ML test is lacking.

> "As regards oscillating or alternating forces, dynamic (thermo-)mechanical loads address many more different requirements in the field than static loads."

As regards oscillating or alternating forces, dynamic (thermo-)mechanical loads address many more different requirements in the field than static loads. Because of the set-up of the modules, these loads may induce internal mechanical stresses at electrical joints or adhesives or, having relevance to the durability of single homogeneous materials, fatigue cracking of the cells or connectors. Research has indicated typical frequencies of around 11Hz to 12Hz as resonance frequencies [4]. In addition, module oscillations in the range of 12Hz to 35Hz caused by surface excitations have been measured as a result of alternating wind forces, but with relatively small deflections of 1.5mm to 3.6mm [5]. Similar resonances could be reproduced in the laboratory from excitation by a loudspeaker. Assmuss et al. proved that free-standing modules can oscillate in their resonance frequencies, the most common being 28Hz [5]. Nevertheless, a 25-year prediction of the feasible amount of wind gusts and accumulated power densities on relevant spectra (or resonance frequencies) is not available.

The question that now remains is how to define an appropriate laboratory testing method which enables a sufficient forecast of the behaviour of PV modules under the influence of alternating mechanical, thermomechanical and vibrating loads.

Dynamic load tests in accordance with EN 12211 and EN12179

In 2007 and 2008 TÜV Rheinland carried out a series of dynamic load tests based on tests for windows and façades. Within the European research project 'Performance' [6], sub-group 6 dealt mainly with adapted testing and standardization situations. Because one major deficiency identified in the test sequence for the estimation of load behaviour was a dynamic load test, research on formulating relevant wind load tests was conducted. As EN 12210 and EN 12179 are benchmark tests for windows and façades, varying pressure and tensile loads form the criteria in characterizing these products in terms of their ability to withstand wind loads while retaining their functions (opening/closing the window, no deformations etc.) [7–9].

Transferring these requirements to PV modules, retaining functions for PV relates to the capability of a product to remain static in the frame, safety of the glass, fixings within the frames, avoidance of permanent deformations of the module construction, coping with minor power loss due to cell cracks or disconnections of electrical joints, etc. According to these standards the specimen has to be mounted

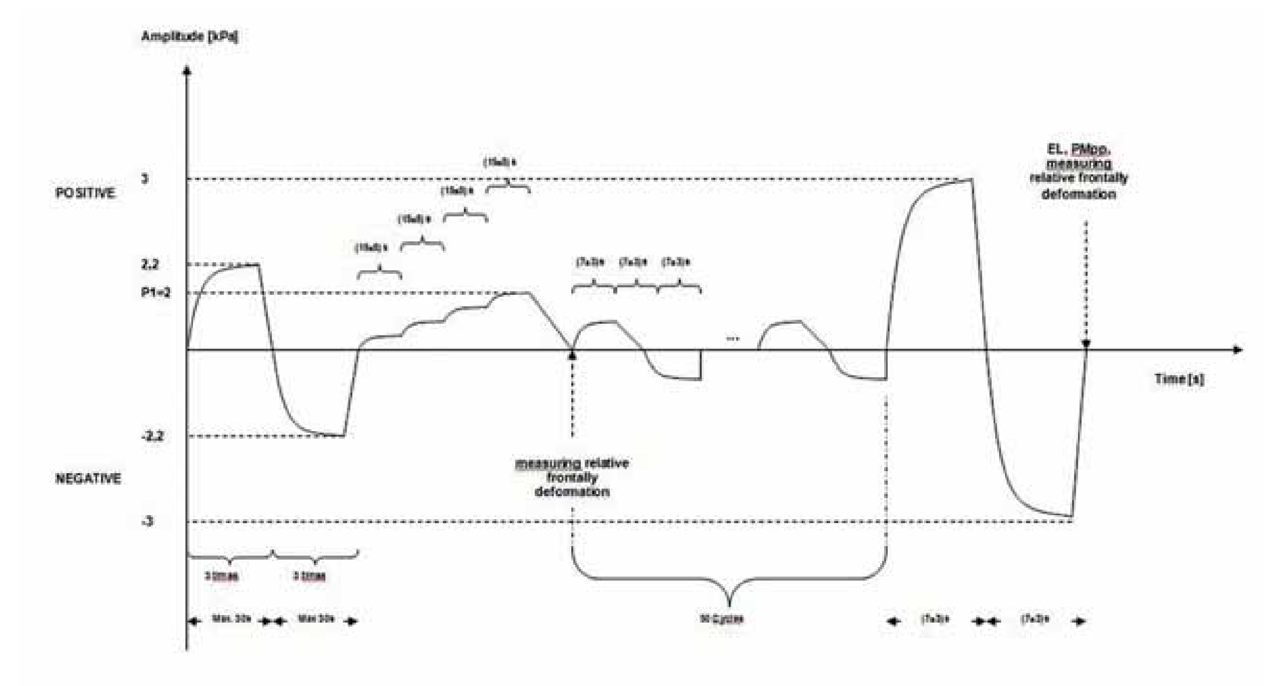

Figure 1. Combined dynamic mechanical stress tests in accordance with EN 12211 and EN 12179 for research test series, carried out at TÜV Rheinland.

in a pressure chamber with sealed edges. In order to include the characterization of a frame under specific dynamic loads as well, a free bending of the module is allowed by adapting the same load frequencies and cycles, amplitudes and measurement methods for determining the deformation.

As a result, a combined testing method (of EN 12210 and 12179) was developed by performing a test sequence which includes the application of various dynamic loads, as shown in Fig. 1. The load amplitudes for each test unit are appropriately lower than the ones specified in IEC 61215, but higher frequencies and alternating changes in load are involved. The pressure and tensile amplitudes of the applied loads were chosen to be those for the highest window class from the classification standard EN 12210: P1 is defined as 2kPa; P2, which provides the load for the 50 load

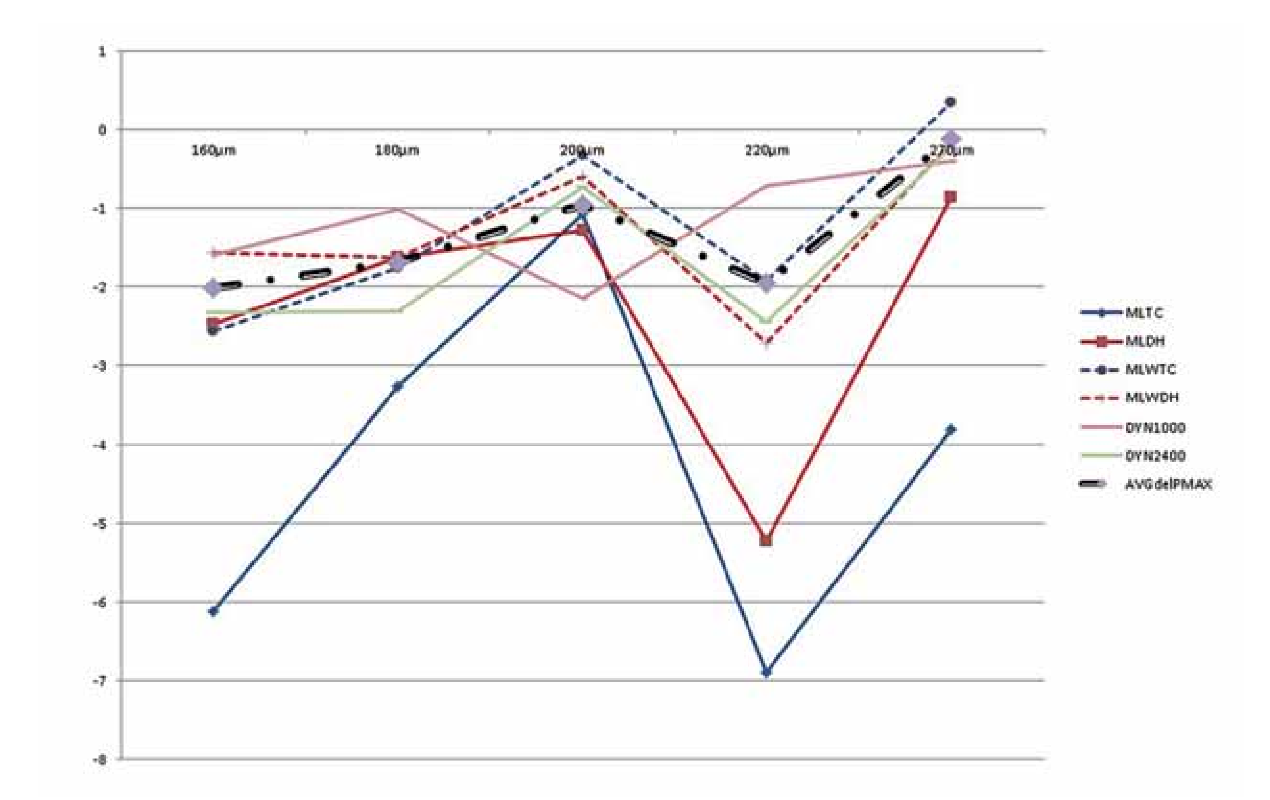

Figure 2. Electrical power measurements after and between static loads with thermomechanical and damp-heat stress testing, compared to dynamic load tests. The increase in the power loss is also clearly defined by TC tests.

cycles directly in the middle of the entire sequence, is set at 1kPa. A final 'safety test' with an excessive load of 3kPa simulates strong wind gusts at intervals of 21±9 sec per half cycle.

The single load peaks are within the limits specified in EN 12210 and, therefore, indicate a high degree of safety in terms of wind gusts with reference to EN 1055-4. A set of four standard polycrystalline glass/foil PV modules with aluminium frames, identical in construction, were exposed to these combined dynamic loads and to the regular IEC static-test loads. Electrical power loss measurements for modules exposed to the static load were about –0.2%; for the dynamic load test, marginal losses were also measured to be about –0.1%. In total, all modules still retained sufficient power-producing capability, and the degradation measurements were all within the measurement uncertainty of the flashlight simulator system. The requirements from the standard benchmark classes were able to be fulfilled. Since all lasting mechanical deformations were below 3mm, the highest window class could be applied to the tested modules – a very helpful result from a building-integrated PV (BIPV) perspective.

Dynamic and thermomechanical loads

On the basis of the findings of the EN 12211/12179 dynamic load tests, the varying load test unit of 50 cycles, with a total time of around 14–30 sec for each cycle, was the focus of further research to serve as a rudimentary tool for indicating possible fatigue behaviour. Although single micro-cracks could be induced by alternating loads, no major or electrically relevant losses, in terms of power or isolation, were caused. This time, 20 polycrystalline PV modules of two different types were exposed in a similar set-up to just ML tests and the aforementioned dynamic load test unit, but using up to 2000 cycles. In addition, further stresses from environmental exposure were included by using the IEC-established thermal-cycling (TC) and damp-heat (DH) tests. As a further interesting aspect, five different cell thicknesses were used.

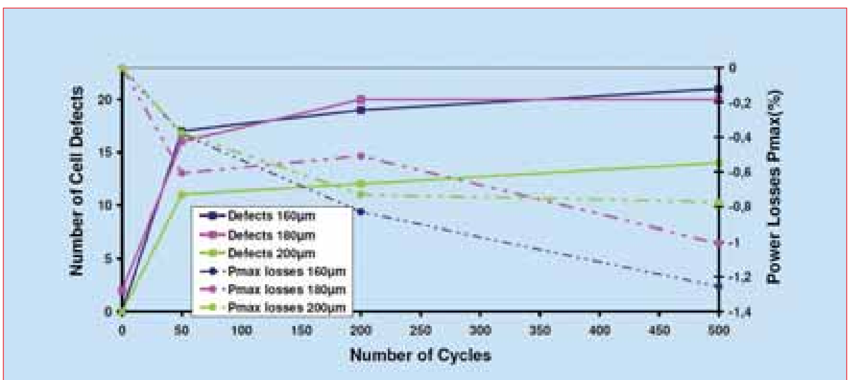

Figure 3. Correlation, for different cell thicknesses, of power losses at P_{MAX} with the number of cell defects.

After the specimen had undergone ML tests combined with subsequent environmental tests, the dynamic load tests were conducted individually without additional thermal or humidity stresses. The goal was to estimate whether any correlation could be found between the cracking behaviour of the cells and the corresponding power loss and cell thicknesses, or whether single dynamic load tests with oscillating forces are capable of providing similar stresses to the combined ML and TC test or the combined ML and DH test from IEC 61215. For practical use, the test sequences are abbreviated as follows: ML(IEC)+TC200(IEC) = MLTC; ML(IEC)+DH(IEC)=MLDH; dynamic loads of ±1000Pa = DYN1000; dynamic loads of ±2400Pa = DYN2400.

Fig. 2 shows the accumulated power losses at ΔP_{MAX} over the range of all tested

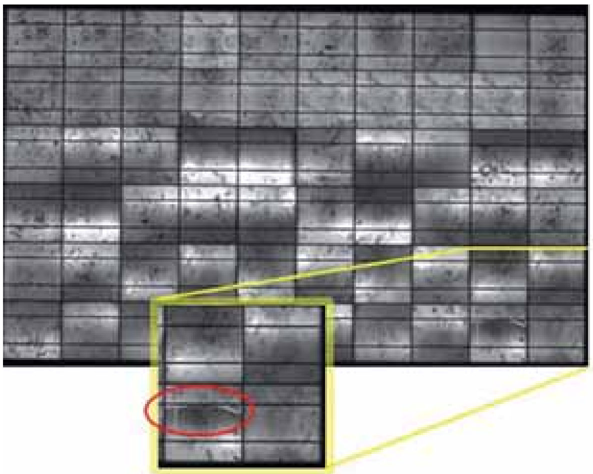

Figure 4. Highlighted cell with a micro-crack in a prepared module, resulting in meandering busbar interruptions.

Figure 5. Affected cell crack with smouldering and arcing along the defect.

modules along with the corresponding cell thicknesses. The individual points indicate the final measurement after the complete test sequences. The combined ML and TC tests subsequently carried out prove to have the highest impact compared to the other test sequences. The main impact on the average power loss for each cell thickness, therefore, depends largely on the results from MLTC. A stronger effect of MLTC, due to thermo-mechanical stresses on thinner wafers, is not clearly defined.

TC, however, exhibits a high degree of damage to cells and busbars, as Fig. 2 demonstrates. The figure shows a direct comparison of static and dynamic load tests without extended tests using the simulated environmental impacts TC and DH. Here, MLWTC stands for ML without TC; similarly, MLWDH is ML without DH.

In these particular measurements, although DYN1000 induces far lower stresses than those caused by DYN2400, the latter leads to almost the same degradation results in comparison to regular ML. In 2008 Wolgemuth et al. [10] worked out that the breakage behaviour of thin crystalline cells is obviously more severe when environmental stress tests, such as 50 thermal cycling (–40°C...+85°C) and 10 humidity freeze cycles, are carried out subsequent to dynamic loads, than for single dynamic loads.

For thinner cell thicknesses, the power losses caused by the application of ±1000Pa correlate very well with the number of cell defects, as determined by electroluminescence for each number of

Figure 6. Hot spots at the cell connectors, caused by higher series resistances from the cell crack and high current load.

cycles. Between 200 and 500 load cycles, the number of cell defects reaches a saturation level (see Fig. 3).

> "The dynamic mechanical loads based on the European standards EN 12211/12179 establish a solid basis for generating the same electrical degradation in modules as the IEC ML test."

In conclusion, the dynamic mechanical loads based on the European standards EN 12211/12179 establish a solid basis for generating the same electrical degradation in modules as the IEC ML test. The higher the load amplitudes chosen, with reference to actual peaks induced by wind gusts, the more severe the damage expected. Indeed, the number of load cycles also plays a certain role, since the number of cell cracks can increase as the number of alternating loads changes.

Reliability and safety issues

A test sequence is at present being developed (in a current German research project concerning the evaluation of fire issues with PV systems) for estimating the risk of PV modules causing electric arcs under accelerated stress. To understand the progression of a degradation process at soldering joints or cell connectors, a combined testing sequence is currently applied to a variety of modules. The objective is to reproduce similar conditions in the modules to those that have already led to single smouldered joints detected in modules in operation in the field. In addition, a forward bias of 1.2–2 times the I_{sc} condition of the modules is applied to achieve a higher temperature in the electrical circuit.

Under the influence of the forward-bias potential, hot spots can be identified at positions where series resistances are higher. By using modules for these tests that have already shown severe hot-spot damage at soldering joints between the cells, even electric arcing in three modules could be induced under the influence of dynamic loads and an intentionally applied forward bias. In one non-aged module containing polycrystalline cells, each connected by two busbars, a meandering course of current was induced by intentionally interrupting the cell interconnectors in an alternating pattern. One cell revealed a cell crack alongside the front busbar. Under an applied forward bias of 1.2 × I_{sc} and dynamic loads of ±2400Pa, the current was forced to run entirely along the cell crack. As a result, with each positive or negative stroke, tiny flashes were created, producing smouldering and burn-through of the backsheet. (Further results will be presented at the IEEE PVSEC in Austin in 2012.)

One result to come out of recent standardization work carried out on the estimation of other dynamic loads is a draft standard (IEC 62759-1) for testing related to transportation issues of PV modules and module stacks, which has been developed under the lead of WG 2 from IEC TC 82.

A higher impact on the modules' breakage behaviour can be expected from resonance frequencies that have been estimated in several crystalline modules, caused by longer-lasting vibrations. After a PV module was subjected to a sinusoidal excitation (acceleration 1g), the resonance frequency was detected from a sweep between 3.5Hz and 15Hz [11]. Fig. 7 shows the damage to a module from the resonance determination with a continuous load for 20 sec for each frequency unit. In this particular case the resonance occurred at a frequency of 11.5Hz and caused a power loss of 8%.

From a resonating material perspective, not only do wind-driven vibration phenomena act on the modules, but also transportation-induced oscillations occur during (for example, truck) transportation. The current draft (IEC 62759-1) projects these influences to complete transportation stacks or package units by applying a random noise spectrum between 5 and 200Hz on the basis of ASTM D4169 [11]. The use of a power spectral density (PSD) profile allows a correlation between power densities (in g^2/Hz) and the individually occurring frequencies. Following these and further individual transportation-specific tests on the shipping unit, environmental tests are then linked into the simulation sequence.

Two testing paths (A and B) are defined

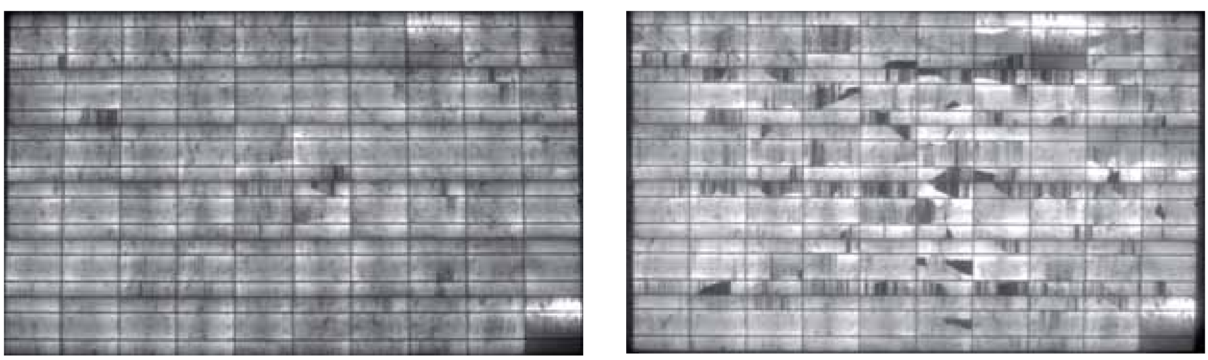

Figure 7. Comparison of EL images of a crystalline module before and after applying vibration frequencies for resonance oscillations.

for the exposure of the modules that are degraded the most from the transportation simulation in order to estimate whether cell cracks or macro damages of the specimen can contribute to a higher performance loss under environmental ageing [12]. Therefore, path A includes a single stress of 200 thermal cycles, whereas path B introduces a sequence of dynamic loads (following EN 12211, 250 cycles, 24 sec/cycle, ±1000Pa), 50 TCs, HF 10 and the regular ML test. From initial experiences, in accordance with the draft transportation-testing standard, path B indicates a stress four times higher in terms of degraded power production than the single 200-TC test for path A.

"Dynamic load tests clearly reveal a different stress potential from that indicated by static mechanical loads."

Conclusion

With reference to accelerated ageing procedures of PV modules, dynamic load tests clearly reveal a different stress potential from that indicated by static mechanical loads. Consequently, fatigue mechanisms for soldered joints or for the cells themselves can be completely determined. The constant application of a forward bias is helpful for generating a higher stress on the cell connectors, for example for addressing arcing issues. In addition, associated environmental tests aid in intensifying the stress on cell connectors [10,13].

Further stress tests will have to be carried out to obtain a more detailed insight into the behaviour of modules under the loads discussed here, to investigate whether higher frequencies and similar load amplitudes will lead to the same reported results. Testing times could be drastically reduced. Moreover, the different research results indicate that the number of load cycles when non-linear breakage behaviour of modules occurs still varies between 200 and 2000 cycles. However, a necessary comparison of adapted test series is important for determining the optimum number of load cycles to be applied, where a saturation level of damage to cells and connectors can be designated.

Acknowledgments

The author would like to thank Dr. Nicolas Bogdanski, J. Althaus, K. Strohkendl, M. Vosen, Dr. Werner Herrmann, A. Sepanski, U. Jahn, Dr. E. Janknecht (TÜV Rheinland Energie und Umwelt GmbH), Dr. H. Schmidt (Fraunhofer Institute ISE), N. Bosco, J. Wolgemuth and S. Kurtz (NREL, USA).

References

[1] IEC 61730:2004 (Standard), "Photovoltaic (PV) module safety qualification – Part 2: Requirements for testing".

[2] IEC 61215:2005 (Standard), "Crystalline silicon terrestrial photovoltaic (PV) modules – Design qualification and type approval".

[3] DIN 1055-4:2005, 2005 (Standard), "Action on structures – Part 4: Wind loads".

[4] Reil, F. 2010, "Dynamische Belastungen von PV-Modulen", *Elektropraktiker PV*.

[5] Assmus, M. et al. 2011, "Measurement and simulation of vibrations of PV-modules induced by dynamic mechanical loads", *Prog. Photovolt: Res. Appl.*, Vol. 19, pp. 688–694.

[6] Jol, J.C. et al. 2009, "New test methods for BIPV: Results from IP performance", *Proc. 24th EU PVSEC*, Hamburg, Germany.

[7] DIN EN 12210: 2003, 2003 (Standard), "Windows and doors – resistance to wind load – classification".

[8] DIN EN 12211: 2000, 2000 (Standard), "Windows and doors – resistance to wind load – test method".

[9] EN 12179: 2000, 2000 (Standard), "Curtain walling – resistance to wind load – test method".

[10] Wolgemuth, J. et al. 2008, "The effect of cell thickness on module reliability", *Proc. 33rd IEEE PVSC*, San Diego, California, USA.

[11] Reil, F. et al. 2010, "The effect of transportation impacts and dynamic load tests on the mechanical and electrical behaviour of crystalline PV modules", *Proc. 25th EU PVSEC*, Valencia, Spain.

[12] IEC 62759-1:2012-04 (Draft Standard), " Transportation testing of photovoltaic (PV) modules – Part 1: Transportation and shipping of PV module stacks".

[13] Reil F. et al. 2011, "Development of a new test standard and experiences of transportation and 'rough handling' testing on PV modules, *Proc. 25th EU PVSEC*, Valencia, Spain.

About the Author

Florian Reil studied mechanical engineering at the University of Applied Sciences Bonn-Rhein-Sieg. He has been working within R&D on applied research in the field of photovoltaics for the TÜV Rheinland Group in Cologne since 2007. In addition to heading the competence centre for BIPV at TÜV Rheinland, Florian is involved with standardization work as a delegate of IEC TC 82 WG3/6, Cenelec TC 82 WG1 and DKE AK 373. He also leads the German research project concerning the fire safety risks of PV systems and developing minimization measures.

Enquiries

Florian Reil
TÜV Rheinland Energie und Umwelt GmbH
Am Grauen Stein
51105 Cologne
Germany
Tel: +49 221 806-2794
Fax: +49 221 806-1350
Email: florian.reil@de.tuv.com
Website: www.tuv.com/pv

Predicted thermal stresses in a photovoltaic module (PVM)

E. Suhir, University of California, Santa Cruz, California, **D. Shangguan**, Flextronics Corporation, Milpitas, California, USA, & **L. Bechou**, IMS Laboratory, University of , Bordeaux, Bordeaux, France

ABSTRACT

Low-temperature thermal stresses in a manufactured photovoltaic module (PVM) based on crystalline silicon (Si), before the PVM is fastened into a metal frame, are assessed using a simple, easy-to-use and physically meaningful analytical (mathematical)predictive model. The PVM considered comprises the front glass, ethylene vinyl acetate (EVA) encapsulant (with silicon cells embedded into it) and a laminate backsheet. The stresses addressed include normal stresses that act in the cross sections of the constituent materials and determine their short- and long-term reliability, as well as the interfacial (shearing and peeling) stresses that affect the assembly's ability to withstand delaminations. The interfacial stresses determine also the cohesive strength of the encapsulant. The calculated data, indicate that the induced stresses can be rather high, especially the peeling stress at the encapsulant-glass interface, so that the structural integrity of the module might be compromised, unless the appropriate design-for-reliability (DfR) measures, including stress prediction and accelerated stress testing, are taken. The authors are convinced that reliability assurance of a photovoltaic (PV) product cannot be delayed until it is manufactured – such an assurance should be considered and secured, first of all, at the design stage.

Introduction

The reliability of a product – including a photovoltaic (PV) product (Fig. 1), whether it is crystalline or a thin-film device (Fig. 2) – is conceived at its design stage and implemented during its manufacturing. The reliability should be evaluated and qualified by testing, and, if necessary and appropriate, maintained in the field during the product's operation. It is the general consensus that if reliability is taken care of at the design phase, the final cost of the product is minimal. If a reliability problem is detected during engineering, the cost of the product goes up by an order of magnitude; if the problem is caught at the production stage, the cost of the product might increase by orders of magnitude. In other words, the product's reliability is too important to be left to the stage when it has already been fabricated – it is too late to change anything at such a late stage.

"The product's reliability is too important to be left to the stage when it has already been fabricated."

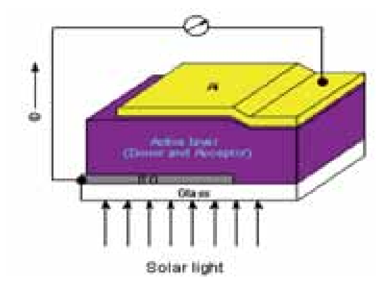

Figure 1. Typical PV device.

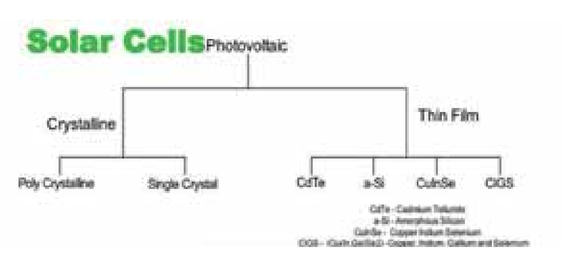

Figure 2. Solar cell (PV) devices.

Credit: Green Econometrics – Wanasa Holdings Company LLC

Elevated thermal stresses are viewed – along with high humidity, UV radiation and other stresses [1–4] – as the major contributor to the finite lifetime of a photovoltaic module (PVM) [5–7], so it takes place in other electronics and photonics systems (see, for example, Schubert et al. [8] and Lau [9]). In the realization that design-for-reliability (DfR) effort is imperative for minimizing the risk that the PV product will not meet the reliability requirements, objectives and expectations, we address in our analysis, an important situation in the manufacturing process of a crystalline silicon (Si) -based module – the low-temperature thermally induced stresses.

Thermal stress failures can be predicted and prevented effectively, provided that adequate predictive modelling, confirmed and validated by field data, is widely and consistently used in addition (and preferably prior) to experimental investigations and reliability testing [10]. Analytical modelling occupies a special place in the modelling effort [11–14]. Not only is such modelling able to clearly indicate the roles of various factors affecting the behaviour of the design of interest, but, more importantly, it is also often able to better explain the reliability physics behind the product performance than finite-element analyses (FEA) and even the experimentation.

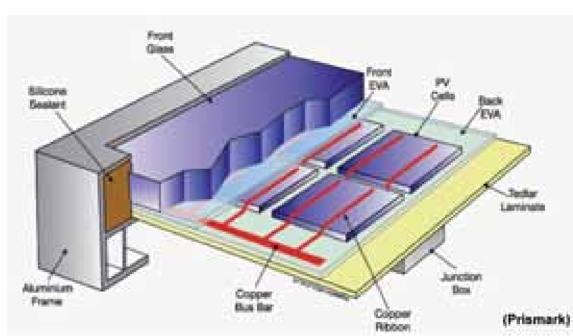

Figure 3. Typical crystalline Si PVM (Prismark).

Accordingly, in the following analysis, an easy-to-use and physically meaningful analytical stress model is developed for evaluating the low-temperature thermal stresses in a crystalline-Si-based PVM (assembly) before it is fastened into a metal frame. The assembly considered comprises the front glass, ethylene vinyl acetate (EVA) encapsulant (with PV silicon cells embedded into it) and a laminate backsheet. The analysis is carried out considering a PVM as shown in Fig. 3.

> "Thermal stress failures can be predicted and prevented effectively, provided that adequate predictive modelling, confirmed and validated by field data, is widely and consistently used."

Analysis

Assumptions

- A structural analysis (strength-of-materials) approach can be applied for the evaluation of the bow and the stresses. As long as this approach is used, no singular stresses can possibly occur. From the theory-of-elasticity standpoint, the predicted stresses can be viewed as suitable design parameters that characterize the state of stress at the assembly edges.
- The assembly constituents (components) can be treated as thin, elongated plates, experiencing small deflection, so that the engineering theory of such plates (see, for example, Suhir [15]) can be employed.
- The interfacial shearing stresses and the assembly curvature can be evaluated without considering the effect of the peeling stresses; the latter stresses can be subsequently determined from the evaluated shearing stresses and the curvature.

Figure 4. Tri-material PV-module schematics.

- Thermal stresses caused by the interaction of the dissimilar EVA and Si materials within the inhomogeneous (composite) encapsulant do not have to be considered when evaluating the forces acting in the PVM components, including the thermally induced force in the inhomogeneous encapsulant itself. These forces can be evaluated by assessing and considering the effective mechanical characteristics – Young's modulus, Poisson's ratio, coefficient of thermal expansion (CTE) – of the EVA-Si composite.
- The above-mentioned stresses caused by the interaction of the dissimilar EVA and Si materials within the inhomogeneous (composite) EVA encapsulant can be evaluated from the computed force acting in the EVA-Si composite. This force is considered to be an external mechanical force applied to the EVA-Si composite layer.
- It is assumed that there might not be a good adhesion between the butt ends of the Si device and the EVA, so that the interaction of these materials is due only to their interfacial interaction. This seems to be a reasonable, and certainly a conservative, assumption.

Normal stresses in the assembly mid-portion

The mid-portion addressed (Fig. 4) consists of component 1 (glass), component 2 (encapsulant with the embedded Si devices) and component 3 (backsheet). The equations of compatibility of the longitudinal thermally induced strains in such a tri-material assembly (that has been fabricated at an elevated temperature and subsequently cooled down to a low temperature) can be written as

$$-\alpha_1\Delta t+\lambda_1T_1^0=-\alpha_2\Delta t+\lambda_2T_2^0=-\alpha_3\Delta t+ \qquad (1)$$

where $\alpha_i, i=1,2,3$, are the CTEs of the materials; Δt is the change in temperature from the manufacturing temperature to the low temperature of interest; $\lambda_i=\frac{1}{E_i^*h_i}, i=1,2,3,$ are the axial compliances of the materials; $E_i^*=\frac{E_i}{1-\nu_i}, i=1,2,3,$ are their effective Young's moduli(that consider the two-dimensional state of stress); $E_i, i=1,2,3$, are the actual Young's moduli of the materials (in the case of the encapsulant composite, it is the modulus of the composite, considering the EVA and Si moduli); $\nu_i, i=1,2,3$, are Poisson's ratios; $h_i, i=1,2,3$, are the layer thicknesses; and $T_i^0, i=1,2,3$, are the thermally induced forces caused by the dissimilar materials in the assembly. The first terms in the expressions of Equation 1 are stress-free (unrestricted) thermal contractions, and the second terms are displacements caused by the thermal forces. In addition to the strain compatibility conditions given in Equation 1, by using the equilibrium condition

$$T_1^0+T_2^0+T_3^0=0\,, \qquad (2)$$

the following expressions for the induced forces are obtained:

$$\left.\begin{aligned} T_1^0&=\frac{\lambda_2(\alpha_1-\alpha_3)+\lambda_3(\alpha_1-\alpha_2)}{\lambda_1\lambda_2+\lambda_2\lambda_3+\lambda_3\lambda_1}\Delta t,\\ T_2^0&=\frac{\lambda_3(\alpha_2-\alpha_1)+\lambda_1(\alpha_2-\alpha_3)}{\lambda_1\lambda_2+\lambda_2\lambda_3+\lambda_3\lambda_1}\Delta t\\ T_3^0&=\frac{\lambda_1(\alpha_3-\alpha_2)+\lambda_2(\alpha_3-\alpha_1)}{\lambda_1\lambda_2+\lambda_2\lambda_3+\lambda_3\lambda_1}\Delta t \end{aligned}\right\} \qquad (3)$$

The stresses acting in the components' cross sections can be found by dividing the forces in Equations 3 by the thickness of the corresponding component.

Interfacial shearing stresses

Basic equations

The longitudinal interfacial displacements of the assembly components can be expressed, in accordance with the assumptions taken, by the formulas:

$$\left.\begin{aligned} u_{11}(x)&=-\alpha_1\Delta tx+\lambda_1\int_0^x T_1(\xi)d\xi-\kappa_1\tau_1(x)+\frac{h_1}{2}w'(x)\\ u_{21}(x)&=-\alpha_2\Delta tx+\lambda_2\int_0^x T_2(\xi)d\xi+\kappa_2\tau_1(x)-\frac{h_2}{2}w'(x)\\ u_{22}(x)&=-\alpha_2\Delta tx+\lambda_2\int_0^x T_2(\xi)d\xi+\kappa_2\tau_2(x)+\frac{h_2}{2}w'(x)\\ u_{32}(x)&=-\alpha_3\Delta tx+\lambda_3\int_0^x T_3(\xi)d\xi-\kappa_3\tau_2(x)-\frac{h_3}{2}w'(x) \end{aligned}\right\} \qquad (4)$$

where $u_{11}(x)$ is the displacement of component 1 (glass) at its interface 1 with component 2 (encapsulant); $u_{21}(x)$ is the displacement of component 2 (encapsulant) at interface 1; $u_{22}(x)$ is the displacement of component 2 (encapsulant) at its interface 2 with component 3 (backsheet); $u_{32}(x)$ is the displacement of the component 3 (backsheet) at interface 2; and Δt is the change in temperature (from the manufacturing temperature to the low temperature of interest). Also,

$$\kappa_1=\frac{h_1}{3G_1},\qquad \kappa_2=\frac{h_2}{G_2},\qquad \kappa_3=\frac{h_3}{3G_3} \qquad (5)$$

are the interfacial compliances of the components [16];

$$T_1(x)=\int_{-\ell}^x\tau_1(\xi)d\xi\,,\quad T_2(x)=-[T_1(x)+T_3(x)],\quad T_3(x)=\int_{-\ell}^x\tau_2(\xi)d\xi \qquad (6)$$

are the thermally induced forces acting in the components' cross sections; G_i, i = 1, 2, 3, are the shear moduli of the materials; ℓ is half the assembly length; $\tau_i(x)$, i = 1, 2, is the interfacial shearing stress at the i^{th} interface; and $w(x)$ is the deflection of the assembly. The origin '0' of the longitudinal coordinate x is at the mid-cross section of the assembly in the mid-plane of the intermediate component 2 (encapsulant).

The conditions $u_{11}(x) = u_{21}(x)$ and $u_{22}(x) = u_{32}(x)$ of the compatibility of the interfacial displacements lead to the following equations for the thus-far unknown axial (longitudinal) forces $T_i(x)$, i = 1, 2, 3:

$$\left.\begin{aligned} &(\lambda_1+\lambda_2)\int_0^x T_1(\xi)d\xi+\lambda_2\int_0^x T_3(\xi)d\xi-\kappa_{12}\tau_1(x)+\frac{h_1+h_2}{2}w'(x)=(\alpha_1-\alpha_2)\Delta tx\\ &\lambda_2\int_0^x T_1(\xi)d\xi+(\lambda_2+\lambda_3)\int_0^x T_3(\xi)d\xi-\kappa_{23}\tau_2(x)-\frac{h_2+h_3}{2}w'(x)=(\alpha_3-\alpha_2)\Delta tx \end{aligned}\right\} \qquad (7)$$

where

$$\kappa_{12}=\kappa_1+\kappa_2\,,\ \kappa_{23}=\kappa_2+\kappa_3 \qquad (8)$$

are the interfacial compliances of the interfaces 1 (between the glass and the encapsulant) and 2 (between the encapsulant and the backsheet), respectively.

The equations of bending of the assembly components can be written as follows:

$$D_1w''(x)=\frac{h_1}{2}T_1(x),\quad D_2w''(x)=\frac{h_2}{2}[T_1(x)-T_3(x)],\quad D_3w''(x)=-\frac{h_3}{2}T_3(x) \qquad (9)$$

where

$$D_i=\frac{E_ih_i^3}{12(1-\nu_i^2)}=\frac{E_i^*h_i^3}{12},\quad i=1,2,3 \qquad (10)$$

are the flexural rigidities of the assembly components. Summing up Equations 9, we have

$$Dw''(x)=\frac{h_1+h_2}{2}T_1(x)-\frac{h_2+h_3}{2}T_3(x) \qquad (11)$$

where $D = D_1 + D_2 + D_3$. Differentiating Equations 9 with respect to the coordinate x and substituting the expression for the curvature $w''(x)$ determined from Equation 11 into the obtained relationships, the following equations for the unknown distributed forces $T_1(x)$ and $T_3(x)$ are obtained:

$$\left.\begin{aligned} \kappa_{12}T_1''(x)-\lambda_{11}T_1(x)+\lambda_{13}T_3(x)&=-(\alpha_1-\alpha_2)\Delta t\\ \kappa_{23}T_3''(x)-\lambda_{33}T_3(x)+\lambda_{13}T_1(x)&=-(\alpha_3-\alpha_2)\Delta t \end{aligned}\right\} \qquad (12)$$

where the axial compliances

$$\left.\begin{aligned} \lambda_{11}&=\frac{(h_1+h_2)^2}{4D}+\lambda_1+\lambda_2\,,\\ \lambda_{33}&=\frac{(h_2+h_3)^2}{4D}+\lambda_2+\lambda_3\,,\\ \lambda_{13}&=\frac{(h_1+h_2)(h_2+h_3)}{4D}-\lambda_2 \end{aligned}\right\} \qquad (13)$$

take into account the effect of the flexural rigidity D of the assembly.

Equations 13 indicate that the consideration of the finite flexural rigidity of the assembly results in higher axial compliances. The solutions to Equations 12 must satisfy the zero boundary conditions

$$T_1(\ell) = T_3(\ell) = 0 \tag{14}$$

These conditions consider that no external axial forces are applied at the end cross sections of the assembly. After the forces $T_1(x)$ and $T_3(x)$ are found, the interfacial shearing stresses $\tau_1(x)$ and $\tau_2(x)$ can be determined, by differentiation, from the first and the third formulas of Equations 6:

$$\tau_1(x) = T_1'(x), \qquad \tau_2(x) = T_3'(x) \tag{15}$$

Separating the functions $T_1(x)$ and $T_3(x)$ in Equations 12, we obtain the following two inhomogeneous differential equations

$$\left.\begin{aligned} T_1^{IV}(x) - (k_1^2 + k_2^2)T_1''(x) + \gamma k_1^2 k_2^2 T_1(x) = \gamma k_1^2 k_2^2 T_1^0 \\ T_3^{IV}(x) - (k_1^2 + k_2^2)T_3''(x) + \gamma k_1^2 k_2^2 T_3(x) = \gamma k_1^2 k_2^2 T_3^0 \end{aligned}\right\} \tag{16}$$

where the notations:

$$k_1 = \sqrt{\frac{\lambda_{11}}{\kappa_{12}}}, \quad k_2 = \sqrt{\frac{\lambda_{33}}{\kappa_{23}}}, \quad \gamma = 1 - \frac{\lambda_{13}^2}{\lambda_{11}\lambda_{33}} \tag{17}$$

are used. The forces T_1^0 and T_3^0 acting in the mid-portion of the assembly are expressed by the first and the third formulas in Equations 3.

Parameter of the interfacial shearing stresses

The homogeneous equation

$$T^{IV}(x) - (k_1^2 + k_2^2)T''(x) + \gamma k_1^2 k_2^2 T(x) = 0 \tag{18}$$

that corresponds to the two inhomogeneous differential Equation 16 turns out to be the same for both of those equations. The characteristic equation

$$k^4 - (k_1^2 + k_2^2)k^2 + \gamma k_1^2 k_2^2 = 0 \tag{19}$$

leads to the following formula

$$k = \sqrt{\frac{k_1^2 + k_2^2}{2}\left[1 + \sqrt{1 - \gamma\left(\frac{2k_1 k_2}{k_1^2 + k_2^2}\right)^2}\right]} \tag{20}$$

for the parameter k of the interfacial shearing stress. Here k_1 and k_2 are the parameters of the shearing stresses $\tau_1(x)$ and $\tau_2(x)$, in the case of a bi-material assembly consisting of components 1 and 2, or of components 2 and 3, respectively. Indeed, the case of a bi-material assembly consisting of components 1 and 2 can be obtained by assuming infinitely large compliance of interface 2 ($k_{23} \to \infty$). The second formula in Equations 17 then results in a zero k_2 value, and Equation 20 yields $k = k_1$. Similarly, the result for the case of an assembly comprising components 2 and 3 can be obtained by letting $k_{12} \to \infty$ in Equations 17 and 20. Consequently, as follows from the first formula in Equations 17, $k_1 = 0$, and Equation 20 yields $k = k_2$.

Axial forces at the assembly ends

The particular solutions to the two inhomogeneous differential equations (Equations 16) are $T_1(x) = T_1^0$ and $T_3(x) = T_3^0$, respectively. These solutions are the thermally induced forces in the mid-portion of the assembly. Considering that the functions $T_1(x)$ and $T_3(x)$ should be symmetric with respect to the mid-cross section ($x = 0$), the general solutions to the differential Equation 16 could be sought as

$$T_1(x) = C_1 \cosh kx + T_1^0, \quad T_3(x) = C_3 \cosh kx + T_3^0 \tag{21}$$

where C_1 and C_3 are constants of integration. The conditions expressed by Equation 14 yield:

$$C_1 = -\frac{T_1^0}{\cosh k\ell}, \qquad C_3 = -\frac{T_3^0}{\cosh k\ell}, \tag{22}$$

so that the distributed longitudinal forces $T_1(x)$ and $T_3(x)$ acting in the cross sections of components 1 and 3 are

$$T_1(x) = T_1^0\left(1 - \frac{\cosh kx}{\cosh k\ell}\right), \qquad T_3(x) = T_3^0\left(1 - \frac{\cosh kx}{\cosh k\ell}\right) \tag{23}$$

The force $T_2(x)$ acting in the encapsulant composite (component 2) can then be determined as

$$T_2(x) = -[T_1(x) + T_3(x)] = T_2^0\left(1 - \frac{\cosh kx}{\cosh k\ell}\right) \tag{24}$$

where the force T_2^0 acting in the mid-portion of a large assembly is given by the second formula in Equations 3.

Predicted interfacial shearing stresses

By taking into account Equations 23 for the distributed longitudinal forces, the interfacial shearing stresses $\tau_i(x)$, $i = 1, 2$, can be determined, by differentiation, from Equations 15:

$$\tau_1(x) = T_1'(x) = -kT_1^0 \frac{\sinh kx}{\cosh k\ell}, \qquad \tau_2(x) = T_3'(x) = -kT_3^0 \frac{\sinh kx}{\cosh k\ell} \tag{25}$$

Peeling stresses

Basic equations

In order to obtain the governing equations for the interfacial peeling stresses $p_1(x)$ and $p_2(x)$ (the interfacial normal stresses acting in the through-thickness direction of the assembly), account should be taken of the fact that the deflection functions $w_i(x)$, $i = 1, 2, 3$, of the assembly components are somewhat different. In the following analysis it is assumed that these functions should satisfy the following conditions of compatibility:

$$w_1(x) - w_2(x) = \delta_{12} p_1(x), \qquad w_2(x) - w_3(x) = \delta_{23} p_2(x) \tag{26}$$

where δ_{12} and δ_{23} are the interfacial through-thickness compliances of the assembly components. These compliances can be determined experimentally, or estimated using the following approximate formulas:

$$\delta_{12} = \frac{h_1}{E_1^*} + \frac{h_2}{2E_2^*}, \qquad \delta_{23} = \frac{h_3}{E_3^*} + \frac{h_2}{2E_2^*} \tag{27}$$

The equations of bending (Equations 9) should also be modified. With consideration of the peeling stresses $p_i(x)$, $i = 1, 2$, and different deflection functions $w_i(x)$, $i = 1, 2, 3$, of the assembly components, these three equations could be written as

$$\left.\begin{aligned} D_1 w_1''(x) &= \frac{h_1}{2}T_1(x) - \int_{-\ell}^{x}\int_{-\ell}^{x} p_1(\xi)d\xi d\xi' \\ D_2 w_2''(x) &= \frac{h_2}{2}[T_1(x) - T_3(x)] + \int_{-\ell}^{x}\int_{-\ell}^{x} [p_1(\xi) - p_2(\xi)]d\xi d\xi' \\ D_3 w_3''(x) &= -\frac{h_3}{2}T_3(x) + \int_{-\ell}^{x}\int_{-\ell}^{x} p_2(\xi)d\xi d\xi' \end{aligned}\right\} \tag{28}$$

The first terms on the right-hand side of these equations are due to the axial thermally induced forces; the second terms are the bending moments due to the peeling stresses. Eliminating the deflection functions $w_i(x)$, $i = 1, 2, 3$, from Equations (26) and (28), the following equations for the peeling stress functions $p_i(x)$, $i = 1, 2$, can be obtained:

$$\left.\begin{aligned} p_1^{IV}(x) + 4s_1^4 p_1(x) - \frac{p_2(x)}{\delta_{12}D_2} &= \frac{h_1 D_2 - h_2 D_1}{2\delta_{12}D_1 D_2}\tau_1'(x) + \frac{h_2}{2\delta_{12}D_2}\tau_2'(x) \\ p_2^{IV}(x) + 4s_2^4 p_2(x) - \frac{p_1(x)}{\delta_{23}D_2} &= \frac{h_3 D_2 - h_2 D_3}{2\delta_{23}D_2 D_3}\tau_2'(x) + \frac{h_2}{2\delta_{23}D_2}\tau_1'(x) \end{aligned}\right\} \tag{29}$$

PV Modules

where

$$s_1 = \sqrt[4]{\frac{D_1 + D_2}{4\delta_{12} D_1 D_2}}\,, \qquad s_2 = \sqrt[4]{\frac{D_2 + I}{4\delta_{23} D_2}} \tag{30}$$

are parameters of the interfacial peeling stresses of bi-material assemblies consisting of components 1 and 2, and components 2 and 3, respectively. From Equations 28 we find, by differentiation,

$$\left.\begin{aligned} D_1 w_1^{IV}(x) &= -\frac{h_1}{2}\tau_1'(x) - p_1(x) \\ D_2 w_2^{IV}(x) &= -\frac{h_2}{2}\left[\tau_1'(x) - \tau_2'(x)\right] + p_1(x) - p_2(x) \\ D_3 w_3^{IV}(x) &= \frac{h_3}{2}\tau_2'(x) + p_2(x) \end{aligned}\right\} \tag{31}$$

As evident from these equations, the lateral loadings acting on components 1 and 3 are

$$q_1(x) = -\frac{h_1}{2}\tau_1'(x) - p_1(x)\,, \qquad q_2(x) = \frac{h_3}{2}\tau_2'(x) + p_2(x) \tag{32}$$

and are due to both peeling and shearing interfacial stresses. Since no loadings other than $q_i(x)$, $i = 1, 2$, act in the through-thickness direction of the assembly, these loadings must be self-equilibrated:

$$\int_0^{\ell} q_i(x)dx = 0\,, \qquad \int_0^{\ell}\int_0^{x} q_i(\xi)d\xi d\xi' = 0\,, \qquad i = 1, 2 \tag{33}$$

Equations 32 and the conditions in Equations 33 therefore result in the following equilibrium conditions for the peeling stress functions $p_i(x)$, $i = 1, 2$:

$$\int_0^{\ell} p_i(x)dx = 0\,, \int_0^{\ell}\int_0^{x} p_i(\xi)d\xi d\xi' = 0\,, \quad i = 1,2 \tag{34}$$

These conditions indicate that the peeling stress loading should be self-equilibrated as well.

Parameter of the peeling stresses

After separating the functions $p_i(x)$, $i = 1, 2$, in Equations 29, we obtain the following two equations of the eighth order for the interfacial peeling stresses acting at the two interfaces:

$$\left.\begin{aligned} p_1^{VIII}(x) + 4(s_1^4 + s_2^4)p_1^{IV}(x) + \delta p_1(x) &= \frac{h_1 D_2 - h_2 D_1}{2\delta_{12} D_1 D_2}\tau_1^{V}(x) + \\ &+ \frac{h_1(D_2 + D_3) - h_2 D_1}{2\delta_{12}\delta_{23} D_1 D_2 D_3}\tau_1'(x) + \frac{h_2}{2\delta_{12} D_2}\tau_2^{V}(x) + \frac{h_2 + h_3}{2\delta_{12}\delta_{23} D_2 D_3}\tau_2'(x) \\ p_2^{VIII}(x) + 4(s_1^4 + s_2^4)p_2^{IV}(x) + \delta p_2(x) &= \frac{h_3 D_2 - h_2 D_3}{2\delta_{23} D_2 D_3}\tau_2^{V}(x) + \\ &+ \frac{h_3(D_1 + D_2) - h_2 D_3}{2\delta_{12}\delta_{23} D_1 D_2 D_3}\tau_2'(x) + \frac{h_2}{2\delta_{23} D_2}\tau_1'(x) + \frac{h_1 + h_2}{2\delta_{12}\delta_{23} D_1 D_2}\tau_1'(x) \end{aligned}\right\} \tag{35}$$

where

$$\delta = \frac{D}{\delta_{12}\delta_{23} D_1 D_2 D_3} \tag{36}$$

The solution to the homogeneous equation

$$p^{VIII}(x) + 4(s_1^4 + s_2^4)p^{IV}(x) + \delta p(x) = 0 \tag{37}$$

can be sought in the form

$$p(x) = C_0 V_0(sx) + C_2 V_2(sx) \tag{38}$$

Here, C_0 and C_2 are the constants of integration, s is the unknown parameter of the interfacial peeling stress and the functions $V_i(sx)$, $i = 0, 1, 2, 3$, are expressed as

$$\left.\begin{aligned} V_0(sx) &= \cosh sx \cos sx\,, \quad V_1(sx) = \frac{1}{\sqrt{2}}(\cosh sx \sin sx + \sinh sx \cos sx) \\ V_2(sx) &= \sinh sx \sin sx\,, \quad V_3(sx) = \frac{1}{\sqrt{2}}(\cosh sx \sin sx - \sinh sx \cos sx) \end{aligned}\right\} \tag{39}$$

The functions $V_i(sx)$, i=1,2,3, obey the following simple rules of differentiation:

$$\left.\begin{aligned} V_0'(sx) &= -s\sqrt{2}\,V_3(sx)\,, & V_1'(sx) &= s\sqrt{2}\,V_0(sx) \\ V_2'(sx) &= s\sqrt{2}\,V_1(sx)\,, & V_3'(sx) &= s\sqrt{2}\,V_2(sx) \end{aligned}\right\} \tag{40}$$

These rules make the use of these functions of convenience. Introducing the sought solution in the form of Equation 38 into the homogeneous Equation 37, we conclude that the following equation for the factor s of the interfacial peeling stress should be fulfilled:

$$s^8 - (s_1^4 + s_2^4)s^4 + \frac{\delta}{16} = 0 \tag{41}$$

The solution to Equation 41 is given by

$$s = \sqrt[4]{\frac{s_1^4 + s_2^4}{2}\left[1 + \sqrt{1 - \frac{\delta}{4(s_1^4 + s_2^4)^2}}\right]} \tag{42}$$

When the through-thickness interfacial compliance δ_{12} or the compliance δ_{23} is infinitely large (such a situation corresponds to the case of a bi-material assembly), then, as evident from Equation 36, $\delta = 0$. If such a bi-material assembly consists of components 1 and 2, then, in addition to $\delta = 0$, one should also let $\delta_{23} \to \infty$; therefore, following from the second formula in Equations 30, $s_2 = 0$. Equations 41 and 42 then yield $s = s_1$. Similarly, for a bi-material assembly consisting of components 2 and 3, one obtains $s = s_2$.

Predicted peeling stresses

Using Equations 25 for the shearing stresses, Equations 29 result in the following equations for the interfacial peeling stresses $p_i(x)$, $i = 1, 2$:

$$\left.\begin{aligned} p_1^{IV}(x) + 4s_1^4 p_1(x) - \frac{p_2(x)}{\delta_{12} D_2} &= -\frac{k^2 h_2}{2\delta_{12} D_2}\left[\left(\frac{h_1}{h_2}\frac{D_2}{D_1} - 1\right)T_1^0 + T_3^0\right]\frac{\cosh kx}{\cosh k\ell} \\ p_2^{IV}(x) + 4s_2^4 p_2(x) - \frac{p_1(x)}{\delta_{23} D_2} &= -\frac{k^2 h_2}{2\delta_{23} D_2}\left[\left(\frac{h_3}{h_2}\frac{D_2}{D_3} - 1\right)T_3^0 + T_1^0\right]\frac{\cosh kx}{\cosh k\ell} \end{aligned}\right\} \tag{43}$$

The particular solutions to these inhomogeneous equations are

$$\bar{p}_1(x) = C_1^*\frac{\cosh kx}{\cosh k\ell}\,, \qquad \bar{p}_2(x) = C_2^*\frac{\cosh kx}{\cosh k\ell} \tag{44}$$

Introducing these solutions into Equations 43 and solving the resulting equations for the constants C_1^* and C_2^*, we obtain the following formulas for these constants:

$$\begin{aligned} C_1^* &= -\frac{k^2 h_2}{2}\frac{\left[1 + \delta_{23} D_2(k^4 + 4s_2^4)\left(\frac{h_1}{h_2}\frac{D_2}{D_1} - 1\right)\right]T_1^0 + \left[\frac{h_3}{h_2}\frac{D_2}{D_3} - 1 + \delta_{23} D_2(k^4 + 4s_2^4)\right]T_3^0}{\delta_{12}\delta_{23} D_2^2(k^4 + 4s_1^4)(k^4 + 4s_2^4) - 1} \\ C_2^* &= -\frac{k^2 h_2}{2}\frac{\left[1 + \delta_{12} D_2(k^4 + 4s_1^4)\left(\frac{h_3}{h_2}\frac{D_2}{D_3} - 1\right)\right]T_3^0 + \left[\frac{h_1}{h_2}\frac{D_2}{D_1} - 1 + \delta_{12} D_2(k^4 + 4s_1^4)\right]T_1^0}{\delta_{12}\delta_{23} D_2^2(k^4 + 4s_1^4)(k^4 + 4s_2^4) - 1} \end{aligned} \tag{45}$$

The general solutions to the inhomogeneous Equations 43 can be sought in the form:

$$\left.\begin{aligned} p_1(x) &= A_0'V_0(sx) + A_2'V_2(sx) + C_1^*\frac{\cosh kx}{\cosh k\ell} \\ p_2(x) &= A_0''V_0(sx) + A_2''V_2(sx) + C_2^*\frac{\cosh kx}{\cosh k\ell} \end{aligned}\right\} \tag{46}$$

where A'_0, A'_2, A''_0 and A''_2 are the constants of integration. Introducing the solutions given by Equations 46 into the equilibrium conditions of Equations 34, we obtain the following equations for the constants A'_0, A'_2, A''_0 and A''_2 of integration:

$$\left.\begin{aligned} V_1(s\ell)A_0' + V_3(s\ell)A_2' &= -\frac{s\sqrt{2}}{k}C_1^*\tanh k\ell \\ V_2(s\ell)A_0' - \left[V_0(s\ell) - 1\right]A_2' &= -\frac{2s^2}{k^2}C_1^* \end{aligned}\right\} \tag{47}$$

and

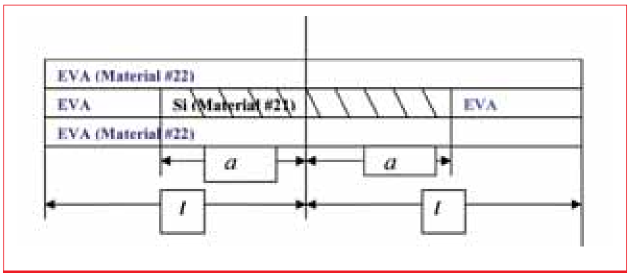

Figure 5. Element of a Si-EVA composite.

$$\left.\begin{aligned} V_1(s\ell)A_0'' + V_3(s\ell)A_2'' &= -\frac{s\sqrt{2}}{k}C_2^* \tanh k\ell \\ V_2(s\ell)A_0'' - [V_0(s\ell)-1]A_2'' &= -\frac{2s^2}{k^2}C_2^* \end{aligned}\right\} \quad (48)$$

The solutions to Equations 47 and 48 are

$$A_0' = -C_1^*\chi_0(s,k),\ A_2' = -C_1^*\chi_2(s,k),\ A_0'' = -C_2^*\chi_0(s,k),\quad A_2'' = -C_2^*\chi_2(s,k) \quad (49)$$

where the functions $\chi_0(s,k)$ and $\chi_2(s,k)$ are expressed as follows:

$$\left.\begin{aligned} \chi_0(s,k) &= \frac{s\sqrt{2}}{k}\,\frac{[V_0(s\ell)-1]\tanh k\ell + \frac{s\sqrt{2}}{k}V_3(s\ell)}{[V_0(s\ell)-1]V_1(s\ell)+V_2(s\ell)V_3(s\ell)} \\ \chi_2(s,k) &= \frac{s\sqrt{2}}{k}\,\frac{V_2(s\ell)\tanh k\ell - \frac{s\sqrt{2}}{k}V_1(s\ell)}{[V_0(s\ell)-1]V_1(s\ell)+V_2(s\ell)V_3(s\ell)} \end{aligned}\right\} \quad (50)$$

Thus, the peeling stresses $p_i(x)$, $i = 1, 2$, can be evaluated using the formula

$$p_i(x) = -C_i^*\left([\chi_0(s,k)V_0(sx)+\chi_2(s,k)V_2(sx)] - \frac{\cosh kx}{\cosh k\ell}\right),\quad i=1,2 \quad (51)$$

where the constants C_1^* are given by Equations 45.

In the case of a long assembly (large ℓ value) with sufficiently stiff interfaces (large k and s values), the following simplified relationships can be obtained for the functions given by Equations 39:

$$\left.\begin{aligned} V_0(s\ell) &\cong \frac{1}{2}e^{s\ell}\cos s\ell, & V_1(s\ell) &\cong \frac{1}{2\sqrt{2}}e^{s\ell}(\sin s\ell + \cos s\ell), \\ V_2(s\ell) &\cong \frac{1}{2}e^{s\ell}\sin s\ell, & V_3(s\ell) &\cong \frac{1}{2\sqrt{2}}e^{s\ell}(\sin s\ell - \cos s\ell) \end{aligned}\right\} \quad (52)$$

Equations 50 then yield

$$\left.\begin{aligned} \chi_0(s,k) &= 4\frac{s}{k}e^{-s\ell}\left[\left(1-\frac{s}{k}\right)\cos s\ell + \frac{s}{k}\sin s\ell\right] \\ \chi_2(s,k) &= 4\frac{s}{k}e^{-s\ell}\left[\left(1-\frac{s}{k}\right)\sin s\ell - \frac{s}{k}\cos s\ell\right] \end{aligned}\right\} \quad (53)$$

and solving Equation 51 results in the following simple formula for the distributed peeling stresses:

$$p_i(x) = C_i\left(e^{-k(\ell-x)} - 2\frac{s}{k}e^{-s(\ell-x)}\left[\left(1-\frac{s}{k}\right)\cos(s(\ell-x)) + \frac{s}{k}\sin(s(\ell-x))\right]\right),\quad i=1,2 \quad (54)$$

In the case of $s << k$, Equation 54 yields $p(l) = C_1^*$. Hence, the constants C_1^* expressed by Equations 45 are, in effect, the maximum peeling stresses at the ends of an assembly for which the parameter of the peeling stress s (through-thickness interfacial compliance) is significantly smaller than the shearing stress parameter k (the longitudinal compliance). At the assembly end we have

$$p_i(l) = C_i^*\left(1 - 2\frac{s}{k} + 2\frac{s^2}{k^2}\right),\quad i=1,2 \quad (55)$$

This relationship indicates that, for the given (calculated) C_1^* values, the peeling stresses at the assembly ends are equal to these values for zero $\frac{s}{k}$ ratios of the parameters of the interfacial peeling and shearing stresses, as well as for the situation when this ratio is equal to one. Equation 55 also indicates that the peeling stresses at the assembly ends have a minimum of for the stress parameter

Property	Thickness h [mm]	Young's Modulus E, [kg/mm^2]***	Poisson's Ratio ν	2D Young's Modulus $E^* = \frac{E}{1-\nu}$, [kg/mm^2]	Shear Modulus $G = \frac{E}{2(1+\nu)}$, *** [1/°C] [kg/mm^2]	CTE $\alpha x 10^6$
# Material			Input data			
1 Glass	5.00	7150	0.22	9167	2930	5.0
21 Silicon	0.20	16000	0.28	22222	6250	2.6
22 EVA 0.30	100	0.35	154	100	100	
2 Si-EVA Composite*	0.50	5506	0.326	8169	2076	42.5
3 Backsheet**	0.25	300	0.40	500	107	33

* Properties were evaluated for a segment of the Si-EVA composite structure (Fig. 2) using the formulas

$$E_{2e} = \frac{a}{l}\left(\frac{E_{21}h_{21} + E_{22}h_{22}}{h_{21} + h_{22}} - E_{22}\right) + E_{22} = \frac{0.34}{0.4}\left(\frac{16000x0.2 + 100x0.3}{0.2 + 0.3} - 100\right) + 100 = 5506 kg/mm^2$$

$$\nu_{2e} = \frac{a}{l}\left(\frac{\nu_{21}h_{21} + \nu_{22}h_{22}}{h_{21} + h_{22}} - \nu_{22}\right) + \nu_{22} = \frac{0.34}{0.4}\left(\frac{0.28x0.2 + 0.35x0.3}{0.2 + 0.3} - 0.35\right) + 0.35 = 0.326$$

$$\alpha_{2e} = \frac{a}{l}\left(\frac{\alpha_{21}E_{21}h_{21} + \alpha_{22}E_{22}h_{22}}{E_{21}h_{21} + E_{22}h_{22}} - \alpha_{22}\right) + \alpha_{22} =$$

$$= \left[\frac{0.34}{0.40}\left(\frac{2.6x16000x0.2 + 100x100x0.3}{1600x0.2 + 100x0.3} - 100\right) + 100\right] x10^{-6} = 42.5x10^{-6} 1/^0 C$$

In these formulas it is assumed that the length of the Si-EVA segment is $2l$=0.80mm, the length of the Si cell in it is $2a$=0.68mm, the cell thickness is h_{21}=0.20mm, the total thickness of the Si-EVA composite is $h_{21}+h_{22}$=0.50mm, and the thickness of the EVA above the Si cell is the same as below it and equal to 0.15mm.

** Polyethylene terephthalate (PET) polyester

*** For details see http://www.americanelements.com/thermal-expansion-coe.html or http://www1.eere.energy.gov/solar/pdfs/pvmrw2011_p41_csi_ebert.pdf. The change in temperature from the EVA curing temperature of 158°C to the room temperature is assumed to be Δt = 30°C.

Table 1. Material properties of the PVM for the numerical example.

ratio of 0.5, and that the peeling stresses can be very high for high stress parameter ratios.

Stresses in the composite EVA-Si layer

The problem

The objective of the following analysis is to address the state of stress within the EVA-Si composite layer (Fig. 5). In addition to the thermal contraction mismatch forces due to the dissimilar Si and EVA materials, the layer is subjected to an external tensile force $\hat{T} = T_2^0$. This force is determined on the basis of the previous analysis, when the effective mechanical characteristics of the Si-EVA composite were considered. In the following analysis, the actual properties of the EVA and Si materials are taken into account, in addition to the geometric characteristics of the Si cells (length and thickness) and the thickness of the EVA encapsulant. The analysis is limited to the evaluation of the normal stresses acting in the cross sections of the Si cells and the EVA materials, and the interfacial shearing stresses that are responsible for the possible delamination of the EVA encapsulant from the Si cells.

Basic equation

The induced axial forces $T_{21}(x)$ and $T_{21}(x)$, acting in the Si device (material 2-1) embedded into the EVA encapsulant and acting in the encapsulant itself (material 2-2), respectively, and caused by the combined action of the thermal and mechanical loading on component 2 of the PV assembly, are related as follows:

$$T_{21}(x) + T_{22}(x) = \hat{T}, \quad T_{21}(x) = 2\int_{-a}^{x} \tau(\xi)d\xi, \quad T_{22}(x) = \hat{T} - 2\int_{-a}^{x} \tau(\xi)d\xi \qquad (56)$$

The origin of the coordinate x is in the mid-cross section of the Si cell. In Equations 56, $\tau(x)$ is the interfacial shearing stress and a is half the Si cell length. Since the upper and the lower parts (layers) of the EVA encapsulant are assumed to be identical, it follows that 1) the stress $\tau(x)$ is the same at the upper and lower Si-EVA interfaces, and 2) the assembly as a whole does not experience bending deformations. Clearly, $\int_{-a}^{a} \tau(\xi)d\xi = 0$ (the shearing stress is anti-symmetric with respect to the mid-cross section of the Si cell). As evident from Equations 56, the boundary conditions $T_{21}(\pm a) = 0$ (this condition is based on our assumption that no external forces are applied directly to the butt end of the Si cell) and $T_{22}(\pm a) = \hat{T}$ are fulfilled for the forces $T_{21}(x)$ and $T_{22}(x)$. From Equations 56 we find, by differentiation,

$$\tau(x) = \frac{1}{2}T_{21}'(x) = -\frac{1}{2}T_{22}'(x) \qquad (57)$$

We seek the longitudinal interfacial displacements of the Si cell and the EVA encapsulant as follows:

$$u_1(x) = -\alpha_{21}\Delta tx + \lambda_{21}\int_0^x T_{21}(\xi)d\xi - 2\kappa_{21}\tau(\xi),$$
$$u_2(x) = -\alpha_{22}\Delta tx + \lambda_{22}\int_0^x T_{22}(\xi)d\xi + 2\kappa_{22}\tau(\xi) \qquad (58)$$

where a_{21} and a_{22} are the CTEs of the Si cell and the EVA materials, respectively; Δt is the change in temperature; $\lambda_{21}=\frac{1-\nu_{21}}{E_{21}h_{21}}$ and $\lambda_{22}=\frac{1-\nu_{22}}{2E_{22}h_{22}}$ are the axial compliances of the cell and the encapsulant; h_{21} is the cell thickness; h_{22} is the thickness of the encapsulant above or beneath the die; E_{21} and E_{22} are the Young's moduli of the Si and the EVA materials; and ν_{21} and ν_{22} are their Poisson's ratios. Also,

$$\kappa_{21}=\frac{h_{21}}{6G_{21}},\ \kappa_{22}=\frac{h_{22}}{3G_{22}} \qquad (59)$$

are the interfacial shearing compliances of the Si cell and each of the EVA layers (above and below the cell), respectively, and $G_{21}=\frac{E_{21}}{2(1+\nu_{21})}$ and $G_{22}=\frac{E_{22}}{2(1+\nu_{22})}$ are the shear moduli of the materials. The first of Equations 59 was obtained in Suhir [18] for a strip subjected to a shear load distributed over both of its long edges and symmetric with respect to its mid-cross section and to the horizontal mid-plane of the strip. The second of Equations 59 was obtained in Suhir [17] for a strip subjected to a shear load distributed over one of its long edges and symmetric with respect to the mid-cross section of the component.

The condition of the compatibility of the displacements given by Equations 58 can be written as

$$u_1(x)=u_2(x)+\kappa_0\tau(x) \qquad (60)$$

where $\kappa_0=\frac{h_0}{G_0}$ is the interfacial compliance of an additional layer, if any, between the Si cell and the encapsulant, h_0 is its thickness and G_0 is the shear modulus of the material. Introducing Equations 58 into the compatibility condition of Equation 60, we obtain the following basic equation for the interfacial shearing stress $\tau(x)$:

$$\tau(x)-\frac{\lambda_{21}}{2\kappa}\int_0^x T_{21}(\xi)d\xi+\frac{\lambda_{22}}{2\kappa}\int_0^x T_{22}(\xi)d\xi=\frac{\varepsilon_t}{2\kappa}x, \qquad (61)$$

where $\varepsilon_t=\Delta\alpha\Delta t=(\alpha_{22}-\alpha_{21})\Delta t$ is the thermal mismatch strain and $\kappa=\kappa_0+\kappa_{21}+\kappa_{22}$ is the total interfacial compliance of the assembly. The integrands in Equation 61 are related to the interfacial shearing stress $\tau(x)$ by the formulas expressed by Equations 56.

From Equation 61 we obtain, by differentiation,

$$\tau'(x)-\frac{\lambda_{21}}{2\kappa}T_{21}(x)+\frac{\lambda_{22}}{2\kappa}T_{22}(x)=\frac{\varepsilon_t}{2\kappa} \qquad (62)$$

This relationship allows the boundary conditions $T_{21}(\pm a)=0$ and $T_{22}(\pm a)=\hat{T}$ for the forces to be translated into the boundary condition for the shearing stress function $r(x)$ as follows:

$$\tau'(a)=-\frac{\lambda_{22}}{2\kappa}\hat{T}+\frac{\varepsilon_t}{2\kappa} \qquad (63)$$

Differentiating Equation 62 with respect to the coordinate x yields the following simple equation for the interfacial shearing stress function $r(x)$:

$$\tau''(x)-k^2\tau(x)=0 \qquad (64)$$

where $k=\sqrt{\frac{\lambda}{\kappa}}$ is the parameter of the interfacial shearing stress, and $\lambda=\lambda_{21}+\lambda_{22}$ is the total axial compliance of the Si-EVA assembly.

Solution to the basic equation

Equation 64 has the following solution that satisfies the boundary condition of Equation 63:

$$\tau(x)=-\frac{1}{2}kT\frac{\sinh kx}{\cosh ka} \qquad (65)$$

where $T = T_m - T_t$ is the force acting in the mid-portion of a Si-EVA assembly with a sufficiently long cell (large a values) and/or with a sufficiently stiff interface (large k values); $T_m=\frac{\lambda_{22}}{\lambda}\hat{T}$ is the tensile force due to the 'external' tensile force; $\hat{T}$ and $T_t=\frac{\varepsilon_t}{\lambda}=\frac{\Delta\alpha\Delta t}{\lambda}$ is the compressive force in the Si cell caused by the thermal contraction mismatch of the Si and the EVA materials.

The reduction factor $\frac{\lambda_{22}}{\lambda}=\frac{1}{1+\frac{\lambda_{21}}{\lambda_{22}}}$ in front of the force $\hat{T}$ is the ratio of the axial compliance of the EVA layer to the total axial compliance of the Si-EVA assembly. When the encapsulant is significantly more compliant than the Si cell ($\lambda_2 \gg \lambda_1$), the ratio $\frac{\lambda_{22}}{\lambda}$ is close to 1, so that the entire external force $\hat{T}$ is transmitted to the Si device. In this case the encapsulant exhibits tensile thermal loading only, i.e. $T_t=\frac{\varepsilon_t}{\lambda_{22}}=2\frac{E_{22}}{1-\nu_{22}}h_{22}\varepsilon_t$. In the hypothetical situation of the encapsulant layer being appreciably less compliant than the Si cell ($\lambda_{22} \ll \lambda_{21}$) – which is certainly not the case for the design in question – the ratio $\frac{\lambda_{22}}{\lambda}$ becomes $\frac{\lambda_{22}}{\lambda_{21}}$. This ratio is close to zero when the EVA encapsulant is significantly less compliant than the Si cell. The Si cell consequently becomes stress free, and it is the encapsulant that experiences the full magnitude of the force $\hat{T}$.

In the case of sufficiently large and/or stiff Si-EVA assemblies ($ka \geq 2.5$), the solution given by Equation 65 can be simplified to $\tau(x)=-\frac{1}{2}kTe^{-k(a-x)}$. This formula indicates that the shearing stress at the Si-EVA interface concentrates at the Si-EVA assembly ends, and decreases exponentially with increasing distance from the ends. In the hypothetical case of a small and/or compliant Si-EVA assembly ($ka \leq 0.25$), the solution (Equation 65) can be simplified to $\tau(x)=-\frac{1}{2}k^2Tx$. In this case the stress is distributed linearly along the Si-EVA interface. As follows from Equation 65, the maximum shearing stress τ_{max} takes place at the end cross sections $x = \pm a$ and is given by $x=\pm a: \tau_{max}=\tau_{max}^{\infty}\chi_\tau(ka)$, where $\tau_{max}^{\infty}=-\frac{1}{2}kT$ is the maximum interfacial shearing stress in an infinitely long assembly, and the function $\chi_\tau(ka)$ = tanh ka accounts for the effect of the assembly size.

Introducing the solution (Equation 65) into the formulas (Equations 56), we obtain

$$T_{21}(x)=T\left(1-\frac{\cosh kx}{\cosh ka}\right),\ T_{22}(x)=\hat{T}-T\left(1-\frac{\cosh kx}{\cosh ka}\right)=T\left(\frac{\lambda_{21}}{\lambda_{22}}+\frac{\cosh kx}{\cosh ka}\right)+T_t\frac{\lambda}{\lambda_{22}} \qquad (66)$$

The force $T_{21}(x)$ acting in the Si cell is greatest in its mid-cross section ($x = 0$) and is given by $T_{21}(0)=T\chi_\sigma(ka)$, where the function $\chi_\sigma(ka)=\frac{T_{21}(0)}{T}=1-\frac{1}{\cosh ka}$ takes into account the effect of the Si-EVA assembly size. For sufficiently long assemblies (large a) and/or assemblies with stiff interfaces (large k), so that $ka \geq 2.5$, we have $T_{21}(0) = T$ For a short (small a) and/or compliant (small k) Si-EVA assembly ($ka \leq 0.25$), the first of Equations 66 yields $T_{21}(x)=T_{21}(0)\left(1-\frac{x^2}{a^2}\right)$, where $T_{21}(0)=T\frac{(ka)^2}{2}$ is the force in the mid-cross section of the device. The corresponding normal stress can be found by dividing the force $T_{21}(x)$ by the Si cell thickness h_{21}. If the product ka is small, then the force $T_{21}(0)$ is small as well. Thus, for lower induced stresses in the cwell, there is an incentive to employ, if possible, small-sized cells and compliant bonding layers, if any, between the Si and the EVA materials.

Numerical example

Fig. 2 shows the structure under consideration, and its material characteristics (input data) are given in Table 1. The calculations are set forth below.

Axial compliances of the assembly components

$$\lambda_1 = \frac{1}{E_1^* h_1} = \frac{1}{9167x5.0} = 2.1817x10^{-5}\, mm/kg,$$

$$\lambda_2 = \frac{1}{E_2^* h_2} = \frac{1}{8169x0.5} = 24.4828x10^{-5}\, mm/kg,$$

$$\lambda_3 = \frac{1}{E_3^* h_3} = \frac{1}{500x0.25} = 8.0000x10^{-5}\, mm/kg,$$

Flexural rigidities of the assembly components

$$D_1 = \frac{E_1 h_1^3}{12(1-\nu_1^2)} = \frac{7150x5.0^3}{12(1-0.22^2)} = 78267.3042 kgmm$$

$$D_2 = \frac{E_2 h_2^3}{12(1-\nu_2^2)} = \frac{5506x0.5^3}{12(1-0.326^2)} = 64.1744 kgmm$$

$$D_3 = \frac{E_3 h_3^3}{12(1-\nu_3^2)} = \frac{300x0.25^3}{12(1-0.4^2)} = 0.4650 kgmm$$

$$D = D_1 + D_2 + D_3 = 78331.9436 kgmm$$

Combined axial compliances of the assembly components

$$\lambda_{11} = \frac{(h_1+h_2)^2}{4D} + \lambda_1 + \lambda_2 = \frac{(5.0+0.5)^2}{4x78331.9436} + 2.1817x10^{-5} + 24.4828x10^{-5} =$$
$$= 36.3189x10^{-5}\, mm/kg$$

$$\lambda_{33} = \frac{(h_2+h_3)^2}{4D} + \lambda_2 + \lambda_3 = \frac{(0.5+0.25)^2}{4x78331.9436} + 24.4828x10^{-5} + 8.0000x10^{-5} =$$
$$= 32.6623x10^{-5}\, mm/kg$$

$$\lambda_{13} = \frac{(h_1+h_2)(h_2+h_3)}{4D} - \lambda_2 = \frac{(5.0+0.5)(0.5+0.25)}{4x78331.9436} - 24.4828x10^{-5} =$$
$$= -23.1663x10^{-5}\, mm/kg$$

Interfacial compliances

$$\kappa_1 = \frac{h_1}{3G_1} = \frac{5.00}{3x2930} = 56.8828x10^{-5}\, mm^3/kg,$$

$$\kappa_2 = \frac{h_2}{G_2} = \frac{0.5}{2076} = 24.0848x10^{-5}\, mm^3/kg,$$

$$\kappa_3 = \frac{h_3}{3G_3} = \frac{0.25}{3x107} = 77.8816x10^{-5}\, mm^3/kg,$$

Combined (coupled) interfacial compliances

$$\kappa_{12} = \kappa_1 + \kappa_2 = 80.9676x10^{-5}\, mm^3/kg, \quad \kappa_{23} = \kappa_2 + \kappa_3 = 101.9664x10^{-5}\, mm^3/kg,$$

Parameter of the interfacial shearing stresses

$$k_1 = \sqrt{\frac{\lambda_{11}}{\kappa_{12}}} = \sqrt{\frac{36.3189x10^{-5}}{80.9676x10^{-5}}} = 0.6697 mm^{-1}; \; k_2 = \sqrt{\frac{\lambda_{33}}{\kappa_{23}}} = \sqrt{\frac{32.6623x10^{-5}}{101.9664x10^{-5}}} = 0.5660 mm^{-1};$$

$$\gamma = 1 - \frac{\lambda_{13}^2}{\lambda_{11}\lambda_{33}} = 1 - \frac{(-23.1663x10^{-5})^2}{36.3189x10^{-5}x32.6623x10^{-5}} = 0.5476,$$

$$k = \sqrt{\frac{k_1^2+k_2^2}{2}\left[1+\sqrt{1-\gamma\left(\frac{2k_1k_2}{k_1^2+k_2^2}\right)^2}\right]} = \sqrt{\frac{0.7689}{2}\left[1+\sqrt{1-0.5476\left(\frac{0.7581}{0.7689}\right)^2}\right]} = 0.8046 mm^{-1}$$

Thermally induced forces acting in the cross sections of the assembly components

$$T_1^0 = \frac{\lambda_2(\alpha_1-\alpha_3)+\lambda_3(\alpha_1-\alpha_2)}{\lambda_1\lambda_2+\lambda_2\lambda_3+\lambda_3\lambda_1}\Delta t =$$
$$= \frac{24.4828x10^{-5}(5.0-33.0)x10^{-6} + 8.0000x10^{-5}(5.0-42.5)x10^{-6}}{2.1817x10^{-5}x24.4828x10^{-5} + 24.4828x10^{-5}x8.0000x10^{-5} + 8.0000x10^{-5}x2.1817x10^{-5}}130 =$$
$$= \frac{-685.5184x10^{-11} - 300.0000x10^{-11}}{53.4141x10^{-10} + 195.8624x10^{-10} + 17.4536x10^{-10}}130 = -\frac{985.5184x10^{-11}}{266.7301x10^{-10}}130 = -48.0326\, kg/mm$$

$$T_2^0 = \frac{\lambda_3(\alpha_2-\alpha_1)+\lambda_1(\alpha_2-\alpha_3)}{\lambda_1\lambda_2+\lambda_2\lambda_3+\lambda_3\lambda_1}\Delta t = \frac{8.0000x10^{-5}x(42.5-5.0)x10^{-6} + 2.1817x10^{-5}(42.5-33)x10^{-6}}{266.7301x10^{-10}}130 =$$
$$= \frac{300.0000x10^{-11} + 20.7262x10^{-11}}{266.7301x10^{-10}}130 = 15.6317\, kg/mm$$

$$T_3^0 = \frac{\lambda_1(\alpha_3-\alpha_2)+\lambda_2(\alpha_3-\alpha_1)}{\lambda_1\lambda_2+\lambda_2\lambda_3+\lambda_3\lambda_1}\Delta t = \frac{2.1817x10^{-5}(33-42.5)x10^{-6} + 24.4828x10^{-5}(33-5)x10^{-6}}{266.7301x10^{-10}}130 =$$
$$= \frac{-20.7262x10^{-11} + 685.5184x10^{-11}}{266.7301x10^{-10}}130 = 32.4009\, kg/mm$$

Normal stresses in the mid-portions of the glass and the backsheet

$$\sigma_1^0 = \frac{T_1^0}{h_1} = -\frac{48.0326}{5.0} = -9.6065 kg/mm^2$$

$$\sigma_3^0 = \frac{T_3^0}{h_3} = \frac{32.4009}{0.25} = 129.6036 kg/mm^2$$

Stress in the EVA material outside the Si cell

$$\sigma_2^0 = \frac{T_2^0}{h_2} = \frac{15.6317}{0.5} = 31.2634 kg/mm^2$$

Axial compliance of the Si-EVA layer

$$\lambda = \frac{1}{E_{21}^* h_{21}} + \frac{1}{E_{22}^* h_{22}} = \frac{1}{22222x0.2} + \frac{1}{154x0.3} = 22.5002x10^{-5} + 2164.5022x10^{-5} =$$
$$= 2187.0022x10^{-5}\, mm/kg$$

Interfacial compliance of the Si-EVA layer

$$\kappa = \frac{h_{21}}{6G_{21}} + \frac{2h_{22}}{3G_{22}} = \frac{0.2}{6x6250} + \frac{2x0.15}{3x100} = 0.5333x10^{-5} + 100x10^{-5} = 100.5333x10^{-5}\, mm^3/kg$$

Parameter of the interfacial shearing stress for the Si-EVA composite

$$k_{Si} = \sqrt{\frac{\lambda}{\kappa}} = \sqrt{\frac{2192.1954x10^{-5}}{100.5333x10^{-5}}} = 4.6697$$

Factor for considering the effect of the finite size of the Si cell on the induced thermal force

$$\chi_\sigma(k_{Si}a) = 1 - \frac{1}{\cosh k_{Si}a} = 1 - \frac{1}{\cosh(4.6697x0.34)} = 0.6076$$

'Mechanical' tensile forces acting on the EVA and Si material within the area where Si cells are located

$$T_{22}^0 = \frac{E_{22}h_{22}T_2^0}{E_{21}h_{21}+E_{22}h_{22}}\chi_\sigma(k_{Si}a) = \frac{100x0.3x15.6317}{16000x0.2+100x0.3}0.6076 = 0.0882 kg/mm$$

$$T_{21}^0 = \frac{E_{21}h_{21}T_2^0}{E_{21}h_{21}+E_{22}h_{22}}\chi_\sigma(k_{Si}a) = \frac{16000x0.2x15.6317}{16000x0.2+100x0.3}0.6076 = 9.4096 kg/mm$$

Thermally induced force in the EVA-Si composite within the area where Si cells are located

$$T_t = \frac{\Delta\alpha\Delta t}{\lambda}\chi_\sigma(k_{Si}a) = \frac{(100-2.6)x10^{-6}x130}{2192.1954x10^{-5}}0.6076 = 0.3509 kg/mm$$

Tensile force in the EVA layer due to the combined action of the external ('mechanical') and thermal loading

$$T_{EVA} = T_{22}^0 + T_t = 0.0882 + 0.3509 = 0.4391 kg/mm$$

Credit: Atersa

European Photovoltaic Technology Platform

7th General Assembly

Photovoltaics : Engine of European Innovation and Development

19 June 2012 - Amsterdam, The Netherlands

PhotoVoltaic TECHNOLOGY PLATFORM

Supported by:

SUSTAINABLE ENERGY WEEK 18-22 JUNE 2012

Coordinator of the Platform Secretariat

EPIA European Photovoltaic Industry Association

Platform Partners

WIP

JRC EUROPEAN COMMISSION

EUREC AGENCY European Renewable Energy Research Centres Agency

More information: www.eupvplatform.org

Normal stress in the EVA layer

$$\sigma_{EVA} = \frac{T_{EVA}}{h_{22}} = \frac{0.4391}{0.3} = 1.4638 kg/mm^2$$

Tensile force in the Si layer within the area where Si cells are located

$$T_{Si} = T_{21}^0 - T_t = 9.4096 - 0.3509 = 9.0587 kg/mm$$

Normal stress in the Si cell within the area where Si cells are located

$$\sigma_{Si} = \frac{T_{Si}}{h_{21}} = \frac{9.0587}{0.2} = 45.2935 kg/mm^2$$

Maximum shearing stress at the Si-EVA interface

$$\tau_{max} = k_{Si} T_{Si} \tanh ka = 4.6697x9.0587x \tanh(4.6697x0.34) = 38.9078 kg/mm^2$$

Maximum shearing stress at the glass-EVA interface

$$\tau_{1,max} = -kT_1^0 = 0.8171x\ 107.0499 = 87.4705 kg/mm^2$$

Maximum shearing stress at the EVA-backsheet interface

$$\tau_{2,max} = -kT_3^0 = -0.8171x\ 22.3519 = -18.2637 kg/mm^2$$

Compliances in the through-thickness direction

$$\delta_{12} = \frac{h_1}{E_1^*} + \frac{h_2}{2E_2^*} = \frac{5.0}{9167} + \frac{0.5}{2x154} = 0.00054543 + 0.00162338 = 0.0021688 mm^3/kg$$

$$\delta_{23} = \frac{h_3}{E_3^*} + \frac{h_2}{2E_2^*} = \frac{0.25}{500} + \frac{0.5}{2x154} = 0.000500 + 0.00162338 = 0.0021234 mm^3/kg$$

$$s_1 = \sqrt[4]{\frac{D_1 + D_2}{4\delta_{12} D_1 D_2}} = \sqrt[4]{\frac{78267.3042 + 64.1744}{4x0.0021688x78267.3042x64.1744}} = 1.1579 mm^{-1}$$

$$s_2 = \sqrt[4]{\frac{D_2 + D_3}{4\delta_{23} D_2 D_3}} = \sqrt[4]{\frac{64.1744 + 0.4650}{4x0.0021234x64.1744x0.4650}} = 3.9962 mm^{-1}$$

$$\delta = \frac{D}{\delta_{12}\delta_{23} D_1 D_2 D_3} = \frac{78331.9436}{0.0021688x0.0021234x78267.3042x64.1744x0.4650} =$$
$$= 7282.7003 mm^{-8}$$

Parameter of the peeling stresses

$$s = \sqrt[4]{\frac{s_1^4 + s_2^4}{2}\left[1 + \sqrt{1 - \frac{\delta}{4(s_1^4 + s_2^4)^2}}\right]} = \sqrt[4]{\frac{1.7976 + 255.0286}{2}\left[1 + \sqrt{1 - \frac{7282.7003}{4x256.8262^2}}\right]} =$$
$$= 3.9963 mm^{-1}$$

Constants in the expression for the peling stress functions

$$C_1^* = -\frac{k^2 h_2}{2} \frac{\left[1 + \delta_{23} D_2 (k^4 + 4s_2^4)\left(\frac{h_1}{h_2}\frac{D_2}{D_1} - 1\right)\right] T_1^0 + \left[\frac{h_3}{h_2}\frac{D_2}{D_3} - 1 + \delta_{23} D_2 (k^4 + 4s_2^4)\right] T_3^0}{\delta_{12}\delta_{23} D_2^2 (k^4 + 4s_1^4)(k^4 + 4s_2^4) - 1} =$$
$$= -0.1618 \frac{6576.8937 + 6709.2759}{146.2830} = -14.6955 kg/mm^2$$

$$C_2^* = -\frac{k^2 h_2}{2} \frac{\left[1 + \delta_{12} D_2 (k^4 + 4s_1^4)\left(\frac{h_3}{h_2}\frac{D_2}{D_3} - 1\right)\right] T_3^0 + \left[\frac{h_1}{h_2}\frac{D_2}{D_1} - 1 + \delta_{12} D_2 (k^4 + 4s_1^4)\right] T_1^0}{\delta_{12}\delta_{23} D_2^2 (k^4 + 4s_1^4)(k^4 + 4s_2^4) - 1} =$$
$$= -0.1618 \frac{2366.0080 - 3.2320}{146.2830} = -2.6134 kg/mm^2$$

Ratio of the peeling stress parameter to the shearing stress parameter

$$\frac{s}{k} = \frac{3.9963}{0.8046} = 4.9668$$

Maximum peeling stresses

$$p_1(l) = C_1\left(1 - 2\frac{s}{k} + 2\frac{s^2}{k^2}\right) = -14.6955x40.4046 = -593.7659 kg/mm^2$$

$$p_2(l) = C_2\left(1 - 2\frac{s}{k} + 2\frac{s^2}{k^2}\right) = -2.6134x40.4046 = -105.5934 kg/mm^2$$

The calculated stresses are summarized in Table 2. The computed data indicate that the interfacial peeling stresses considerably exceed the interfacial shearing stresses and could possibly lead, in combination with the effect of the shearing stresses, to delaminations. These data also indicate that delaminations at the glass-encapsulant interface are more likely than delaminations at the backsheet-encapsulant interface. As for the stresses acting in the components' cross sections, these are greatest in the backsheet, and need to be taken into consideration when the material and the thickness of the backsheet are selected and established.

Material (layer)	Stress in the component cross section [kg/mm²]	Maximum interfacial stresses [kg/mm²]	
		Shearing	Peeling
Glass	–9.6		
Glass-EVA Interface		87.5	593.7
EVA	+31.3		
EVA-Si Interface		38.9	-
Si	+45.3		
Si-EVA Interface		38.9	-
EVA	+31.3		
EVA-Backsheet Interface		18.3	105.6
Backsheet	+129.6		

Table 2. Calculated stresses for the numerical example.

> "Important as the reliability and performance of a PV device itself is, it is the module – or the 'package' – that is the most vulnerable element of a PVM."

Some major challenges and future work

Since solar energy is abundant worldwide, cell/PV technology is an attractive option in the renewable energy field, but there is still a long way to go before viable and promising devices based on PV technology become reliable and cost-effective products. Here are a few of the main questions that are typically asked and some of the major challenges envisioned:

- Since some (far from perfect) PV products have been in the field for just a couple of years, no well-established qualification specifications and test methodologies exist yet. For this reason, the only way to make adequate short- and long-term reliability predictions, as far as the possible failure modes and mechanisms are concerned, is through properly designed, carefully conducted and clearly interpreted failure-oriented accelerated testing (FOAT). What stimuli and reliability criteria should be included in such FOAT methodologies and testing procedures? Should we be aiming (perhaps unrealistically) for a 20-year PVM lifetime, or possibly settle for a shorter lifetime?
- How will actual loading (thermal, dynamic) and environmental (temperature, humidity, earthquake, etc.) conditions

encountered in different geographic areas affect the useful and cost-effective lifetime of the PV system of interest, and what should be the criteria?

- The major effort today centres on improving the effectiveness and reliability of PV devices per se. However, it is clear that, important as the reliability and performance of a PV device itself is, it is the module – or the 'package' – that is the most vulnerable element of a PVM. Should the PVM engineering and business-oriented communities, concurrently with the continuing effort to make the PV devices more efficient and more robust, place more emphasis on the general reliability of PVM systems (structures)? Are the existing PV qualification test methodologies and procedures – such as IEC 61215 (for crystalline-Si-based devices), IEC 61646 (for thin-film-based devices) and IEC 62108 (for concentration-based devices (CPV)) – adequate? Do PV industries need new approaches to qualify their products?

- The most critical aspect of today's PV technologies seems to be the way(s) in which a PVM is packaged (optical, electrical, materials, thermo-mechanical, etc.) to protect the given PVM design from the harsh environment, in order to enhance what the PV devices can do and to guarantee, with a reasonably high certainty, their durability. There is a crucial need to consider and to develop effective and goal-oriented PVM packaging directions – what is the best way to do this and how can it be done in a timely fashion? To what extent could previous experience, accumulated in the fields of electronics, opto-electronics, photonics, MEMS and MOEMS technologies, be employed?

- In many areas of opto-electronic engineering, predictive modelling has proved to be a highly useful and time-effective means of both understanding the physics of failure and designing the most helpful FOAT. There is certainly a need for developing such models in the PV field, with an emphasis on validating observed field failures. Which models might be needed most: thermal, environmental or mechanical – or combinations of all these?

- There are indications that some PVM degradation (ageing) and failure mechanisms have been found in the field that were not detected by the existing accelerated tests, such as temperature cycling, temperature-humidity bias (THB), nominal operating cell temperature (NOCT), hail (solid precipitation) tests and high-voltage (high-potential, or 'high-pot') tests. How can a minimum list of crucial tests and stimuli be established?

- There are currently several different PV technologies (key approaches to solar-based electricity), such as solar thermal, crystalline Si, thin film, concentrators and, perhaps, combinations of these. Each of these technologies has its merits and shortcomings. Should the packaging and FOAT approaches be developed separately for all these technologies, or might there be unified and cost- and time-effective ways of addressing reliability and packaging issues for them? Is there a possibility that one or two existing PV technologies will predominate (or perhaps already do so), and that packaging and reliability efforts should be directed accordingly?

- There are many PVM reliability concerns that are more or less well established – some examples are:
  - if new materials and/or new physical (structural) designs are introduced, how will this affect the short- and long-term reliability of the PV device and/or the PVM and/or the PVM system as a whole?
  - to what extent could impurities in the silicon result in light-induced degradation of the material?
  - how might arcing, grounding, power conditioning and other system-related problems affect the PV system's reliability?
  - given that annual degradation rates of typically 0–1% might be difficult to measure, how could one measure, using existing metrological techniques, even lower degradation rates (less than 0.1%) in the field? Could better metrological means be developed, and what role might modelling play in such a situation?
  - edge seals in the moisture-resistant device structures may allow water penetration; at the same time it has been established that thermal stresses due to dissimilar materials concentrate at the assembly ends. How could this thermo-mechanical-environmental problem, as well as many other adhesion-related problems, be resolved?

- The process involved in going from creating something in a lab to marketing an industrial product is a lengthy one. Could this be shortened?

- The measurement of degradation rates takes several years. Could physically meaningful ALT (accelerated-life test)-FOAT methodologies be developed?

Based on the authors' expertise in many areas of reliability and packaging of electronic systems, a list is presented below of the most crucial engineering problems that could be addressed and successfully solved, and that are, at the same time, of the utmost interest to the PV manufacturing community.

- Review and analyze existing PVM physical designs and the geographical areas in which these modules are, or will be, installed.

- Review and analyze the existing qualification testing specifications and test conditions used by Flextronics to qualify its PVM systems.

- Review and analyze any observed field failures of the PV products.

- Address the adequacy of the existing Flextronics specifications and accelerated test methodologies and practices from the standpoint of their ability to prevent field failures.

- Improve in a timely fashion and to the extent possible the existing qualification methodologies.

- Select the most indicative and most vulnerable structural item (the 'bottle-neck') in the existing Flextronics PVM design, and then consider the application to the selected structural element of the recently suggested (rather general) novel and effective approach [18–20] for qualifying electronic and similar products.

- Design an adequate FOAT procedure, conduct the accelerated life testing, develop the appropriate predictive models and predict the reliability of failure of the selected structural element in the field.

- On the basis of the results obtained, make a prediction, using primarily predictive modelling approaches and techniques (both computer-aided and analytical), of the probability of failure of the entire PVM system in the field under the anticipating loading conditions and after the given time in operation.

- Establish what changes, if any, to the existing design and in the qualification specifications could or should be made.

Experimental and modelling (both computer-aided and analytical) approaches should and will be widely used to address these issues.

“The model can also be used for stress analysis and reliability predictions for bonded joints in applications outside of the PV technology field.”

PV Modules

Conclusions

Low-temperature thermally induced stresses in a crystalline-Si-based PVM (assembly) have been evaluated on the basis of a rather general analytical ('mathematical') predictive stress model for a tri-material assembly. A special predictive model was developed for the evaluation of the effective elastic constants and the CTE of component 2 (EVA-Si composite) consisting of a low-modulus and high-expansion EVA encapsulant and high-modulus and low-expansion Si cells, so that the module of interest could be treated as a tri-material body. The calculated data indicated that the induced stresses can be rather high, especially the peeling stress at the glass interface, which means that the structural integrity of the PVM might be compromised unless the appropriate DfR measures are taken. It is well known that the reliability of a product should be conceived and, to the extent possible, assured at the design stage – as far as such an effort is concerned, the developed model can be helpful. The model can also be used for stress analysis and reliability predictions for bonded joints in applications outside of the PV technology field.

References

[1] Meydbray, J. et al. 2007, "Solder joint degradation in high efficiency all back contact solar cells", *Proc. 22nd EU PVSEC*, Milan, Italy.

[2] Osterwald, C. & McMahon, T. 2008, "History of accelerated and qualification testing of terrestrial photovoltaic modules: A literature review", *Prog. Photovolt: Res. Appl.*, Vol. 17.

[3] Wohlgemuth, J.H. et al. 2008, "Using accelerated tests and field data to predict module reliability and lifetime", *Proc. 23rd EU PVSEC*, Valencia, Spain.

[4] Jacobson, M.Z. 2008, "Review of solutions to global warming, air pollution, and energy security", The Energy Seminar, Stanford University, October 1 [available online at http://www.stanford.edu/group/efmh/jacobson/Articles/I/ReviewSolGW09.pdf].

[5] Hacke, P. et al. 2010, "Test-to-failure of crystalline silicon modules", *Proc. 35th IEEE PVSC*, Honolulu, Hawaii, USA.

[6] Dietrich, S. et al. 2010, "Mechanical and thermo-mechanical assessment of encapsulated solar cells by finite-element-simulation", *Proc. SPIE - Optics and Photonics*, San Diego, California, USA.

[7] Meier, R. et al. 2010, "Thermal and mechanical induced loading on cell interconnectors in crystalline photovoltaic modules", *Proc. 25th EU PVSEC*, Valencia, Spain.

[8] Schubbert, C. et al. 2010, "Exemplary results of temperature-dependent mechanical load tests under variation of glass and foil parameters and investigation of different load types", *Proc. 25th EU PVSEC*, Valencia, Spain.

[9] Lau, J.H. (Ed.) 1993, *Thermal Stress and Strain in Microelectronics Packaging*. New York: Van-Nostrand Reinhold.

[10] Lang, G.A. et al. 1970, "Thermal fatigue in silicon power devices", *IEEE Trans. Electron. Dev.*, Vol. 17.

[11] Suhir, E. 1999, "Modeling of thermal stress in microelectronic and photonic systems", *Future Circuits*, No. 5.

[12] Timoshenko, S. 1925, "Analysis of bi-metal thermostats", *J. Opt. Soc. Am.*, Vol. 11.

[13] Suhir, E. 2002, "Analytical stress-strain modeling in photonics engineering: Its role, attributes and interaction with the finite-element method", *Laser Focus World* (May).

[14] Ceniga, L. 2008, *Analytical Models of Thermal Stresses in Composite Materials*. New York: Nova Science Publishers.

[15] Suhir, E. 2009, "Analytical thermal stress modeling in electronic and photonic systems", *ASME Appl. Mech. Rev.*, Vol. 62, No. 4.

[16] Timoshenko, S.P. & Woinowsky-Krieger, S. 2007, *Theory of Plates and Shells*, 2nd ed. Knovel (online).

[17] Suhir, E. 1986, "Stresses in bi-metal thermostats", *ASME J. Appl. Mech.*, Vol. 55, No. 1.

[18] Suhir, E. 1999, "Adhesively bonded assemblies with identical nondeformable adherends: Predicted thermal stresses in the adhesive layer", *Composite Interfaces*, Vol. 6, No. 2.

[19] Suhir, E. 2010, "Probabilistic design for reliability", *ChipScale Reviews*, Vol. 14, No. 6.

[20] Suhir, E. & Mahajan, R. 2011, "Are current qualification practices adequate?", *Circuit Assembly* (April).

About the Authors

Dr. E. Suhir is with the University of California, Santa Cruz, CA, USA. He is a Fellow of IEEE, APS, ASME, IoP (UK) and SPE, co-founder of the ASME *Journal of Electronic Packaging* and served as its Editor-in-Chief for eight years (1993–2001). Dr. Suhir holds 22 US patents and has authored about 250 technical publications (papers, book chapters and books). He has received many professional awards, including: the 2004 ASME Worcester Read Warner Medal for establishing a new discipline: Structural Analysis of Microelectronic and Photonic Systems.

Dr. Dongkai Shangguan received his B.S. in mechanical engineering from Tsinghua University, China; his Ph.D. in materials from the University of Oxford; and his M.B.A. from San Jose State University. He conducted post-doctoral teaching at the Universities of Cambridge and Alabama, and is a guest professor at Shanghai University. Dongkai joined Flextronics International in 2001, where he is Senior Director with the Corporate Technology Group. He has 20 US and international patents and is a senior member of IEEE and SME. Dongkai has received the "Total Excellence in Electronics Manufacturing Award" from the SME.

Dr. Laurent Bechou received his Ph.D. in electronics from the University of Bordeaux 1 (France) in 1998. He then joined the Integration of Material to System Laboratory (IMS), where he has held the title of professor since 2010. His research field addresses characterization, failure mechanisms modelling and methods for reliability prediction of optoelectronic/photonic devices and systems. He is currently the manager of the "Reliability Assessment of Micro and Nano-assemblied Devices" Research Group (EDMiNA) at IMS Laboratory and the co-author of more than 80 regular papers and contributions to international conferences.

Enquiries

E. Suhir
suhire@aol.com

D. Shangguan
Dongkai.Shangguan@flextronics.com

L. Bechou
Laurent.bechou@ims-bordeaux.fr

Power Generation

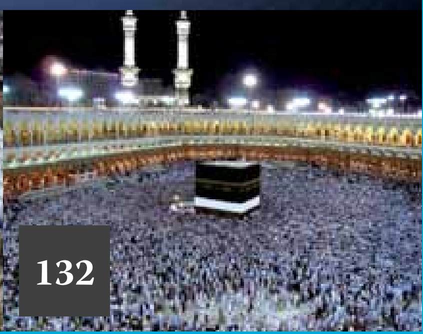

Solar power was 'most-installed' power in Europe in 2011, says EPIA

The European Photovoltaic Industry Association (EPIA) has reported that, for the first time ever, solar PV power became the most installed energy source in Europe in 2011. The increased uptake of solar power, which rose 63% to reach 21.9GW last year, has been attributed to the implementation of incentive schemes and widespread subsidization by governments.

European countries have enjoyed reduced module and panel prices in recent months and were responsible for 75% of newly installed global capacity, producing around 26TWh of solar energy. Solar power is leading the way in renewable energy production in Europe, generating more than new wind and gas projects combined, which each had 9.5GW of capacity installed in 2011.

Italy and Germany were responsible for 60% of Europe's installed solar PV capacity in 2011.

Global PV capacity reached 29.7GW in 2011, an increase of almost 13GW (44%) of capacity when compared to the installation capacity of 16.8GW for 2010. Predictably the German and Italian PV markets led the way in Europe, together accounting for more than 60% of the installed capacity, 7.5GW and 9.3GW respectively.

However, the EPIA also insisted that these installation growths are unsustainable at their current rates, largely because countries will reach a subsidy cap where governments will have spent all finances reserved for renewable energy subsidization. A decrease to anything from 21.6 to 9.4GW of new European capacity has been suggested.

Asia & Oceania News Focus

Shanghai Alex Solar to develop over 1GW of PV capacity in Jinchang City

Under an agreement signed by the Jinchang Municipal Government and Shanghai Alex Solar Energy Science and Technology, Alex Solar will be developing 1GW of PV capacity in the Jinchang city development centre under a five-year plan that takes the agreement until 2016. Alex Solar advised that this marked the beginning of its long-term growth plan to expand in the Jinchang municipality.

The US$1.74 billion (11 billion Yuan) is to be owned, financed and developed by Alex Solar. The company will construct solar power stations in the western slope of Jinchang City and plans to open a new factory in the area known as the new Economic and Technological Development Zone, which holds a 300MW scale in itself.

State of Gujarat to construct rooftop PV systems in five cities

The Indian state of Gujarat has announced plans to install rooftop PV systems in five different cities based upon the PV rooftop system in Gandhinagar. The International Finance Corporation (IFC) supports this enterprise. The cities that will have such systems installed are Mehsana, Rajkot, Vadodara, Surat and the city of Bhavnagar.

Gujarat and the IFC are developing policy frameworks based on the Gandhinagar system operating experience. Under this program, Azure Power India and SunEdison will both provide 2.5MW of energy, which will be installed on rented rooftops across the cities.

State of Gujarat expands the Gandhinagar PV Rooftop Program to five other cities.

Funding will be provided by public-private partnerships and the businesses renting out the rooftops will receive a small part of the revenues, although they cannot use any of the generated energy themselves. The Gujarat Energy Research and Management Institute (GERMI) and the Gujarat Power Corporation will manage the projects. Developers will be chosen through a competitive bidding process.

Japan to exclude net-metering from new FiT

The Japanese Ministry of Economy, Trade and Industry, has announced it will omit net-metering purchase prices from the new feed-in tariffs due to be implemented in July. Instead, the government has decided that in order to avoid confusion, current rates will be extended for three months until June and kept separate from the feed-in tariff.

Jefferies has lauded the government's proposals and is predicting a solar success in Japan. The new tariffs include residential facilities of less than 10kW at ¥42/kWh, although hybrid systems will only receive ¥34/kWh. Non-residential facilities and residential facilities of 10kW or more will be due for ¥40/kWh and hybrid systems at ¥32/kWh. Rates for facilities installed before 2010 will be set at ¥24/kWh and for hybrid systems ¥20/kWh.

CEFC to provide AUD$10 billion to Australian solar industry

Following the release of the IPART report this week, Expert Review Panel has issued directives to the Australian government on the Clean Energy Finance Corporation (CEFC). The CEFC will finance Australia's clean energy in order to address the barriers currently inhibiting investment.

The CEFC will finance Australia's clean energy in order to address the barriers currently inhibiting investment.

Expected to commence operations in July, the AUD$10 billion CEFC has been set up to provide funding to a broad range of renewable projects, with a focus on large-scale projects. Smaller projects would need to turn to third-parties for financing. However, the CEFC requires that all projects are co-financed alongside private sector investments as well as the CEFC.

This could also cover hybrid projects as well as supporting infrastructure. Investment in projects to create renewable energy certificates are also a priority. Eligible projects will be required to achieve an emissions intensity of 50% or lower than the electricity grid average – 0.415 tonnes of CO_2 per megawatt hour of electricity.

Europe News Focus

News

Report: Serbian government officials sign memorandum to build 1,000MW solar park

Representatives from Serbia's government and the Securum Equity Partners Europe signed a memorandum for the development of what is being called the world's largest solar park. Minister of the Environment, Oliver Dulić, and members of Securum's management board, including Alessio Colussi and Ivan Matejak, signed the memo in the presence of Prime Minister Mirko Cvetković.

Source: Tanjug

Securum management, along with Oliver Dulic (right), Minister of the Environment, sign the memorandum with Prime Minister Mirko Cvetkovic (back) looking on.

The solar park will have a 1,000MWp capacity and be built over 7,413 acres of land. Its total value is near €2 billion with construction on the project anticipated to take place over a three- to five-year period. Almost 3,000 people will be involved in the development and, Dulić pointed out, the finished park will employ between 500 to 600 workers.

MX Group will work on the project and it is expected that the company will move its panel production to Serbia. Dulić additionally noted that the country has no financial commitment in the investment, but he expects the country to collect €750 million in taxes over the next 20 years. Matejak pointed out that construction could begin early next year, providing that the appropriate land is found and permits are secured. He confirmed that, among other factors, the company chose Serbia because of its solar irradiation being 40% higher than other parts of Southeast Europe. The country plans to lease the land for the solar park free of charge for 25 years.

ET Solar completes 4MW of rooftop PV projects in France

ET Solar has announced the completion of four rooftop projects, totalling 4MW generating capacity, in partnership with French developer Langa Solar. The projects are expected to begin power production by June, 2012.

Source: ET Solar

ET Solar connected a 2.65MW PV plant to the grid in France in October 2011.

The two companies jointly designed, installed and financed the four projects with ET Solar supplying the PV modules for the plants.

JinkoSolar renews Valencia Football Club sponsorship

JinkoSolar will continue to sponsor Valencia Football Club for two more years following the signing of a new contract.

Source: SportsProMedia

JinkoSolar's logo will be featured on Valencia's home and away shirts throughout the season.

Valencia recently finished third in Spain's La Liga and will play in the European Champions League next year. JinkoSolar will remain the club's main sponsor and the company's logo will be featured on Valencia's home and away shirts throughout the season.

Solaria and Convert Italia partner to deliver world's largest low concentrating PV solar power plant

Module manufacturer Solaria Corporation has joined forces with renewable energy project developer Convert Italia to create the largest low concentrating PV solar plant in the world. The plant, located in Puglia, southern Italy, recently came online and will deliver an annual generation of 2MW to the Italian grid.

Convert Italia will own and operate the solar plant but use Solaria's advanced low concentration modules on the system.

IKEA Italy installs 7MW of Q-Cells' modules

IKEA has announced that it will equip the roof of its main warehouse in Piacenza, Northern Italy, with 7MW of Q-Cells' CIGS thin-film modules. The rooftop installation was developed in collaboration with GreenTechPower and F. Ili Zaffaroni.

German company tops IMS Research PV System Integrator rankings for second year running

According to the latest PV System Integrators report from IMS Research, a German company held onto the top spot for the second year running. The report also demonstrated how Chinese integrators made the biggest gains in 2011, with three companies appearing in the top 10.

The report, which tracks the activities and pipelines of more than 550 global

World PV System Integrator Market Rankings - 2010 & 2011

For All PV Systems > 10 kW

HQ Location	Company Name	2010 Rank	2011 Rank
Germany	BELECTRIC	1	1
China	China Power Investment Corporation	>10	2
USA	First Solar	7	3
USA	SunEdison	5	4
USA	SunPower Corporation	3	5
Germany	Juwi	2	6
Germany	Solarhybrid	>10	7
Germany	Q-Cells International	6	8
China	Huanghe Hydropower Development Company	>10	9
China	CGN Solar Energy Development	>10	10
Austria	Activ Solar	>10	11
Belgium	Enfinity	8	12
France	EDF Energies Nouvelles	4	13
Germany	Phoenix Solar	9	14
Germany	Enerparc	10	15

Source: IMS Research 's Quarterly PV System Integrator Report www.pvmarketresearch.com

Source: IMS Research

IMS Research's top 10 PV System Integrator rankings.

system integrators and EPCs, found that Belectric maintained its position as the world's largest PV system integrator in 2011, with close to 400MW of new PV capacity developed. Belectric was followed by China Power Investment Corporation (CPI) which was responsible for 380MW of new PV capacity in China in 2011.

Though the biggest gains were made by Chinese integrators in 2011, a high level of project completion performance was also achieved by US-based companies First Solar, SunEdison and SunPower which were ranked third, fourth and fifth respectively. German-based companies dominated the rest of the rankings.


Source: Caribbean Energies Group

Caribbean Energies Group chose ESA Renewables as the designer and constructor for the 24MW Jamaican PV project.

Americas News Focus

Satcon enters strategic manufacturing agreement with Sanmina-SCI

Renewable energy solutions provider Satcon Technology has entered into a strategic manufacturing agreement with Sanmina-SCI, the company has announced. Under the agreement, Sanmina will begin producing Satcon's PowerGate Plus 50, 100, 250 and 500kW inverters well as the company's Prism Platform solutions at its Canadian factory. The production of the utility-scale inverters in Ontario, Canada, is necessary to comply with Ontario's FiT program.

Yingli Solar and partners to deliver solar power to Brazil's Estadio do Maracanã

Yingli Green Energy will team up with Light ESCO, EDF Energy and Rio de Janeiro State to Brazil's best known football stadium, the Estadio do Maracanã. Project developer Light ESCO, which is also the majority owner of the project, will work with EDF to install and construct the system. The power produced will then be supplied to the State of Rio de Janeiro.

The stadium, which has a capacity of 82,238 spectators, will have more than 1,500 YGE 245 series modules fitted to its iconic circular roof. The Estadio do Maracanã is owned by the government and will be an important football venue when Brazil hosts the 2014 FIFA World Cup, eventually hosting the final.

ESA Renewables develops 24MW solar park in Jamaica

ESA Renewables, US project developer, has been chosen by Jamaica-based Caribbean Energies Group (CEG) to construct a 24MW PV plant in Jamaica. ESA is responsible for the design and the maintenance of the plant as well as the legal permits and other requirements.

Furthermore, ESA Renewables will conduct the assessment of the system and administrate the necessary studies. Construction of the plant is expected to commence in 2012 but a completion date has not yet been established. CEG, who will finance the project, has not disclosed the costs.

Enbridge, First Solar complete 50MW Silver State North project in Nevada

Ken Salazar, US Secretary of the Interior, was on hand today with representatives from Enbridge and First Solar to celebrate the completion of the 50MW Silver State North Solar Project in Clark County, Nevada. This is the first utility-scale solar facility to be built on public lands.


Source: Northern Gas Pipelines

Ken Salazar, US Secretary of the Interior, flipped the switch for Enbridge and First Solar's 50MW Silver State North Solar Project.

Enbridge bought Silver State North in March from First Solar, which developed and constructed the project using over 800,000 of its thin-film PV modules. First Solar will operate and maintain the project and advised that it expects to recognize revenue from the project in Q2 2012. NV


Source: AE

The Estadio do Maracanã was opened in 1950 and at the time had the world record for the spectator capacity, over 199,000.

Energy will buy the facility's output under a 25-year PPA.

US and Japan launch three new clean energy initiatives as part of energy partnership

US President Barack Obama has said that the US plans to strengthen its cooperation on energy issues with Japan. Obama made the comments at the White House recently after talks with Japanese Prime Minister Yoshihiko Noda.

Source: The White House

Prime Minister Noda and US President Obama pictured during a bilateral meeting on April 30, 2012.

The alliance, named the Clean Energy Policy Dialogue, will see the countries partner on the research and development of renewable energy sources through the launch of three new clean energy initiatives. As part of the program, green communities will be built in Japan's Tohaku region and community-scale microgrid systems and green energy technologies will also be developed.

The countries will continue their discussion on clean energy issues at the 4th Clean Energy Policy Dialogue in Fukushima later this year.

Africa & the Middle East

Report: Angola to invest in 130 solar projects

According to a report by Bloomberg, Angola has revealed its plans to invest in around 130 solar projects. The solar installations will help power schools

Source: Wikimedia Commons

The African country of Angola to invest in 130 solar projects.

and health centres as reported by Agencia Angola Press. Energy Minister Joao Baptista Borges noted that solar power equipment suppliers may benefit from tax incentives. No further information about a timeline of investment or construciton was revealed.

Gestamp Renewable Industries confirms its South African presence

Gestamp Renewable Industries, a division of Gonvarri Steel Industries, has established its presence in the South African Renewable Energy components market by signing new joint venture agreements between its Gestamp Wind Steel and Gestamp Solar Steel divisions and South African industrial partners.

Gestamp Solar Steel, which specializes in the integration of solar solutions by developing metal structures for the solar industry, will set up a new manufacturing facility in Johannesburg by the end of 2012. The company aims to manufacture up to 350MW of PV and CSP per annum.

Saudi Arabia targets 41GW of solar installations by 2032

Representatives from the King Abdullah City for Atomic and Renewable Energy (KA-CARE), the government body directing alternative energy development, have announced the country's ambitious long-term goals for solar power. The oil-rich kingdom aims to have installed 41GW of concentrated solar power (CSP) and solar PV projects by 2032, 25GW and 16GW respectively.

Plans to construct geothermal, biomass, wind and nuclear plants were also announced on at the Saudi Solar Energy Forum in Riyadh on May 8, 2012. The proposed framework would cost tens of billions of dollars and see Saudi Arabia producing almost 25% of its electricity from solar power installations. Solar PV projects will supply the country's daytime electricity demand, while high-capacity CSP plants will provide the majority of solar power, while including thermal storage facilities.

If the plans come to fruition, Saudi Arabia will become one of the world's largest solar power producers. The plans are currently under assessment from the KA-CARE board, though approval is expected to be granted for the scheme in the coming weeks.

Masdar announces plans for solar projects in Tonga and Afghanistan

Renewable energy company Masdar has announced the development of solar projects in Afghanistan and Tonga. The development is part of the United Nations' Sustainable Energy for All initiative.

Source: USAID

Masdar will develop PV projects as part of a UN initiative.

The company plans to install one system on the Tonga island of Vava'u. In Afghanistan, Masdar will install 600 residential solar systems to supply isolated villages with energy.

Source: Constable Research

Saudi Arabia has high levels of solar irradiance and huge areas of desert but is only just beginning to take advantage of them for solar power.

Product Reviews

ABB

ABB's 630kW central inverter series provides integrator flexibility

Product Outline: The new 630kW PVS800 central inverter from ABB has a claimed high total efficiency with one of the most compact designs on the market. The operating temperature range is extended and a new modular DC input design provides flexibility for integrators.

Problem: A 45% higher power density compared to earlier ABB central inverters makes this one of the most compact inverters on the market by footprint and volume per kW. This reduces installation and container space and lowers transportation costs.

Solution: The new ABB central inverter has a 98.6% maximum efficiency with an improved efficiency at partial loads to provide a Euro efficiency of 98.4%. This, together with a very low auxiliary power consumption of only 600W at nominal power, results in an inverter with a very high total efficiency. The central inverter offers a wider operational temperature range, up to 45°C at nominal power and up to 55°C with power derating. This makes the product suitable for hot temperature conditions. At lower temperatures, the ABB central inverter provides up to 10% power overloading capability, up to a maximum power output of 700kW at 25°C.

Applications: The ABB central inverter series is designed for multi-megawatt PV power plants as well as large and medium sized commercial and industrial PV installations.

Platform: The 630kW ABB central inverter is available with eight 250A inputs, suitable for 16 string junction boxes. Optionally, the inverter is also available with four 400A or 12 160A inputs. With the ABB central inverter's certificates and advanced and flexible grid support functions it is possible to meet all applicable network connection requirements, regardless of where the project is located.

Availability: March 2012 onwards.

AlsoEnergy

AlsoEnergy enhances PowerTrack Energy Management Services software

Product Outline: AlsoEnergy has developed several new reporting and collaboration enhancements to its cloud-based PowerTrack Energy Management Services software. The newest features allow developers and investors in solar energy systems to create performance models and compare operations between sites and models to detect underperforming components and generate better system returns.

Problem: PV power plant owners, operators and investors need to be able to correctly react to underperforming zones and be able to undertake performance modeling based on actual weather conditions. However there is a need for interpreting site operational and financial performance data that can be difficult to accurately and precisely analyze.

Solution: PowerTrack's new features include Individual Utility Billing Integration, which enables users to integrate individual real-time utility rate schedules with different time of day charges, providing more accurate predictive analysis data platform on which developers and financiers can establish invoicing. PPA providers can automatically invoice for production based on actual utility rates. PowerTrack can also create interactive reports including production and consumption comparisons, demand reduction, actual revenue versus predicted revenue and live performance data.

Applications: PV power plant asset management and energy monitoring software solutions.

Platform: Beyond the reporting features, PowerTrack pairs with PowerLobby, a customizable marketing display for end-users that can show data such as sun tracking, number of kWh saved, information about the end-user's sustainability goals or other customer-oriented messaging.

Availability: March 2012 onwards.

Amphenol

Helios H4 PV connector from Amphenol is UL certified to 1000V

Product Outline: Amphenol Industrial Global Operations has had its Helios H4 UL certified to 1000V. This UL rating allows Amphenol's connectors to be used in existing systems as well as in new ones that require more voltage without having to increase cable size. The increase in voltage rating allows higher voltage systems to be created with a lower percentage of voltage drop. It also decreases the use of copper and the dollar per watt through electrical efficiency.

Problem: Renewed focus on BOS costs means that all areas of electrical wiring system for large-scale PV power plants are coming under scrutiny. Obtaining increased voltage rating for interconnect systems while maintaining quality and safety could reduce material costs and overall BOS costs.

Solution: The PV connector features Amphenol's RADSOK technology, offering higher current ratings and lower contact resistance claimed to result in lower power losses. The Helios H4 is compatible with industry standard connectors. Designed for applications that use solar inverters, combiner boxes and installers, the H4 connector helps feed power from a solar panel into an inverter or combiner box and features quick snap lock mating for easy panel mount installation and termination to either box. The connector meets NEC 2008 requirements without the need for extra locking collars or locking sleeves.

Applications: Large-scale PV power plants.

Platform: The RoHS-compliant connector is available in four different gauges including 14 AWG rated at 32A, 12 AWG rated at 40A, 10 AWG rated at 44A and 8 AWG rated at 65A.

Availability: April 2012 onwards from Amphenol's solar distribution network.

eIQ Energy

vBoost 600 converter module from eIQ Energy lowers installation costs

Product Outline: eIQ Energy has launched a high-capacity addition to its vBoost DC Parallel System – the new vBoost 600 DC-to-DC converter module. It employs fewer vBoosts per solar array, enabling system installers and operators to save on both materials and labour on solar installations.

Problem: Studies have shown that up-front costs are lower for a Parallel Solar installation, because cable and combiner box requirements are cut by more than an order of magnitude; this also slashes the amount of on-site interconnection labour. Parallel wiring also removes many design and installation constraints.

Solution: The new vBoost 600 modules boost the output of solar panels to a predictable, constant voltage while providing up to 600W of power capacity – enough to handle two crystalline silicon PV panels or multiple thin-film panels. The new modules use fewer components and provide more efficient power conversion than eIQ Energy's previous 250 and 350W modules. The vBoost converters also provide distributed maximum power point tracking (MPPT), simplifying array design, extends the life of system components and is claimed to increase power harvest by five to 30%. The vBoost DC Parallel System's parallel wiring architecture enables well over 100 thin-film solar panels to be connected on a single cable, 20 times more than traditional series wiring schemes permit, according to the company.

Applications: PV module system installations, including c-Si and thin film modules.

Platform: vBoost DC Parallel System includes vBoost converter modules, vComm communication modules and web-based Monitoring System software.

Availability: March 2012 onwards.

Eltek

Eltek's MultiSite Monitor capable of tracking 3,000 DC solar power systems

Product Outline: Eltek has released MultiSite Monitor, an IP-based monitoring service for its DC power systems. Enabling carriers to monitor remote power systems around the world for both green power performance and for system health.

Problem: Cost savings and environmental responsibility have been the driving reasons for looking to high-efficiency (HE) technology to power telecommunications networks. But new services like cloud, VoIP, IPTV and others are becoming an important component of network operator sales and profitability. As new networks are built and new computing services deployed to provision these services, energy efficiency is quickly becoming a tool for growth in addition to operating expense (OPEX) savings.

Solution: The MultiSite Monitor software can watch up to 3,000 sites worldwide that use a wide range of Eltek DC power system controllers including its flagship Flatpack2 HE power system. The software gives managers a map overview of the status of all of the connected systems showing alarms, warnings and online/offline status. The system also allows carriers to set and monitor key performance indicators related to power sources such as use of solar or diesel generators. The energy logs, key parameters and status are sent to the MultiSite Monitor server.

Applications: Power telecommunications networks employing renewable energy.

Platform: The TCP/IP-based monitoring traffic is firewall friendly. The server uses TCP/IP-JSON to communicate with the controllers and collect data. If sites are to be connected through the open internet, IPsec encryption is recommended.

Availability: For deployment from Q2, 2012 onwards.

Evonik Cyro

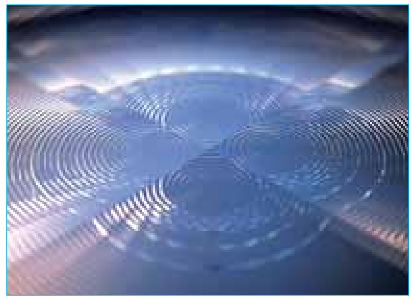

Evonik Cyro offers pre-fab lens panels for CPV modules

Product Outline: Evonik Cyro has launched ACRYLITE Solar Pre-Fab acrylic lens panels, which are combined with a Secondary Optical Element (SOE) to create a complete optical train package for assembly directly onto CPV modules. This allows customers to bypass purchasing the tooling device needed to create the product and avoid the required time-consuming installation process.

Problem: The need to reduce BOS costs of CPV also applies to assembly of the system. Often, optical train designs are unique and require specialized tooling and assembly. Providing a modular pre-assembled system could reduce manufacturing costs.

Solution: The optical lens package utilizes Light Prescriptions Innovators patented Fresnel-Köhler optical design. The ACRYLITE Solar Pre-Fab lens panels serve as the Primary Optical Element, which collects light over its entire area. This POE is coupled with a Secondary Optical Element, either Evonik's SAVOSIL, or LPI's glass SOE, which focuses light over a smaller area homogenizing the light in order to maximize its usefulness to a solar cell. The system is claimed to provide excellent light transmission, high-mechanical strength and outstanding resistance to weathering and UV light.

Applications: ACRYLITE Solar Pre-Fab is offered in three sets of quantities – 10 panels, 50 panels and 300 panels.

Platform: These new lens panels are part of the ACRYLITE Solar product portfolio, which consists of specialty acrylic molding compounds and sheet products for solar applications.

Availability: April 2012 onwards.

Product Reviews

Satcon Technology

Satcon Equinox LC inverters for the light commercial solar market

Product Outline: Satcon Technology has expanded its product portfolio to include certified inverter solutions for the light commercial solar market segment with the launch of Equinox LC with a maximum efficiency of 98.2%. The new product line will include four UL certified power ratings of 12kW, 16kW, 20kW and 24kW, alongside five CE certified power ratings of 8kW, 10kW, 13kW, 17kW and 20kW.

Problem: The light commercial inverter market segment is claimed to be rapidly expanding, supporting the growing need for improved levelized cost of energy (LCOE). The market therefore requires a broader range of inverter power ratings that meet the growing market demand for high efficiency, low cost, lightweight, highly reliable solutions.

Solution: Satcon's Equinox LC is said to be highly reliable, transformerless and three-phase, with a maximum efficiency of 98.2% combined with an innovative and effective MPPT that allows for high energy yield of PV power systems from 12kW to 500kW or larger. Equinox LC solutions are designed to be compact, lightweight and quickly installed on a simple mounting plate with an integrated data logger. The rugged design allows for both indoor and outdoor applications.

Applications: Inverter solutions for the light commercial solar market.

Platform: The Equinox LC series includes four UL certified power and five CE certified power ratings. These lightweight, high efficiency inverters come in NEMA4/IP65 enclosures

Availability: March 2012 onwards.

Schüco

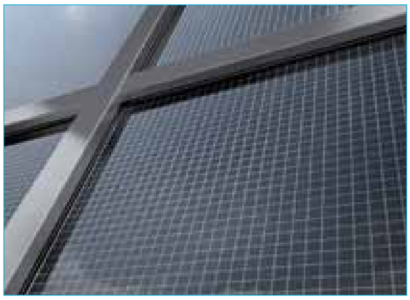

Schüco offers ProSol TF+ tandem junction thin-film module for architectural design

Product Outline: Schüco has launched an up-rated version of its ProSol TF module, claiming a 30% increase in electrical output over its standard offering. The new thin-film module, ProSol TF+, is a tandem junction module capable of being customized for a range of BIPV applications.

Problem: BIPV applications demand flexibility in the PV module having both an aesthetic and functional role.

Solution: The ProSol TF+ is a tandem junction silicon thin film cell design. As a result the surface is of deep anthracite colour, meeting many aesthetic requirements in BIPV applications. However, in addition to a standard rectangle form factor, the modules can, for the first time, be specified in a variety of alternative shapes including triangles, parallelograms and rhomboids. While the modules are supplied opaque for maximum power output, they can be customized by laser-cutting to present varying degrees of transparency ranging from 5% to 25%.

Applications: Available either as single glass panes for use in Schüco rain screen façade systems or as part of double- or triple-glazed units incorporated into Schüco insulated façade systems.

Platform: The ProSol TF+ is typically 80Wp/m^2, employing a tandem cell structure that incorporates dual layers of microcrystalline and amorphous silicon, together with a special laminate foil. ProSol TF+ can also act as both insulation and as solar shading, resulting in a significant reduction in the need for heating and air-conditioning. Sizes range from 200mm × 300mm up to 2300mm × 2600mm with even larger sizes being possible using a patchwork technique.

Availability: April 2012 onwards.

Shanghai TAOKE

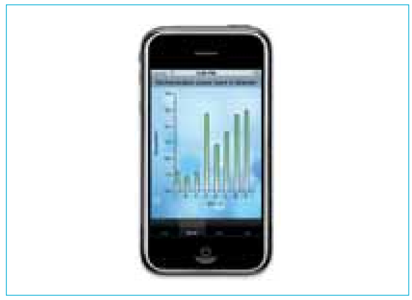

TAOKE 'IOT' designed to improve operating efficiency of PV power plants

Product Outline: Shanghai TAOKE Network Technology has developed the GPRS photovoltaic data acquisition, TK-G10-01/08/16/08S/16S and ethernet PV data acquisition, the TK-E20-01/08/16/08S/16S/32D systems for a wide range of PV power plant applications, designed to protect and improve the operating efficiency of the PV system.

Problem: Correct PV power plant maintenance is required to provide optimum yield of the system and to provide the best ROI. However, many internet-based monitoring equipment is either single function or too expensive.

Solution: TAOKE develops and produces third-party remote monitoring systems for PV power plants, using a self-developed mini-PV data acquisition box. The built-in embedded operating system provides monitoring features of the overall network architecture, data acquisition delay control in less than two seconds and is capable of operating in cloud computing centre network platform. The PV power plant data acquisition intervals as low as one minute, while the 485 bus acquisition equipment reduces installation and cabling costs. GPRS PV data logger runs logic control and is said to significantly reduce GPRS traffic costs.

Applications: The system is applicable to a variety of different forms of PV plants, from small residential to roof-top power plant and large-scale PV power plants power station type.

Platform: TAOKE has two kinds of products, the GPRS photovoltaic data acquisition (TK-G10-01/08/16/08S/16S) and ethernet PV data acquisition the (TK-E20-01/08/16/08S/16S/32D), suitable for the demand of different users. The system is compatible with more than 36 global inverter brands and certified by TUV and FCC.

Availability: April 2012 onwards.



Fab & Facilities

Materials

Cell Processing

Thin Film

PV Modules

Power Generation

Market Watch

The myth of PV module manufacturers' bankability in project financing

Felix Holz, Vice President / Head of Industry Expert Team Greentech, Deutsche Bank AG, Berlin, Germany

ABSTRACT

A typical financial structure for a utility-scale (i.e. larger than a few MW) PV project is the so-called 'non-recourse project financing.' Experience shows that lenders may occasionally refuse financing because they dislike a technology or even a certain supplier. This past behaviour has created the 'myth of bankability' and the perceived necessity of manufacturers to get onto the banks' 'bankability lists.' But there is no strictly defined process for doing this, and many of the experienced banks do not even work with such lists for good reason. Moreover, 'bankability' is not a feature that a manufacturer or a product can achieve or maintain forever.

Figure 1. View of a 10MW utility-scale PV installation in Osa de la Vega, Spain.

Introduction

There are two basic financing structures in the market: 'corporate financing' and 'project financing,' the latter often being referred to as 'non-recourse (project) financing.' Both structures, and even combinations of the two, can be found in the PV installation financing market.

Corporate financing

If a company wants to install a PV plant on its roof or land, the easiest way is to ask its corporate banks for a loan. The company typically has different divisions and a diversified business model. A consolidated balance sheet with a historical track record exists and is well known to the banks. Assets and cash flows of the company have been analyzed many times: the banks have a clear understanding of its securities and liabilities. Therefore, having a good idea of sustainability of the company's business model derived from historical financials, a bank can, as part of its daily business, calculate the remaining debt capacity of the company. If there is enough margin, financing is straightforward and the banks do not need to concern themselves with details about the PV installation. The bank's internal processes are smooth and therefore its fees are limited – bankability is not an issue.

> "Bankability in the case of non-recourse project financing is always related to a certain project and its structure and not to a supplier."

Project financing

For a non-recourse project finance structure, a new company – or special purpose vehicle (SPV) – is founded and acts as the borrower. The business model is limited to construction, ownership and operation of the PV plant, and no historical data are available. The SPV is equipped with a certain amount of equity provided by the investor. 'Non-recourse' means that there is no obligation of the investor to increase the equity portion if unforeseen situations occur. The debt provider's decision has to be based on the estimation of the expected cash flow that the PV power plant will generate. Only future cash flows and assets of the SPV are accessible. No further securities other than for the project itself will be provided to the lender. Such a project structure is typical of larger PV installations that present to the banks in order to ask for loans. The necessary due diligence implies a high workload for all stakeholders, with additional cost for the project. Bankability in the case of non-recourse project financing is therefore always related to a certain project and its structure and not to a supplier.

The process

When assessing a request for project finance, the lender has to evaluate how safe the expected cash flow really is. Three major areas have to be evaluated independently:

- The basis of the cash-flow assessment is the yield prediction for the project. This should be prepared or reviewed by an independent, experienced institution. In the next step, a site-related legal due diligence has to demonstrate that all necessary prerequisites (land-lease contracts, permissions, grid access, etc.) are fulfilled.
- In order to translate the yield into a safe cash flow in a further step, the framework (legal, economic, etc.) has to be examined. In a country with a feed-in tariff, the resulting basis is the country risk accompanied by a currency risk if the tariff is paid in the local currency and the debt service requires a different currency.
- Last, but not least, an assessment of technology, suppliers and stakeholders is necessary to complete the picture.

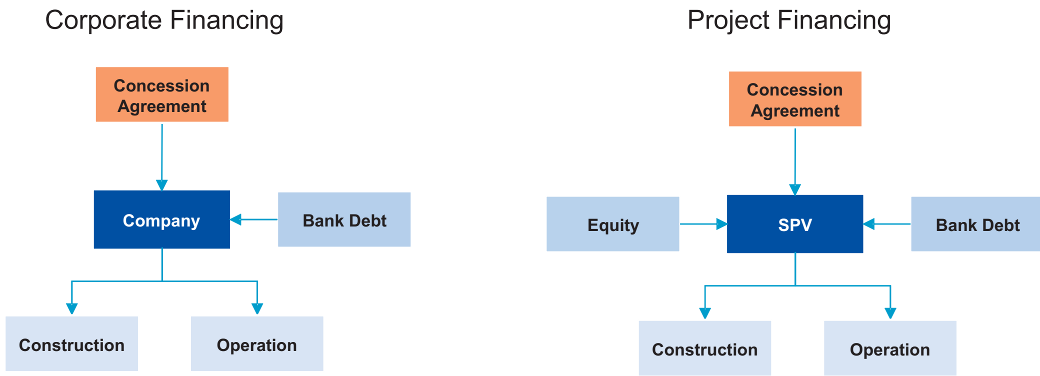

Corporate Financing

- Borrower: company with mostly different divisions and diversification within a broader business model
- Accounting: consolidate balance sheet of the corporate / group
- Security and liability: assets and cash flows of the whole group
- Debt capacity: sustainability of the business model of the company and historical financials

Project Financing

- Borrower: SPV with limited business model
- Accounting: balance sheet of the SPV; possibility of 'off balance' solutions
- Security and liability: future cash flows and assets of the SPV
- Debt capacity: future cash flows

Figure 2. Differences between corporate and project financing structures.

Among yield predictions, country and region, permitting status, grid access, legal framework and so on, only very few are directly related to technology. However, in order to avoid unnecessary workload, it makes sense to look for 'no-goes' first, because just one of these will lead to project rejection. But technology-related show stoppers are the easiest and fastest to identify; lots of past rejections have therefore been argued for technology-related reasons, which may have helped to create the 'myth of bankability'. Nevertheless, most of the rejected projects that had disregarded some key requirements concerning technology showed deficiencies in other areas too.

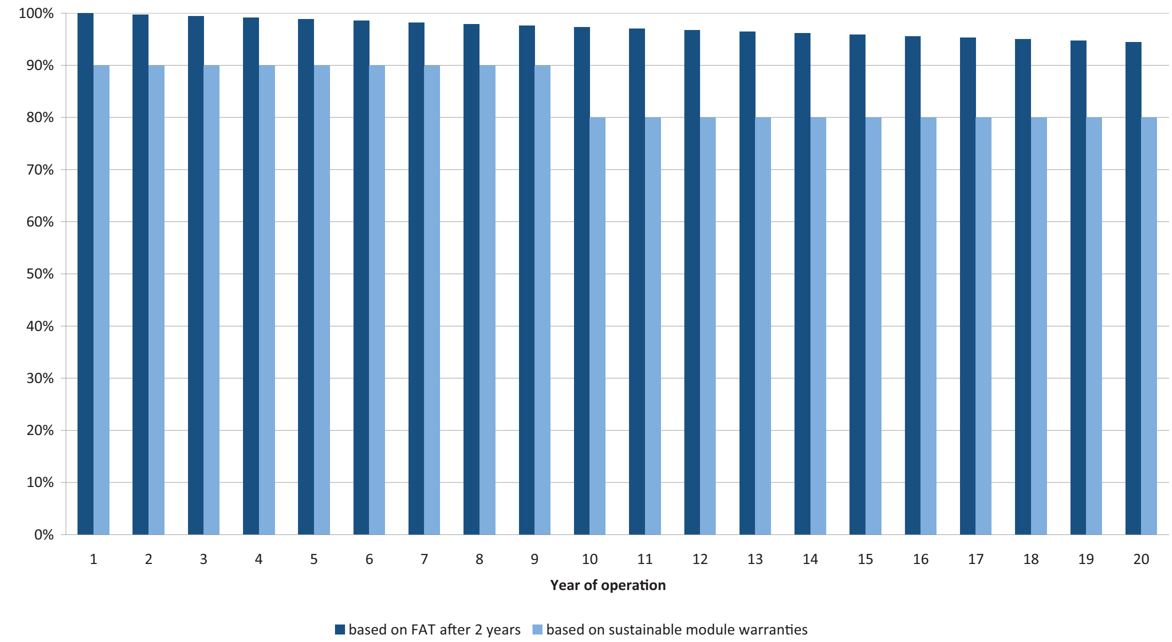

Figure 3. Safe project revenues according to yield prediction.

Technology-related requirements

A principle of project finance is that debt should not bear the risk of the technology. Two key aspects are therefore: 1) project debt providers are not keen on any kind of prototype-like technology; and 2) the warranties of the suppliers must be sustainable and therefore supported by financial strength.

> "A principle of project finance is that debt should not bear the risk of the technology."

In order to minimize the first technology-related risk, modules have to be certified in accordance with international standards. Unfortunately, it is common knowledge that a successful certification is not enough for predicting the expected lifetime of a module: a failure in a certification process only suggests that a long life is unlikely. Certification is therefore a necessity but not sufficient. There are several approaches that attempt to stress test modules using more stringent procedures than the requirements of the official international standards. But, for as long as even these tests are unable to predict the module lifetime in the field and such lifetime is not guaranteed by the testing laboratory, these types of approach cannot be considered sufficient.

A selection of approaches for tackling the technical challenge of lifetime estimation from a lender's perspective will now be discussed.

Field data from real installations provide a much better indication of actual performance than laboratory data. For PV projects, at least two years' field experience is expected before a new supplier or technology is accepted. This has to be supported by data assessment performed by a trusted third party, typically an experienced expert institute.

It can happen that even experienced first-choice best-quality suppliers supply underperforming equipment. This has been demonstrated in many cases in PV as well as in mature industries such as the automotive industry, where, from time to time, recall actions can be found in the news. It is unrealistic to expect the PV industry to be free of faults. There will always be the "What if?" questions to be answered, especially: "What if the modules in the project show defects which harm the cash flow?" All PV modules come with warranties covering 20+ years, but these are provided by companies with track records of only a few years and who currently face a challenging environment of oversupply and consolidation. Considering these warranties to be sustainable is difficult at best.

On the other hand, field experience shows that the lifetime of a fault-free manufactured PV module should exceed 20 years. A pragmatic approach to the challenge described, at least for large projects, is to try to detect production faults in time. Fortunately, most critical production faults already show up during the first two years of operation. If a final acceptance test (FAT) is carried out in the field after that time – which includes visual inspections as well as technical tests such as infrared photography, and is not restricted to simple performance measurements – most of the potentially faulty modules can be identified. These should be exchanged and this can be part of the supply contract if considered necessary. The advantage of this approach is evident. After two years, the project yield consists of essentially fault-free manufactured modules, and so any module-related downside risk to cash-flow projections should be minimized. The sustainability of the supplier's warranty must therefore be credible and trustworthy for a period of two years. An analysis of the financial strength of a supplier for the near future can be done by standard banking procedures in combination with existing sector intelligence.

The resulting advice will be to use modules from suppliers with a strong balance sheet and a sustainable business model and who are able and willing to fulfil the warranties for the next two years at least. The acceptance of exchange requests after the FAT should be addressed during supply contract negotiations.

A further possibility would be to use an engineering, procurement, production (EPC) provider with a strong balance sheet who is able and willing to support the warranties and also accepts the described procedures. In this case the selection of the module can be left to the EPC contractor. Bankability of the module manufacturer would not be an issue at all in this case. Unfortunately the number of EPC contractors with strong balance sheets in the PV project area is even smaller than the number of module suppliers with strong balance sheets. Typical EPC contractors are obliged to rely on sustainable back-to-back contracts for the module warranties.

And for those who are strong enough, the added value of taking the risk is often not sufficiently high.

For projects suggesting components that do not completely meet these requirements, a lower leverage (e.g. more equity, less debt) can sometimes be a possible solution. Even a combination of a small portion of some of these non-compliant components into well-established modules from well-known suppliers may solve the problem, if this is acceptable to the equity investor, since the risk is then borne by the equity.

An entirely different approach is to use an insurance wrap for the product warranty offered (20+ years): this separates the warranty risk from the debt. The task of the insurance company is to assess technical risk, assign a price tag to it and then take the risk. Having such insurance in place solves both debt requirements. The technology risk has been assessed by an institution with the competence to do so and the financial ability to take it. In that way, the risk related to the financial strength of the supplier is transferred to the balance sheet of the insurance company as well. The debt provider will assess the financials of the insurance company instead, and in principle an assessment of the technology is made redundant. But here the devil is in the details. Not every bank will accept every insurance plan on the market. The risk increases and is not widely accepted, especially if the tenor is shorter than the tenor of the debt, or a termination is possible before the debt is completely repaid. On the contrary, the project evaluation on the debt side will now raise the question as to why a competent technical risk evaluation has led to the need for limiting the risk exposure. The logical answer would clearly be to assume a hidden risk which should not be borne by the debt. The same argument has to be addressed if an upper financial limit comes with the insurance.

Conclusion

As highlighted here, the bankability of a project depends on lots of factors, and technology is only a very small part of the equation. There are several different possible ways to approach the lender's needs, and bankability, therefore, is never associated with a product or a supplier. Furthermore, the validity of a bankability list would be limited, since the financial strength of the different suppliers may change rapidly, particularly in the current environment of consolidation.

> "If providing an insurance solution is a consideration, it should be ensured that this is supported by the major banks."

Nevertheless, if module manufacturers aim to supply to the utility-scale PV project market, they should consider adhering to some recommended guidelines:

- Because the track record in the field is crucial, this aspect should be taken into account when presenting technical developments. In particular, changes regarding (for example) efficiency that do not affect degradation and/or lifetime should be presented as improvements. This allows the lender to base its decision on the history for the already-known generation and does not force a new assessment.

- No attempt should be made to hide technical difficulties. It is accepted that mistakes happen – the question is how suppliers react and solve problems. If in doubt, it is advisable to take care of replacements and argue about cost later, but to help keep the cash flow of the project running. Otherwise, the project runs the risk of breaking contracts. Having such a project under surveillance may suddenly create an immediate 'no go', and a bank will remember this incident for years. Moreover, large projects are typically served by a number of banks, which means that all concerned parties speak to each other, and talk of misbehaviour begins to quickly snowball.

- The balance sheet should be kept intact. The quality of a project depends on the perceived sustainability of the warranties. The current market is heavily oversupplied with modules, so there is no reason to invest time and money in project setups if the ability or willingness to support warranties is doubtful.

- If providing an insurance solution is a consideration, it should be ensured that this is supported by the major banks. The insurer should be asked which banks they have talked to and who their reference contact is, and time should be taken to call them. During the bank's process of making the decision as to whether or not to finance a particular project, there is no time to study insurance solutions in detail: there are just too many projects to consider. If the insurance is critical to the decision process and has not previously been accepted by the banks, it will probably not be approved under a tight timescale.

About the Author

Felix Holz is currently vice president of Deutsche Bank, where he is the head of the industry expert team Greentech. Prior to this he held various positions at Conergy AG, and was the head of off-grid systems at Fraunhofer ISE. Felix has a degree in physics from the University of Kiel, Germany.

Enquiries

Felix Holz
Vice President / Head of Industry Expert Team Greentech
Deutsche Bank AG
German Midcaps
Unter den Linden 13–15
10117 Berlin
Germany

Tel: +49(30)3407-4079
Fax: +49(30)3407-4077
Email: felix.holz@db.com

Reduced solar capital costs in India

Mohit Anand, Senior Consultant, BRIDGE TO INDIA, New Delhi, India

ABSTRACT

India is a unique market. As part of an India-specific strategy on the part of the players, solar capital costs in India have significantly fallen in relation to the global average. This paper describes the trend for lower cost modules and services to be offered by module suppliers and EPC companies in order to capture the greatest share of the Indian market. In this context, more importance is being given to gaining a greater market share than earning a higher return.

Introduction

The National Solar Mission (NSM) in India has set installation targets of 20GW of grid-connected and 2GW of off-grid solar power by 2022. In the first of its three phases, from 2010 to 2013, the government is incentivizing the construction of 1000MW of grid-connected power plants, encouraging the more developed PV technology as well as concentrated solar power (CSP) equally with 500MW each [1]. Projects are allocated by a process of reverse bidding under which bidders are selected on the basis of the maximum discount they can offer on the proposed feed-in tariff (FiT). Many Indian states that have allotted solar projects have also adopted a similar reverse bidding procedure.

> "The average system cost in India is now 14% lower than the global average."

A fall in the cost of solar power to the end consumer is indicated by the latest round of reverse bidding under India's NSM Phase I Batch II in December 2011 [2] and in the Indian state of Odisha in February 2012. Tariffs offered for the allotted projects have fallen to as low as INR7 per kWh. This is being attributed to low solar capital investment cost in the Indian solar market. The cost of installing a PV plant of 1MWp was INR120m (€1.76m) in January 2011. Costs fell to about INR90m in January 2012, and there were further falls by about 10% to INR81.5m (€1.2m) in early March 2012. The average system cost in India is now 14% lower than the global average. A precise calculation of solar costs depends on the location and the cost of finance available to the owner of the solar installation, but, on average, global system costs are INR95m per MW.

Gaining strategic market share

This difference between the average Indian system cost and the global average can primarily be attributed to the difference in cost of modules, which typically account for the largest share (about 65%) of solar capital investment. In India, the cost of modules is 10% lower than in global

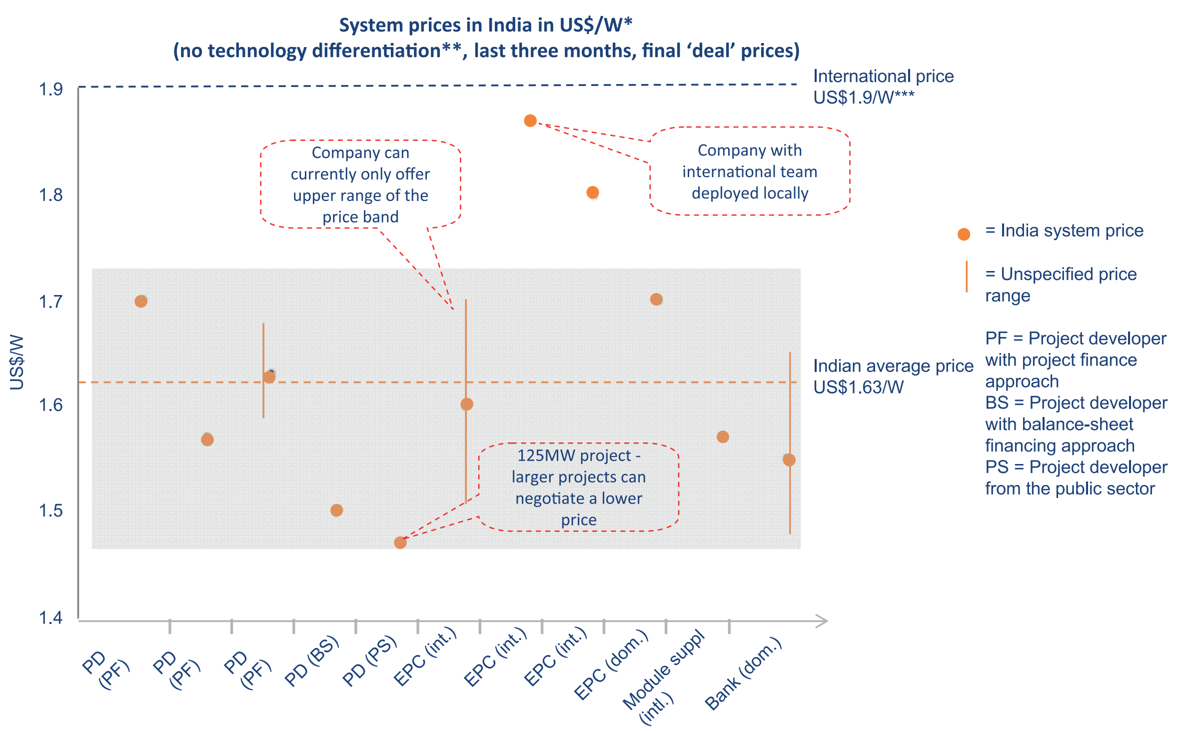

* All data was gathered in US$/W to avoid effect of fluctuating exchange rates.
** None of the respondents thought a differentiation between thin film and crystalline relevant (if anything, it was pointed out that after recent cost reductions, crystalline is more attractive in India – benefit of thin film (e.g. price/temperature coefficient) is marginal. Project developers were unconcerned with technology.
*** As given by one of the respondents ('current spot price').

Credit: BRIDGE TO INDIA market interviews, 16th to 19th February 2012.

Figure 1. System prices in India.

markets: INR41.5m per MW as opposed to a global average of INR47m per MW.

Module manufacturers see India as a key strategic market for the next few decades. Players want to gain strategic market entry and offer modules at lower prices to gain market share in India. At the current lowest Indian feed-in tariff (FiT) of INR7 per kWh, it is unlikely that these manufacturers are making sufficiently high margins on the sale of modules to the Indian market. Moreover, Indian buyers are aware of the strategic relevance of their market and are therefore using this knowledge to pressurize suppliers to provide them with modules at the lowest cost.

Providing cheap modules can also be seen as a factor of portfolio risk management on the part of the suppliers. Manufacturers designate supply quotas for every country and then allow local sales teams to play with the price in order to drive modules to acquire greater market share. Hence, suppliers prefer to sell a certain number of modules in a new market like India, in order to reduce their dependence on traditional markets.

Certain suppliers treat the Indian market as the last resort: they see it as the last market to sell to in an attempt to unload or dump surplus production capacity. Module suppliers think in terms of a 'merit order' – they first sell to attractive markets with high margins and then work their way down to markets with low margins, such as the Indian market. Manufacturers believe that it is better to sell excess capacity below manufacturing cost than to maintain inventory.

In addition, Indian module sales take place through direct negotiations between project developers and manufacturers. Given the early stage of the solar market in India, new and inexperienced project developers are entering the growing market. In such a scenario, price has become the paramount criterion for these first-time project developers to make their choice, thus increasing the competitive pressure among module suppliers.

> "In the Indian market, project developers procure modules directly from suppliers rather than through EPC companies."

Globally, so far, Engineering, Procurement and Construction (EPC) companies have procured modules and provided a composite solution for developers. From a technical point of view, choosing the appropriate modules for their system design has allowed EPC players to give a comprehensive performance guarantee for their plants. From a commercial point of view, EPC players have charged a margin on the modules to the developer, which has helped cover the cost of the performance guarantees. However, in the Indian market, project developers procure modules directly from suppliers rather than through EPC companies. This has allowed the developers to avoid paying the margin that would have been involved if they were to rely on the EPC companies for the procurement. This has contributed to lower project costs for the developers.

Unawareness of realistic execution challenges

According to EPC players in the industry, tier II and first-time system integrators are setting unrealistic price benchmarks. Some EPC companies are quoting extremely low prices and offering impractical guarantees, without understanding the actual execution challenges. Further, there are project developers in the industry who are vertically integrated and offer EPC services. Such developers are able to drastically bring down capital costs for their projects, which forces pure EPC companies to push down service costs.

Conclusion: the strategy for gaining more projects in India

Project developers are keen to get a foot into the first phase of the NSM. They see this as a crucial opportunity to strategically position

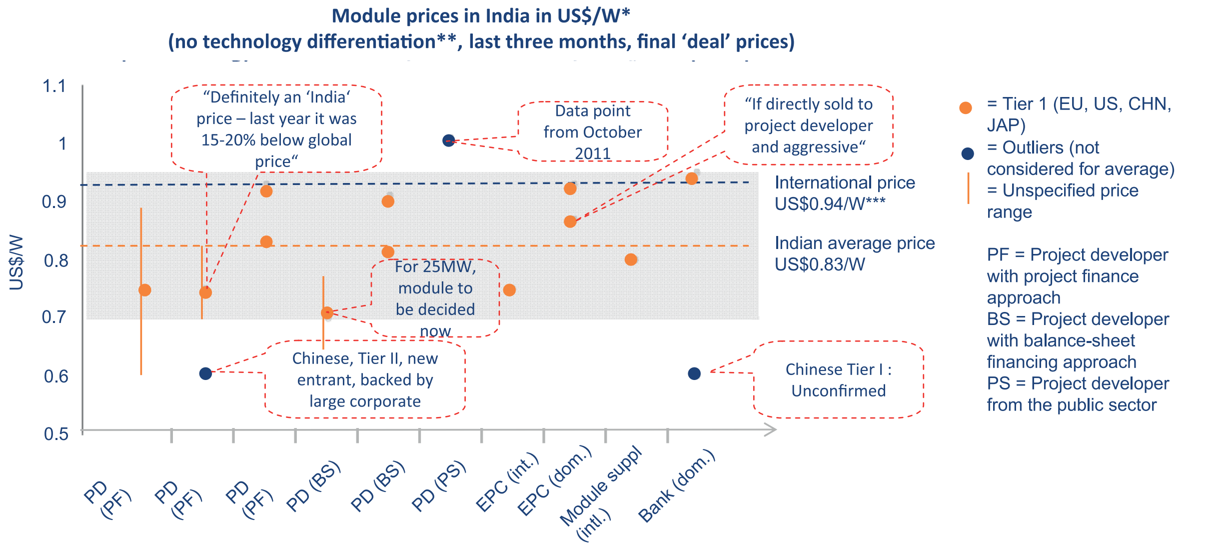

* All data was gathered in US$/W to avoid effect of fluctuating exchange rates.
** None of the respondents thought a differentiation between thin film and crystalline relevant (if anything, it was pointed out that after recent cost reductions, crystalline is more attractive in India – benefit of thin film (e.g. price/temperature coefficient) is marginal. Project developers were unconcerned with technology.
*** As given by one of the respondents ('current spot price').

Credit: BRIDGE TO INDIA market interviews, 16th to 19th February 2012.

Figure 2. Module prices in India.

themselves as leading solar players. At this stage, they see having a place in the NSM as being more important than achieving high returns. Many are also looking to build a portfolio of projects with the option of selling these projects as the market develops further. The reverse bidding procedure of project allotment in India increases the competitive pressure between investors in the Indian market. Investors are compelled to accept a lower internal rate of return (IRR) in order to acquire a greater number of projects. Low system costs, along with competitive pressures in the market, have led to the fall in the overall consumer price of solar power in India.

References

[1] MNRE National Solar Mission 2010. "Guidelines for new grid-connected solar power projects", July.
[2] BRIDGE TO INDIA 2012, "The India solar compass", January, pp. 5–6.

About the Author

Mohit Anand is responsible for the Market Intelligence team at BRIDGE TO INDIA and has significant expertise in analyzing the Indian solar market. With a team of solar experts he leads the development of products like the INDIA SOLAR NAVIGATOR. He also develops solar business opportunities and executes consulting projects on market-entry strategies for international solar companies. Mohit writes regularly for several leading publications about solar power in India.

Enquiries

Mohit Anand
Email: mohit.anand@bridgetoindia.com
Website: www.bridgetoindia.com

INDIAN SOLAR
INVESTMENT & TECHNOLOGY
SUMMIT & EXHIBITION 2013

INDIAN SOLAR 2013 INVESTMENT & TECHNOLOGY

MAKING INDIA'S NATIONAL SOLAR MISSION A REALITY

SUMMIT & EXHIBITION
18 – 21 APRIL 2013, GANDHINAGAR, GUJARAT



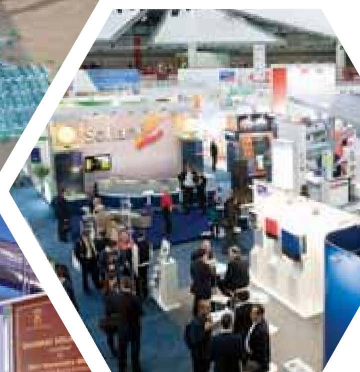

THE 2012 INDIAN SOLAR SUMMIT, WITH THE INSTITUTIONAL SUPPORT OF THE GOVERNMENT OF GUJARAT AND THE GUJARAT POWER CORPORATION, ATTRACTED:

- 50 conference delegates
- 50 exhibitors
- 1,800 exhibition visitors
- More than 10,000 attendees to the official launch of the 200MW Charanka Solar Park
- More than 45 speakers, including senior representatives from other State governments

DON'T MISS YOUR OPPORTUNITY TO SECURE A PLACE IN 2013 AT THE FIRST EXHIBITION AND CONFERENCE SET IN THE GATEWAY TO SOLAR INDIA, GUJARAT.

IMAGES FROM INDIAN SOLAR 2012



WWW.SOLARSUMMITINDIA.COM

Contact us now for further information on how you can attend the event:
Call +44 20 7871 0123 or email: info@solarsummitindia.com

ORGANISED BY — SOLAR MEDIA
CO-HOSTED BY
MEDIA PARTNERS — PV TECH, PV TECH PRO, DESIGN-BUILD SOLAR, SOLAR POWER PORTAL, semi, PV Group, PANCHABUTA

Market Watch

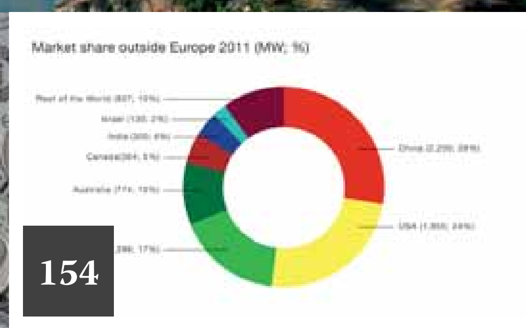

News

President-elect François Hollande pledges commitment to renewables industry

Decanter

Hollande has promised a 25% reduction in nuclear facilities by 2020, an investment in alternative energy generation and improving energy efficiency.

Socialist François Hollande has been elected as President of France, bringing further concerns and hopes to the country's already flagging solar industry. Dubbed "Mr Normal", he has promised a 25% reduction in nuclear facilities by 2020, an investment in alternative energy generation and improving energy efficiency.

In a speech earlier this year, the President-elect said nuclear power would remain an important component of France's energy consumption, but all facilities were sorely in need of inspection. Bloomberg has reported that Hollande asserted his government would decommission EDF's oldest reactor in a bid to boost alternative energy generation.

EDF CEO, Henri Proglio, has also been cited as one of the most prominent victims of the President's salary cap initiative on French high-earning executives. EDF has also suffered a loss with shares dropping by as much as 3.2%. Shares have lost about 43% over the past year, reports Bloomberg.

Hollande's victory "doesn't bode well for regulated activities," said Chicuong Dong, analyst at Richelieu Finance in Paris. "There are worries that measures to boost growth will involve spending for EDF." With this attack on energy regulators, it remains to be seen the effect it will have on solar manufacturers.

Financial and Business News Focus

Report: Solar Trust of America receives over US$43 million in capital loans, letters of credit

Solar Trust of America has bought some more time in its bankruptcy proceedings as Bloomberg reports that the company was approved for new loans while it continually pursues the sale of its assets. The company will receive financing arranged by Mason Capital Management, which includes US$25 million in working capital loans and US$18.3 million in letters of credit.

The funding takes the place of the US$3.9 million interim financing, which the bankruptcy court originally approved April 3, one day after the company filed for Chapter 11 insolvency. At the time, NextEra Energy Resources was set to provide the interim funding. Solar Trust the developer of solar thermal power plants in various US States, including the 1,000MW Blythe project in Riverside County, California.

Canadian Solar and Bank of China agree CAD$120 million solar construction financing agreement

A CAD$120 million ground-breaking financing agreement between Canadian Solar and Bank of China has been signed. The loan facility will be used to support the construction of solar power projects owned by Canadian Solar and which are expected to be built during 2012, 2013, and into 2014.

Source: The Globe and Mail

A CAD$120 million ground-breaking financing agreement between Canadian Solar and Bank of China has been signed.

Timminco sale produces business split

Although subject to court approval, a successful action sale of bankrupt firm Timminco has taken place. QSI Partners has acquired silicon metal business and assets of Bécancour Silicon, including its 51% ownership interest in Québec Silicon for approximately US$31.87 million. The solar-grade silicon business and assets of Timminco Solar, a division of Bécancour Silicon, were sold to Grupo FerroAtlántica for approximately US$2.7 million.

QSI previously provided US$4,250,000 of debtor-in-possession financing to BSI which was said to be repaid with interest and applied to the cash purchase price. Closure is expected to take several months.

US Bancorp to invest US$150 million in Sunrun residential systems

US Bancorp is continuing with the expansion of its portfolio with its new partnership with Sunrun. The move will support the purchase and installation of more than US$150 million in residential solar systems across the United States. This is Sunrun's sixth renewable energy tax equity commitment from US Bancorp.

Sunrun owns, insures, monitors and maintains the solar panels on a homeowner's roof, while families pay a low rate for clean energy and fixed electric costs for 20 years. Sunrun claims its customers pay a lower rate for solar energy than what they pay for electricity

Source: CalFinder

This is Sunrun's sixth renewable energy tax equity commitment from US Bancorp.

from their utility companies. Sunrun installs over US$1.5 million in solar every day and has more than 20,000 customers in 10 states.

A recent report from Sunrun and PV Solar Report, an authority on solar market data, shows solar power service has grown 174% in California in the first two months of 2012 compared to the first two months of 2011. It has generated over US$100 million in growth for the California economy so far in 2012.

Seminole Financial Services closes five solar project lending deals in Q1 2012

Seminole Financial Services has announced closing loan deals for five solar projects in Q1 of 2012. The projects are ground-mounted and rooftop installations as well as canopies, ranging in size from 600kW to 2.4MW. The loans totalled US$13.8 million for all five projects. Of the five projects, two are located in New Jersey, another two in North Carolina and one in Oregon. The first quarter of 2012 follows a busy 2011, during which Seminole lent a total of US$88 million in construction loans and US$25 million in permanent loans. Since 2009, Seminole has closed over $162 million in construction

Source: Black Platinum

Seminole focuses on construction and permanent loans between US$2 million and US$30 million.

financing and permanent debt financing for solar projects as well as wind projects.

Market Trends & Developments

Jefferies report: Japanese FiT announcement "positive" for industry growth

On April 25, chairperson of the Purchase Price Calculation Committee, Professor Kazhiro Ueda, announced proposals for the new FiT program expected to start in July. Jefferies, global securities and investment banking group, has released a report in support of the government's proposals to develop solar PV on a grander scale. However, the report also highlights that many manufacturers, too much involved with Europe, may lose out on investment opportunities in the emerging market in Asia.

Jefferies' confidence in the Japanese FiT is as a result of the following:

1. Investors do not appreciate that Japanese solar IRRs have the potential to be the largest globally at <20%, which should allow a fast-growing market.

2. On the heels of the new FiT, a new master energy plan is being revised in Japan and it may target up to 100GW of cumulative PV capacity by 2030, from 4.7GW installed at the end of 2011.

3. Japanese installation and panel prices are the highest globally.

Independent report confirms growth of Indian solar industry

As Phase 1 of India's National Solar Mission reaches half way, India stops to take stock of its progress with an independent report conducted by the National Resources Defence Council (NRDC) and the Council on Energy, Environment and Water (CEEQ).

Source: Famous Wonders

As Phase 1 of India's National Solar Mission reaches half way, India stops to take stock of its progress.

The report has been drawn from extensive discussions with stakeholders and research and analysis of national, state and international programs, with the aim of aiding the government in overcoming obstacles to achieving the Mission's goal of 20GW by 2022. The NRDC and CEEQ are calling on the government to encourage financing in order to boost domestic manufacturing and create an environment conducive to renewable energy generation.

Jamaican minister demands a "call to action" over rising energy bills

Citing high energy bills as a result of the colossal cost of importing electricity, the Jamaica Energy Council assembled on April 20 to discuss the implementation of an energy policy. The main points of the meeting involved the haulage, storage and distribution of conventional energy resources, including but not limited to oil and coal/petroleum coke; oil and gas exploration; petroleum refinery. Furthermore, energy access (urban and rural electrification) and affordable prices; implementing a governance framework for the energy sector, including fiscal and non-fiscal incentives to stimulate investments into the sector towards achieving the 2003 – 2030 Energy Policy goals.

Source: Travelanthropist

The Jefferies report estimates Japanese PV production to grow to over 10% of the global market.

Source: US Solar Institute

The Jamaica Energy Council assembled on April 20 to discuss the implementation of an energy policy.

Source: Jamaica Page

Minister of Science, Technology, Energy and Mining, Phillip Paulwell wants the nation's outrage and dissatisfaction with rising energy prices to be translated into a "call to action".

CASM releases interpretation of China's new Five-Year Plan for the solar industry

According to commissioned analysis done by Wiley Rein for the Coalition for American Solar Manufacturing (CASM), China's 12th Five-Year Plan for its solar industry shows heightened signs of government control and support of its industry through numerous government initiatives, including new policy and financial and price subsidies.

Additionally, the report is said to call for more support in industry, financial and tax policy and more aid with development and production of equipment for polysilicon silicon ingots, wafers, cells and panels within the crystalline-silicon solar industry. CASM noted that the plan provides support for industrialization of the country's thin-film industry by harnessing silicon and copper indium gallium diselenide solar technologies.

The Five-Year Plan is part of China's broader 12th Five-Year Plan for its national economic and social development, which was released in February. The plan, according to Wiley Rein, is said to designate solar one of seven "strategic emerging industries" that deserve extra government support, preferential treatment and tight control.

Asia and Oceania

Australia

The Australian government has announced plans to establish a AUD$10 billion clean energy agency next July that will be responsible for providing financing for renewable energy, low-emissions and energy efficiency projects. The commercially oriented Clean Energy Finance Corporation (CEFC) will focus on supporting large-scale projects with the intention of making a positive return on its investments. Smaller projects would need to turn to third-parties for financing. Projects that receive CEFC financing will be required to also obtain financing from the private sector.

China

With Europe cutting back solar incentive schemes and imposing moratoriums, China is poised to be amongst the emerging nations set to monopolize the solar market in 2012. China is expected to add between 3–5GW this year with new annual capacity rising to 4.5–10GW in 2016.

At €1.088/watt for BIPV systems and €0.846/watt for PV residential systems, it is not surprising that China is in the top five for market leaders in 2011. Utility-scale tariffs remain at €0.88. China had recently raised the target of solar energy to 15–GW by 2015 from 10–GW as solar energy has grown amazingly fast in the recent past.

Japan

New tariffs due to be implemented in July 2012, include residential facilities of less than 10kW at ¥42/kWh, although hybrid systems will only receive ¥34/kWh. Non-residential facilities and residential facilities of 10kW or more will be due for ¥40/kWh and hybrid systems at ¥32/kWh. Rates for facilities installed before 2010 will be set at ¥24/kWh and for hybrid systems ¥20/kWh. However, the Japanese Ministry of Economy, Trade and Industry has announced it will omit net-metering purchase prices from these rates in order to avoid confusion. Current rates will be extended for three months until June and kept separate from the feed-in tariff. The ministry is expected to officially announce the FiT rates by the end of May.

Europe

France

The CRE has made further cuts to the feed-in tariff. Residential BIPV applications amounted to 37.4MW and non-residential applications were 102.4MW resulting in a decrease to the FiT of 4.5% and 9.5% respectively. Ground-mounted installations will fall to €0.1079 and residential BIPV arrays have been set to a maximum of €0.1934. President-elect François Hollande has promised a 25% reduction in nuclear facilities by 2020 with an investment in renewables and improving energy efficiency.

Germany

Starting April 1st, 2012 new feed-in tariff payments for rooftop PV plants smaller than 10kW will be €0.195/kWh, rates for rooftop PV up to 1MW will be €0.165/kWh and rates for ground-mounted and rooftop PV of 1–10MW in size will be €0.135/kWh. Germany's Federal Network Agency announced that as a result, during January and February this year, the country collectively installed around 650MW of solar panels — almost double the amount installed for the same period in 2011.

Italy

Energy agency Gestore dei Servizi Energetici SpA (GSE) will charge PV installation owners between €2 and €5 per kW, depending on its size upon registration. The second tax requires imminent and current owners to pay €0.001 per kWh produced. With Italy's current 13GW of installed power and an annual output of 1,300kWh, the second tax could in theory generate an annual income of €17 million for the GSE. However, electricity demand in Italy is apparently falling which could make this quite a generous estimate in the current climate.

The draft has been submitted to the State-Regions Conference, although a date for completion is yet to be announced.

Americas

Canada

The government has proposed to cut the microFiT (projects under 10kWh) by 31.5% with rooftop installations earning CAD$0.549 and ground-mounted CAD$0.445.

Ground-mount microFIT projects would not be able to be located on residential property, lands with CLI 1, 2 or 3 per OMAFRA maps and commercial and industrial lands, unless intended for secondary use. An application security paid to the OPA of CAD$20/kW of a proposed contract capacity for PV projects and CAD$10/kW of proposed contract capacity for all other renewables would be imposed

A CAD$10 million solar development capital fund has been launched across Ontario, Canada by JSM Capital. The investment will leverage the province's current feed-in tariff program to finance early-stage PV projects installed on large commercial and industrial buildings.

The fund will target application-ready projects awaiting submission to the Ontario Power Authority application window and provide capital for FiT application fees, structural engineering assessments, FiT security deposits and grid-connection impact assessment costs. The fund will also invest in Ontario-based FiT contracted projects that have not yet reached commercial operation.

Africa and Middle East

Saudi Arabia

Representatives from the King Abdullah City for Atomic and Renewable Energy (KA-CARE), the government body directing alternative energy development, have announced the country's ambitious long-term goals for solar power. The oil-rich kingdom aims to have installed 41GW of concentrated solar power (CSP) and solar PV projects by 2032, 25GW and 16GW respectively.

KA-CARE announced it would conduct two bidding rounds for the sale of approximately 5GW worth of solar plants. The first round of bidding will be in the first quarter of 2013, where 1.1GW worth of PV project and 0.9GW of CSP will be up for sale. The second round of bidding will take place in the third/fourth quarter of 2014, when KA-CARE will be offering 1.3GW worth of PV project and 1.2GW of CSP. The minimum project size for sale is expected to be 5MW.

Plans to construct geothermal, biomass, wind and nuclear plants were also announced at the Saudi Solar Energy Forum in Riyadh on May 8. The proposed framework would cost tens of billions of dollars and see Saudi Arabia producing almost 25% of its electricity from solar power installations. Solar PV projects will supply the country's daytime electricity demand, while high-capacity CSP plants will provide the majority of solar power, while including thermal storage facilities.

If the plans come to fruition, Saudi Arabia will become one of the world's largest solar power producers. The plans are currently under assessment from the KA-CARE board, though approval is expected to be granted for the scheme imminently.

Compiled by Nilima Choudhury
Web and Publications Editor,
Solar Media Ltd.

The market outlook for PV until 2016

Gaëtan Masson, European Photovoltaic Industry Association (EPIA), Brussels, Belgium

ABSTRACT

Solar photovoltaic (PV) electricity continued its remarkable growth trend in 2011, even in the midst of a financial and economic crisis and despite the PV industry going through a difficult period. Once again PV markets grew faster than anyone had expected, just as they have done for the past decade, especially in Europe but also around the world. While such a rapid growth rate cannot be expected to last forever in Europe, prospects for growth around the world remain high. The results of 2011 – and indeed the outlook for the next several years – show that under the right policy conditions, PV can continue its progress towards competitiveness in key electricity markets and be a mainstream energy source. The major system-price decrease that was experienced in 2011, combined with measures taken in Germany and Italy after the Fukushima nuclear disaster, allowed the market to further develop in 2011, particularly in these two countries. However, the price decrease also helped weaken the policy support in many countries, with policymakers facing growing discontent with regard to the perceived cost of PV and the ailing PV industry in Europe.

Introduction

EPIA's new report "Global Market Outlook for Photovoltaics until 2016" assesses the European and global markets for PV in 2011, and makes forecasts for the next five years. It is based on an internal analysis of data from industry members, national associations, government agencies and electric utilities. The figures presented in the report were discussed and analyzed by key players from the PV industry at the 7th EPIA Market Workshop in Brussels (March 2012).

The major findings for 2011 include:

- **29.7GW of PV systems were connected to the grid in 2011**, up from 16.8GW in 2010; PV is now the third most important renewable energy source (after hydro and wind power) in the European Union in terms of globally installed capacity.
- **21.9GW were connected in Europe in 2011**, compared to 13.4 in 2010; Europe still accounts for the predominant share of the global PV market, with 75% of all new capacity in 2011.
- **Italy, with 9.3GW connected, was the top market for the year**, followed by Germany with 7.5GW (out of which probably 1GW was not yet connected); Italy and Germany accounted for nearly 60% of global market growth during the year.
- **China, with 2.2GW installed, was the top non-European PV market in 2011**, followed by the USA with 1.85GW and Japan with 1.3GW.
- **The number of markets achieving close to or above 1GW of additional PV capacity during 2011 rose from three to seven**: Italy, Germany, France, China, Japan, USA and Belgium.

2011 in a nutshell

Forecasting the PV market is a difficult exercise for at least one reason: energy has always been a policy-driven field, and PV is no exception. On the contrary, the market for PV systems exists in most cases because of the commitment of policymakers to making it possible. The necessary fine-tuning of feed-in tariffs (FiTs) requires a strong political commitment to ensure the development of a sustainable market growth for PV systems. And this fine-tuning was put under significant pressure in several key markets throughout 2011.

The Fukushima disaster clearly led to a revision of policies in Germany and Italy that contributed to helping achieve the incredibly high level of new systems connected to the grid in these two countries in 2011. A closer look at market evolution reveals that the first half of the year was affected by FiT changes and the market fell during an overproduction situation. The rapid price decrease that followed triggered a market growth in the second part of the year, but at a level that was not high enough to cope with high-level production capacities. This led to the prices remaining quite low until the end of the year and into 2012.

> "The growth rate of PV during 2011 reached almost 70% – an outstanding level among all renewable technologies."

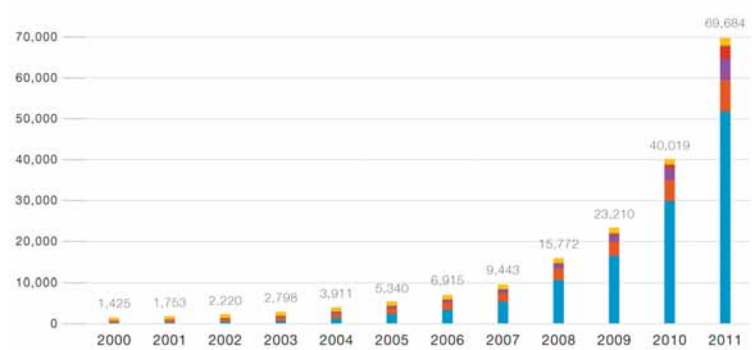

	2000	2001	2002	2003	2004	2005	2006	2007	2008	2009	2010	2011
ROW	751	807	887	964	993	1,003	1,108	1,150	1,226	1,306	1,209	1,717
MEA	N/A	N/A	N/A	N/A	N/A	N/A	N/A	N/A	N/A	21	205	336
China	19	30	45	55	64	68	80	100	145	373	893	3,093
America	146	177	222	287	379	496	645	856	1,205	1,744	2,820	5,053
APAC	355	491	677	902	1,178	1,475	1,797	2,080	2,643	3,409	5,116	7,769
Europe	154	248	389	590	1,297	2,299	3,285	5,257	10,554	16,357	29,777	51,716
Total	**1,425**	**1,753**	**2,220**	**2,798**	**3,911**	**5,340**	**6,915**	**9,443**	**15,772**	**23,210**	**40,019**	**69,684**

Figure 1. Evolution of global cumulative installed capacity 2000–2011 (MW).

The consequences are still visible today, with the industry in several parts of the world, and especially in Europe and the USA, battling to remain profitable in that environment of low prices. In addition, an awareness that these low prices could be normal has spread in the minds of policymakers. This frame of mind, combined with the rapid market growth in some countries, is pushing several administrations to drastically reduce the

level of the incentives – too much and too quickly. Should the price rise again, this could become a serious issue for market development in several EU countries.

Market growth in Europe and globally

Until now, growth has continued to accelerate, fuelled by the European market development and, in 2011, by development of the markets in China, USA, Japan and Australia. Towards the end of 2009 the world's cumulative installed PV capacity was approaching 23GW (Fig. 1). One year later it exceeded 40GW. By the end of 2011 a cumulative capacity of more than 69GW had been installed globally, which will produce at least 85TWh of electricity every year. This energy volume is sufficient to cover the annual power supply needs of over 20 million European-style households. In terms of globally installed capacity, PV is currently the third most important renewable energy source in Europe, after hydro and wind power. The growth rate of PV during 2011 reached almost 70% – an outstanding level among all renewable technologies.

In terms of global cumulative installed capacity, the EU still leads the way, with more than 51GW installed as of 2011: this represents about 75% of the world's total cumulative PV capacity. Next in the ranking are Japan (5GW) and the USA (4.4GW), followed by China (3.1GW), which reached its first GW during 2011. Many of the markets outside the EU – in particular China, the USA and Japan, but also Australia (1.3GW) and India (0.46GW) – have addressed only a very small part of their enormous potential; several countries from large sunbelt regions such as Africa, the Middle East, Asia and South America are on the brink of starting their PV development. Even so, the cumulative installed capacity outside Europe almost doubled between 2010 and 2011, demonstrating the ongoing rebalancing between the EU and the rest of the world, and reflecting more closely the patterns in electricity consumption.

Growing connections but stable demand in 2011 in Europe

The EU has developed from an annual market of less than 1GW in 2003 to one of over 13GW in 2010 and 21.9GW in 2011 (Fig. 2). Given the difficult economic circumstances and varying levels of opposition to PV in some countries, many expected at best a stabilization of PV markets in 2011 compared to 2010. Looking at the newly connected capacity in 2011, one can consider that the PV market has again exceeded all expectations. However, due to variable delays (depending on the country) in connecting PV systems to the grid, some installations from 2010 were only connected in 2011. This will be discussed in detail next.

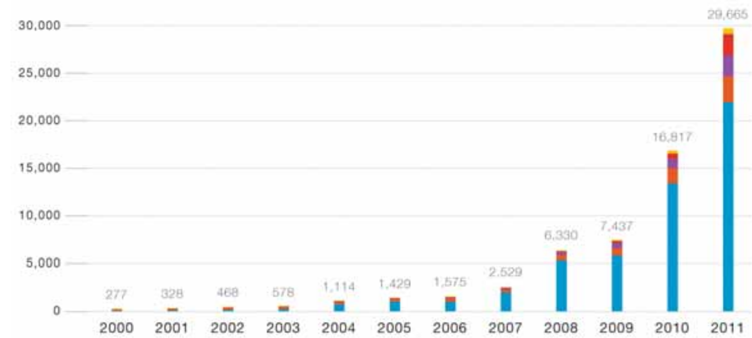

	2000	2001	2002	2003	2004	2005	2006	2007	2008	2009	2010	2011
ROW	88	56	80	77	29	10	105	42	76	80	284	508
MEA	N/A	N/A	N/A	N/A	N/A	N/A	N/A	N/A	N/A	21	45	131
China	0	11	15	10	9	4	12	20	45	228	520	2,200
America	23	31	46	65	92	117	149	212	349	539	983	2,234
APAC	114	136	186	225	276	296	322	283	563	766	1,618	2,653
Europe	53	94	142	201	708	1,002	987	1,972	5,297	5,803	13,367	21,939
Total	277	328	468	578	1,114	1,429	1,575	2,529	6,330	7,437	16,817	29,665

Figure 2. Evolution of global annual installations 2000–2011 (MW).

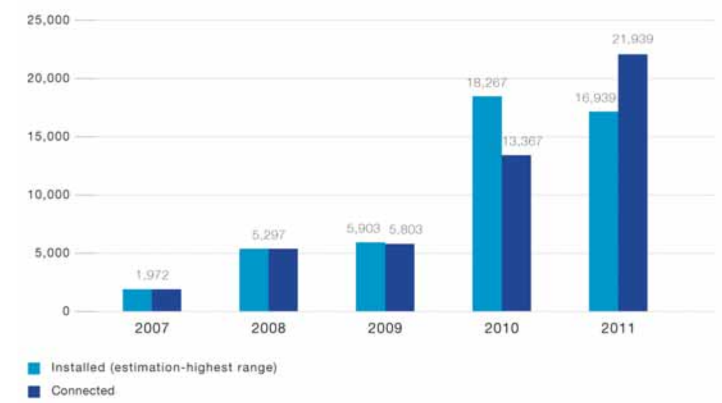

Figure 3. Annual differences between installations and grid-connected systems in Europe (MW).

> "Italy, in 2011, became the top PV market for the first time, with 9.3GW of newly connected systems."

As regards systems newly connected to the grid, Italy, in 2011, became the top PV market for the first time, with 9.3GW of newly connected systems after several years of Germany's having led the market (excluding the Spanish episode in 2008). Together, Italy and Germany (7.5GW) accounted for nearly 60% of global market growth during 2011. These two markets were followed by France (1.7GW), Belgium (974MW) and the UK (784MW); the last two countries both showed surprisingly strong growth in 2011. Many other markets have begun to show significant development: Greece (426MW, despite difficult economic conditions), Slovakia (reaching 321MW), and Bulgaria and Switzerland (with around 100MW each). As a result of constraining policies, Spain disappointed again with 372MW connected.

For several years now, the EU has continued to retain its leadership share of the global PV market, with four markets close to or above the GW mark. Europe's market development is the result of a few countries that have taken the lead year after year, with Germany showing a constant commitment from policymakers to supporting the development of PV.

Installations and connections

While most market reports give installation figures, EPIA reports quote newly grid-connected capacities. The reason for this is simple: there is no reliable methodology for counting installations, and most official bodies report systems connected to the grid. Installation figures are interesting for the PV industry (they describe the demand for PV systems), but

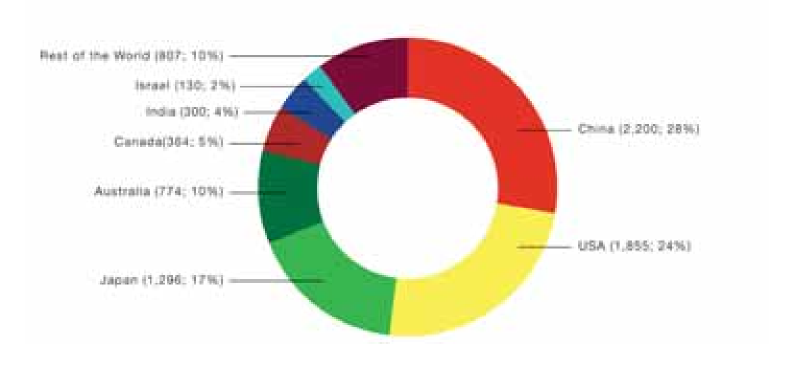

Figure 4. Market share outside Europe for 2011 (MW; %).

grid-connection data are more relevant when considering the increasing share of PV in the electricity mix (and the expenditures in FiTs).

The gap between installations and connections is not new; discrepancies have been noted in France and Belgium in recent years. However, the gap increased significantly in 2010 because of two country-specific situations. The first was in Italy, where the so-called 'Salva Alcoa' decree allowed system owners to receive the 2010 FiT if a system installed in 2010 was connected by June 2011; this led to a rush of installations of nearly 3.5GW by the end of 2010. The second situation occurred in France, where very long delays observed between the end of a project's commissioning and its actual connection by the main grid operator (ERDF) amounted to more than 18 months in some cases. Had those numbers been confirmed, the European demand for PV systems would have shifted up by 5GW in 2010: instead of some 13GW connected in 2010 in Europe, there would have therefore been around 18GW of installations (reflecting the demand for PV systems). In 2011, however, there would then have been only 16.7GW instead of 21.9GW – completely changing the interpretation of the market evolution during those two years.

In reality the situation is more complex, since installation numbers are difficult to obtain. For example, reports from Italy indicate that a part of those 3.5GW was not really *installed* in 2010, but *reported* as having been installed. And, in Germany, the concept of 'commercial commissioning' of PV systems – which can allow the reporting of systems that are not yet installed or connected – creates another complication in the counting of PV systems. It could be argued that part of the 3GW reported in Germany in December 2011 was not really connected, again lowering the 2011 installation count. The final numbers for 2010 and 2011, then, probably lie somewhere between the number of GWs shipped and the 18GW that were installed in 2010, and (due to the German situation) between 15 and 21.7GW installed in 2011. So, while grid-connected PV capacity rose in 2011, the actual demand for PV remained essentially flat between 2010 and 2011. This explains the reality of the PV market in 2011 better than the growth of connected systems.

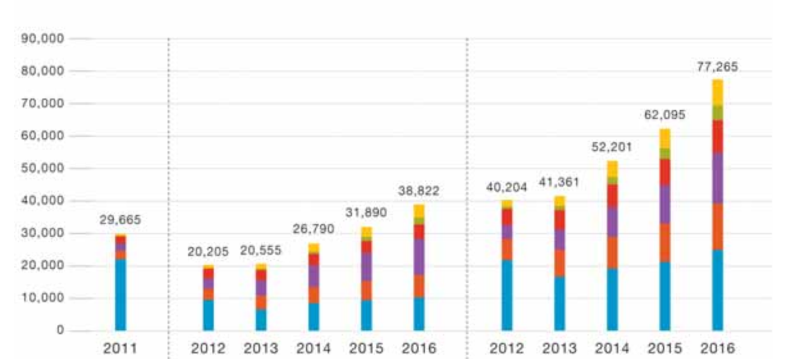

	Historical data	EPIA Moderate					EPIA Policy-Driven				
	2011	2012	2013	2014	2015	2016	2012	2013	2014	2015	2016
ROW	508	1,000	1,500	2,500	3,000	4,000	2,000	3,000	5,000	6,000	8,000
MEA	131	160	350	650	1,250	2,100	700	1,250	2,200	3,250	4,500
China	2,200	3,000	3,250	3,500	3,750	4,500	5,000	6,000	7,000	8,000	10,000
America	2,234	3,250	4,650	6,650	8,650	11,150	4,350	6,250	9,200	11,900	15,700
APAC	2,653	3,360	4,290	5,030	5,890	6,800	6,520	8,270	9,760	11,780	14,220
Europe	21,939	9,435	6,515	8,460	9,350	10,272	21,634	16,591	19,041	21,165	24,845
Total	29,665	20,205	20,555	26,790	31,890	38,822	40,204	41,361	52,201	62,095	77,265

Figure 5. Evolution of global annual market scenarios per region (MW).

Promising global growth

Outside the EU, China has joined Japan and the USA in the group of countries with more than 1GW of newly installed PV capacity in 2011. India and Thailand could also quickly reach that threshold, but it will take several years before other medium-sized markets achieve the same level of development. There was rapid development in Australia, though its future growth over the short term remains constrained by political decisions.

Regionally, the EU is followed by the Asia-Pacific (APAC) region, which – in addition to Japan and China – includes Korea, Australia, Taiwan and Thailand as existing markets. The third leading region is North America, with Canada developing steadily alongside the USA. Elsewhere, the Middle East and North Africa (MENA) region represents untapped potential for the medium term, with some initiatives in Morocco, Saudi Arabia and the Emirates. PV also shows great potential in South America and Africa, where electricity demands will grow significantly in the coming years.

With 7.7GW installed outside Europe, compared to 3GW in 2010, the expected rebalancing still has some way to go before it will be clearly visible. China, with 2.2GW, took first place among the countries outside of the EU, followed by the USA with 1.8GW and Japan with 1.3GW; all are expected to see continued growth in 2012. Australia expanded rapidly in 2011, with 771MW installed last year. Canada has expanded more slowly than some have expected, achieving 364MW. The potentially strong market in India seems to have finally taken off, with 300MW installed in 2011.

An examination of the total installed capacity reveals greater contrasts. The development of the market outside Europe in recent years has not yet caught up with the existing installations in China, USA, Japan and Australia, but the time is near. Outside Europe, the market is well balanced: three countries with a huge potential lead the pack, followed by an emerging secondary market. Except for the Australian boom in 2011, the market remains under control in most countries. With that potential progressively unleashed, the share of PV installations outside Europe can only increase, rebalancing in the right direction.

Where will new growth occur?

With close to 30GW of PV systems having been added in 2011, the PV market is at the crossroads of its development. The expected growth of markets outside Europe will not compensate for a slowed-down market in Europe before 2016 in the pessimistic 'moderate' scenario. This assumes a negative perspective in most markets in the next five years, especially in Europe.

But what is the likelihood of such a negative evolution in the coming years? Two main drivers must be considered here: 1) the existence of open markets that could absorb a part of the excess supply of PV systems; and 2) the evolution of PV module and system prices. The acceleration of PV module price decreases that were experienced in 2011 comes from a huge imbalance between the high demand (close to 30GW) and an even higher supply (around 50GW). The inability of existing markets to absorb more GWs pushed prices even lower in the early months of 2012. A slower market should trigger new price decreases, at least in the short term, favouring development in markets without regulatory restraints.

Yet for most of the industry, lowering costs is becoming less of an option. Moreover, the number of established markets with growth potential is limited, with more and more of them becoming constrained by registries or caps imposed by policymakers. Further rapid price drops could lead to production plant closures all over the world; in that case, prices would stabilize, with markets progressing less rapidly in Europe than they are today. So this evolution will depend mainly on the evolution of markets in Europe and the ability of policymakers to maintain market conditions at an acceptable level. In the policy-driven scenario, the European market would stabilize at around 20–25GW in the coming years, accompanying the development of markets outside Europe. In that respect, the market could top more than 75GW in 2016, with two-thirds of this coming from new markets outside Europe. These new markets could help ensure a major growth even in 2012, and drive market development in the following years.

Ensuring growth with a declining European market

European markets in which the PV market developed tremendously in the past have reached – at least for the time being – a level that will not be easy to replicate in the next two years. In addition, the rebalancing of market growth outside Europe that has started will not immediately offset the fading growth within Europe itself. The consequence of this will be that, in the case of a confirmed market decline in Europe, new markets around the world will have to be opened up to drive PV development in the coming decade, just as Europe accounted for it until now.

Many existing markets – in particular China, the USA and Japan, but also India – have addressed only a very small part of their enormous potential for PV development. Moreover, several countries from large sunbelt regions such as Africa, the Middle East, Southeast Asia and South America are on the brink of starting their development, impelled by an increasing awareness of the potential of solar PV. As a whole, the global PV market will be more balanced in the coming years, and will grow more sustainably, driven by competitiveness of PV solutions rather than just by financial support schemes. But this paradigm shift will not happen overnight.

> “Sudden, stop-and-start policies can create a boom-and-bust cycle that threatens PV’s growth momentum and moves the competitiveness goal further away.”

Finally, in Europe, the game is not over yet. For now, as long as the Spanish and Czech markets are not growing at all, there are no outstanding contenders to replace Germany and Italy as the two leading European markets. Germany, Belgium, Greece, Italy and the UK will, to varying extents, continue to draw investors. In all, with the right policies in place, there is the potential for around 20 to 25GW in Europe in the coming years. Without these policies, however, the market will collapse to possibly less than 10GW a year. The effects of this will be felt globally: low demand, companies suffering from low prices, and a negative effect on the global PV industry.

Conclusion

If any general lesson can be learned from the various market analyses, it is this: sudden, stop-and-start policies (making harsh and/or frequent changes in the FiTs, for example) can create a boom-and-bust cycle that threatens PV’s growth momentum and moves the competitiveness goal further away. What is needed is a more measured response to market developments. This balanced approach will lead PV out of the FiT era and into one in which the technology is competitive with all electricity sources, and in which governments continue to support market development in other ways – for example by removing bureaucratic barriers, encouraging innovation and ensuring grid access.

About the Author

Gaëtan Masson is head of EPIA’s business intelligence unit, which is dedicated to studying the market and industry development, and the technology and sustainability impacts of PV. The unit also deals with short- and long-term PV scenarios, grid parity, competitiveness with conventional energy sources and integration of all renewable energies in the electricity sector, as well as contributing to IEA-PVPS task 1. Having a broad experience in the financial sector, including financing tools and markets, Gaëtan holds a master’s degree in engineering from the Université Libre de Bruxelles in Belgium. He also holds master’s degrees in political sciences, in management (from the Solvay Business School) and in environment studies.

Enquiries

Gaëtan Masson
Tel: +32 (0) 2 400 10 58
Email: g.masson@epia.org

Global PV mix offers remedy for quarterly mood swings

Finlay Colville, NPD Solarbuzz, London, UK

ABSTRACT

Recently, PV demand forecasting has seen greater contributions from countries that had previously been lumped together in the rest-of-world (RoW) bucket – a category previously reserved for the collective PV demand from countries or regions outside of major (FiT-stimulated) European PV markets. Research has shown that PV adoption outside Europe will not simply increase overall PV demand levels, but will assist in smoothing out erratic demand cyclicality.

Introduction

At first glance, the increased gigawattage of demand being added from the rest-of-world (RoW) grouping provides an essential component in driving long-term industry growth scenarios. Non-European PV demand is forecast to increase from approximately 30% to 60% of global PV demand between 2011 and 2016.

However, more tangible benefits of having an increased number of countries feeding into the global demand mix extend beyond just the significant 'growth' potential this situation offers to the PV supply chain. Of these various benefits, perhaps the one that will provide the greatest level of comfort to the PV supply chain will be a collective 'smoothing' effect in quarterly demand swings. This should have a positive effect on factory shipment schedules and hopefully provide an end to some of the boom-and-bust cycles that have negatively impacted the fortunes of the PV supply chain during 2010 and 2011.

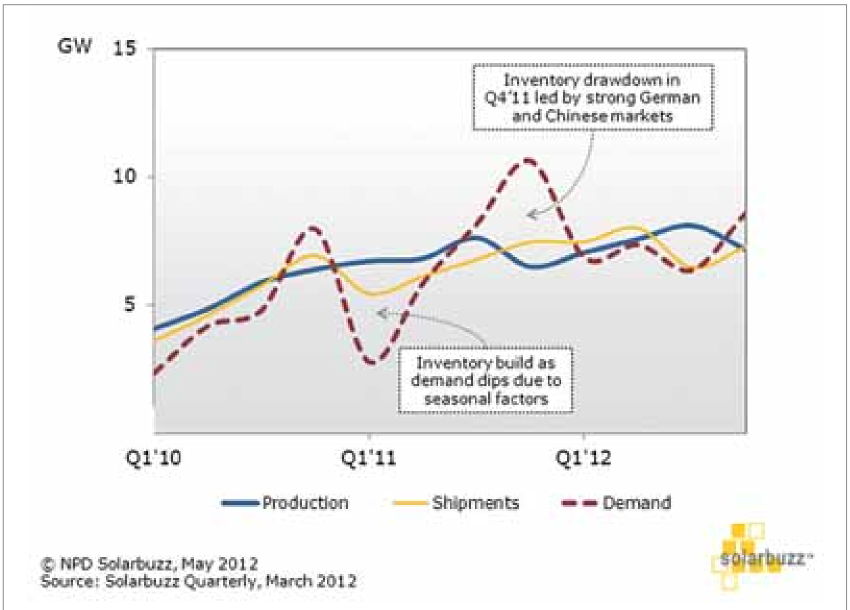

Figure 1. The PV industry has been plagued by quarterly demand cycles, driven by a select group of European countries that accounted for the majority of PV demand each quarter.

Europe captures the headlines, but masks the long-term objectives

Demand from key European countries has dominated the global PV industry in recent years. During 2011, demand from Germany and Italy represented 50% of worldwide demand. This created over-dependence on the quarterly phasing of demand from these regions; this trend continues to dominate short-term corporate tactics and thinking through 2012 as the impact of pending FiT revisions is played out.

In fact, just three countries (Germany, Italy and China) provided 66% of the Q4'11 global PV demand of 10.6GW. European PV demand accounted for 64% of the Q4'11 total, only marginally down quarter-on-quarter compared to Q3'11 (71%) and year-on-year compared to Q4'10 (80%). As a result, any policy change (predicted or not) in just one or two of these countries can dramatically alter the outcome for all PV participants in any given quarter – or indeed, for the full calendar-year period.

Transitioning from an over-dependence on European PV demand cannot come quickly enough for the PV industry. Today, PV policy risk across European countries can at best be summarized as 'moderate to high', while policies across all non-European regions fall more into the 'low risk' or 'moderate risk' categories.

"Just three countries (Germany, Italy and China) provided 66% of the Q4'11 global PV demand of 10.6GW."

The consequence of start-stop demand variations has typically been a surge in inventory levels: often first seen in the downstream/demand side, followed by a similar spike in the upstream/supply portion of the value chain as manufacturers react too late to any rapid downturn in end-market demand. While creating havoc with production and shipment schedules, the full impact is felt most when significant reductions in employee headcount are announced after consecutive quarters of negative demand growth. And of course, the events of 2011 have shown just how quickly ASPs can be eroded as a result of any increase in either upstream or downstream inventory channels.

Fig. 1 illustrates the global supply/demand balance between Q1'10 and Q4'12, showing the dramatic demand cycles that have plagued the PV industry in the past few years, with strong inventory build during Q1'11 followed by an equally emphatic drawdown at the end of last year.

Moving on from single-market demand volatility

Irrespective of the overall demand levels forecast for 2013–15, global PV demand is certain to be comprised of a much greater number of countries feeding into the overall demand figure. Furthermore, since all countries' demand levels are still

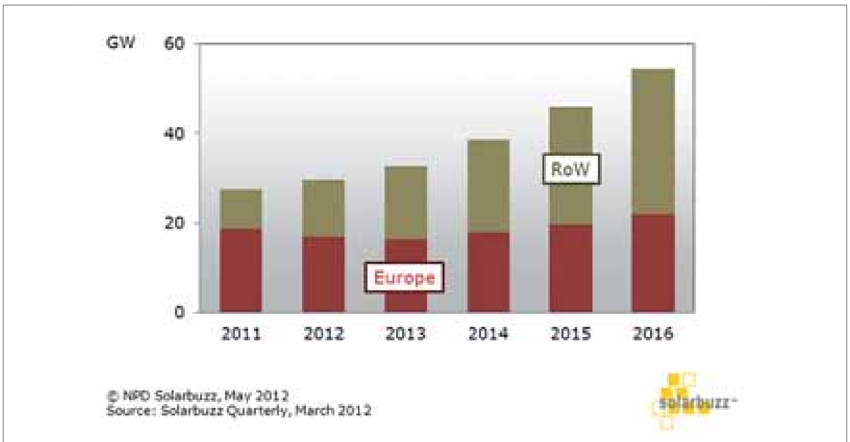

Figure 2. The contribution of PV demand from European countries is forecast to decline significantly out to 2016, with a greater number of countries contributing to the overall global demand.

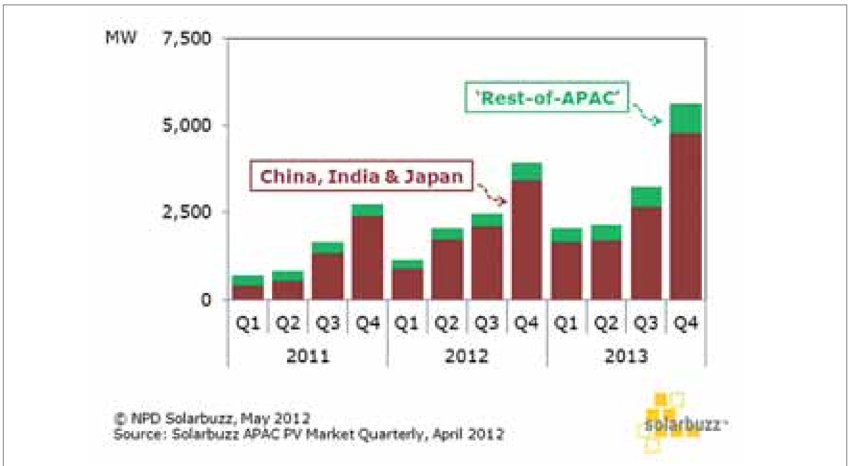

Figure 3. Demand from China, India and Japan is forecast to dominate APAC PV demand out to Q4'13, with regional seasonality and policy structures impacting the overall APAC quarterly demand phasing.

largely policy driven, there will inevitably be quarterly cycles at the country-specific level before and after any policy-related expiration.

However, unlike previous years, the effect of strong cyclic demand changes in any one country will now have a much softer impact on global PV demand. Therefore, the industry's obsession with pending uncertainty from single markets such as Germany should become less important to suppliers' overall global strategies and production/shipment schedules.

> "The industry's obsession with pending uncertainty from single markets such as Germany should become less important."

Fig. 2 shows the expected transition in global PV demand levels to 2016, when comparing demand from Europe with the RoW category (defined in this graphic as all demand from outside Europe). The share of European PV demand is projected to decrease from 69% in 2011 to 40% by 2016, as policy-related changes take effect to curb market growth rates during 2012 and 2013.

The shift in annual demand to non-European countries provides one source of comfort to PV suppliers. But the real benefit will likely be played out when the quarterly phasing of demand unfolds beyond 2012. The expectation is for less severe quarterly demand spikes than seen during 2010 and 2011, in particular when Q4'11 demand was four to five times higher than Q1'11 – a situation that will provide a more stable demand environment to plan production schedules and fab utilization rates.

Indeed, such an environment should enable more controlled module inventory levels, and lessen the requirement for distributors and dealers to act aggressively at quarter- or year-end to cut inventory levels. Transitioning inventory management to a process that is dictated by supply-chain corporate strategy – and not by unpredictable macroeconomic external influences – would be a considerable achievement for the PV industry moving forward.

Another feature that should be removed through PV globalization is that of single-country or single-region seasonality. In recent years, the impact of mild or harsh winter months has introduced one extra variable to take into account, over and above any year-end policy expiry dates.

APAC end-market growth to the rescue

No region characterizes the broader geographic contribution to PV more today than emerging growth across the APAC region. PV demand here is forecast to grow 60% year-on-year during 2012, driven by recent upward revisions to expected demand from China this year (see Fig. 3).

However, short-term cyclicality in the collective APAC demand during 2012 and 2013 is to be expected here also. Again, seasonality and policy deadlines are the culprits driving large quarterly demand variations. This is illustrated by the decline in Q1'12, largely attributed to strong seasonality in ground-mount installations in China, which typically peak in Q4 due to weather conditions and policy structures.

In fact, with a range of incentive terms across the APAC region being revised or expiring in early 2012, many project segments are forecast to experience slight declines in Q1 and Q2'12, as reduced incentive terms take effect. This creates the linear 'ramp' in demand across 2012 shown in Fig. 3, with a large quantity of module shipment occurring during Q2 and Q3'12 ahead of year-end installations within China.

By 2016, however, the demand from the APAC region is forecast to reach approximately 25GW, with the majority of growth coming from China, Japan and India, driven by national incentive programs. By 2016, China and Japan combined are now forecast to account for 70% of APAC demand.

North America drive to self-sustaining status offers further hope

Through a combination of diversified and innovative policies/regulations at the federal/state levels, the US PV market has experienced steady growth until now. The diversification of initiatives has made the US market less vulnerable (and less dependent) on any single national incentive program. And almost by default, this has helped to avoid some of the significant boom-and-bust demand cycles discussed earlier for the major European PV countries. In fact, by avoiding the temptation to introduce FiT-type programs, US authorities have sought to create and implement incentives that were tailored specifically to meet local conditions and requirements.

The case study in this regard is California. Prior to implementing the California Solar Initiative (CSI) – the nation's largest ratepayer-funded program – California had operated several renewable energy programs. Back in 2006, the state represented 63% of the national market (140MW). But some of the legacy programs were operated on an annual basis with limited budgets, which caused undesirable stop-start demand cycles with further instability within the industry.

> "The diversification of initiatives has made the US market less vulnerable."

Now, one of the key components of the initiative is that incentive levels are automatically reduced over the duration of the program in 10 steps, based on the market demand (MW volume of confirmed reservations issues). The incentive levels are then tailored to adapt to dynamic market conditions: the greater the market demand, the faster the incentive level declines and the slower the market grows with reductions in incentives.

Most importantly, industry participants – from PV module makers to installers and consumers – understand the projected rate reduction schedule, and therefore market demand (reservation status) conditions are constantly updated, providing predictability and stability. Compared to some of the other PV-leading countries, the US PV market has witnessed relatively steady growth (see Fig. 4).

It has, however, already experienced two setbacks. The 30% Investment Tax Credit (ITC) originally became available in 2006 for residential and corporate taxpayers for two years (2006 and 2007), but congress extended this to 2008. During 2008, the industry was left waiting nervously, not knowing whether the ITC would be extended. This caused a surge in PV installations. In December 2008, the government extended the ITC for eight years at a fixed rate of 30%, leading to a slowdown in market growth. Similarly, the recent expiry of the Federal Cash Grant caused a surge in installations at the end of 2011 in order to qualify for the grant in time. It is anticipated that the market in 2012 will see considerably slower growth rates.

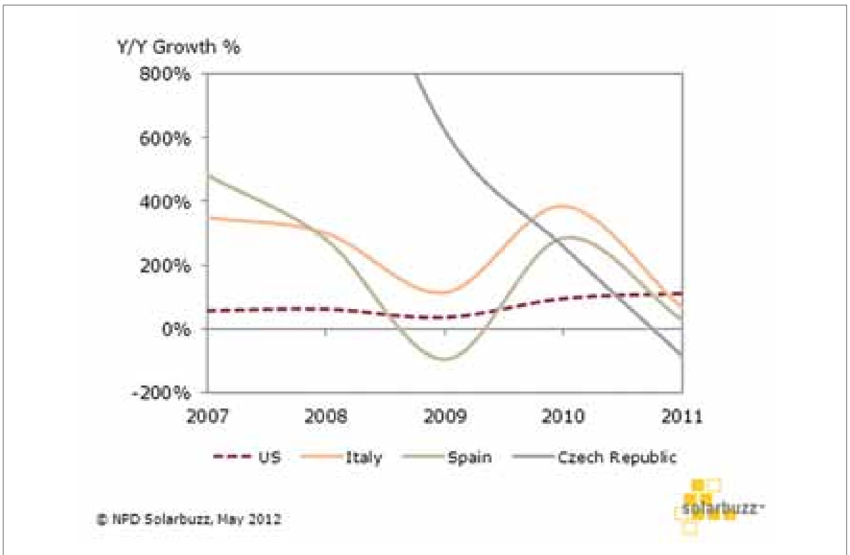

Figure 4. Growth rates within the US show a more moderate – and less erratic – growth trajectory, when compared to year-on-year growth variations for European countries such as Italy, Spain and the Czech Republic.

However, the success of the CSI program does highlight that the market can grow against a backdrop of reduced incentive rates when presented in a predictable and transparent manner. Combined with the other non-European PV market growth, it is hoped that quarterly global demand phasing will start to become less pronounced and more predictable, and that the days of dramatic quarterly demand cycles from policy changes in any single country will be issues only for the PV historians to ponder over.

About the Author

As vice president, **Dr. Finlay Colville** leads the NPD Solarbuzz team of analysts dedicated to PV market research and strategic consulting activities. Since 2010, he has co-authored the PV Equipment Quarterly report. He previously served as Director of Strategic Marketing for Coherent, Inc.'s solar business unit. Dr. Colville holds a B.Sc. in physics from the University of Glasgow and a Ph.D. in nonlinear photonics from the University of St. Andrews.

Enquiries

Email: finlay.colville@solarbuzz.com

Advertisers & Web Index

Photovoltaics International

DON'T MISS: Module encapsulant creep testing | Picosecond laser structuring of CIGS cells | Screen-printed PERC cell development

I would like to purchase a subscription.

Price: ☐ 1 x Issue **$59.00 USD** (includes international delivery)
☐ 4 x Issue **$199.00 USD** (includes international delivery) Please start my subscription with edition ....

Method of payment: ☐ Credit Card ☐ Bank Transfer

Name: ....
Job Title: .... Job Function: ....
Company: .... Div/Dept: ....
Street Address: ....
City: .... Post Code/Zip: ....
Country: ....
Telephone Number: .... Web URL: ....
E-mail: ....
For the purposes of our circulation audit, please indicate the last digit of your birth year (YYYY): ....

Company Activity (tick where appropriate):

☐ PV Manufacturer (inc. Thin Film & Module) ☐ Materials Supplier ☐ Equipment Supplier

If you ticked any of the above three options, please indicate the company technology type by ticking one or more of the boxes below:

☐ Si Cell ☐ Thin Film ☐ Module ☐ Concentrator ☐ Emerging ☐ Polysilicon ☐ Ingot/Wafer

☐ University ☐ Energy Utility Supplier ☐ Government Agency
☐ R&D Facility ☐ Financial Community ☐ Other (please specify ....)

In order to continually improve Photovoltaics International we require your feedback. We would be very grateful if you would answer the following questions:

(Q) Which section(s) of the publication are of interest to you? (please tick)

☐ Fab + Facilities ☐ Materials ☐ Cell Processing ☐ Thin Film
☐ PV Modules ☐ Power Generation ☐ Market Watch

(Q) What technical subjects do you wish to see in future editions?...

....

Signature:.. Date ....

Payment Details:

Fax on +44 (0) 20 7871 0101 or email info@pv-tech.org:

Type of credit card: ☐ VISA ☐ MasterCard ☐ American Express

Card Number: ....
Expiry Date: ....
3 Digit CVV Code (back of card): ....
Cardholder's name: ....

Post: Make cheques payable to **"Solar Media Ltd."**
Photovoltaics International, Trans-World House,
100 City Road, London EC1Y 2BP, UK
Online: PayPal - visit **www.photovoltaicsinternational.com/subscriptions**

To request an invoice please call on 020 7871 0148
or **email:** subscriptions@pv-tech.org

Bank Transfer Details:

Account Name:	Solar Media Ltd.
Account Number:	80686832
Sort Code:	20-39-53
Swift Code:	BARC GB 22
IBAN Number:	GB 42 BARC 203953 80 68 68 32
Bank:	Barclays Bank Plc, 10 Hart Street, Henley-on-Thames, Oxon, RG9 2AX.

All invoices are calculated in Pounds Sterling.

Any payments made in US$ must be made according to the appropriate exchange rate at the time of payment.

US military takes solar to the frontline

The US military is not where you'd expect to find America's greatest climate warriors wanting to save the planet. But it's where you will find the country's staunchest allies when it comes to support for renewable energy - because it saves lives.

US Department of Defense is the highest consumer of energy in the world with a thirst for 300,000 barrels of oil a day. But reducing the DoD's carbon boot print from the barracks to the battlefield has become mission critical.

Source: Fine Art America

In 2007 in Iraq and Afghanistan, a total of more than 3,000 army personnel and contractors were wounded or killed in action from attacks on fuel and water resupply convoys.

Major General Anthony Jackson said at a Pew Charitable Trusts forum at Stanford University last year: "I know the cost of oil. I know it up close and personal. If you have never seen the mixture of blood and sand, it's a harsh purple on the desert floor.

"There is an urgent need for our nation to lead the world in renewables and conservation and getting a grip on the strategic vice that one three letter word has around our neck. For every 50 trucks we put on the road someone is killed or loses a limb."

President George Bush started this strategy for energy security that Barack Obama has accelerated. Over the past four years, DoD clean energy investments in biofuels, solar technology and advanced batteries have increased 200%, from US$400m to US$1.2bn.

US Marines reinforced the DoD's goal by taking renewable energy to the frontline with the deployment of solar panels at bases and solar battery charging packs for patrols. Marines in Afghanistan use about 200,000 gallons of fuel a day to power their "war fighting capabilities" and forward operating bases require a minimum of 300 gallons of diesel a day.

Solar panels are a useful alternative to noisy diesel generators at military posts in Afghanistan where US troops at a US Marine Command Operation Centre are testing the Ground Renewable Expeditionary Energy Network System (GREENS) to power phones, laptops and air conditioners. But the clean conversion doesn't come cheap at US$500,000 for a 1000W system.

"Lightening the load" for those with boots on the ground is also vital as batteries account for around 20% of the weight of a soldier's pack and a typical infantry battalion uses US$150,000 worth of batteries a year.

Meanwhile, the US army has committed to sourcing 25% of its electricity come from renewable sources by 2025, the equivalent of 2.5 million MWh.

A report earlier this year, the Solar Energy Development on Department of Defense Installations in the Mojave and Colorado Deserts, estimated that more than 7,000GW of solar energy development is technically feasible and financially viable.

Financier and integrator Borrego Solar earlier this year cut the ribbon on a 3.4MW solar installation at Edwards Air Force Base in San Diego. Borrego Solar financed the project and has a 10-year power purchase agreement to sell the electricity to the base.

Investors will be buoyed at the prospect of private partnership powered by military financial might: after all DoD procurement helped create scalable cost-competitive markets for computers, the internet and GPS.

"Market pull and signal for investors is strong enough that it's going to significantly accelerate those cost reductions and they are going to allow the commercial marketplace to come in and adopt the technologies," said Jonathan Gensler, a project manager at Borrego Solar.

"The DoD has been the primary first adopter for virtually every major new technology that the world has seen over the last 50 years. There's nothing inherently different about energy that should make the case different here, it's just the timelines are a little bit longer and the scales necessary are a little bit larger."

But the DoD procurement has wider political implications as renewables are deployed in more conservative communities, he said.

"There's a lot of political pushback against using renewables in a lot of these communities. But once the people who live there see the military adopting renewable energy and understanding the benefits to their economy, we'll see those spill-over effects and political opposition go away once they start to realise the benefits of a clean energy economy."

This will be especially beneficial as the military's clean energy mission that started under the Bush administration now seems to be on the hit list for Republicans.

One of the neat tricks of the US government is that the US president is also the commander in chief. The US military is following executive orders to follow a lower-carbon path and there is little Congress can do.

Republicans are slowly waking up to this "command and control" by stealth, but Obama appears to have secured enough territory and support for protecting American soldiers to keep these renewable trends safe from the right-wing axe for now.

This column is a revised version of a blog that originally appeared on PV-Tech.org.

Felicity Carus is a regular freelance blogger for PV-Tech.

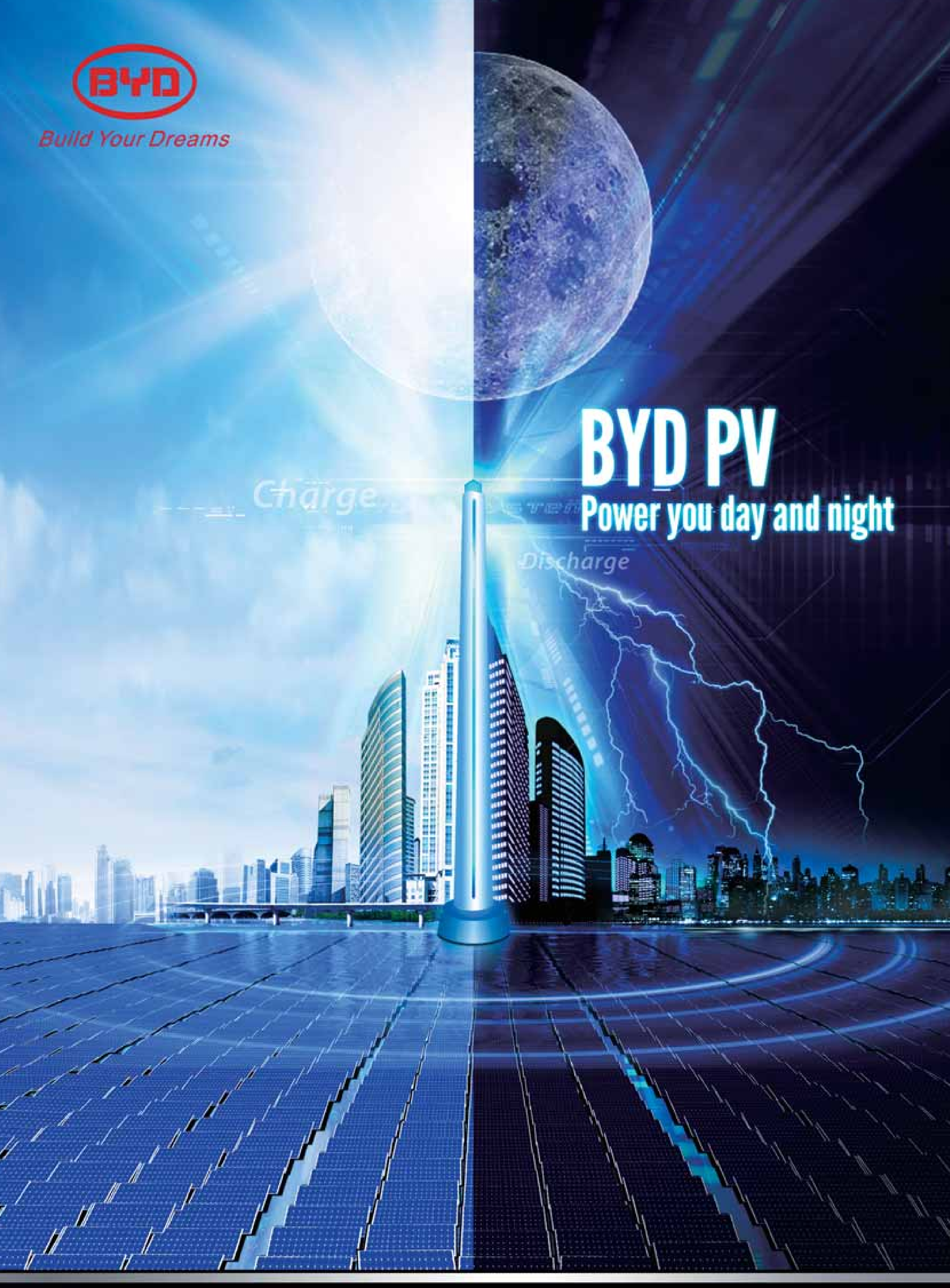

To find out more about BYD New Energy, please go to http://www.bydenergy.com or contact us at bydenergy@byd.com